Institut für Nutzpflanzenwissenschaften und Ressourcenschutz (INRES)
Fachbereich Pflanzenzüchtung

The genetic and molecular architecture controlling flowering time in interaction with the environment in winter wheat

Dissertation

zur Erlangung des Grades

Doktorin der Agrarwissenschaften (Dr. agr.)

der Landwirtschaftlichen Fakultät

der Rheinischen Friedrich-Wilhelms-Universität Bonn

vorgelegt von

Dipl. Ing. agr

Salma Benaouda

aus Elhoceima, Marokko

Bonn 2022

Referent	Prof. Dr. Jens Léon
Koreferent	Prof. Dr. Frank Hochholdinger
Tag der mündlichen Prüfung	16.02.2022

Angefertigt mit Genehmigung der Landwirtschaftlichen Fakultät der Universität Bonn

Acknowledgments

By writing the last words in my thesis, the memories take me back to the day I started my Ph.D., a long trip full of emotions and challenges, failure and success. A way in which I got to know people that changed me somehow. Ph.D. is more than understanding a natural phenomenon scientifically, it is a life experience through which I rediscovered myself, I learned a lot and I learned to get adapted to the difficulties of researching. I kept in mind, every day, that I am in the right place doing the right job. I would never have been able to finish my Ph.D. without the support I received from many good hands, good minds, and good hearts.

I am deeply thankful to my supervisor Prof. Dr. Jens Léon for offering me the chance to work on this thesis, providing me with all necessary facilities for the work, for his time to discuss and face the research issues, for his guidance, and for his confidence in my competence to assume this part of the flowering time project. Sir, I can never forget your words as I finished my master thesis and I applied for this Ph.D. position. You saw in me someone who deserves this chance, your trust was an honor for me. I feel very lucky that I worked under your supervision for the last 5 years before retiring, and even after, you kept being close to your students and continued your ennobling mission. I wish you all the best in your retirement, Sir.

To Dr. Agim Ballvora, "Maître" Agim, as I call him most of the time, I am more than grateful, for his patience to answer my daily questions, for teaching me genetics, for his effort to make this work better, step by step, for his help to elaborate new ideas and ways for the research, for motivating me when I was tired or stressed, and for offering me the positive energy that was in many times very needed. I will never forget what you said always: Wenn die Forschung so einfach ist, dann bleiben wir alle zuhause! It was a pleasure and honor to work with you, maître.

I want to acknowledge Prof. Dr. Frank Hochholdinger, Prof. Dr. Mathias Becker, and Prof. Dr. Heinrich W. Scherer for accepting to be part of the examination committee and for their time and attention to read my thesis.

I express my gratitude to Dr. Said Wali Dadshani, who helped me a lot as a master's student, then as a colleague in my research. One of the best experts in statistics in the plant breeding group, his assistance improved my work significantly! Thank you Said Wali for your considerable effort over all those years.

I thank Prof. Dr. Heiko Shoof and Ph.D. candidate Tyll Stöcker from the bioinformatic department for their nice cooperation in transcriptomics analysis.

"Un grand Merci" to Karin Woitol for her help in translating the summary of this thesis into the German language and for the technical aid. Karin, you are more than a lab assistant in our group, you are our "mother Theresa". To you and Rania Raafat: I never imagined having better friends than you. Your friendship is a precious present that I want to keep forever. God bless you.

I owe many thanks to my ex officemate Dr. Benedict Oyiga for his friendly advice during my Ph.D. time. I am also indebted to PD. Dr. Boby Mathew for his assistance in the R program and to PD. Dr. Ali Naz, who has gently answered my questions and gave some tips during the coffee break!

My gratitude is extended to: Dr. Patrice Koua, Dr. Diana Daurte, Dr. Shumaila Muzammil and Dr. Hasina Bigum. Thank you for being supportive colleagues. I say thank you and good luck to all Ph.D. candidates: Kamaruzaman, Nurialam, Majid, Andreas, Maissa, Karolin, and Bahman. My thanks go also to Karola Müller, Anne Reinders, Andrea Ott, and Dr. Henrik Schuman. Thank you Martina Ruland for your help with different stuff.

My special thanks go to Lea Hördemann who assisted me greatly in some experiments while working on her master thesis. Without forgetting the precious help of Inci Vogt and Sarah Schult. Thank you to the Klein Altendorf team and Gardner Team in Poppelsdorf for supporting my experiments.

I want to thank Prof. Dr. Annaliease Mason for enabling me to finish my Ph.D. in good condition and for her constructive remarks about my work.

My last acknowledgment word I reserved to my parents, my first teachers, your prayers for me, encouragement, and unconditional love give me the force during my whole life and sustained me so far. I hope you are proud of me and I dedicate to you my “Doctor” title as a symbol of gratitude for what you did for me. I love you too much! My sister, my brothers, my nephews, and nieces, to all of you I say thank you for being part of me as I am part of you.

My Lord, Almighty God, you show me the way to follow, you give me the insight to find the light, you offer me the mercy and the grace, and you guide me to recognize you through what you have created. All praise is due to you as befits the majesty of your countenance and the greatness of your authority.

TABLE OF CONTENT

LISTE OF FIGURES

Chapter 1:

Chapter 3:

Chapter 4:

LISTE OF TABLES

Chapter 3:

GENERAL SUMMARY

The time of flowering is a key factor for global adaptability to diverse conditions and a critical agronomical factor for successful reproduction. This high potential is resulting from a natural variation that has remained largely unexplored so far. For this reason, the present research endeavors to decrypt the genetic and molecular architecture of flowering time regulation in winter wheat in interaction with the environment. We used a diverse collection set made of 213 elite bread wheat cultivars from Germany, central Europe, and other countries. Three complementary studies were conducted:

The first study evinced through the phenotypic evaluation, that the genotypic response to climatic parameters variation depending on location and year revealed that the spring temperature dominates other climatic stimuli in reducing the number of days to heading in low and middle latitudes, while the very low yearly thermal change uncovered the implication of photoperiod in promoting heading in the higher ones. The solar radiation is mostly delaying flowering time, whereas the precipitations showed locations and seasonal depending effect on heading date.

The outcomes of the second study showed out of the screening of all cultivars for the known vernalization and photoperiod genes that the allele combination *vrn-1/Vrn-2/Ppd-D1b* is responsible for winter growth habit in 95% of the adapted cultivars. QTL × environments analysis detected a novel locus TaHd102 on chromosome 5A, which is stable across all environments and explains 13.8% of the genetic variance. The allelic variation at TaHd102 alters flowering time by 1.2 days. Including the non-adapted cultivars in the analysis, an exotic allele at QTL TaHd044 on chromosome 3A could be identified. The latter explains up to 33% of the genetic variance and has an allele effect of 5.6 days. The genetic response to climatic stimuli selects thermo-sensitive and circadian clock loci in the lower and higher latitudes, respectively for inducing heading. A novel locus TaHd098 located on the small arm of chromosome 5A, which showed multiple epistatic interactions with 15 known regulators of flowering time was uncovered.

In the third study, QTL mapping provided by the previous genetic analysis was combined with transcriptomics. The early flowering cultivar “Kontrast” and the late flowering one “Basalt”, developed in Germany, were selected for this analysis. 664 and 1075 differentially expressed genes in Kontrast” compared to “Basalt” in the apex and leaves respectively, could be identified in 23 QTL intervals for heading date. In transition apex, Histone *H3-K36* methylation and regulation of circadian rhythm are both controlled by the same homoeologous genes/QTL TaHd112, TaHd124, and TaHd137. In the double ridge stage, the gene *FLOWERING TIME LOCUS T* located on chromosome 7D acts as a flowering repressor due to polymorphisms in the coding sequence. The wheat orthologous of the transcription factor *ASYMMETRIC LEAVES* 1 (*AS1*), mapped in TaHd102 is uncovered in the late reproductive stage. In its promoter region, *AS1* exhibits a deletion of eight single nucleotides in the binding site of the *SUPPRESSOR OF CONSTANS OVEREXPRESSION 1 (SOC1)* gene. Both genes induce flowering time in response to Gibberellin biosynthesis in *Arabidopsis thaliana* background.

ALLGEMEINE ZUSAMMENFASSUNG

Der Zeitpunkt der Blüte ist ein Schlüsselfaktor für die globale Anpassungsfähigkeit an unterschiedliche Bedingungen und ein entscheidender agronomischer Faktor für eine erfolgreiche Reproduktion. Dieses hohe Potenzial ist das Ergebnis einer natürlichen Variation, die bisher weitgehend unerforscht ist. Aus diesem Grund wird in der vorliegenden Arbeit versucht, die genetische und molekulare Architektur der Blühzeitregulierung bei Winterweizen in Wechselwirkung mit der Umwelt zu entschlüsseln. Wir verwendeten eine vielfältige Sammlung von 213 Elite-Brotweizensorten aus Deutschland, Mitteleuropa und anderen Ländern. Es wurden drei sich ergänzende Studien durchgeführt:

Die erste Studie zeigte anhand der phänotypischen Auswertung, dass der Einfluss der Frühlingstemperatur andere Faktoren bei der Regulierung des Blühzeitpunkts in den niedrigen und mittleren Breiten überwiegt. Die sehr geringen jährlichen Temperaturschwankungen haben die Bedeutung der Photoperiode bei der Förderung des Blühbeginns in höheren Breiten deutlich gemacht, Die Sonneneinstrahlung verzögert die Blütezeit am meisten, während die Niederschläge einen standort- und jahreszeitabhängigen Einfluss auf das Ährenschiebendatum haben.

Die Ergebnisse der zweiten Studie zeigten, dass die Allelkombination *vrn-1/Vrn-2/Ppd-D1b* bei 95 % der adaptierten Sorten für das Winterwachstum verantwortlich ist. Die Analyse von QTL $^{\times}$ Umwelt ergab einen neuen Locus TaHd102 auf Chromosom 5A, der über alle Umwelten hinweg stabil ist und 13,8 % der genetischen Varianz erklärt. Die allelische Variation an TaHd102 verändert die Blütezeit um 1,2 Tage. Unter Einbeziehung der nicht angepassten Sorten in die Analyse wurde ein exotisches Allel am QTL TaHd044 auf Chromosom 3A identifiziert. Dieses letztere erklärt bis zu 33 % der genetischen Varianz und hat einen Allel-Effekt von 5,6 Tagen. Die genetische Reaktion auf klimatische Stimuli selektiert thermosensitive und zirkadiane Uhr-Loci in den niedrigeren bzw. höheren Breitengraden für die Induktion des Blühzeitpunktes. Die Analyse der Epistase führte zur Entdeckung eines neuen Locus TaHd098 auf dem kleinen Arm von Chromosom 5A, der signifikante Interaktionen mit 15 bekannten Operatoren der Blütezeitregulierung zeigte,

In der dritten Studie wurde die QTL-Kartierung aus der vorangegangenen genetischen Analyse mit Transkriptomik kombiniert. Für diese Analyse wurden die früh blühende Sorte "Kontrast" und die spät blühende Sorte "Basalt", die in Deutschland gezüchtet wurde, ausgewählt. 664 und 1075 Gene, die in Kontrast" im Vergleich zu Basalt" in dem Sproßmeristem bzw. in den Blättern unterschiedlich exprimiert werden, konnten in 23 QTL-Intervallen für den Blühzeitpunkt identifiziert werden. Im Sproßmeristem werden sowohl die Histon-*H3-K36*-Methylierung als auch die Regulierung des zirkadianen Rhythmus von denselben homöologen Genen/QTL TaHd112, TaHd124 und TaHd137 kontrolliert. Im Doppelrippenstadium wirkt das auf Chromosom 7D gelegene Gen *FLOWERING TIME LOCUS T* aufgrund von Polymorphismen in der kodierenden Sequenz als Blühunterdrücker. Das Weizenortholog des Transkriptionsfaktors *ASYMMETRIC LEAVES 1 (AS1)*, das auf TaHd102 kartiert

ist, wurde im späten Reproduktionsstadium entdeckt. In seiner Promotorregion weist *AS1* eine Deletion von acht einzelnen Nukleotiden in der Bindungsstelle des *SUPPRESSOR OF CONSTANS OVEREXPRESSION 1 (SOC1)* Gens auf. Beide Gene induzieren die Blütezeit als Reaktion auf die Gibberellin-Biosynthese in *Arabidopsis thaliana.*

Chapter 1: Literature overview

1.1 Introduction

Wheat (*Triticum aestivum* L.) contributes to about 20 % of all calories consumed by humans worldwide. It is a staple source of nutrients for around 40% of the world's population and is highly used for animal feed or fuel production as well (FAO, 2019). This crop is growing worldwide and expanded in different geographical regions from 67°N to 45°S (Gustafson et al., 2009). The cultivation of hexaploid wheat in a wide range of temperatures 3 to 32 °C results in satisfactory yields (Curtis et al., 2002). The global production stands at 776.7 million tons (Figure1.1), with this, wheat is the second most cultivated cereal worldwide (Supply & Brief, 2020). With a predicted world population of almost 10 billion by 2050, the demand for wheat is expected to increase further by 60% (Alexandratos & Bruinsma, 2012). To meet this demand, annual wheat yield increases must rise from the current level of below 1% to at least 1.6%. This task becomes more complex considering that land for productive agriculture has been lost to urbanization as well as environmental degradation (Godfray et al., 2010). Possible solutions are, for instance, improved cultivation on marginal lands or intensified cultivation of existing agricultural areas (Shahid & Al-Shankiti, 2013). A key challenge in increasing global wheat production is to understand the causes for differences in yield. Multiple factors such as low water availability, differences in soil characteristics, or extreme temperatures are challenging yield potential and rising issues triggered by climate change are expected (Beniston et al., 2007). The adaptability of wheat to a wide climatic conditions derived from large natural variation which has been favored by allelic diversity in genes regulating growth and developmental stages especially growth habit and flowering time (Worland, 2001).

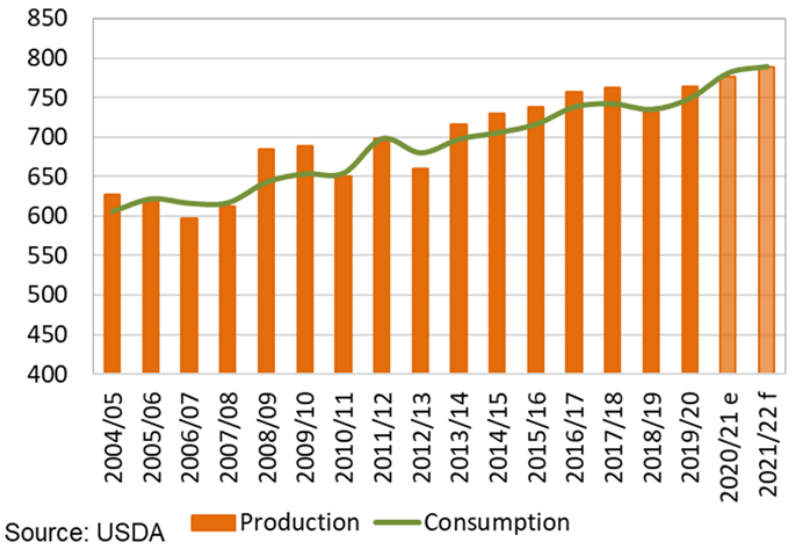

Figure 1. 1: Global wheat production and consumption in million tons until 2022.

https://mecardo.com.au/record-global-wheat-crop-on-its-way/

1.2 Life cycle and growth stages of temperate wheat

Winter wheat growth and development are physiologically and morphologically classified according to the BBCH scale (Biologische Bundesanstalt, Bundessortenamt und Chemische Industrie) (Meier, 1997). The life cycle of a wheat plant can be divided into three main development phases: vegetative phase (BBCH0-29), reproductive phase (BBCH30-69), and grain development phase (BBCH70-99) (Figure 1.2). For winter wheat, the vegetative phase starts from autumn to the end of winter and includes germination, emergence, and tillering. The optimal temperature for germination ranges between 12° and 25°C (Acevedo, 1987). The seed size is associated with seedling growth, a higher number of fertile tillers per plant, and a higher grain yield (Spilde, 1989). The emergence is marked by the initiation of three to four leaf primordia through the coleoptile and the tip is visible above the soil surface (Baker & Gallagher, 1983). Then, the bud differentiates into tillers, which grow from the axils of the main shoot leaves. The beginning of the reproductive phase is indicated by the change of shoot apex shape from dome to more elongated apex and formation of the single ridge then double ridge. The stem elongation synchronizes with the appearance of the terminal spikelet. Next, the ligule of last leaf merges. The heading begins when the first ear (spikelet) is visible and ends when all ears are out of the sheath. The flowering time (anthesis) is marked by the appearance of the first anther on the top of the ear and is completed to the bottom of the ear. In the last growth phase, grain filling is designed by milky and mealy development and the milk grain becomes a dough. The spikes continue ripening to the maturity stage when all ears components, internodes, and leaves lose green color (Bonnett, 1936; Zadoks et al., 1974).

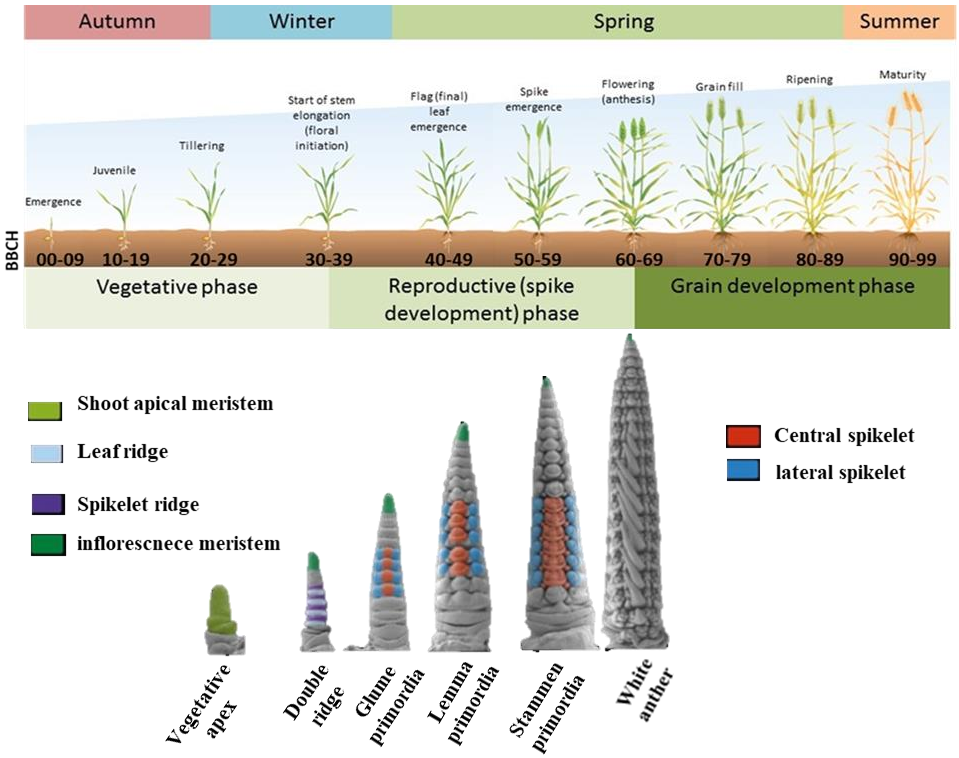

Figure 1. 2: The life cycle of wheat and key development stages and phases relative to seasons of the year. https://grdc.com.au (modified), and profile views of wheat/barley spike developmental stages from the vegetative apex to white anther.

1.3 Flowering time and plant adaptability

Heading date (HD) is one of the most purposed traits in breeding programs which have the ultimate goal to breed performing cultivars that fit different climatic conditions while maintaining a high and stable yield production over years (Ferrara et al., 1997). Setting the reproductive organs for pollination and seed development at an appropriate and optimum time is depending on the adaptability to environmental conditions (Cockram et al., 2007). Adaptability means that the plant can avoid inappropriate stress factors such as frost, heat, and drought by adjusting its flowering time to seasonal changing and protecting its floral organs by delaying heading (Fjellheim et al., 2014). Such an adaptive mechanism of controlling the timing of starting the transition from vegetative to reproductive phase is a result of resilient genetic variability which can be a tool for selecting cultivars that match different climates and geographical regions and even to adapt regional cultivars to coming climate changes (Guedira et al., 2016). It has become evident that HD is highly associated with yield improvement and yield stability (Cuesta-Marcos et al., 2009; Pasam et al., 2012). In addition, other agronomical traits such as leaf area, plant height, tillering, and grain number are subsequently based on the synchronization of HD (Fischer & Kohn, 1966; Kato et al., 2000).

1.4 Seasonal control of flowering time in winter wheat

The development of wheat is depending on day length and temperature that control two major flowering seasonal responses based on vernalization and photoperiod. A long time ago, researchers figured out that exposure to cold during winter is a critical factor and a mandate to promote flowering in temperate cereals, in such a way that those plants lack to flower when sown in spring (Chouard, 1960; Gassner, 1918; McKinney, 1940). This phenomenon of cold requirement came later to be referred to as vernalization (Chouard, 1960).

Cold responsive varieties of wheat are sown in autumn. After vernalization, the irreversible transition from the vegetative phase to the reproductive phase is promoted at the shoot apex (Flood & Halloran, 1984). The vernalization effect is cumulative. Increasing the duration of exposure to cold until saturation of vernalization response induces rapidly the flowering process (Gott et al., 1955). Nevertheless, there is an optimal temperature range between 0 and 10°C, required for initiating vernalization and the effectiveness of vernalization is both time and temperature-dependent (Chouard, 1960; Gassner, 1918). However, increasing day length during spring is a prerequisite for fluorescence development after vernalization (Purvis, 1934). Consequently, the combination of vernalization demand and daylength sensitivity ensures the postponement of flowering until an optimum time after winter, to protect the sensitive floral organs from frost damage. The response to long days is accelerated during spring before summer comes to avoid heat and water deficiency effect on the reproductive organs (King & Heide, 2009; Thomas & Vince-Prue, 1996) (Figure1.3).

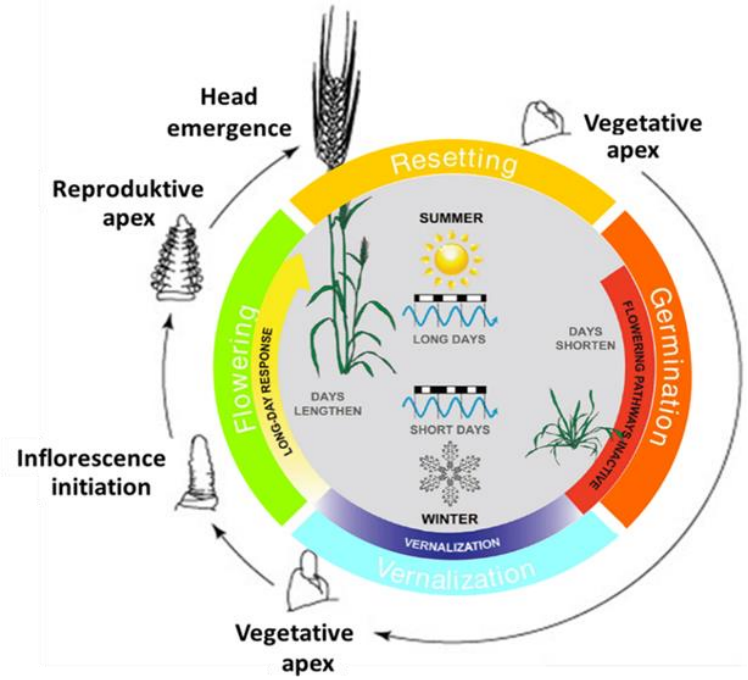

Figure 1. 3: Seasonal flowering responses of temperate cereals.

The flowering of in autumn-sown cereal plants is retarded during winter as a response to the inactivation of vernalization and daylength pathways. The vernalized plants are competent to respond to lengthening days during spring. Consequently, the flowering is started and proceeds to the formation of the reproductive apex and later the emergence of the spikelet. https://www.publish.csiro.au/fp/Fulltext/fp10056 (modified).

1.5 Mechanisms and pathways of flowering time in hexaploid wheat

Four distinct pathways interact to control flowering time in wheat: vernalization, photoperiod, earliness *per se (Eps)*, and plant hormones (Distelfeld et al., 2009; Herndl et al., 2008; Kamran et al., 2014; Snape et al., 2001). For winter wheat, *Eps* and endogenous hormones are involved in the growth and developmental process during the vegetative stage. Then vernalization and photoperiod integrate exogenous signals of environmental stimuli to promote spikelet, floret initiation, and spike development (Figure 1.4.a). Thus, vernalization, photoperiod, and exogenous hormones are external players that determine the time of heading, while, endogenous hormones and *Eps* are internal regulators that control the duration of the wheat heading stage (Alvarez et al., 2016; Dennis & Peacock, 2009; Distelfeld et al., 2009; Laurie, 1997; Turner et al., 2005; Worland, 1996; Zikhali et al., 2015). The four pathways controlling flowering time in wheat will be reviewed in the next sections.

1.5.1 Genetic regulation of vernalization response

The group of vernalization (*VRN)* genes regulates the molecular mechanisms for the requirement of vernalization and exposure to cold in wheat (Allard et al., 2012; A Distelfeld et al., 2009; Trevaskis et al., 2007). The four vernalization loci have been cloned from wheat by using a positional cloning approach: *VRN1* (Yan et al., 2003), *VRN2* (Yan et al., 2004), *VRN3* (Yan et al., 2006), and *VRN-D4* (Kippes et al., 2015) (Figure 1.4.b). Natural allelic variation in one or many of *VRN* genes leads to the

differentiation between winter and spring growth habits. The alleles *Vrn1*, *Vrn3*, and *Vrn4* genes are dominant for the spring growth habit and confer partial or no sensitivity to cold treatment, whereas *Vrn2* is dominant in controlling the winter growth habit and requires exposure to cold for a certain period before the start of flowering (Danyluk et al., 2003; Fu et al., 2005; Kippes et al., 2016; Trevaskis et al., 2003; Yan et al., 2003, 2004).

1.5.1.1 Vernalization gene VRN1

The three homoeologous genes of VRN1 *(Vrn-A1, Vrn-B1, and Vrn-D1)* are mapped on chromosomes 5A, 5B, and 5D, respectively (Dubcovsky et al., 1998; Fu et al., 2005; Pugsley, 1971; Snape et al., 1976). At least three different *Vrn* alleles could be characterized in hexaploid wheat due to insertion and/or deletion of polymorphisms at the dominant *Vrn-A1* locus (Yan et al., 2004). The promoter region of *Vrn-A1a* is duplicated. In addition, *Vrn-A1a* contains two insertions of 222bp and 131 bp within the promoter region. *Vrn-A1b* exhibits two mutations in the insertion sites of *Vrn-A1a* besides the deletion of 20-bp in the 5′ untranslated region. *Vrn-A1c* differentiates from other alleles by a large deletion in intron 1. At the *Vrn-B1* locus, the dominant allele *Vrn-B1a* is a result of a 440-bp deletion in Intron 1 compared to the recessive winter allele *vrn-B1*. Further deletion of 36bp led to emerging the *Vrn-B1b* allele (Santra et al., 2009). *Vrn-D1a* is characterized by a deletion in intron 1 at the *Vrn-D1*. A further SNP in the CArG box gives rise to another spring allele *Vrn-D1b* (Zhang et al., 2012). Mutations in A-genome confer the greatest effect in reducing vernalization requirement compared to B- and D-genomes (Trevaskis et al., 2003). The first intron of *VRN1* bears the binding site for wheat glycine-rich RNA-binding protein 2 (*TaGRP2*), which represses *VRN1* expression in absence of low temperature. Deletions in the first intron include the *TaGRP2*-binding sites, and this loss is associated with a moderate need for vernalization (Kippes et al., 2018; Shujuan Xu et al., 2019). *VRN1* encodes a conserved 60 amino-acid fragment belonging to MADS-box transcription factor *MIKC-type* protein, which is highly identical to *Arabidopsis* meristem identity protein *APETALA1 (AP1)* (Kippes et al., 2015; Yan et al., 2003). Before vernalization, modification in chromatin methylation and histone activity at the promoter and first intron of *VRN1* lead to its repression until it is released by low temperature (Oliver et al., 2009). *VRN1* is initially transcribed at very low levels and increased gradually during prolonged vernalization (Murai et al., 2003). The accumulation of *VRN1* transcripts in the shoot apex induces the switch to the reproductive

phase, while increasing *VRN* transcription levels in leaves mediate the flowering under long-day conditions after winter.

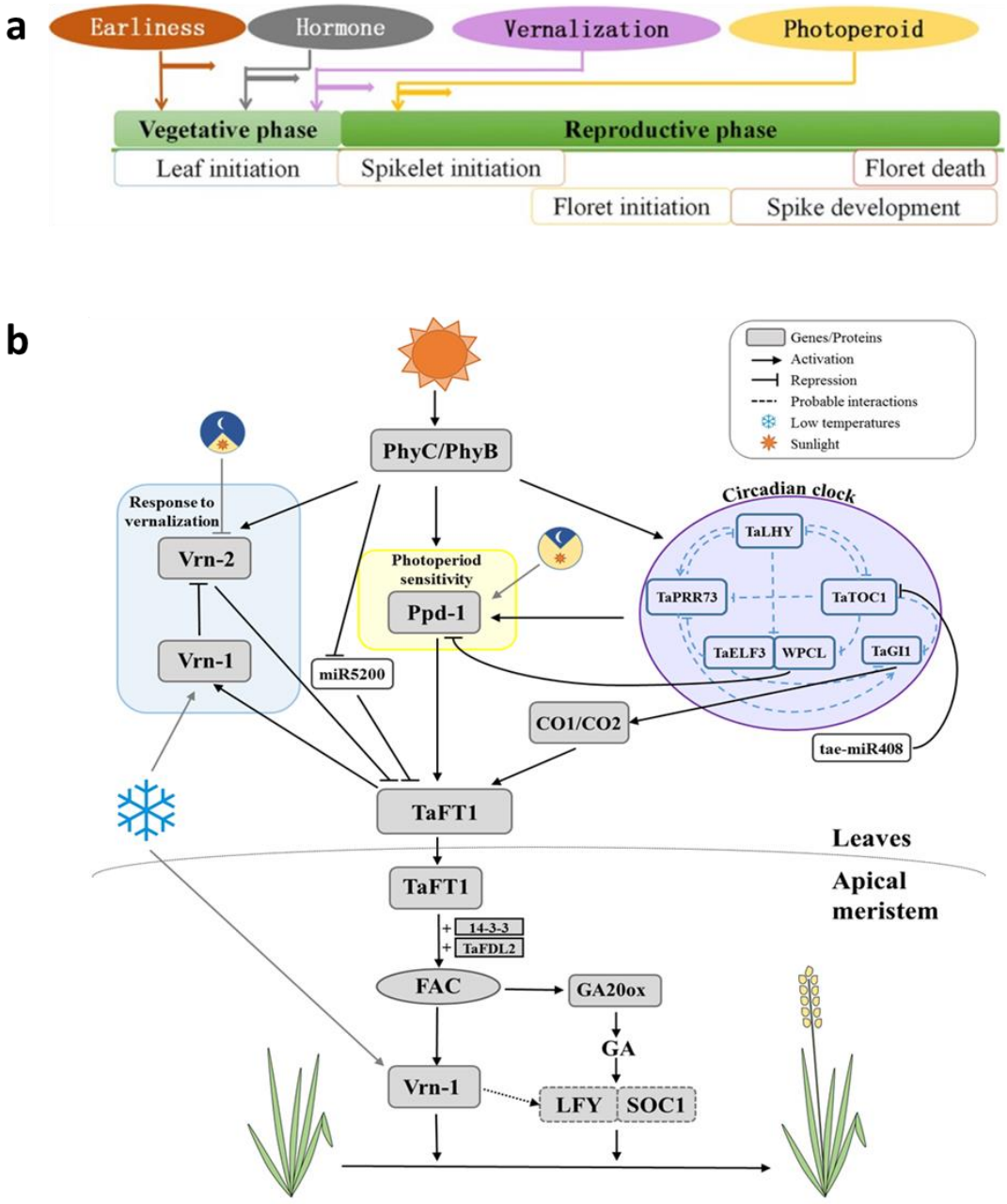

Figure 1. 4: Major flowering pathways during development of bread wheat.

a. Major flowering pathways during development of bread wheat (*Triticum aestivum* L.) (Shi et al., 2019). b. Schematic summary of the wheat heading stage regulatory network (Kiseleva & Salina, 2018)

1.5.1.2 Vernalization gene VRN2

Vrn-B2 and *Vrn-D2* series genes of *VRN2* are located on chromosomes 4B and 4D (Tan & Yan, 2016), while *Vrn-A2* is mapped on chromosome 5A (Dubcovsky et al., 1998). *VRN2* gene codes for two similar *zinc finger-CCT* domain transcription factors (Yan et al., 2004). The *CCT* domain is a conserved 43-

amino acid segment that is referred to the proteins *CONSTANS (CO), CONSTANS-like (COL),* and *TIMING OF CAB1 (TOC1)* that were described first in *Arabidopsis* (Putterill et al., 1995; Robson et al., 2001; Strayer et al., 2000). *CCT* domain is involved in the regulation of light signaling, circadian rhythms, and photoperiod pathway (Wenkel et al., 2006). The recessive *vrn2* is characterized by loss of function necessarily in all copies of *ZCCT* genes in A, B, and D genomes, caused by missense mutations within the *CCT* domain (non-functional *ZCCT* genes) (Distelfeld et al., 2009) or deletion of the complete *CCT* genes (null *ZCCT* genes) (Zhu et al., 2011). Thus, dominant *Vrn2* contains at least one single functional allele, which is sufficient to confer some vernalization requirements. *VRN2* is a flowering repressor with no orthologs in rice or *Arabidopsis,* and it seems that this gene is a flowering-specific regulatory element, developed by the genomes of grass species during their evolution (Liuling Yan et al., 2004). During and after vernalization, RNA level of *VRN2* are significantly reduced by the up-regulated *VRN1* (Yan et al., 2004; Chen & Dubcovsky, 2012; Deng et al., 2015). A part of *VRN2* regulation is achieved through photoperiod and ambient temperature under long days (Dubcovsky et al., 2006).

1.5.1.3 Vernalization gene VRN3

VRN3 (known as *VRN-B3*) encodes an *RAF* kinase inhibitor–like protein that promotes flowering time in wheat and shows high similarity to *FLOWERING LOCUS T (FT)* in *Arabidopsis* (Yan et al., 2006). Natural mutations for *VRN3* have been found only in the B genome (Yan et al., 2006). *VRN3* expression is induced under long days, which leads to suggest that *VRN3* acts as a bridge integrating vernalization and photoperiod signals. Introgression of a *VRN3* allele with an inserted transposable element in the promoter into winter wheat lines results in increased *VRN1* expression and consequently early flowering. This confirms the effect of *VRN3* in positive regulation of *VRN1* and overcomes the vernalization requirement (Li & Dubcovsky, 2008). Additionally, *VRN3* may be suppressed by the repressor *VRN2*. Low *VRN3* transcript levels were observed in wheat lines overexpressing *VRN2* (Hemming et al., 2008).

1.5.1.4 Vernalization gene VRN4

Finally, the gene *VRN4* mapped on chromosome 5D, derived from translocation of the region that includes *VRN1* from the long arm of chromosome 5A into the short arm of chromosome 5D (Kippes et al., 2014). *VRN4* exists only in D-genome, thus known as *VRN-D4*. Likewise *VRN1*, the paralog *VRN4* encodes a protein very similar to *(AP1) in Arabidopsis. VRN1* is considered duplicated in the wheat genome. Therefore, the copy *VRN1* at the *VRN-D4* locus carries a deletion of the *TaGRP2* binding site (described above) leading potentially to an increase in *VRN1* transcripts levels in wheat lines containing *VRN-D4* (Kippes et al., 2015).

For recapitulating the vernalization response in wheat, vernalization-mediated activation of *VRN1* expression downregulates *VRN2*. Increasing *VRN3* induced by long days contributes to the up-regulation of *VRN1* expression in leaves, which creates a positive feedback loop, when is active it induces an

irreversibly flowering process (Distelfeld et al., 2009; Shimada et al., 2009; Yan et al., 2006). *VRN-D4* is believed to act upstream of this feedback loop (Kippes et al., 2015).

1.5.2 Genetic regulation of photoperiod response

Wheat is a photoperiod sensitive crop, flowering after accumulation of critical daylength has been satisfied. The regulation of photoperiodic flowering is largely determined by *PHOTOPERIOD1 (PPD1)* gene (Figure 1.4.b) with three homoeologous alleles *Ppd-A1*, *Ppd-B1*, *Ppd-D1* mapped in collinear positions on chromosomes 2A, 2B and 2D, respectively (Law et al., 1978; Welsh, 1973). *PPD1* is a member of the *pseudo response regulator (PRR)* family and is also known as *PRR37* (Mizuno & Nakamichi, 2005). *PPD1*conatins a *CCT* domain, which relates this gene to the circadian clock. The expression of the wild-type allele of *Ppd-D1b* follows a rhythmic diurnal oscillation, reaches its peak in the middle of the day, and shows daylength sensitivity, where flowering is promoted under long days (Díaz et al., 2012; Shaw et al., 2012). Deletion of 2089-bp in the promoter region of wild type gives arise to *Ppd-D1a*, the major source of insensitivity to photoperiod that can induce early emergence of ear and accelerates flowering independently of daylength, compared to the sensitive allele *Ppd-D1b* (González et al., 2005; Grogan et al., 2016; Worland et al., 1988). *Ppd-D1a* causes upregulation of the floral activator *VRN3* which leads to insensitivity to photoperiod and enhances flowering time (Beales et al., 2007). The *Ppd-D1a* allele is widely distributed in Eastern and Southern European and Eurasian varieties. It was introduced at the beginning of the twentieth century from Japanese germplasm to provide adaptation to a broad range of environments with high summer temperature, thus escaping the heat and drought period and avoiding consequential damages in the early growth stages (Bentley et al., 2013; Rajaram & Ginkel, 2001). The insensitive alleles of the homoeologous *Ppd-A1a* and *Ppd-B1a* are promising a similarly strong effect on accelerating flowering time as *Ppd-D1a* in the Japanese background (Nishida et al., 2013). The crucial role of *PPD1* is derived from the crosstalk between photoreceptors and circadian clock-regulated genes in the coordination of the day-length response (Mizuno & Nakamichi, 2005).

1.5.2.1 Circadian clock

The circadian clock is the intrinsic mechanism used by plants as a timekeeper to synchronize internal biological processes with the periodic oscillation of light and temperature between day and night (Dodd et al., 2005). In daylength response, the circadian clock regulates photosynthesis, metabolism, and the response to biotic and abiotic stress to maintain synchrony between internal processes and signal changes due to external modification caused by day/night rhythm over 24 hours approximately (Harmer, 2009). The circadian clock has been studied intensively in *Arabidopsis*. This mechanism and its components seem to be conserved in cereals. The clock comprises negative feedback loops that result in rhythmic waves or oscillations of gene expression through the day-night cycle (Hsu & Harmer, 2014). Key genes related to the circadian clock are maintained by a three-loop repressors model as follows:

C*IRCADIAN CLOCK ASSOCIATED 1* (*CCA1*) and *LATE ELONGATED HYPOCOTYL* (*LHY*) are expressed in the morning, reach peak transcript levels at dawn, then they are downregulated gradually during the day by the *PSEUDO RESPONSE REGULATORS* (*PRRs*), *PRR5, PRR7, PRR9, TIMING OF CAB EXPRESSION 1* (*TOC1 / PRR1*) that are in turn repressed by the evening complex (EC) composed of *ARRHYTHMO/PHYTOCLOCK (LUX/PCL), EARLY FLOWERING 3 (ELF3)* and *EARLY FLOWERING 4 (ELF4)* (Nusinow et al., 2011). *CCA1* and *LHY* close the loop by suppressing the evening complex genes the next morning (Covington & Harmer, 2007; Hazen et al., 2005; Pokhilko et al., 2012; Schaffer et al., 1998; Somers et al., 2004). Other components are integral to maintaining the circadian rhythm such as *GIGANTEA (GI)* (Park et al., 1999). In *Arabidopsis*, the circadian clock regulates the photoperiodic flowering through a light-sensitive zinc-finger transcription factor *CONSTANS (CO)* (Putterill et al., 1995), which triggers *FT* induction under long days conditions (Kobayashi et al., 1999). Once activated, *FT* is transcribed in leaves and migrates through the phloem to reach the shoot apex where it provokes the transition from vegetative to reproductive phase (Corbesier et al., 2007; Jaeger & Wigge, 2007; Turck et al., 2008). *TaHD1* is the ortholog of *CO* in the wheat genome. Likewise *CO, TaHD1* expression profile is strong in the day and low at the night, which hints more that daylength sensing is regulated similarly in cereals as in *Arabidopsis* (Beales et al., 2007).

1.5.2.2 Response to light

Light signal components are involved in the Posttranslational regulation of *CO* protein (Valverde et al., 2004). Far-red and blue-light signals control *CO* stability during the day, while red light signals destabilize it (Möglich et al., 2010). Flowering plants use photoreceptors including phytochromes to perceive light signals (Lin, 2000). Phytochromes contain three clades of genes designed as *PHYTOCHROME A (PHYA), PHYTOCHROME B (PHYB),* and *PHYTOCHROME C (PHYC)* (Mathews, 2010). Monocotyledon species comprise only one single copy of each *PHYTOCHROME* gene, whereas the duplication event leads to emerging *PHYD* and *PHYE* genes derived from *PHYB* in dicotyledon lineage (Li et al., 2015). *PHYA* is required for photomorphogenesis establishment in seedlings and regulates the response to de-etiolation and low light (Casal et al., 2014). *PHYB* is involved in the shade-avoidance regulation under low ratios of the red light to the far-red light (Franklin & Quail, 2010). *PHYC* plays a minor role in the photomorphogenesis in *Arabidopsis* and rice, where the activation of *PHYC* is depending on *PHYA* and *PHYB* functionality (Takano et al., 2005). By contrast, *PHYC* in wheat acts independently of the other photoreceptors (Monte et al., 2003). *PHYC* is a primary element for the light activation of the *PPD1* and *FT* and accelerates flowering over long days. A flowering delay of up to 100 days was observed in the *phyC*-null mutant of wheat compared to the control (Chen et al., 2014). The *phyC*-null mutants exhibit accentuated flowering postponement than the *ppd1*-null or *ft1*-null mutants (Chen et al., 2014; Lv et al., 2014; Shaw et al., 2013). This leads to suggest that *PHYC* regulates very likely other floral pathways in addition to *PPD1-FT* activation (Chen et al., 2014; Pearce et al., 2016).

1.5.3 Earliness *per se*

(Eps) or Intrinsic Earliness (IE) (also named narrow-sense earliness) is referred to as the remaining earliness inducing variation in heading and flowering time when the vernalization requirements and the photoperiodic sensitivity are fulfilled (Worland, 1996; Yasuda & Shimoyama, 1965). The genetic effect of *Eps* loci is relatively small and is more contributing to fine-tuning for environment adaptation (Appendino et al., 2003; Zikhali et al., 2014). The *Eps* genes are believed to be involved in various growth phases mainly stem elongation, heading, and spike development that determines grain yield components (Griffiths et al., 2009; Lewis et al., 2008). Allelic variation in *Eps* genes was found associated with HD alterations ranging from a few days to a few weeks (Appendino et al., 2003; Zikhali et al., 2014). No *Eps* genes have been cloned in wheat so far. Leastways, near-isogenic lines (NILs), were used to map approximately some *Eps* loci in the wheat genome and potential candidate genes orthologous of *Eps* in *Arabidopsis*. The few known cereal *Eps* genes are related to the components of the circadian clock. Two main *Eps* genes have been fine-mapped in the diploid wheat on chromosomes 1A and 3A, respectively (Faricelli et al., 2010; Gawroński & Schnurbusch, 2012). The *Eps-3A*^{m} gene of *Triticum monococcum* is an ortholog of the *LUX/PCL* gene in *Arabidopsis* (Gawroński & Schnurbusch, 2012), while *Eps* locus, *Eps-A1*^{m} shows a deletion in the loci of the wheat *ELF3* gene (Zikhali et al., 2014). It was thought that *Eps* is an autonomous pathway that is not controlled by environmental cues (Slafer, 1996), but, there are some insights relating the earliness effect to sensitivity to temperature (Snape et al., 2001). In this sense, Ochagavía et al., (2019) reported that the effect of *Eps* genes increases when the temperature decreases. The late reproductive phase in the flowering process is mostly affected by the interaction *Eps* ^{x} temperature during heading according to the same study (Ochagavía et al., 2019). The expression of the *ELF3* gene, which is proposed to underly the *Eps-A1*^{m} locus, is changing with the daily temperature variation (Ford et al., 2016; Salomé & McClung, 2005). Finally, how *Eps* regulates the heading stage remains poorly understood in comparison to vernalization and photoperiod mechanisms.

1.5.4 Phytohormones

The plant hormones are other important factors, which influence the flowering time in wheat. The role of phytohormones in controlling flowering time is extensively investigated in *Arabidopsis* through the exogenous application to mimic the natural influence of endogenous hormones (Davis, 2009). Since a long time ago, it is known that Gibberellin acid (GA) induces flowering and bolting, and this function is conserved in the vernalized grasses (Lang, 1957; MacMillan et al., 2005). For common wheat, GA accelerates flowering for winter and spring types under long days (Evans et al., 1995; Razumov, 1960). However, under short days, GA can promote spike development only in wheat lines expressing *VRN1* (Pearce et al., 2013). In the model proposed by Pearce et al. (2013), the activated gene *VRN3 (FT)* under long days moves from leaves to apical meristem where it upregulates *VRN1* and GA biosynthetic gene *GA20ox,* both prerequisites for regulating *SOC1* and *LFY* that trigger the spike development. Cytokinin

(CK) is secreted in massive concentration in the apical meristem of many plants during the flowering transition (Corbesier et al., 2003). The dynamic of CK is essential in the regulation of meristematic activity and inflorescence branching in plants (Wang et al., 2018). Cytokinin oxidase/dehydrogenase (*CKX)* are major enzymes that strongly regulate CK content in plants (Werner et al., 2006). In total, 11 to 14 gene family members have been identified in bread wheat (Ogonowska et al., 2019; Shoaib et al., 2019). The gene *OsCKX9* in rice is strongly expressed in the heading stage (Duan et al., 2019), but no ortholog in wheat with a similar function is identified so far. However, a previous study showed that CK promotes the flowering of *Arabidopsis* via transcriptional activation of *TWIN SISTER OF FT (TSF)* (D'Aloia et al., 2011). Abscisic acid (ABA) exhibits antagonistic effects to CK on flowering time in *Arabidopsis*. On one hand, ABA genes *ABI4* and *ABI5* promote directly the transcription of *FLC*, a repressor of *flowering time locus T (FT*), and negatively control Gibberellin biogenesis that initiates flowering as well, thus flowering is postponed (Shu et al., 2016; Wang et al., 2013). On the other hand, under drought stress, the elevated ABA level induces *miRNA172* expression, and subsequently, *miRNA172* suppresses its target flowering repressors such as *WRKY44* and *TARGET OF EAT1 (TOE1)*; this stimulates early flowering and the plant escapes the drought stress (Han et al., 2013; Li et al., 2016). In cereals, a recent study in barley (*Hordeum vulgare* L.) highlights the implication of photoperiod gene *Ppd-H1* in drought response orchestrated by ABA signaling (Gol et al., 2021). Another endogenous hormone that delay flowering is the Jasmonate acid (JA). JA forms a complex with *ZIM* domain JAZ that interact with *TOE1* and *TOE2* to inactivate *FT* (Zhai et al., 2015). In the opposite, Salicylic acid (SA) promotes the floral transition. This mechanism is poorly understood, but it seems that SA involves the photoperiod and autonomous pathways to regulate flowering (Martínez et al., 2004). Finally, auxin related genes play primordial roles in flowering, as auxin accumulation in the periphery of the shoot apical meristem specifies the site of leaf or floral primordium initiation. Auxin regulates floral organ initiation, growth, patterning and ensures the reproductive success of the mature flower (Krizek, 2011). After this outline of the role of the most important phytohormones in the flowering time pathway, several phytohormones biosynthesizes remain less uncovered in cereals in general and in wheat specifically.

1.6 Grain yield improvement in the light of flowering time regulation

Producing higher-yielding varieties with a great genetic fitness to adapt to different environments is the ultimate goal of plant breeding. Flowering time is a key factor that permits the plants to adjust their growth to a given milieu and climate. The timely occurrence of flowering as well as the duration of spike development starting from the heading stage to the end of anthesis are determinant factors for grain yield (Reynolds et al., 2012; Slafer et al., 2001). Many regulatory elements of flowering time have an extended pleiotropic impact on yield components. The indirect contribution of vernalization genes to yield potential has been already mentioned (Iqbal et al., 2007). High yielding was reported to be associated with the presence of at least two dominant *VRN1* spring loci in specific alleles combination in the Canadian wheat germplasm (Randhawa et al., 2014). For winter wheat, an approach adopted in

the arid and semi-arid areas such as Iran showed that decreasing the vernalization requirement could increase the yield (Shourbalal et al., 2019). This approach is based on shortening the exposure time to cold and promoting flowering by spraying plant growth regulators, which resulted in optimum yield potential. *PPD-D1* gene is not only a major regulator of photoperiod sensitivity in wheat, but it is also a control element in inflorescence architecture and paired spikelet development (Boden et al., 2015). For this gene also, spring genotypes carrying the insensitive allele *Ppd-D1a*, produce larger grains and harvest higher yields in southern Europe (Worland et al., 1998). The *reduced height-1* (*Rht1*) gene, responsible for the semi-dwarf phenotype and reduced plant height in wheat is the iconic symbol of the green revolution (Borlaug, 1983). This gene shows an important pleiotropic effect on the ears development and the increasing number of grains in the spikes (Börner et al., 1993). *Rht1* is insensitive to GA, and thus, it regulates indirectly flowering time. *Rht1* and *Rht2*, mapped in the small arms of chromosomes 4B and 4D, respectively, are homoeologous loci of the *DELLA* gene, a known repressor of GA that promotes flowering time (Pearce et al., 2011; Peng et al., 1999). Interestingly, another height-reduced gene *Rht12* showed an additive effect in presence of *Ppd-D1a*, which lead to the early flowering and improved yield in the Chinese cultivars containing this allele combination (Chen et al., 2018). Environmental factors such as the ambient temperature can enhance the yield potential. In wheat, *Eps* genes were reported to take part in yield improvement. The previously reviewed *Eps-A1*^{m} and *Eps-3A*^{m} genes participate in determining the number of spikelets and number of grains per spike (Lewis et al., 2008). Considering the *Eps* ^{x} temperature interaction, a more comprehensive understanding is essential to determine which specific sub-phases of heading and flowering processes are more sensitive to temperature, because it is during these pheno-sub-phases that the development of tillers, spikelets and florets, resulting later in yield components, will occur (Slafer, 2003).

1.7 Identification of flowering time genes

Various strategies have been developed to study the genetic architecture of flowering time in wheat. The most-reported approaches used to achieve this goal and have proved their success are summarized and discussed in this section.

1.7.1 Positional cloning

Also known as map-based cloning is a useful method to clone genes of interest. This method of gene identification concerns more the narrowing down the chromosomal location of a gene related to a specific phenotype or disease (Wallace et al., 1990). The practical use of this strategy in crops is described as follows (Review by Li et al., (2020)): First, molecular markers, residing in the vicinity of the locus of interest, are identified and used to create the mapping for biparental populations. Making use of genetic recombination, a few hundred plants are generated, and genotyped for allelic segregation. The genetic map is produced by integrating phenotypic and molecular marker data. Then, yeast artificial (YAC) or bacterial artificial (BAC) chromosome libraries for overlapping clones containing an insertion

of the target gene are screened using other closest markers flanking the locus, which generate a contig map. Chromosome walking is applied to piece the sequenced segments together into a physical map and thus, the approximate position and the sequence of the target gene are identified (Keller et al., 2005; Lukowitz et al., 2000; Staskawicz et al., 1995). The molecular markers: restriction fragment length polymorphism (RFLP) were widely used in this technique for mapping many genes in *Arabidopsis* (Chang et al., 1988; Nam et al., 1989) and some disease resistance genes in tomato (*Solanum lycopersicum* L.*)*, rice (*Oryza sativa* L.), maize (*Zea mays* L.), and wheat (Feuillet et al., 2003; Johal & Briggs, 1992; Martin et al., 1993; Song et al., 1995). For flowering time, map-based cloning was successfully exploited to identify the major vernalization genes *VRN1* in diploid wheat, *VRN2, VRN3,* and *VRN4* in hexaploid wheat (Kippes et al., 2015; Yan et al., 2006; Yan et al., 2003, 2004) as well the photoperiod gene *Ppd-H1* in barley (Turner et al., 2005). Notably, positional cloning does not prerequire a prior knowledge of the function of the gene or mutation in question.

1.7.2 Candidate gene approach

Identifying genes underlying complex agronomic traits in many crops is achieved through candidate gene association studies that have been proven to be successful in many instances in plants (González-Martínez et al., 2007), cultivated crops (Tabor et al., 2002; Wilson et al., 2004), and human diseases (Ueda et al., 2003; Vaisse et al., 2000). For a given trait, the candidate gene approach focuses on the relationship between genetic variation within a previously known gene of interest and the observed phenotype and consequently enables to conduct a genetic association study for this trait (Kwon & Goate, 2000; Zhu & Zhao, 2007). This strategy requires a *priori* knowledge of the biological function and pathway of the selected genes. The hypothesis behind it is that specific allelic polymorphisms in certain genomic regions result in a change in gene function and lead to phenotype alteration (Kwon & Goate, 2000; Zhu & Zhao, 2007). Practically, candidate genes provided from the forward genetic approaches were further used in many candidate gene researches to dissect genetic pathways underlying agronomically significant traits (Ehrenreich et al., 2007). In this context, flowering time, due to its complexity, was a suitable and attractive trait for the candidate gene approach in several model and crop species, including wheat (Bentley et al., 2013; Eagles et al., 2009, 2010; Ehrenreich et al., 2009; Rousset et al., 2011). Using this strategy in a collection of wheat germplasm with worldwide geographical origins, Rousset et al., (2011) demonstrated that a high proportion of growth habit variation was associated with allelic variation at the *VRN-1* locus, specifically, in the promoter region and coding sequence of *Vrn-A1* and the intron 1 of *Vrn-B1* and *Vrn-D1*. While Bentley et al., (2013) showed that photoperiod insensitive alleles *Ppd-A1a* and *Ppd-D1a* have comparable early flowering effect, which is stronger than the effect of their homolog *Ppd-B1a* by running candidate gene approach in a BC_2F_4 British lines.

1.7.3 Genetic mapping

Genetic mapping aims to identify the loci responsible for the natural phenotypic variation of a quantitative trait within a population. Initially, a quantitative trait is a phenotypic feature controlled by one or many genes (mono or polygenic), and this characteristic is varying and quantitative (Falconer, 1996; Kearsey, 1998; Lynch & Walsh, 1998). From here comes the definition of QTL (Quantitative Trait Locus), which is a genomic region that associates and correlates with the variations of a quantitative trait of the phenotype (Geldermann, 1975). Two approaches: linkage mapping and association mapping are successfully used for unlocking the genetic architecture of complex traits in several crop species. The specificity of each method and the fundamental differences between them are reviewed and summarized in the coming section.

1.7.3.1 Linkage mapping

Linkage mapping, called also family-based mapping is when QTL mapping is conducted in progenies of biparental or multiparent crossings (Kearsey & Farquhar, 1998; Xu, 1998). Linkage mapping requires the construction of a population that segregates for the trait of interest, which may be F_2 generation, backcrosses (BC), doubled haploids (DH), recombinant inbred lines (RIL), or near-isogenic lines (NIL) (Morrell et al., 2012). Each population presents strengths and weaknesses concerning the construction, estimation of QTL dominant effect, number of recombination, and time requirement (Reviewed by Xu et al., 2017). Generally, steps of linkage mapping include the collection of parental lines showing contrasting phenotypes for the studied trait (1), genotyping the parental lines for detecting the genetic polymorphism that distinguishes them by using molecular markers such as amplified fragment length polymorphism (AFLP), restriction fragment length polymorphism (RFLP), simple sequence repeat (SSR), diversity arrays technology (DArT) or single nucleotide polymorphism (SNP) (2), construction of mapping population as cited above (3), genotyping and phenotyping the mapping population for the trait (4) then identifying marker-trait associations or QTL using an adequate statistical model (Reviewed by Xu et al., 2017). Linkage mapping has the disadvantages of low allele richness and a limited number of recombination events, which generates low-resolution mappings and inheritance of larger linkage blocks providing high linkage disequilibrium (LD) (Asins, 2002; Bernardo, 2002; Doerge, 2002). LD is referred to the non-random association of alleles at different loci (Slatkin, 2008). Additionally, the magnitude of phenotypic variation of the two parental strains may not necessarily or always represents the highest genetic diversity in the species. This small genetic variation plus the fact that only two alleles segregate at any locus limit the number of captured QTL. To overcome partially the limitation of biparental population, mapping populations deriving from inter-crossing multiple parents were designed and implemented in linkage mapping, hence the emergence of nested association mapping (NAM) and multiparent advanced generation intercrosses (MAGIC) (Reviewed by Scott et al., 2020). Different designed biparental populations were developed in the European wheat for identifying flowering time QTL in linkage mapping such as BC_2F_4 population (Bentley et al., 2013), DH population (Griffiths et

al., 2009), and F_2 of recombinant substitution lines (Pánková et al., 2008). Four-parent and eight-parent MAGIC populations were developed in wheat for linkage mapping QTL underlying height and hectoliter weight traits (Huang et al., 2012) and presence/absence of awn trait (Mackay et al., 2014), respectively. Some flowering time QTL could be mapped using eight-parent MAGIC populations for linkage QTL mapping in wheat (Camargo et al., 2016) and (Afsharyan et al., 2020; Sannemann et al., 2015) and a NAM population in maize (Buckler et al., 2009).

1.7.3.2 Association mapping

Association mapping, known as natural population-based mapping, consists of the collection of lines without existing kinship and containing a potential genetic diversity due to greater allele numbers deriving from natural recombination events that occurred over hundreds of years for mapping QTL of target traits. In other words, the key distinction to linkage mapping is that in association mapping the meiotic cycles happened in genetically independent individuals/lines of a population, not in the family (Pritchard et al., 2000; Risch & Merikangas, 1996). Advanced statistical models, precision phenotyping, and high-throughput genotyping are tools that together fully exploit the potentialities of association mapping populations for a global QTL mapping of complex quantitative traits over the entire genome of species. This broad investigation is called genome-wide association study (GWAS) (Tanksley & Nelson, 1996; Visscher et al., 2012). By incorporating distantly related and heterogeneous lines, the level of genetic relatedness should be estimated by calculating LD. Thence, the historical meiotic events, accumulated through hundreds of generations with the historical LD, are conserved in the selected lines, and this leads to a rapid decay of LD, which improves the resolution of the map (Rafalski, 2010). Performing a GWAS necessitates firstly the collection of diverse genetic material, which can be elite cultivars, landraces, wild relatives, and exotic accessions (1), phenotyping the trait and estimating broad-sense heritability (2) genotyping the collected germplasm (3), estimation of LD extent of the population (4), define the population structure and the derived clusters (5) and calculation of phenotype-genotype associations using a suitable statistical model (6) (Reviewed by Alqudah et al., 2020). A part of GWAS robustness is indebted to the immense genotyping upswing. The massive advances in the last years in sequencing technologies made DNA sequencing information very abundant and more available. The high throughput of next-generation sequencing (e.g.) genotyping-by-sequencing (GBS) provides thousands of SNPs in a time and cost-efficient manner with improved genome coverage (Bevan & Uauy, 2013; Elshire et al., 2011; He et al., 2014; Poland et al., 2012). GWAS for flowering time QTL using GBS were reported by many studies in wheat (Kobayashi et al., 2016; Langer et al., 2014; Rahimi et al., 2019), maize (Larsson et al., 2013), and *Brachypodium distachyon* (Wilson et al., 2019). GWAS owes much also to array-based genotyping platforms. A series of high-density SNP arrays were developed and utilized in wheat like Illumina 9K iSelect (Cavanagh et al., 2013), 90K iSelect (Wang et al., 2014), 15K SNP array (Boeven et al., 2016), Axiom Exome Capture 660K (Cui et al., 2017), Axiom Exome Capture 820K (Winfield et al., 2016), Wheat Breeders' 35K Axiom array (Allen et al., 2017) and 135K

Axiom Exome Capture Array (Voss-Fels et al., 2019). Numerous QTL for heading date in wheat were identified using SNPs chip in GWAS (Benaouda et al., under review; Gizaw et al., 2018; Reif et al., 2011; Zanke et al., 2014; Zhang et al., 2018). Association mapping and linkage mapping differ in the power and resolution in detecting and mapping QTL, but they are still two complementary approaches, when combined together, they overcome each other's limitations (Brachi et al., 2010).

7.3.3 Major limitations of GWAS

The complexity of the target trait creates two scenarios: either the trait is underpinned by few loci with large effect size (rare variants of large effect), or the trait is controlled by many loci with small effect size (common variants of small effect) (Reviewed by Korte & Farlow, 2013). A concrete example of that: a single locus can explain up to 86% of the flowering time variation in the interspecific Sorghum (*Sorghum bicolor* L.) population (Lin et al., 1995), while 50 % of the variation in the kernel oil concentration in maize represents the total effect of 50 QTL (Laurie et al., 2004). Detecting or missing the true causative variants (rare or common) is the challenge that faces the dissection of genetic architecture for many complex traits. Using GWAS for this goal, many factors can limit its potential to provide true results and detect accurate associations. These factors are discussed as follows:

- ✓ Phenotypic variation

Analyzing the phenotypic variation is highly recommended because of the outliers that should be removed from the phenotypic data; otherwise, they can affect the normal distribution of data. Nevertheless, taking out the outliers should not influence the phenotypic variation accounted as a basic agent in the association analysis. Broad-sense heritability is to be estimated after filtration of phenotypic data. Heritability indicates the proportion of the phenotypic variation that can be explained by the genetic variance (Wray & Visscher, 2008). Hence, traits with very low heritability are not recommended for GWAS. Replacing row phenotypic values by best linear unbiased predictor (BLUP) or best linear unbiased estimator (BLUE) (Piepho et al., 2008) will generate adjusted phenotypic data by minimizing the environmental effect and consequently increase the broad-sense heritability.

- ✓ Population size

The sample size is a critical variable in GWAS that reflects the variation of the phenotypes and genotypes. A large number of individuals improve the power for uncovering meaningful associations. Selecting geographically distant accessions will certainly heighten the genetic variance but may also increase the genetic heterogeneity, which leads possibly to the detection of non-causative loci and missing the major ones. To find a balance between the effect size and the genetic diversity, it is proposed to include a major locus with a competing effect as a cofactor within the statistical model (Segura et al., 2012). This gives chance to loci with small effects to be unscrambled. Practical use of this approach for flowering time in wheat is reported by Langer et al., (2014). Going for low heterogeneity by picking out locally adapted and phenotypically diverse individuals in large number will not avoid the drawback of

decreasing allele frequency of relevant variants relative to the global phenotypic diversity in the trait (Platt et al., 2010).

- ✓ Population structure

It is a confounding variable aiming to characterize the structural diversity and calculate the kinship correlations among individuals within the population since not all accessions have genetically the same degree of distant relatedness to each other. This is to be taken into account due to different backgrounds of individuals (geography, growth habit, etc…), and many markers correlate strongly with ecotypic differentiation, the fact that generates clusters or subpopulations (Cardon & Palmer, 2003). Disregarding this parameter can result in false positives. With help of specific programs, population structure can be corrected either by treating the population membership as a covariate with a fixed effect or unmeasured (structured association) (Pritchard et al., 2000) or by analyzing the genotypic data using principal component analysis that considers linear combinations to reduce the number of dimensions that explain as much the genetic variation (Price et al., 2006). Both approaches are widely applied and get at correcting single-SNP association tests for the population structure. The statistical modeling and computation of these methods are reviewed by Wu et al., (2011).

- ✓ Allele frequency

Another constraint factor for GWAS is the detection of functional alleles that are present at low frequency. Alleles should exist at a minimum frequency of 5 %. Otherwise, with minor allele frequency (MAF) less than 0.05, rare alleles are hardly detected even when they have an enormous effect on phenotype. Several studies have shown that rare alleles could explain a large proportion of natural variation for many traits. Unfortunately, the domestication bottleneck in many crops has affected clearly the allele frequency by favoring the selection of frequent common alleles related to benefic traits and discriminating the rare ones. Furthermore, allele frequency can be skewed through the careful selection of individuals for a specific phenotype for traits that depend strongly on selection. Therefore, an association panel based on a more assorted selection of accession including diverse germplasms such as landrace, wild relatives exotic and adapted genetic materials when genotyped with high throughput genotyping technology can raise the frequency of the less representative alleles due to the increased SNP number and consequently, rare alleles can be detected via GWAS (Reviewed by Soto-Cerda & Cloutier, 2012).

- ✓ Linkage disequilibrium (LD)

LD is the culprit responsible for retaining both causative and non-causative alleles until advanced analysis steps in GWAS and leads to spurious QTLs if the non-random associations between two markers/alleles at different loci are underestimated (Reviewed by Alqudah et al., 2020). The tighter the linkage between two markers is, the stronger the LD. Hence, resolution mapping is a function of the rate at which LD decays over genetic or physical distance (Gupta et al., 2005). a large number of markers

lead to LD declines rapidly, which improves the resolution mapping (Reviewed by Myles et al., 2009). Therefore, the calculation of LD as the first step in GWAS will indicate if the utilized genotyping tool (GBS, SNP arrays, etc…) was suitable for constructing a high dense map considering the size of the genome. The factors influencing LD such as recombination and mutation rates, mating system, genetic diversity, population size and population structure, genetic drift, and selection, in addition to the statistics used to estimate LD are reviewed by many authors, I cite as examples Semagn et al., (2010) and Soto-Cerda & Cloutier, (2012).

1.7.3.4 Statistical analysis in genetic mapping

Choosing a compatible statistical model is a critical factor that can accurately detect true biological associations and reduce as much the false positives. For linkage mapping, three known approaches are widely used: (i) Single-marker analysis that identifies QTL by calculating the difference between the average phenotypes of all genotypes without including the linkage information (Broman et al., 2003). (ii) Interval Mapping (IM) is based on incorporating the maximum likelihood in estimating the position of one QTL between two flanking markers (Lander & Botstein, 1989). The multiple regression method was introduced later to IM (Haley & Knott, 1992). IM supposes that only one locus is controlling a quantitative trait and thus, analyses one interval at a time, whence the possible biased localization of other QTLs. (iii) Composite interval mapping (CIM) integrates IM and the multiple-marker regression analysis that verifies the effect of loci from other regions on the tested QTL (Zeng, 1993).

Statistical approaches used in the association mapping fall into two categories: Single-locus and multiple-locus models. In the single locus approach, a one-dimensional genome scan is based on testing one marker at a time and iteratively for every marker. The most popular deriving models from this approach are: (i) General linear model (GLM) corrects only false positives resulting from the population structure (Bradbury et al., 2007), (ii) mixed linear model (MLM) corrects both population structure and kinship (Yu et al., 2006), (iii) compressed MLM is decreasing the effect of sample size by clustering individuals into groups based on kinship (Zhang et al., 2010). The single-locus method examines each locus separately, which is not adequate for complex traits controlled by many loci simultaneously (Wang et al., 2016). To cope with this problem, the multilocus approach has been recommended. It is based on a forward selection of all potentially associated SNPs, which are later inserted into iterative cycles of the multilocus QTL model (Bauer et al., 2009; Kilpikari & Sillanpää, 2003). Some examples of multi-locus-based models utilized in different crops are described in Kaler et al., (2020) and Li et al., (2018).

Finally, an overcorrection or overfitting of the model can lead to false negatives. Multiple comparisons are conducted to check the statistical significance using commonly Bonferroni correction (Holm, 1979) and false discovery rate (FDR) (Benjamini & Hochberg, 1995) for fixing a threshold of significance. Overly conservative thresholds may cause the missing of potentially important associations (Liu et al., 2016).

1.8. Epistasis

Bateson, (1909), was the first to use the term epistasis to describe a qualitative "masking" effect whereby the expression of an allele on one locus is blocked by another locus. Later, Fisher, (1919), defined "quantitative epistasis". Since that time, different meanings of epistasis emerged in various subdisciplines of biology. One of many definitions of epistasis reported by Phillips, (2008), and commonly used in evolutionary and quantitative genetics is referred to as the dependence of phenotypic effect variation of an allele at a given locus on the allelic combination in other loci. Epistatic interactions have been studied in various traits and many taxa (Carlborg et al., 2003; Huang et al., 2012; Kelly & Mojica, 2011; Moore, 2003). The contribution of quantitative epistasis in genetic variance has been shown in *Arabidopsis* (Kusterer et al., 2007; Malmberg et al., 2005), maize (Lamkey et al., 1995; Lukens & Doebley, 1999), rice (Li et al., 2008; Shen et al., 2014), in cotton (*Gossypium arboretum* L.) (Lee et al., 1968), and wheat (Crossa et al., 2010; Jiang et al., 2017).

Understanding the genetic architecture of a quantitative trait requires more knowledge about the extent and nature (synergetic or antagonistic) of the epistatic interaction between loci controlling this trait (Mackay, 2001; Phillips et al., 2000). To measure epistatic effects, one experimental approach is to use a mutation in a specific allele as a starting point and measure its effect in interaction with other mutations in the genetic background (Malmberg et al., 2005). This approach was used for example to uncover epistatic interactions for flowering time in *Arabidopsis* by examining the effect of the null mutant at *Frigida* locus on other flowering time genes such as the *FLC* gene (Koornneef et al., 1994; Michaels & Amasino, 1999; Schläppi, 2001). The second approach is mapping QTL epistasis. Several methods have been proposed to get this target. These methods are either based on a one-dimensional genome scan that considers a simple case in which the trait is controlled by a simple locus (Jannink & Jansen, 2001) or simultaneous mapping of epistatic QTL using multi-dimensional genome scan for simultaneous multiple interactions (Carlborg et al., 2000). As for the QTL multilocus approach, the same method can be extended by including all possible pairwise interactions to estimate the two-way epistatic effects of QTL (Kärkkäinen et al., 2015; Li & Sillanpää, 2012; Xu, 2007). The multilocus approach was applied for identifying epistatic interactions regulating flowering time in wheat (Benaouda et al., under review; Langer et al., 2014), barley (Afsharyan et al., 2020; Mathew et al., 2018), maize (Buckler et al., 2009; Durand et al., 2012), and rice (Ahsan et al., 2019; Liu et al., 2021).

The difficulty in running epistatic analysis is mainly due to the multiple testing for pairwise epistasis. To tackle this problem, GWAS can be used first to identify loci with significant additive effects, then perform pairwise tests only for the selected variants (Carlson et al., 2004). Another alternative is to relax the multiple test correction threshold (Benjamini & Hochberg, 1995).

1.9 Transcriptomic: RNA-Sequencing

The transcriptome encompasses all classes of RNA molecules and their quantity, expressed in a specific organ (cell, tissue, or whole genome) in a particular developmental stage or physiological condition (Piétu et al., 1999; Velculescu et al., 1997). Transcriptomics aims to inventory all transcripts including messenger RNAs, non-coding RNAs, small interfering RNAs, transferase RNAs, and micro-RNAs, determine the transcriptional structure of genes (sequence, splicing pattern, and posttranscriptional modifications) and quantify the expression level and kinetic of transcripts in time and organ-specific manner (Wang et al., 2009). Various technologies have been developed to explore the transcriptome such as tiling microarray (hybridization-based approach) (Bertone et al., 2004), cDNA or expressed sequence tag (EST) sequencing (Gerhard et al., 2004), and RNA-Seq (high throughput sequencing-based approach). This later offers clear advantages and efficacy over other approaches regarding the range to quantify gene expression level (>8000 fold), required amount of RNA (low), resolution (high), and cost for mapping transcriptomes of large genomes (favorable costs) (Wang et al., 2009). RNA-seq revolutionized how gene structure and expression (identify and quantify transcribed sequences) are analyzed. Making use of short-read sequencing technologies such as the Roche 454, SOLiD, and Solexa/Illumina platforms, it becomes more feasible to perform *de novo* transcriptome sequencing (Li et al., 2010; Mortazavi et al., 2008; Nagalakshmi et al., 2008; Wilhelm et al., 2008).

By far, the most widespread usage of RNA-seq in crops is detecting the differentially expressed genes (DEGs) associated with contrasting phenotypes for a trait in two or a group of selected individuals. Constantly improving algorithms and advancing bioinformatics tools are called to address this issue (Anders et al., 2013; Law et al., 2014; Robinson et al., 2010; Soneson & Delorenzi, 2013; Wang et al., 2010). In short, RNA-seq analysis consists of several common steps: (i) Quality control of RNA-seq data, (ii) trimming by elimination of the adapter sequences and the removal of poor-quality nucleotides to increase reads mapping rate, (iii) alignment of the mapped reads to a reference genome or transcriptome, (iv) normalization procedure to remove probable sequencing bias and finally (v) detect (DEGs) between two or more conditions (Reviewed by Corchete et al., 2020). As the number of options available at each step is increasing, the complexity of RNA-seq lies with choosing between many possible algorithms and tools in each step and combining them in form of the best or most accurate workflow to pass from the RNA-seq reads to the differential gene expression. Consequently, there is no favorable consensus including appropriate pipelines to analyze RNA-seq data. Validating the gene expression via qRT-PCR decides about the degree of reliability of the chosen workflow (Consortium, 2014).

RNA-seq served to investigate the genetic shape of flowering time in many crops under abiotic stresses such as drought stress in maize (Kim et al., 2021; Song et al., 2017), heat stress in *Arabidopsis* and soybean (Blair et al., 2019; Xu et al., 2019), frost stress in wheat (Song et al., 2017) as well in biotic stress resistance in various plant species (Fabian et al., 2021; Liu et al., 2011; Lyons et al., 2015).

Chapter 2: Hypothesizes and objectives

2.1. Background and overview of the research

The chronology and progress of publications about flowering time using the European adapted wheat are following the betterment and advances in genotyping, sequencing, statistical models, and bioinformatic arsenal that together radically transformed how several polygenic agronomical traits are explored. In addition, the researchers exploited diverse sources of phenotypic variation in hexaploid wheat like advanced backcrossing population (Bentley et al., 2013), biparental DH populations (Griffiths et al., 2009; Zikhali et al., 2017), F_2 of recombinant substitution lines (Pánková et al., 2008) and NILs (Zikhali et al., 2014). By far, three studies made use of association panels from central Europe including elite cultivars mostly developed in France and Germany (Reif et al., 2011; Zanke et al., 2014), or in border European countries (Langer et al., 2014). Reif et al., (2011) used 115 SSR markers, while Zanke et al., (2014) merged 770 SSR and 7934 SNP markers deriving from 90K iSelect illumina chip for genotyping. GBS resulting in 23,371 SNP markers was reported by Langer et al., (2014). Comparing the results of these studies are included in chapter 5. Flowering time is highly dependent on the environment. This factor was not deeply analyzed by the previous publications that aimed to identify the genetic shape of flowering time in the European wheat. Thence, exploring QTL through environment interactions will enrich our knowledge about the regulatory elements that adjust the flowering time in the adapted material. Furthermore, epistatic interactions are a considerable source of variation. Reif et al., (2011) and Langer et al., (2014) reported divergent results despite that they used the same material. This fact deserves to be analyzed one more time. The mechanistic basis of flowering time in wheat gained more attention in recent years, but still very few publications about it could be found in the literature (Pearce et al., 2016; Li et al., 2018; Yang et al., 2021). The molecular regulation of a such complex trait is studied in specific experimental conditions that lead to specific responses. To uncover the mechanisms that control the time to heading in the studied adapted material, a transcriptome profiling was conducted. This study is the first one for flowering time using European germplasm.

The present Ph.D. research was conducted in the framework of a project funded by the German Research Foundation (DFG). The project is a part of a priority program in which 17 institutions from all over Germany were involved. This research should investigate the environmental effect on the genetic and molecular architecture underlying flowering time regulation in winter wheat. To achieve this goal, we performed combined environmental, genetic, and molecular experiments to dissect the causes leading to variations in the heading time. An association panel was chosen to display a high genetic diversity and represented the breeding history of the last 60 years of wheat. For that, we selected locations with variations in the environmental factors and repeated the experiments for three years, coming to 17 environments. Both these prerequisites are essential to perform the envisaged study. Further, this population was deeply genotyped using the most updated SNP technology. For the data analysis, we used partially in-house developed algorithms to perform the genotype-environment interaction analysis.

To the best of our knowledge, this is the first comprehensive analysis of heading time under so many various environments using a unique and well genetically characterized wheat germplasm.

2.2 Hypothesizes and objectives

Based on this background the following research questions were put forward:

- Is there any genotype by environment interaction for flowering time in wheat and how does the genetic control occur?
- What are the mechanistic bases of the transition to flowering?

The following hypothesizes were elaborated for building the bases of the scientific work:

1. After vernalization, the time of flowering induction is depending on location and year;
2. The genetic response to climatic stimuli is mastered by a spatial factor;
3. Flowering time regulation involves, besides the known regulators, digenic interactions and allelic variation at so far uncovered loci/genes;
4. The floral switch is regulated in a stage-organ-specific manner.
5. The uncovered loci harbor stage and tissue-specific genes responsible for heading variation.

The main objective of this thesis is to identify novel QTL harboring genes that operate in flowering-regulation in interaction with the environment for understanding the mechanisms of the genetic architecture underlying flowering time in wheat.

The workflow of the research leans on three approaches:

A. Analysis of the genetic response to local and seasonal interplays of environmental factors and its effect on flowering time variation;

B. Search for stable genetic factors and fine tuners controlling flowering time in response to latitude dependent drivers;

C. Comparative transcriptome analysis at the transition time in combination with genetic mapping

A couple of steps were elaborated to reach the goals of each approach:

A.1 Assessment of the environmental impact on heading date variation;
A.2 Comparison of the induced genetic responses in the German geographical context;
B.1 Determination of the growth habits of the used germplasm;
B.2 Identification of loci associated with heading trait in interaction with the environment;
B.3 Analysis of epistasis and its involvement in flowering time control;
C.1 Evaluation of flowering behaviors in different conditions;
C.2 Exploration of the responses revealed by the gene expression analysis;
C.3 Integration of the genetic and molecular outcomes.

Chapter 3: Flowering time control in interaction with the environment

3.1 Introduction

HD, representing the initiation of flowering time, is one of the most targeted and extensively studied traits in breeding programs designed to improve yield stability under various climatic conditions. The Plant capable to adapt to extreme climates can avoid inappropriate stress factors such as frost, heat, and drought by adjusting its flowering time to seasonal conditions to protect the floral organs (Fjellheim et al., 2014). Such an adaptive mechanism of controlling the timing of starting the transition from vegetative to reproductive phase is a useful tool for selecting cultivars that match different environments and geographical regions and even to adapt regional cultivars to coming climate change scenarios (Guedira et al., 2016).

Wheat is a leading food grain crop and a staple source of nutrients for around 40% of the world's population (FAO, 2019). The adaptability of wheat to wide climatic regimes derived from large natural variations, which has been favored by allelic diversity in genes regulating growth and developmental stages including the flowering time pathway (Worland, 2001). Three distinct pathways interact to control flowering time in wheat: vernalization, photoperiod, and earliness *per se* (Distelfeld et al., 2009; Herndl et al., 2008; Kamran et al., 2014; Snape et al., 2001). The group of four vernalization *(VRN)* genes regulates the molecular mechanisms for the requirement of vernalization and exposure to cold in wheat (Allard et al., 2012; Distelfeld et al., 2009; Trevaskis et al., 2007). *VRN1* and its paralog *VRN-D4* encode *a MADS*-box gene with high similarity to *Arabidopsis* meristem identity protein *APETALA1 (AP1)* (Kippes et al., 2015; Yan et al., 2003). *VRN2* locus includes two tandemly duplicated genes *ZCCT1* and *ZCCT2* (Yan et al., 2004). These genes encode proteins carrying a putative zinc finger and a *CCT* domain referred to as *CONSTANS (CO), CONSTANS-like (COL),* and *TIMING OF CAB1 (TOC1*) (Putterill et al., 1995; Robson et al., 2001; Strayer et al., 2000). *VRN3* is a homolog of the Arabidopsis photoperiod gene *FLOWERING LOCUS T* (Yan et al., 2006). Natural allelic variation in one or many of *VRN* genes leads to the differentiation between winter and spring growth habits. Hexaploid wheat bearing a dominant allele at *VRN1* or *VRN3* loci requires less cold treatment to flower (spring habit), while the presence of recessive alleles at both loci increases the demand for vernalization (winter habit) (Turner et al., 2013). Dominant and recessive alleles at the *VRN2* locus act adversely (Yan et al., 2004). Winter bread wheat is a long day plant and a photoperiod sensitive crop that flowers after accumulation of a critical day length (Fjellheim et al., 2014). The day length responsive gene, *Ppd-D1*, is an ortholog of *pseudo-response regulator (PRR)* of Arabidopsis in wheat (Beales et al., 2007; Turner et al., 2005). The semi-dominant deletion of 2,089 bp upstream from the coding region in the allele *Ppd-D1a* causes insensitivity to photoperiod and accelerates flowering time (Beales et al., 2007; Shaw et al., 2012). Earliness *per se (Eps)* is referred to the remaining earliness of flowering time when vernalization requirements and photoperiodic sensitivity are fulfilled (Worland, 1996; Yasuda & Shimoyama, 1965). Numerous strategies have been adopted to decipher the genetic control of flowering time in wheat such as the candidate gene approach (Bentley et al., 2013; Eagles et al., 2009, 2010; Rousset et al., 2011), and the meta-QTL analysis, which includes individual and separate QTL studies, was used firstly in

maize and was conducted in wheat as well using either biparental populations or collections of association panels (Bentley et al., 2013; Griffiths et al., 2009; Hanocq et al., 2007; Kamran, Iqbal, et al., 2014; Reif et al., 2011). Additionally, facilities gained via high-throughput genotyping and sequencing technologies besides the development of powerful statistical tools based on linkage disequilibrium (LD) could be exploited in genome-wide scans (Flint-Garcia et al., 2005; Frazer et al., 2007; Jander et al., 2002; Kang et al., 2008; Pletcher et al., 2004). Identification of genetic and molecular interactions improved the understanding of the mechanisms underlying complex traits (Patrick C Phillips, 2008b). The epistasis is referring to an interaction between a pair of loci in a dependent manner making that the resulting phenotype of one locus is conditioned by the genotype at the second locus (Carlborg & Haley, 2004). Therefore, many genome-wide scan studies used epistatic analysis as a complementary approach to discover more genomic regions associated with intricate traits in different crops including maize, wheat, and rapeseed (Buckler et al., 2009; Liu et al., 2012; Steinhoff et al., 2012; Würschum et al., 2013).

In Europe, most of the reported studies on flowering time in the field use 1st January or sowing day as the date for starting the scoring until the anthesis stage. Both dates are including the vernalization period, where the winter wheat is facing low temperature (frost and even snow cover), and consequently, HD is delayed for protecting the shoot meristems to be damaged until the environmental conditions become favorable (Law & Worland, 1997). Thermal time or growing degree day (GDD) estimated by different statistical models is the variable mostly used for predicting the timing in days for the transition from one phenological stage to the next (Eagles et al. 2010; Rousset et al. 2011; Allard et al. 2012; Cane et al. 2013).

Given this background, this study aimed to dissect the genetic regulation of flowering time and the detection of novel QTL and epistatic interactions underlying HD in winter wheat in different environments across Germany. The particular goals of the current study were (1) to accurately assess the seasonal depending interaction of flowering time with the environmental stimuli in a geographical context; (2) to investigate the implication of *VRN* and *PPD* genes in flowering time control; (3) to provide insights into stable and fine-tuning genetic factors controlling HD, (4) and to evaluate the contribution of epistasis in the genetic architecture of the flowering time.

3.2 Material and Methods

3.2.1 Plant material

We used a collection set made of 213 elite bread wheat cultivars released between 1966 and 2016 (Voss-Fels et al., 2019). The set was containing 162 cultivars from Germany (winter type that needs vernalization and requires long days to start flowering), 34 from other Western European countries, and 17 exotic cultivars from Mexico, India, USA, Australia, Moldava, and Chile (winter and facultative types). We used two subsets for GWAS. Subset1 refers to the 162 wheat cultivars developed and adapted in Germany. Subset2 is grouping all the 213 wheat cultivars.

3.2.2 Experimental set-up

The experiments were conducted in three consecutive years from 2015 to 2017 at six locations across Germany following a gradient latitude: Moosburg an der Isar 48°28′ N/11°56′E (Loc1), Klein-Altendorf 50°37'N /6°59´E (Loc2), Rauischholzhausen 50°46'N/8°53'E (Loc3), Quedlinburg 51°47'N/11°09'E (Loc4), Hannover 52°22'N/9°44'E (Loc5) and Kiel 54°19'N/10°08'E (Loc6). In total 17 environments were included in the study (Loc3 was analyzed only in 2015 and 2016).

3.2.3 Scoring of heading date and measurements of environmental factors

HD was recorded according to two reference dates: the first one (HD_winter), as the number of days from January 1st until the day when 75% of the ears of an observation plot are visible according to stage BBCH58 (Biologische Bundesanstalt, Bundessortenamt und Chemische Industrie) (Meier, 1997). The second one (HD_spring) was recorded from the first day where GDD kept being positive for at least five consecutive days until the day of reaching the BBCH58 stage (day/date of heading) in each environment as shown in Figure 3. 1a. The accumulated GDD is calculated using the Peterson equation (Peterson, 1965): GDD = $\sum_{i=1}^{n}\left\{\left(\frac{Tmax+Tmin}{2}\right)-Tb\right\}$, where n = the number of days taken for the completion of a particular growth phase. The basic threshold temperature used for wheat is (Tb) = 4.0°C (Cao & Moss, 1989). The spring reference date is used to calculate the real number of days needed to complete the phenological stage heading based on positive accumulated GDD after winter (Figure 3. 1a). By adopting this approach, we observed that the first day from which GDD keeps being positive corresponds to different dates in each location*year (Figure 3. 1b). We calculated the cold period (winter) from 1st January until the day in which GDD started to be irreversibly positive. We observed that the cold period varied from year to year within the same location and between locations in the same year (Figure 3. 1c). When the cold period is short, this signifies that heading was early induced. Consequently, we reason it makes sense to fix a spring reference date for each environment instead of one arbitrary date for all environments. The cold period will not be included in spring reference date because it is not synchronizing with heading initiation. The measurements of the environmental stimuli were recorded beginning from both reference dates until the day of heading. The daily measurements of temperatures, global solar radiation and precipitations were obtained from local weather stations placed directly at the experimental field in each location (Appendix 3. 6). For temperature, the maximal (Tmax) and minimal (Tmin) values were calculated from reference date until the day of heading for a given cultivar. For the other factors, the accumulated values of daily measurements starting from the reference date until the day of heading were used. Daylength, including civil twilight (h), was computed daily following Forsythe et al., (1995).

Field trials were conducted in plots of sizes between 4.5 and 12 m^2. The experimental sites had diverse soil characteristics and the sowing density was 330 viable seeds per m^2 in two replicates (See supplementary Table 3 in Voss-Fels et al., 2019).

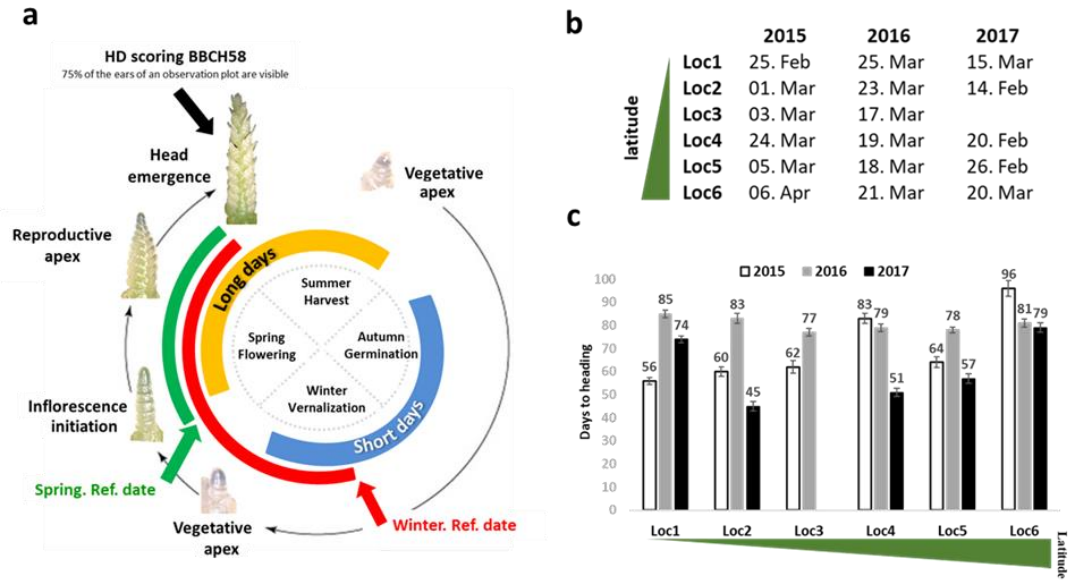

Figure 3. 1: HD scoring based on winter and spring reference dates

a. Schema showing the seasonal control of heading in temperate wheat (winter type). After sowing in autumn, the plant vernalizes and the vegetative apex is growing slowly over winter and short days. Flowering time is delayed to protect the floral organ to be damaged because of cold (frost). When the days lengthen in spring, the vegetative apex transits into the reproductive apex, which indicates the inflorescence initiation as a response to favorite conditions of ambient temperature and long days. b. Reference dates corresponding to the first day from which growing degree day (GDD) kept being positive until the day of reaching the heading stage BBCH58 in each location ^{x} year. Abbreviations: Feb: February, Mar: March, Apr: April. c. The cold periods (in days) calculated from 1st January until the first day from which growing degree day kept being positive until the day of reaching the heading stage BBCH58 in each location ^{x} year.

3.2.4 Allelic variation analysis of flowering time known genes

All cultivars were screened for known vernalization (*VNR1, VRN2, and VRN3*) and photoperiod genes (*Ppd1*). The genotyping included the recessive and dominant alleles of *VRN-A1*(*vrn-A1*, *Vrn-A1a*, *Vrn-A1b*, *Vrn-A1c)* (Yan et al., 2004), *VRN-B1 (vrn-B1*, *Vrn-B1)* (Chu et al., 2011), *VRN-D1 (vrn-D1*, *Vrn-D1a*, *Vrn-D1b)* (Fu et al., 2005), null alleles *ZCCT-A1*, *ZCCT-B1* and *ZCCT-D1* (X. Zhu et al., 2011) and functional alleles *ZCCT-A2*, *ZCCT-B2* and *ZCCT-D2* of *VRN2* (Distelfeld et al., 2009; Kippes et al., 2016), *VRN3 (vrn-B3*, *Vrn-B3a*, *Vrn-B3b*, *Vrn-B3c)* (Chen et al., 2013), photoperiod-insensitive alleles *Ppd-A1a*, *Ppd-B1a*, *Ppd-D1a and* sensitive alleles *Ppd-A1b*, *Ppd-B1b* and *Ppd-D1b* of *Ppd1* (Beales et al., 2007; Nishida et al., 2013). The primers and the protocols used to amplify the target fragments are summarized in Appendix 3. 7. DNA extraction was conducted following the protocol of DNAeasy Plant Mini Kit (Qiagen, Hilden, Germany). The polymerase chain reactions (PCR) were performed in a 25 µL reaction volume containing 100 ng of genomic DNA, 1×Taq DNA polymerase

reaction buffer, 10 µM of forward and reverse primers, 0.2 mM of dNTP, and 0.5 unit of Taq DNA polymerase (NEB, Frankfurt, Germany). The PCRs were conducted in the thermocycler Flex cycler (Analytik GmbH, Jena, Germany). PCR profiles were visualized by electrophoresis on a 1% agarose gel stained with peqGreen (0.04 µl/mL; VWR, Darmstadt, Germany).

3.2.5 Phenotypic data analysis

Analysis of variance (ANOVA) was performed adopting the general linear model (Gilmour et al., 1995) in Proc Mixed procedure in SAS 9.4 (SAS Institute, 2015). Variance components of genotypes (G), locations (L), years (Y) as well as their interactions (G ^{x} Y), (G ^{x} L), and (G ^{x} L ^{x} Y) were determined by the restricted maximum likelihood (REML) method assuming a random model in SAS 9.4. Broad-sense heritability (H^2) estimation was calculated following the method described by Holland et al. (2003): $H^2 = \frac{V_G}{V_G + \frac{V_{G*E}}{E} + \frac{V_E}{E}}$ where V_G: genetic variance, V_{G*E}: variance of genotype × environment, E: environment, V_E: variance of error term. Principal component analysis (PCA) was run using the function prcomp built-in R. Calculation of Pearson coefficients of the correlation and the partial correlation was performed in R using "cor" and "pcor" functions (Kim, 2015).

3.2.6 QTL mapping

The diversity panel was genotyped using the map of 24,216 informative SNP markers based on the Infinium iSelect 15K chip and the 135K Axiom Exome Capture Arrays (Dadshani et al., 2021). Principal component analysis was performed by using the prcomp core function in R (Team, 2013). Marker-based identical-by-state (IBS) kinship matrix was calculated with the "A.mat" function of the R package rrBLUP (Endelman, 2011)**,** and the Pair-wise measures of linkage disequilibrium (LD) between two SNP with the package PLINK version 1.9 (Chang et al., 2015). For QTL mapping a multiple QTL model using the PROC MIXED procedure in SAS 9.4 was utilized. Iteratively, the forward selection and backward elimination approach described in (Bauer et al., 2009) were used to reduce the number of false-positives and endorse the true QTL. Threshold of *P*-value ≤0.001 and false discovery rate (FDR) was set at 5% for the iterative multi-locus approach in the QTL model (Kilpikari & Sillanpää, 2003). QTL with a LOD ($-\log_{10}(p)$) score higher than six were identified as QTL and reported here Further increase of accuracy for detection of true QTL was achieved by the implementation of 10-fold cross-validation procedure with 20% leave out. QTL analysis was conducted following the linear model: $Y_{ik} = \mu + M_i + E_{k+} M_i * E_k + \varepsilon_{ijk}$, where Y_{ik} is the vector of phenotypic values, µ: general mean, M_i: the fixed effect of i-th marker; E_k: the fixed effect of k-th environment (location-by-year), $M_i * E_k$: the fixed interaction effect of i-th marker with the k-th environment, and ε_{ijk}: the residual. The genetic variance explained by a single SNP marker (P^G) was calculated as follows: $P^G = SQ_M/SQ_g$, where SQ_M is the sum of squares of $_{i\_th}$ marker and SQ_g was calculated as the type I sum of squares (Type I SS) of the genotype in the ANOVA model. The total proportion of the genotypic variance P_G for each marker was calculated by including all markers with QTL effect in the ANOVA model.

3.2.7 Epistatic interactions

In PROC MIXED procedure in SAS 9.4, the two-way multilocus approach was used for epistatic interactions involving the environment factor in the following model: $Y_{ijk}=\mu+M_{1i}+M_{2j}+M_{1i}\times M_{2j}+ E_k +M_{1i}\times M_{2j}\times E_k +\varepsilon_{ijk}$, where Y_{ijk}: the vector of phenotypic values; μ: general mean; M_{1i}: the fixed effect of $_{i\text{-th}}$ marker1, M_{2j}: the fixed effect of $_{j\text{-th}}$ marker2, $M_{1i}\times M_{2j}$: the fixed interaction effect of $_{i\text{-th}}$ marker1 with $_{j\text{-th}}$ marker2, E_k : fixed effect of $_{k\text{-th}}$ environment (location ^{x} year), $M_{1i}\times M_{2j}\times E_k$: fixed interaction of the $_{i\text{-th}}$ marker1 with the $_{j\text{-th}}$ marker2 genotype and $_{k\text{-th}}$ environment; ε_{ijk}: the residual. Thresholds of *P*-value ≤0.001 and FDR < 5% were implemented in the model for more accuracy in detecting true epistatic interactions. The proportion of the genotypic variance explained by every single epistatic interaction was estimated in the same way as the genetic variance for a single SNP marker.

3.2.8 *In silico* analysis

The known vernalization *VRN* and photoperiod *PPD* genes were mapped physically on the wheat genome sequence ((Zhu et al., 2021), https://urgi.versailles.inrae.fr/download/iwgsc/IWGSC_RefSeq_Assemblies/v2.1/) using the following approach: the core sequence information of markers was blasted against the genome sequence draft (Appendix 3. 8). Further, the genes included in the flanking regions were downloaded and their annotations were checked using the last updated version of the gene annotation from the International Wheat Genome Sequencing Consortium and EnsemblPlants platforms. The start position of each gene was extracted from blasting outputs and was exploited later in the QTL and epistatic analyses. For some reported SSR markers only the primer sequences were available in the Grain Genes database (wheat.pw.usda.gov). In this case, the sequence of the primers was blasted to find the corresponding physical positions, and the same steps were followed for blasting using the IWGSC RefSeq v1.1 gene annotation platform.

3.3 Results

3.3.1 Phenotypic assessment of heading date-by-environment

To characterize the phenotypic performance, the genotypes of subset1 and subset2 were tested in six different locations for three years. The mean HD_winter across all environments ranged from 148.9 and 143 to 159.3 for subset1 (10.4 days) and subset2 (16.2 days), respectively (Table 3. 1). The variance components of genotype and interactions genotype-by-year, genotype-by-location, and genotype-by-location-by-year are increased in subset2 compared with subset 1. The Student's *t*-test showed a highly significant difference ($p \leq 0.01$) between HD scorings of subset1 and subset 2 (Appendix 3. 9). The heritability estimation was high by 0.89 for adapted cultivars and 0.96 by including the exotic ones. The exotic cultivars originating from Australia, Mexico, Serbia, Moldova, and the USA were found in the

early flowering group (Figure 3. 2). Cultivars from France are the earliest flowering ones in the European germplasm. All latest flowering cultivars originate from Germany.

Table 3. 1: Summary statistics for heading date for subset1 and 2

	Subset1	Subset2
Max	159.32	159.32
Min	148.93	143.07
Mean	154.13	151.2
SD	6.03	6.36
CV	3.93	4.18
σ^2_G	1.13***	2.54***
$\sigma^2_{G \times Y}$	2.14***	3.04***
$\sigma^2_{G \times L}$	4.99***	6.87***
$\sigma^2_{G \times L \times Y}$	11.94***	14.37***
σ^2_{error}	2.52	2.51
H^2	0.89	0.96

Abbreviations: Standard deviation SD. Coefficient of variation CV (in percentage). Variance components for genotypic variance (σ^2_G), genotype-by-year variance ($\sigma^2_{G \times Y}$), genotype-by-location variance ($\sigma^2_{G \times L}$) genotype-by-location-by-year variance ($\sigma^2_{G \times L \times Y}$). *** Significance at <0.001 probability level. Heritability H2

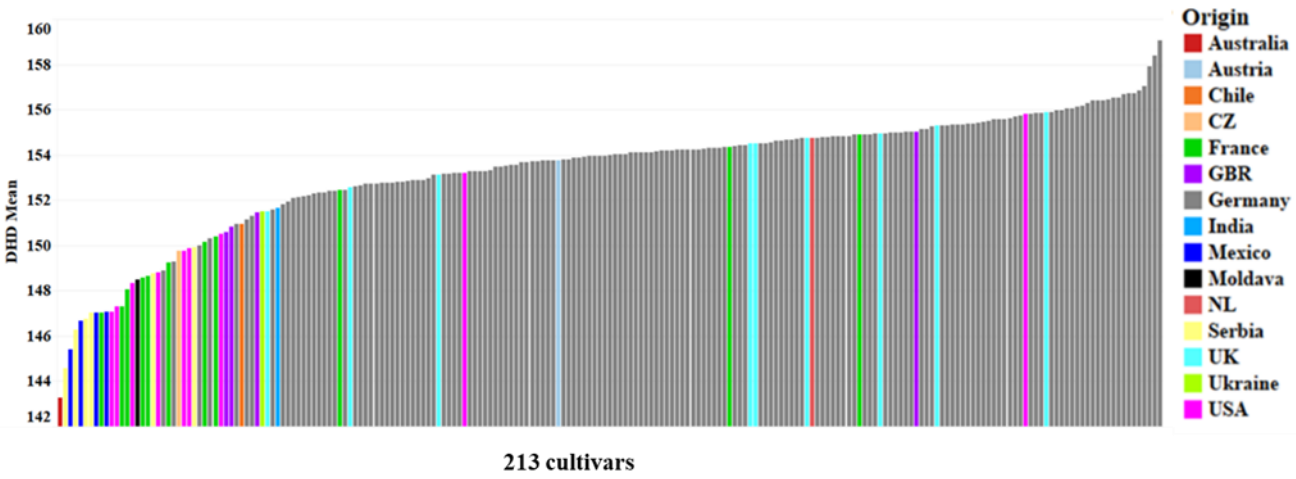

Figure 3. 2: Phenotypic distribution of HD_winter in mean value per country of origin of 213 cultivars of the diversity wheat panel (subset2).

The mean is based on data collected from six locations across Germany and over three years 2015, 2016 and 2017

For a close estimation of the environment effect, HD was evaluated using two reference dates for scoring. HD_winter revealed less distinctness among environments due to overlapping of the scorings in all locations over the three years. An exception is Loc6 (North), where HD was delayed by 14.5 days in 2015 compared to 2016 and 2017. Loc1 (South) recorded an advanced HD by 12.6 days in 2016 compared to other years (Figure 3. 3a). According to HD_spring, an overlapping of HD scorings over years was noticed exclusively in Loc6, while in other locations, two to three distinguishable clusters could be differentiated. In 2016, we observed a reduction of days to heading in Loc1, Loc2, Loc3, and

Loc5 by 54, 59, 68, and 72 days, respectively, except in Loc6 (Figure 3. 3b). PC analysis was conducted to identify the combination of variables that better explained the environmental variability in Germany. The first two axes of the PCA accounted for ca 71% (Figure 3. 3c). Day length, Tmax of spring, Tmin of winter, and global radiation of spring contribute the most by 13.7%, 13.5%, 12.6%, and 11.6%, respectively in explaining the total environment variability (Figure 3. 3d). The genotype effect on HD variation in interaction with environmental factors, selected by PCA, was checked via ANOVA. The location influenced the HD variation due to the genotypic response to Tmax, day length, and global radiation by 53%, 34%, and 13%, respectively. The genetic response to the yearly change of Tmax (Appendix 3. 10) explained 70% of HD variation, while genotypic interactions with daylength and global radiation seem to be stable from year to year and lead to very weak HD alterations. Significant hierarchical clustering (p-value <0.05) uncovers how similar is the flowering behavior between 17 environments based on the genetic response to the fluctuation of the most important climatic factors (based on PCA and ANOVA). Tmax of spring lead to the most similar clustering to the HD pattern given in Figure 3. 3a, compared with other parameters, showing high closeness between low and middle latitude in 2016 (Loc1 and Loc2, r>0.9), as well as in high ones (Loc5 and Loc6, r>0.9). The global radiation of spring revealed a strong cluster grouping over all the years in loc6 as well. HD variation based on winter reference date (Figure 3. 3b) narrows tightly the grouping based on day length, which revealed the dissimilarity of loc1-2016 and loc6-2015 to the other environments (Appendix 3. 2)

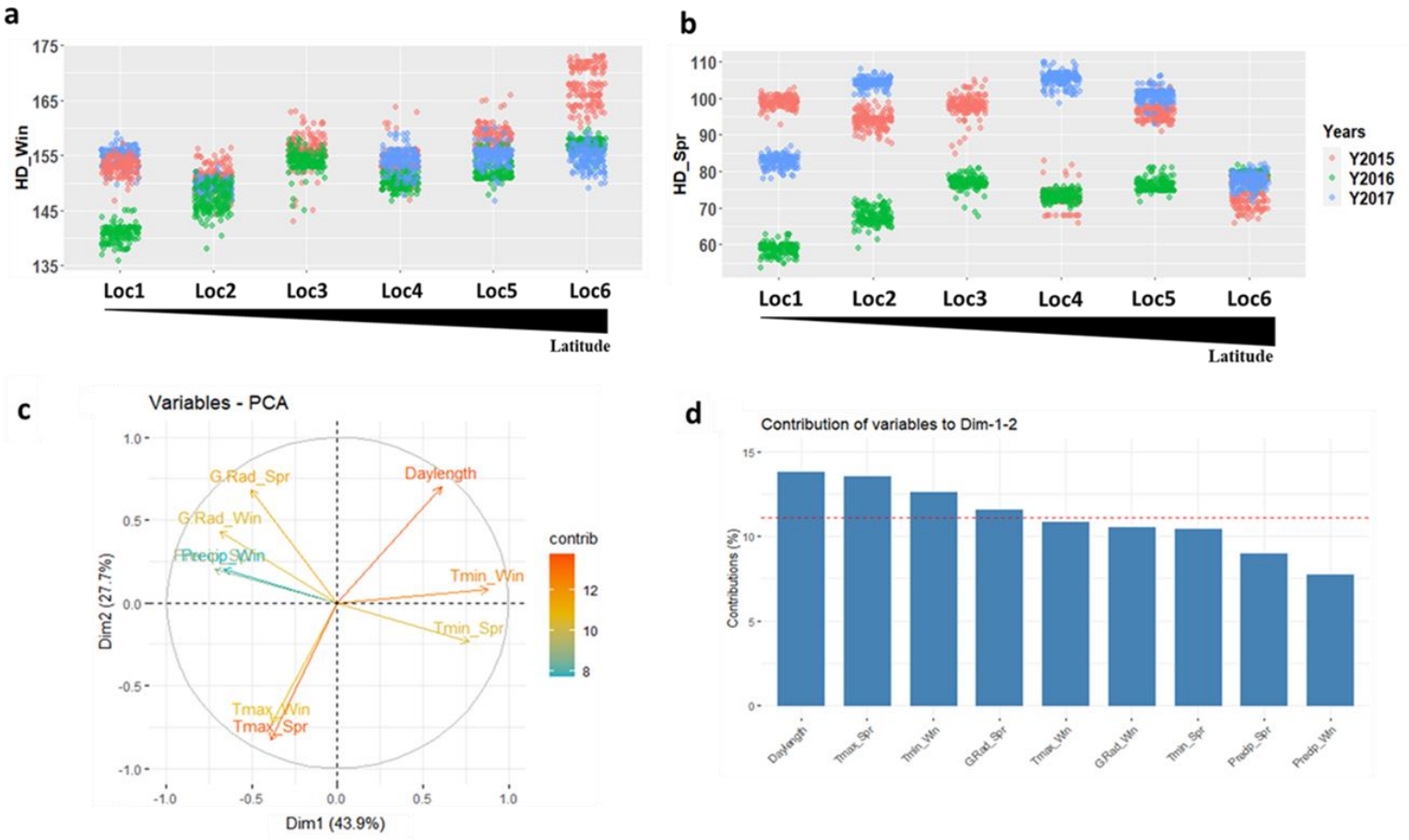

Figure 3. 3: Comparison of HD variation based on winter and spring reference dates of scoring.

Comparison of HD variation based on winter and spring reference dates of scoring. a: for HD_winter and b, for HD_Spring. Locations are denoted on the x-axis, HD scorings are denoted on the y-axis. The colors refer to years. c: Visualization of Principal Component Analysis of the variability among the environmental factors. The contributions of each environmental variable to the principal components Dim1 and Dim2 are indicated by percentage and colors. d) Summary of the contribution of each environmental variable by combining Dim1 and Dim2. The red dashed line indicates the expected average contribution. The environmental factors that are below the red threshold of the expected average contribution are considered less important

3.3.2 Effect of latitude-associated genetic response on HD variation

To identify the environment-associated effect of climatic parameters on HD variation, correlation analysis in each location was performed. For spring measurements, comparing Pearson coefficients of correlation (r) and partial correlation (r´) revealed that Tmax reduced strongly the days to heading from the South (r = -0.99 in Loc1) to the North (r = -0.26 in Loc6) (Appendix 3. 3, Appendix 3. 11)This effect did not change much if the global radiation (r´= -0.83 in Loc1, r´= -0.35 in Loc6) or Tmin (r´= -0.89 in Loc1, r´= -0.20 in Loc6) are considered as constant. The impact of Tmin is following the same trend and showed a high inducing HD effect with r = -0.98 in Loc1, -0.79 in Loc2, -0.81 in Loc3, and 0.04 in Loc6. Similarly, Tmax and the global radiation did not influence the Tmin effect on HD. The global radiation correlates positively with HD in almost all locations, except in the higher latitude, where Tmax minimizes greatly the effect of the global radiation (r = 0.33, r´= 0.85) on HD. Using the winter reference date, all three factors show a moderate partial correlation with each other and HD without a clear tendency to latitude. The correlation between HD and the precipitations goes from strongly positive to strongly negative for both reference dates, with high dependence on all other factors. Focusing on spring records, ANOVA revealed that the genotype response to Tmax change explained HD variation by 98.4% in the South and 10.7% in the North, showing a strong reliance on latitude gradient across locations. The response to day length is highly dependent on latitude as well but follows the opposite trend than Tmax. The interaction genotype-by-day length altered very weekly HD in the South and central regions. From Loc4, the effect of the response to daylength increased to 89% in the North. No significant HD change could be explained by the genotype-by-radiation interaction in all locations (Table 3. 2).

Table 3. 2: ANOVA output

		Loc1 (South)		**Loc2**		**Loc3**		**Loc4**		**Loc5**		**Loc6 (North)**	
Source of variance	**DF**	MQ	**%**	MQ	**%**	MQ	**%**	MQ	**%**	MQ	**%**	MQ	**%**
Genotype*Tmax_Spr	161	788.43	**98.4****	696.98	**85.4****	184.67	**96.4****	546.45	**77.3****	40.35	**10.5****	12.98	**10.7****
Genotype*Daylength	161	9.41	**1.2****	49.41	**6.1****	6.89	**3.6****	159.33	**22.5****	293.34	**76.3****	107.61	**89****
Genotype*G.Rad_Spr	161	3.65	**0.5****	69.31	**8.5****	0.00	**0.00**	1.06	**0.00**	50.54	**0.13****	0.23	**0.00**
Error		0.12		0.13		0.02		0.10		0.33		0.17	

Percentage of the mean of squares extracted from ANOVA for the genotype interaction with environmental variables and heading date in subset1 (adapted germplasm) including six locations following latitude gradient.

Abbreviations: Degree of freedom DF. Mean squares MQ. ** Significance at the 0.01 probability level. Loc: Location. The maximal temperature of spring Tmax_Spr. Global radiation of spring G.Rad_Spr.

3.3.3 Genotyping the population for major flowering time regulatory genes

To identify the growth habit of the cultivars, the genotypes were screened at the known flowering time *VRN* and *PPD* loci (Appendix 3. 12). For subset1, the analysis based on allele-specific primers using PCR revealed the presence of three recessive alleles *vrnA1*, *vrn-B1*, *vrn-D1*, at locus *VRN1* and consequently a recessive *vrn1*. The screening showed the presence of null alleles *ZCCT-A1*, *ZCCT-D1*, and absence of *ZCCT-B1*, as well the existence of the functional alleles *ZCCT-B2*, *ZCCT-D2*, and the missing of *ZCCT-A2* at *VRN2*, which leads to conclude that the German cultivars carry a dominant *Vrn-2*. The spring allele *Vrn-3B*, photoperiod insensitive allele *Ppd-D1a*, and sensitive allele *Ppd-D1b* could be detected too. In total, 95% of the adapted germplasm carries the allelic combination *vrn-1/Vrn-2/Vrn-3Bc/Ppd-D1b* (Figure 3. 4). Except for *Vrn-3Bc* (Appendix 3. 4), which is a spring allele, *vrn-1/Vrn-2/Ppd-D1b* is responsible for the strict winter growth habit of the majority of the German cultivars. Only a minority (5%) harbors the insensitive allele *Ppd-D1a* beside the same *VRN* alleles. For subset2, *VRN-D1/ Ppd-D1* appears to be the allelic pair mostly associated with growth habits for the European cultivars. Referring to the origin of selected cultivars, 88% of those from central Europe follow a winter growth attitude. The facultative behavior related to *Vrn-D1a/ Ppd-D1a* was detected in 9 % of the south-European cultivars (France and Serbia), while 3% of cultivars harbor *Vrn-D1a/ Ppd-D1a* (France). Different *VRN/PPD* allelic associations identified in the non-European wheat collection included mostly spring alleles (*Vrn-A1*, *Vrn-B1*, *Ppd-A1a*, and *Ppd-B1a)*.

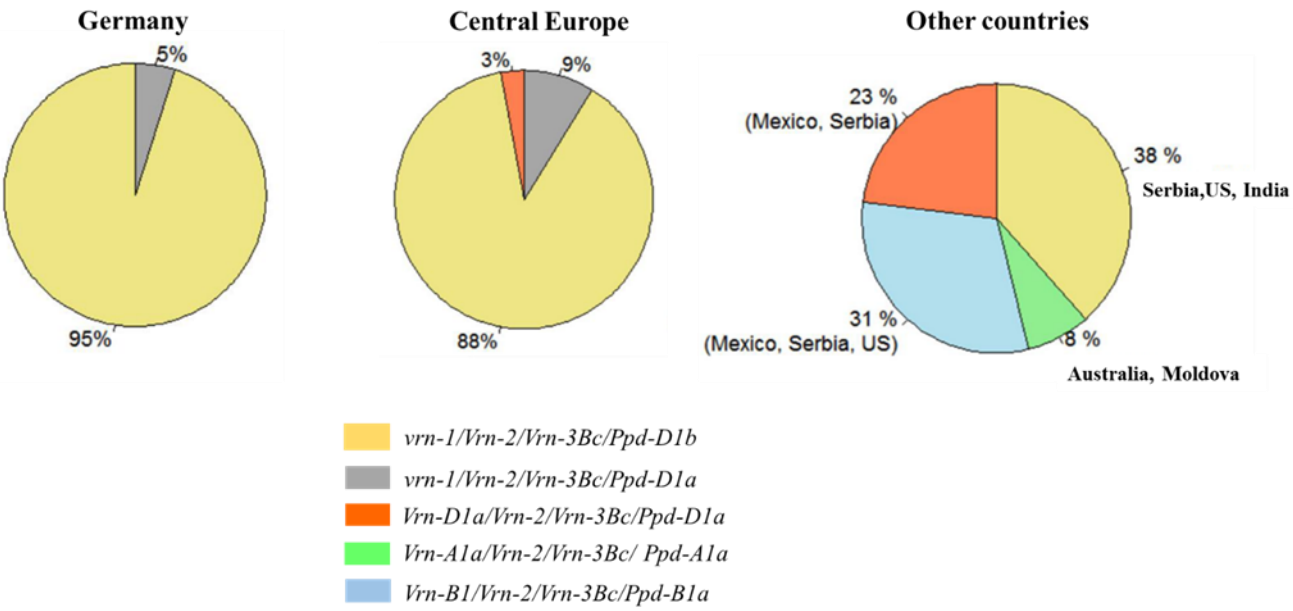

Figure 3. 4: Frequency in the percentage of allele combinations of *VRN* and *PPD* genes detected in different wheat germplasm according to the country of origin.

For vernalization genes, dominant and recessive alleles are designed with capital and small letters, respectively. For photoperiod genes, the letter "a" designs the insensitive allele and the letter "b" indicates the sensitive one.

3.3.4 Identification of stable and fine-tuning QTL for heading date

We aimed to identify stable genetic regions controlling HD independently of environmental factors. For that, GWAS including phenotypic data from all locations and years was performed. For subset1, four loci mapped on chromosomes 5A and 5B were selected as significantly associated with HD. The marker GENE_3500_336 mapped at 117,4Mbp, in QTL TaHd102, explains the highest proportion of the genotypic variance (13.18%) with an SNP effect of 1.2 days (Figure 3. 5a, Table 3). By including the exotic cultivars into GWAS, five QTL, different from the ones found in subset 1, could be identified in subset 2 and distributed on chromosomes 2B, 3A, 4A, 5B, and 7B (Figure 3. 5b, Table 3. 3). The strongest effect was shown by the peak marker AX-111134276, mapped at 556.60 Mbp of QTL TaHd044 on chromosome 3A, which explained 33% of the genetic variance. The allelic variation at this locus alters HD by 5.63 days. Looking at the allelic level, the adapted cultivars revealed a very high monomorphism at the five loci identified in subset 2. No QTL related to *VRN* and *PPD* genes were detected in subset1, while loci bearing *VRN-A1*, *VRN-A2*, *VRN-B1*, *VRN-D2*, *Ppd-A1*, and *Ppd-B1*genes were identified in subset 2 (Table 3. 3). The proportions of detected QTL related to candidate genes in explaining the genetic variance are very low compared to the locus TaHd044 (Appendix 3. 13)

Figure 3. 5: GWAS for heading date including phenotypic data from all locations and years using

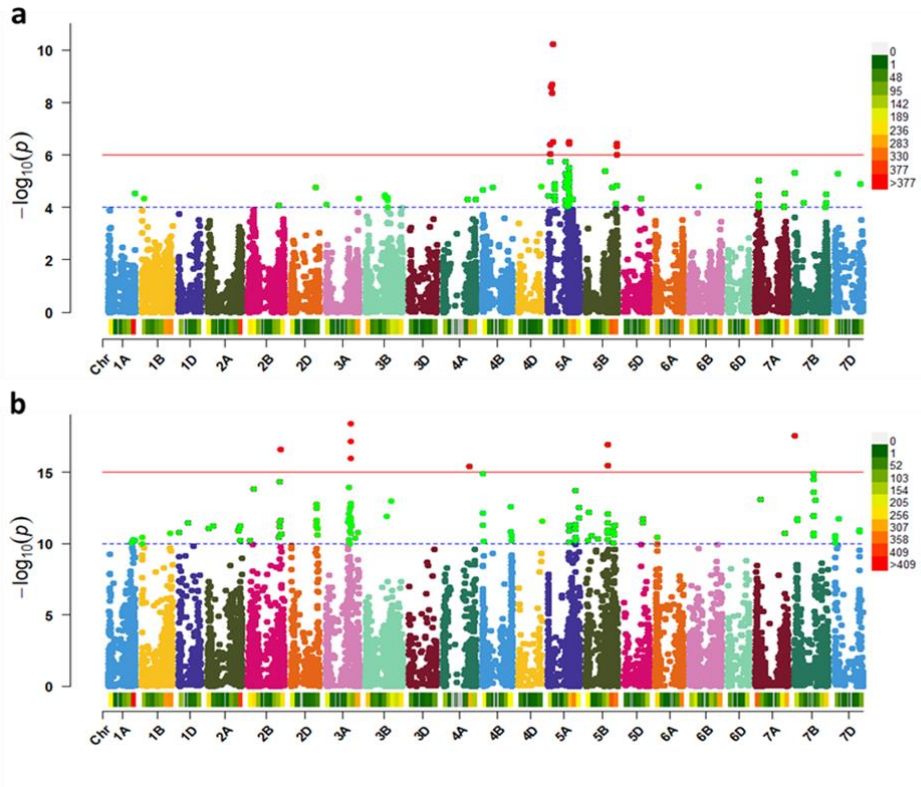

adapted (subset1) and adapted plus non-adapted (subset2) winter wheat cultivars.

a and b Manhattan plots show the identified QTL in subset1 and subset2, respectively. The y-axes refer to the –log10 (P) values of the SNP markers. The chromosomes are denoted on the x-axes. The red dots refer to the significant SNP markers above the cut-off red line. The SNP markers density per chromosome for each subset is shown above the x-axis. The number of SNP markers within 10 Mbp window size is indicated in categories and colors on the right side of the Manhattan plot.

Table 3. 3: Significant QTL for flowering time detected in the winter wheat association panels of subset1 und subset2

	QTL	Marker[a]	Chr[b]	Position[c]	Flanking region[d]	MAF[e]	F_Value[f]	*P*[g]	-Log$_{10}$(*P*)	FDR[h]	*PG*[i]	Allele effect[j]	Present allele	RefSeqv2.1
Panel 1	TaHd098	Ra_c69221_1167	5A	41,427,451	36,273,096 - 51,590,002	0.37	26.06	9.40E-07	6.03	9.00E-04	2.78	0.97	T	T
	TaHd102	GENE_3500_336	5A	117,495,484	98,329,421 - 125,143,323	0.47	49.3	6.14E-11	10.21	4.25E-07	13.18	-1.2	T	T
	TaHd112	BS00022191_51	5A	476,402,782	461,485,853 - 481,199,152	0.35	28.54	3.14E-07	6.5	4.72E-04	2.46	1.05	T	C
	TaHd132	BS00024829_51	5B	693,611,551	691,411,951 - 697,289,998	0.26	28.11	3.75E-07	6.43	4.72E-04	2.21	-1.19	T	T
Panel 2	TaHd034	AX-158603420	2B	720,796,133	720,796,133 - 730,190,623	0.11	120.4	2.45E-17	16.61	5.54E-19	1.54	5.09	A	C
	TaHd044	AX-111134276	3A	556,662,059	556,548,610 - 564,943,896	0.1	159.69	4.25E-19	18.37	1.97E-23	33.01	5.63	A	A
	TaHd072	AX-158581720	4A	593,486,064	581,869,248 - 596,506,881	0.12	113.35	3.86E-16	15.41	3.45E-18	1.77	6.27	A	G
	TaHd125	Jagger_c3991_101	5B	488,820,722	478,130,002 - 490,769,429	0.08	126.61	1.14E-17	16.94	8.06E-20	1.82	6.01	T	C
	TaHd171	AX-158601566	7B	2,944,225	1,980,522 - 3,500,643	0.09	155.01	2.68E-18	17.57	4.31E-23	7.09	5.83	A	G
Candidate genes in panel 2	*PPD-A1*	AX-158573607	2A	70,940,322	70,877,024 - 71,318,288	0.38	44.44	1.13E-11	10.95	7.97E-09	2.02	-1.73	A	A
	PPD-B1	Exca_rep_c68899_1400	2B	91,836,538	89,552,942 - 93,545,484	0.14	71.37	8.15E-13	12.09	6.26E-13	0.04	1.66	A	A
	VRN-D2	RAC875_c8642_231	4D	509,666,717	498,241,876 - 512,102,050	0.08	91.32	1.12E-14	13.95	1.09E-15	2.02	1.55	T	C
	VRN-A1	AX-111486916	5A	587,411,454	586,141,645 - 588,872,113	0.11	17.12	5.07E-05	4.29	3.76E-04	1.21	-1.98	A	G
	VRN-A2	BobWhite_c8266_227	5A	698,507,476	689,913,529 - 708,418,214	0.08	101.31	3.34E-15	14.48	6.18E-17	1.17	2.12	T	G

[a] The peak marker of QTL for flowering time showing the highest -Log10(P)

[b] The chromosome harboring the peak marker.

[c] The physical position in bp of the peak marker

[d] The physical interval of the most significant QTL harboring the peak marker

[e] The minor allele frequency set to >5%

[f] F-test statistic value

[g] *p* value threshold set to $p \leq 0.001$

[h] False discovery rate (FDR) set to ≤0.05

[i] Proportion of the genotypic variance explained by the QTL in %

[j] Effect in days of the allele substitution on flowering time

Further, for a better understanding of the genetic modulation or fine tuners of the transition to the reproductive phase, we performed the genome-wide scan per each environment separately. In total, 95 SNPs distributed across 17 environments were identified (Appendix 3. 14). Some shared QTL among the specific location-by-year combinations were detected. In 2015, three possibly homoeologous QTL (TaHd024, TaHd036, TaHd040) were uncovered at the very distal end of chromosomes 2A, 2B, and 2D, respectively. This region was shared by locations at lower latitudes until the middle part of Germany (Loc1 to Loc3), whereas northern regions (Loc5 and Loc6) had a common QTL (TaHd122) on the short arm of chromosome 5A. The year 2016 was the warmest among the three years of the experiment in the southern and central locations that share the loci TaHd059 and TaHd088 on chromosomes 3B and 4B, respectively. The loci detected in 2017 followed no trend with latitude gradient. The overall effect of revealed fine-tuning QTL spans from inducing early flowering time by 2.6 days (Loc5-2016) to delaying it by 4.45 days (Loc2-2015).

Since all genotypes were tested in 17 environments, we were able to calculate the flowering time response to various meteorological parameters for each genotype separately after vernalization. We calculated the Pearson correlation coefficients between HD and the mean records of climate variables in February, March, and April and used these as new traits in GWAS. This approach leads to the detection of a few significant QTL. We only counted the annotated genes associated with the detected loci and identified four QTL for temperature, seven for day length, and five for radiation (Appendix 3. 15).

3.3.5 Identification of epistatic interactions involved in heading date control in winter wheat

To evaluate how the interaction among genetic loci affects flowering time, genome-wide epistatic interaction analysis was performed. Using subset1, 32 significant epistatic interactions were detected and explained up to 3.8% of the genetic variance (Appendix 3. 16). One locus on chromosome 5A (TaHd120) at 698.10 Mbp was involved in 14 epistatic interactions with loci located on chromosomes 1B, 2B, 3B, 4A, 4B, 5A, 5B, and 5D including the strongest QTL TaHd102 identified in the same subset (Figure 3. 6a). This locus is located 37 kb upstream of *ZCCT2*, the core protein of the *VRN2* gene. We detected 30 significant epistatic interactions using subset 2, which explained up to 7.8% of the genetic variance (Appendix 3. 17). Two loci mapped on chromosomes 1B (TaHd015) and 5A (TaHd104) at 158.2Mbp and 654.70 Mbp, respectively, showed the strongest epistatic interaction in the subset2, explaining 7.8% of the genetic variance. The combination of minor alleles of both regions induced HD by 4.64 days earlier compared with that of major alleles. The locus TaHd098 showing QTL effect in subset1 was implicated in 15 digenic interactions in subset 2 (Figure 3. 6b)

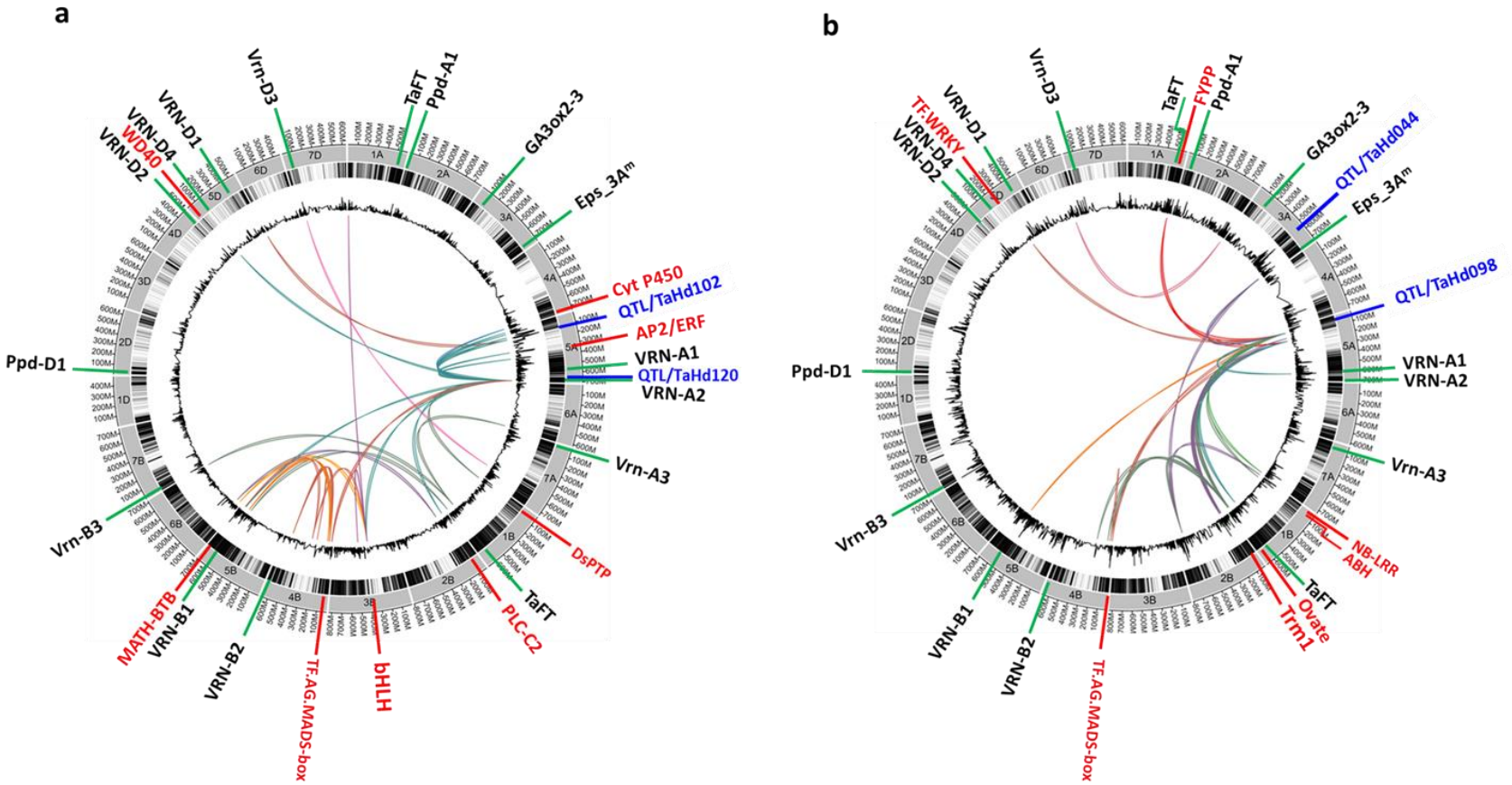

Figure 3. 6: Epistatic interactions detected in subset1 (a) and subset2 (b).

From outside to inside, the layers indicate the length of chromosomes in Mb, then the organization of chromosomes per subgenome A, B, and D, then the mapping of SNP markers used for GWAS, then the QTLs presented according to their –log10 P values extracted from GWAS. The last inner curved lines indicate significant interactions between SNP markers highlighted in colors. The known flowering time genes are indicated with a green arrow. The detected genes are highlighted in red. The blue color designs the QTL with epistatic effect.

3.4 Discussion

3.4.1 Response of heading date to local and seasonal interplays of environmental factors

HD variation occurs between individuals across very small temporal and spatial scales, where local climatic conditions caused a part of within-population variation (Dahlgren, von Zeipel & Ehrlén 2007). This explains the heading interval of 10.4 days among the adapted cultivars within a latitude range of around 6°. The reduced genotypic variance of HD in subset1 compared to subset2 is attributed to the local adaptation impact of the German cultivars. The genetic response of HD is more dependent on location than on year. This indicates the importance of multi-location trials with broad distribution for the genetic estimation of a highly heritable trait such as HD (Holland, Nyquist & Cervantes-Martínez 2003). Moreover, the high variance of genotype-by-location-by-year interaction for both sets shows that all cultivars respond very differently to the 17 environments. This confirms that the European/German germplasm has a high genetic potential appropriate to study complex and polygenic traits like flowering time.

The interplay of climatic factors is influencing all phenological events of plants including flowering time in barley (Jones & Thornton, 2003), rice (Mall & Aggarwal, 2002; Prasad et al., 2006), and wheat (Manderscheid et al., 2003; Kouchaki & Nasiri, 2008). Exploiting GDD as an indicator of the beginning of heading revealed that Tmax and Tmin of spring dominate strongly other factors in reducing days to heading from the lowest latitude to the middle ones. The HD inducing effect of temperature is reported by other studies (Menzel et al. 2006; Miller-Rushing et al. 2007; Record 2009; Moore & Lauenroth 2017). The elevated solar radiation accumulation was highly associated with delayed HD. The high UV-B radiation plays a crucial regulatory role in plant growth and morphology (Bornman et al., 2015), however, many reports confirm the delay of flowering time as a response to high natural UV-B radiation in different plant species, such as maize (Saile-Mark et al., 1996), pot roses (Terfa et al., 2014) and pea (*Pisum sativum* L.) (Roro et al., 2016). Although other factors such as soil moisture and soil temperature could affect HD, nevertheless, the PCA showed that 71% of the environmental variation was explained by the variables considered in the study.

3.4.2 Substituted effect of latitude dependent temperature and daylength on heading date

Latitude as a complex environmental determinant plays a pivotal role in temperature regimes, photoperiod, and solar radiation fluctuations, which influence the growth and reproduction of plants (Craufurd & Wheeler, 2009; B. Li et al., 1998). With all measurements performed in this study, we did not see a linear relationship between latitude and HD. Villegas et al., (2016) reported that the long day length is more responsible for short “sowing to anthesis” duration than the temperature in a latitude range of 22°. However, the climatic stimulus that induces flowering time in one location, is not necessarily the same in another (Wilczek et al., 2010). As day length and Tmax of spring contribute mostly and quite equally in explaining the environmental variability in Germany, the genotypic response

to day length in dependency on Tmax should be considered to understand the HD variation in respect of latitude. It is noteworthy that a dramatic acceleration of flowering with increasing light amount as a response to daylength was certainly observed in several annual plant species (Tsegay et al., 2005; Opseth, Holefors, Rosnes, Lee & Olsen, 2016; Chiang et al., 2018). By contrast, it was reported as well that daylength has no or less effect when flowering is induced by milder temperatures between 15°C and 22°C (King, Pate & Johnston, 1996; Sønsteby & Heide, 2008). Indeed, the seasonal change of daylength is prolonged faster during the spring season in the North than in the South at the time when HD began, while Tmax recorded higher values (17-21°C) in the South than in the North (11-17°C) in the same period (Figure 3. 7), which explains the opposite genetic responses to temperature and daylength. Hence, the impact of high seasonal change of temperature in the South on HD seems to compete with the immense daylength seasonal variation occurring in the North when moving from winter to spring. Consequently, plants are adapted to use temperature as a sensor of favorable conditions in lower latitudes, whereas photoperiod is a more reliable indicator of the changing seasons than the temperature in the higher ones for starting HD. Furthermore, because the yearly thermal change is greater in the lower latitude and more stable in the higher ones, and as the seasonal alteration of daylength is the only environmental input that is constant from year to year, this might explain the unchangeable HD behavior in the North and the increased HD variation as we headed further South.

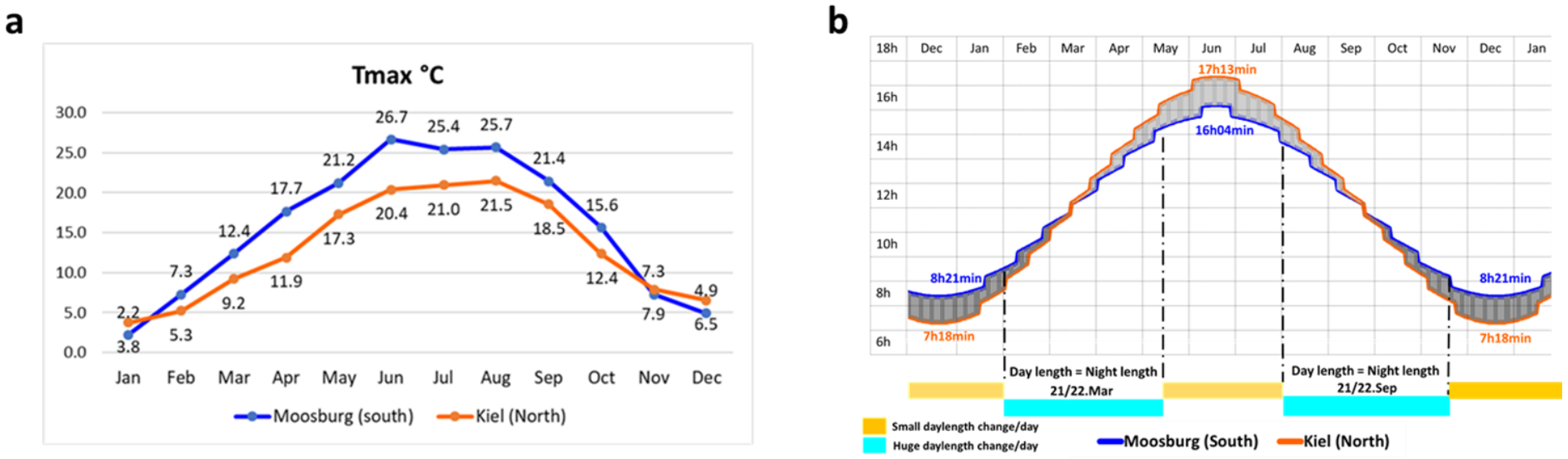

Figure 3. 7: Seasonal change of Tmax (a) and daylength (b) including three years in loc1 (Moosburg) and in loc6 (Kiel).

The mean of Tmax per month is indicated in numbers. Daylength, including civil twilight (h), was computed daily following Forsythe et al. (1995).

3.4.3 The roles of *VRN* and *PPD* genes in flowering time control

The candidate gene approach was used for identifying allelic variations of known *VRN* and *PPD* genes and studying their effect on flowering time in wheat in many researches (Eagles et al., 2009; Rousset et al., 2011; Bentley et al., 2013). The allele combination *vrn1/Vrn2/vrn3* confers the strict winter growth habit due to the dominance of *VRN2* and recessiveness of *VRN1* and *VRN3* (Takahashi, 1970; Yan et al., 2006). Indeed, the adapted germplasm carries the winter allele *vrn1* due to the three homoeologous recessive alleles *vrnA1, vrn-B1, vrn-D1*. No recessive null *ZCCT-1* gene is segregating in the German winter wheat because of the missing null allele *ZCCT-B1* despite the detection of null alleles *ZCCT-A1* and ZCCT-D1. By contrast, the presence of two functional alleles *ZCCT-B2* and *ZCCT-D2* leads to dominant *Vrn2* (even one functional allele is enough) and consequently, an increase in vernalization requirement (Distelfeld et al., 2009; Kippes et al., 2016). The presence of photoperiod sensitive allele *Ppd-D1b* validates the strict winter growth habit in the adapted germplasm owing to allele combination *vrn1/Vrn2/Ppd-D1b*. Our results are in line with Langer et al., (2014), who reported that 82% of the European winter wheat cultivars harbor daylength sensitive allele *Ppd-D1b* with 100% dominance of winter allele *vrn-1*. Contrary to the same study, we found that all European cultivars carry the spring alleles *Vrn-B3c* while the recessive form *vrn-B3* (winter allele) could not be detected. However, the presence of spring allele *Vrn-B3c* did not reduce the long exposure to the low temperature needed by the winter European wheat cultivars for heading initiation. Chen et al., (2013) reported that the genotype carrying *Vrn-B3c* headed and flowered only one day later than the genotypes with winter allele *vrn-B3*. Moreover, the winter allele *vrn-A1* has a greater impact on flowering time than the *Vrn-B3* gene (Chen et al., 2013). Since the majority (95%) of the adapted cultivars carry the same allelic variation at *VRN* genes, neither the HD range of 10.4 days nor the genetic variance showed by the German cultivars can be convincingly explained by the allelic variation at *Ppd-D1* locus, as only 5% of the cultivars harbor the insensitive allele *Ppd-D1a.* The candidate gene approach disclosed the presence of *VRN* and *PPD* alleles established as a result of long-term adaptation to winter conditions. Nevertheless, the HD variation due to genetic variance and interaction with the environment is very likely involving more genetic regulators responsible for HD variation after fulfillment of vernalization and photoperiod requirements. On the other hand, spring alleles at *VRN* and *PPD* were more frequent in the exotic cultivars. The insensitive alleles at *Ppd-A1* and *Ppd-B1* reported by Nishida et al., (2013) have an equal HD inducing effect as *Ppd-D1*.

3.4.4 Novel stable QTL alleles regulating the time of heading

The overall effect (20.6%) of the four detected stable QTL is higher compared with that of six QTL (9.5%) reported by Langer et al., (2014) that tested more European winter wheat cultivars but in very close locations for one single year. Granted that the size of the population is a determinant factor in GWAS, the incorporation of QTL × environment interaction, which maintains the genetic variance, may improve the power of GWAS to find relevant and broadly adapted QTL (Cantor et al., 2010; Thomas,

2010). TaHd102 is a novel locus regulating HD and explaining 13.15% of genetic variance in the German germplasm is located distantly from the reported SSR marker *Xgwm293* in the small arm of chromosome 5A, involved in the genetic control of height in wheat (Griffiths et al., 2009) (Appendix 3. 5). The novel adapted allele that attributes a stable effect independently of the environment can be used for the autonomous adjustment of HD in wide geographical regions. The missing QTL related to *VRN* genes in subset 1 is explained by the fact that all German cultivars are adapted to the same vernalization conditions, a fact that is confirmed by PCR screening. *Ppd-A1* and *Ppd-B1* do not harbor any polymorphism that segregates in the European germplasm as shown by Langer et al., (2014). Although *Ppd-D1* is segregating in the adapted cultivars, no related QTL was detected via GWAS. This might be explained by the low LD decay in chromosome 2D especially around the region harboring *Ppd-D1* (Bentley et al., 2013). Increasing the phenotypic variance is highly required for high-resolution mapping and allele mining (Ersoz et al., 2007; Uchiyama et al., 2013). The incorporation of the non-adapted cultivars uncovers the strongest QTL TaHd044. This later is flanked by two previously reported SSR markers Xbarc45 (Griffiths et al., 2009) and WMC264 (Zanke et al., 2014). The identification of the QTL related to *VRN* genes in subset2 is most probably due to different vernalization requirements, caused by the exotic alleles, which could carry natural variations that lead to a need for shorter exposure to cold (Yan et al., 2004; Fu et al., 2005; Kippes et al., 2015). Despite the expected differences in photoperiod adaptations of the exotic cultivars, no QTL related to *Ppd-D1* could be detected, due very likely to the selective sweep around *Ppd-D1* as explained above. The detected exotic alleles enable the introgression into the adapted breeding wheat cultivars of improved adaptability to face the challenging climate changes.

3.4.5 Fine-tuning QTL undergo the competition of latitude dependent climatic variables

The fine-tuning QTL of specific microenvironments are matching with the latitudinal competition of environmental cues affecting HD. In the lower latitude, where Tmax dominates the interaction with HD, the three uncovered QTL bear genes that are involved in annotated mechanisms related to temperature response mainly the response to ambient T°C in *Arabidopsis* (Liu et al., 2012) (TaHd036, 2015), heat-inducing cytokinin biosynthesis and control of spikelets number in rice (Chao Wu et al., 2017) (TaHd059, 2016) and thermotolerance regulation by *DnaJ* protein in tomato (Wang et al., 2019) (TaHd088, 2016). The locus TaHd122 on chromosome 5A, found to be a member of Auxin/B3 appeared exclusively in the higher latitudes, where the photoperiod acts as a reliable proxy for initiating the floral transition. Auxin is known to promote floral timing in *Arabidopsis* (Ueda et al., 2008), while transcriptional and growth responses to auxin are modulated by the circadian clock (Covington & Harmer, 2007). Despite their small effect, thermo-sensitive genes play an essential role in adaptation to specific climatic conditions (Lewis et al., 2008; Snape et al., 2001), and can be exploited to enhance the adaptability to different environments.

.

3.4.6 Epistatic interactions

One locus TaHd120 located in the *VRN2* gene region that is implicated in 14 genetic interactions could be identified. This strongly suggests that *VRN-A2* plays a central role in the regulatory network controlling heading time in the German germplasm. The epistatic effect of *VRN* loci in the genetic control of flowering time in the European winter wheat was reported by Reif et al., (2011) who found that the *VRN-A1* gene is involved in four epistatic interactions. The identification of ORFs in the intervals interacting with *VRN2* revealed the Apetala2/Ethylene (AP2/ERF) on chromosome 5A explaining 2.14% of the genetic variance. The class of AP2/ERF genes is well described in the flowering pathway in *Arabidopsis* for regulating the correct timing of the transition of the spikelet meristem to the floral meristem in maize (Chuck et al., 1998). Similarly, we found that the other chromosomal regions interacting with the *VRN2* harbor protein families such as *MATH-BTB, bHLH, WD40, Agamous/MADSbox, DsPTP1, and PLC-C2*, known to contribute to flowering time regulation in other plant species (Liyuan Chen et al., 2015; Georges et al., 2009; Hazebroek & Metzger, 1990; Ito et al., 2012; Lingyan Jiang et al., 2018; Sheldon et al., 1999; Yanofsky et al., 1990). Interestingly, the novel locus TaHd098 which has a small QTL effect in adapted germplasm, showed a strong epistatic effect when adding the exotic cultivars to the analysis. Some of the 15 interacting loci were mapped very close to key regulatory elements of flowering time in *Arabidopsis* like *FYPP* (Kim et al., 2002), *Alpha-Beta hydrolase (ABH)* (Sun & Ni, 2011), *and tRNA methyltransferase (Trm1)* (Chen et al., 2010; Guo et al., 2019) on chromosomes 1A, 1B and 2B, respectively and in wheat*: TaFT3, Eps-3A, VRN-B1,* and *Vrn-3/FT* genes on chromosomes 1A, 1B, 3A, 5B, 7A, respectively.

3.5 Conclusion

In this study, we elucidated a part of the complex interaction of the environmental factors with flowering time. The impact of high seasonal changes of temperature in the lower latitudes on HD competes with great daylength seasonal variation occurring in the higher ones when moving from winter to spring. The resulted genetic response selects thermo-sensitive loci in the South and photoperiod susceptible loci in the northern location for starting the transition to the reproductive phase. The allele combinations of known *VRN* and *PPD* genes responsible for the winter and facultative growth habits of adapted and exotic cultivars were determined. We were able to enrich the flowering time pathway in wheat with potential QTL attributing a stable effect across different environments (TaHd102) and exotic alleles (at TaHd044) that induce greater HD alteration. In addition, fine-tuning QTL that responds to specific environmental stimuli was identified. A novel locus TaHd098, detected on chromosome 5A, gained more epistatic implications for controlling flowering time in non-adapted winter wheat. Further, we propose a pivotal epistatic role of *VRN2* based on its multiple genetic interactions with key regulatory elements in the adapted germplasm. Our findings offer new insights into understanding the mechanisms

of the genetic architecture underlying flowering time in winter wheat and be leveraged for the wheat breeding process for developing cultivars adapted to different environments.

Chapter 4: Mechanistic basis of flowering time regulation

4.1 Introduction

A precise adjustment of flowering time to suitable environmental conditions is a critical agronomical factor for successful reproduction (Andrés & Coupland, 2012). This adaptive trait of transition from vegetative to the reproductive stage is controlled genetically by monitoring and responding to specific seasonal stimuli such as temperature and photoperiod with additional involvement of nutrient availability (Lee & Amasino, 1995; Romera-Branchat et al., 2014). Most of the knowledge and understanding of flowering time regulation is gained from the diploid model dicotyledonous plant *Arabidopsis.* Floral transition in *Arabidopsis* implicates six known pathways: age, vernalization, Gibberellin (GA), ambient temperature, photoperiod-dependent, and autonomous mechanisms (Blümel et al., 2015; Fornara et al., 2010; Henderson & Dean, 2004; Ó'Maoiléidigh et al., 2014). In *Arabidopsis*, the vernalization genes are induced by low temperature over the cold period, and this leads to suppressing *FLOWERING LOCUS C (FLC)* that represses the floral transition (Michaels & Amasino, 1999; Sheldon et al., 1999). The photoperiod mechanism consists of photoreceptors and circadian clock (Searle & Coupland, 2004) that involves two primary genes *CONSTANS (CO), and FLOWERING LOCUS T (FT)* (Putterill et al., 1995). During the light period, *CO* is overexpressed, resulting in the activation of *FT* which acts as mobile florigen that is expressed in leaves, moves through the phloem to reach the shoot apical meristem, and activates floral identify genes *APETALA1 (AP1)* and *LEAVES FLY (LFY)* (Abe et al., 2005; Golembeski & Imaizumi, 2015). The endogenous growth regulator GA upregulates the transcription of *SUPPRESSOR OF OVEREXPRESSION OF CO1 (SOC1)* known as an activator of *LFY* (Moon et al., 2003). In monocotyledonous plants, flowering time regulation has been intensively investigated in most economically important crops such as maize, rice, barley*)*, and wheat, for which, vernalization, photoperiod, and earliness per se pathways were identified (Laurie, 1997; Kamran et al., 2014). For winter wheat, vernalization induced *VRN1* (= *AP1*) that expresses in leaves and acts as a repressor of *VRN2 (=FLC)* which promotes the transcription of *VRN3* (= *FT1*) when days get longer in spring (Chen et al., 2013; Yan et al., 2006). The photoperiod pathway in wheat is regulated by homoeo-allelic gene series *PPD,* which encodes a pseudo-response regulator (*PRR*) family protein gene orthologous to the *Arabidopsis PRR7* gene. Wheat *Heading date 1 (TaHD1)* gene is the homolog of *CO* in wheat and exhibits diurnal rhythm (peak during the day, low at night) under long days (Nemoto et al., 2003). In wheat, *PHYTOCHROME C (PHYC)* is the elementary light receptor that transmits light input to the photoperiod pathway, by promoting the transcription of *PPD1* and accelerates flowering via *VRN3* in long days (Chen et al., 2014). Earliness *per se*, which corresponds to the autonomous flowering pathway in *Arabidopsis* involved genes such as the *Eps-3A*^{m} gene of *Triticum monococcum* which is an orthologue of the *Arabidopsis LUX/PCL* gene (Gawroński & Schnurbusch, 2012) and *Eps-1A*^{m} related to wheat *ELF3* gene (Zikhali et al., 2014). It was reported that many *Eps* genes are active in a temperature-dependent manner, correspond to components of the circadian clock, and mediate light signaling (Ford et al., 2016; Ochagavía et al., 2019). Phytohormones such as Abscisic acid, Cytokinins,

Ethylene, and Brassinosteroids contribute to the flowering process in *Arabidopsis* (Achard et al., 2007; Barth et al., 2006; Bernier, 2013). Thus, exogenous and endogenous floral integrators crosstalk with each other and channelize the signals via several regulatory elements to control the floral switch.

To identify genes underlying complex traits, quantification of gene expression levels using RNA sequencing (RNA-seq) analysis is a powerful technique to achieve this goal (Wang et al., 2009). In plants, RNA-seq was exploited to investigate biotic and abiotic stress resistance (Liu et al., 2011), tillering (Palmer et al., 2012), flower development (Grogan et al., 2016; Singh & Jain, 2014), and fruit formation (Jiang et al., 2015). The transition to the reproductive phase was subject to large-scale transcriptome analyses in many important cereal crops such as maize (Eveland et al., 2014), rice (Harrop et al., 2016), barley (Digel et al., 2015), and wheat (Feng et al., 2017). RNA-seq has also proven to be a time and cost-effective method for detecting single nucleotide polymorphisms (SNPs) in transcribed genes and consequently analyzing the allele mining that harbors a target locus (Cavanagh et al., 2013). The identification of such genomic loci and their related SNPs resulting from natural variation and accounting for significant phenotypic alteration of a given trait is the ultimate target of GWAS (Rafalski, 2010). Despite the high reliability of GWAS, it does not lead necessarily and directly to the gene (s) responsible for phenotypic variation because of insufficient marker density and/or decay of linkage disequilibrium in some cases. Combining QTL mapping with analysis of RNA-seq data to improve the interpretation of GWAS results has previously proven to be efficient in plant-based studies (Habib et al., 2018; Jian et al., 2019; Ramirez-Gonzalez et al., 2015).

Pre-anthesis (heading) development in cereals is divided into three distinctive phases based on the morphological changes of the shoot apical meristem: the vegetative phase, the early reproductive phase, and the late reproductive phase (Slafer & Rawson, 1994). Waddington et al., (1983) developed a quantitative and developmental scale that describes the morphogenesis and progression of the shoot apex and carpels.

In this study, we joined significant QTL mapping provided by previous GWAS to transcriptome sequencing analysis for identifying candidate genes underpinning the detected QTL that underlay flowering time regulation in winter wheat (Benaouda et al., under review). The particular goals of the current study were to (1) assess the correlation between the observed flowering time trait in the field with microscopical phenotyping of trait-specific organ and stage, (2) to identify and map the genes differentially expressed in the early and late flowering cultivars in trait-specific organ and stage, (3) to explore the pathways and responses revealed by RNA-seq in QTL intervals and finally (4) to compare transcription levels of some selected genes mapped in significant QTL with relative gene expression via RT-PCR and identify polymorphisms in coding sequences and promoter regions of those genes.

4.2 Material and methods

4.2.1 Plant material and growth conditions

For this study, we selected two bred winter cultivars developed in Germany showing contrasting and stable flowering behavior in different environments (

Appendix 4. 1). The mean value of the heading date (HD) of both cultivars is based on the phenotyping data collected from six locations across Germany over three years (Benaouda et al., under review). “Kontrast” is the earliest flowering one in the adapted cultivars, which is released in 1990, and flowers 10 days earlier than the latest flowering cultivar “Basalt”, developed in 1980 (Voss-Fels et al., 2019). The Australian cultivar Triple dirk "S", which flowers five days earlier than “Kontrast” in the field, is cultivated since 1968 and was used as control. The seeds were sown in 96-well growing plates and kept in the greenhouse over two weeks for germination at 18°C. Subsequently, the plants were transferred to a climate chamber to vernalize for 8 weeks in short-day conditions (8 h light at 22°C and 16 h dark at 18°C). Then, the plants were shifted to long-day conditions (14 h, 22°C light; 10 h, 18°C dark) until flowering.

4.2.2 Microscopical phenotyping of shoot apical meristem

The phenotyping of the shoot apical (SAM) was performed by dissecting the plants every two days after vernalization. After removing the leaves covering the floral organ, the apex was cut very quickly using a microsurgical disposable blade under a binocular microscope to avoid dehydration of the apex. The development of SAM was observed using the digital microscope KEYENCE model VHX-900F (KEYENCE Corporation, Osaka, Japan). The morphogenetic advancement of SAM was determined according to the developmental scale as described by Waddington et al., (1983).

4.2.3 Statistical analysis

HD was scored in field und under climate chamber conditions. The phenotypic data were compared between all cultivars by running a paired student’s t-test. Significance was compared to *p*-value <0.01. The regression slopes were calculated in excel.

4.2.3 Tissues collection for RNA analysis

The SAM and leaves materials were collected at three Waddington stages (W): W1.25-W1.75 (transition apex phase TAP), W2.0-W2.5 (double ridge stage DRS), and W3.0-W5.0 (late reproductive phase LRP), which correspond to time points 5, 13, and 25 days after the end of vernalization (DAV**)**. Depending on the development stages of each cultivar at the time of collection, the pooling of 20 to 60 shoot apices was needed to reach the minimum weight of tissue required for RNA extraction. We strictly selected shoot apices that showed a uniform morphological development per time point. The distal part of leaves samples was harvested at the same time points as mentioned above and from the same plants from which

SAM was collected. For each cultivar, three biological replicates were collected. The samples were frozen immediately in liquid nitrogen and stored at -80°C.

4.2.4 RNA-seq analysis and data processing

Total RNA extraction from the collected tissues, initial quality control, and sequencing analysis were performed commercially at Novogene Co. Ltd. (HK, China). Considering two cultivars*two tissues* three-time points*three biological replications, 36 libraries were constructed and sequencing based on the sequencing platform NovaSeq 6000 (Illumina) using the sequencing strategy paired-end 150 (=PE150) yielded on average 52.76 million 100 bp paired-end reads per sample We used the RAW-ABS workflow for automated quality control and preprocessing of the RNAseq reads (https://github.com/tgstoecker/RAW-ABS/tree/v1.0; DOI: 10.5281/zenodo.3865747). Quality assessment of reading libraries was performed using FastQC v0.11.8 and Trimmomatic version 0.3 (Bolger et al., 2014) to remove low-quality reads and remaining adapter sequences from each dataset. Specifically, a sliding window approach was used, in which a read was clipped if the average quality in a window of four bp fell below a Phred quality score of 20. BBDuk of the BBTools suite (https://jgi.doe.gov/data-and-tools/bbtools/) was employed to remove rRNA reads from the datasets using a kmer length of 27 as filtering threshold for decontamination. The splice-aware STAR aligner v2.7.3a (Dobin et al., 2013) was used to align the remaining reads against a genome index of the bread wheat reference sequence and annotation - IWGSC "RefSeq v1.0" & "RefSeq Annotation v1.1" (Appels et al., 2018). Multi-mapping reads that mapped to more than one position were excluded from subsequent steps by considering only reads, which mapped in a single location (outFilterMultimapNmax 1). On average, 50.8 million reads per sample aligned to unique positions in the gene set of the RefSeq v1.0 wheat reference genome with 120,744 predicted coding and non-coding gene models (EnsemblPlants release 46, (Bolser et al., 2017)). The aligned paired-end reads were ordered according to their position and transformed to .bam files with the software samtools (version 1.9, (Li et al., 2009)). We employed featureCounts v1.6.4 (Liao et al., 2014) to obtain aggregate counts of aligned reads at exon-level and to construct a gene-level matrix of these counts comprising all samples. The transcripts have been mapped in the previous four identified QTL for heading in the adapted germplasm (Benaouda et al., under review). The list has been extended to 23 QTL that are statistically significant to explore as much as possible the pathways and responses revealed by RNA-seq (Appendix 4. 3).

4.2.5 Differential gene expression analysis

DEGs were identified with the package "edgeR" version 3.26.4 (Robinson et al., 2010) using the R language (Team, 2013). Differential expression analysis was based on comparing DEGs between the genotypes at the three-time points. Only genes passing a false discovery rate FDR <0.05 and a fold change > (±) 2 were considered differentially expressed.

4.2.6 Gene ontology term and pathway enrichment analyses

We performed de-novo functional annotation of the RefSeq v1.1 gene models with human-readable descriptions, including GO terms using AHRD (manuscript under review; https://github.com/groupschoof/AHRD). GO functional enrichment analysis was conducted using the database AgriGO v2.0 (Tian et al., 2017) to study the functions of DEGs. First, all DEGs were mapped to GO terms in the database, and then were used hypergeometric tests to find significantly enriched GO terms in the sets of DEGs. *P*-value ≤0.05 was taken as a threshold after Bonferroni correction.

4.2.7 RNA extraction, cDNA synthesis, and gene expression analysis

Total RNA extraction from SAM and leaves was performed using RNAeasy Plant Mini Kit (Qiagen, Hilden, Germany, following the manufacturer's instructions by using 100 mg tissue. The obtained RNA was subsequently treated with DNase to remove possible DNA contaminations using my-Budget DNase I (Krefeld, Germany, Bio-Budget Technologies). The quality of RNA was visualized by gel electrophoresis on 1% of agarose gel and quantified with a Spectrophotometer (ND-1000 Spectrophotometer, NanoDrop Technologies, USA). cDNA was synthesized from 1µg total RNA using RevertAid First Strand cDNA Synthesis Kit (Thermo Scientific, Waltham, MA, USA) according to the manufacturer's instructions. The possible contamination of cDNA with DNA was checked via PCR by *TaActin* gene (TraesCS1B02G283900) using designed primers flanking an intron (5'-CCATCATGAAGTGTGACGTGG-3', 5'-TCCAAGGATGAGTACGACGAG-3', Ta= 58°C), The quantification of expression levels of the target genes was performed by RT-qPCR using DyNAmo ColorFlash SYBR Green qPCR Kit (Thermo Fisher Scientific Inc, Massachusetts, USA) and Applied Biosystems 7500 Real-Time PCR System (Life Technologies, Carlsbad, CA, USA) following the manufacturer's instructions. The *TaEf-1.2* gene (Oyiga et al., 2018) was used as an internal control. The average Ct values of three technical replicates per reaction were calculated and used as input to estimate the expression of the target genes relative to *TaEf-1.2* using the $2^{-\Delta\Delta CT}$ method (Livak & Schmittgen, 2001). The primers used in RT-qPCR for each selected gene are listed in Appendix 4. 4.

4.2.8 Analysis of promoter region and coding sequence of candidate genes

The amplification of the promoter region and coding sequence of targeted candidate genes was performed via PCR. For this, DNA from cultivars "Kontrast", "Basalt", and control was extracted following the protocol of DNeasy Plant Mini Kit (Qiagen, Hilden, Germany). The PCR amplification reactions were performed in a 25µL reaction volume containing 100 ng of genomic DNA, 1 ^{x} One Taq standard buffer, 10 µM of forward and reverse primers each, 0.2 mM of dNTP, and 0.5 unit of Taq DNA polymerase (NEB, Frankfurt, Germany). The PCRs were conducted in the thermocycler Flex cycler (Analytik GmbH, Jena, Germany). PCR profiles were visualized by electrophoresis on a 1% agarose gel stained with peqGreen (0.04 µl/mL; VWR, Darmstadt, Germany). The obtained PCR products were purified using the Purelink Quick PCR kit (Invitrogen, Waltham, MA, USA) and after undergoing

sequencing from both ends. The primers used for PCR and Sänger-approach based sequencing are listed in Appendix 4. 4. The sequencing was carried out by Eurofins Genomics GmbH (Ebersberg, Germany). The obtained sequence information was then *in silico* analyzed to identify specific motifs and transcription binding sites (TBS) within the promoter region using PlantTFDB v5.0 (Ovcharenko et al., 2005). The alignment of sequenced coding regions was performed using the MegAlign Pro tool of DNASTAR software (DNASTAR. Madison, WI). Identification of putative start and stop codons and exons-introns regions was carried out using the Ensembl database (http://plants.ensembl.org).

4.3 Results

4.3.1 Morpho-histological phenotyping of shoot apex development at the transition phase

To investigate the heading shift observed in the field between cultivar "Kontrast" and "Basalt", a comparative analysis of the SAM morpho-histological development was performed. The climate chamber conditions accelerated significantly ($P<0.01$) the days to heading by 93.5, 81.2, and 65.6 days for cultivars "Basalt", "Kontrast" and control, respectively (Figure 4. 1a). HD range moved from 10.4 in the field to 12.3 days between the early and late adapted cultivars, while the control headed 8 days earlier than "Kontrast". In the field and under climate chamber conditions, the same heading behavior and ranking were observed. The quantitative development of shoot apex revealed distinguishable SAM progresses observed in the three cultivars without overlapping at any Waddington stage. Paired student's t-test showed differences between Waddington scores of SAM development in the three cultivars during the observation phase that extended to 35 DAV (Appendix 4. 5, Appendix 4. 6, Appendix 4. 7). "Basalt" showed the slowest SAM growth compared to "Kontrast" and control. The slope of regression lines were 0.08, 0.12, and 0.18 for "Basalt", "Kontrast" and control, respectively (Figure 4. 2b). The microscopic phenotyping of SAM showed that the DRS was reached by "Basalt", "Kontrast" and the control approximately at 25, 13, and 5 DAV, respectively. The shoot apex persisted in the vegetative phase (W0.5-W1.0) in "Basalt" until day 10. Then, the slow transition to the DRS lasted 15 days. The control moved very early to TAP at day 2, which needed only 5 days to reach DRS, while "Kontrast" took 13 days to reach the same stage (Figure 4. 1c). The days 5, 13, and 25 after vernalization were considered for further analysis.

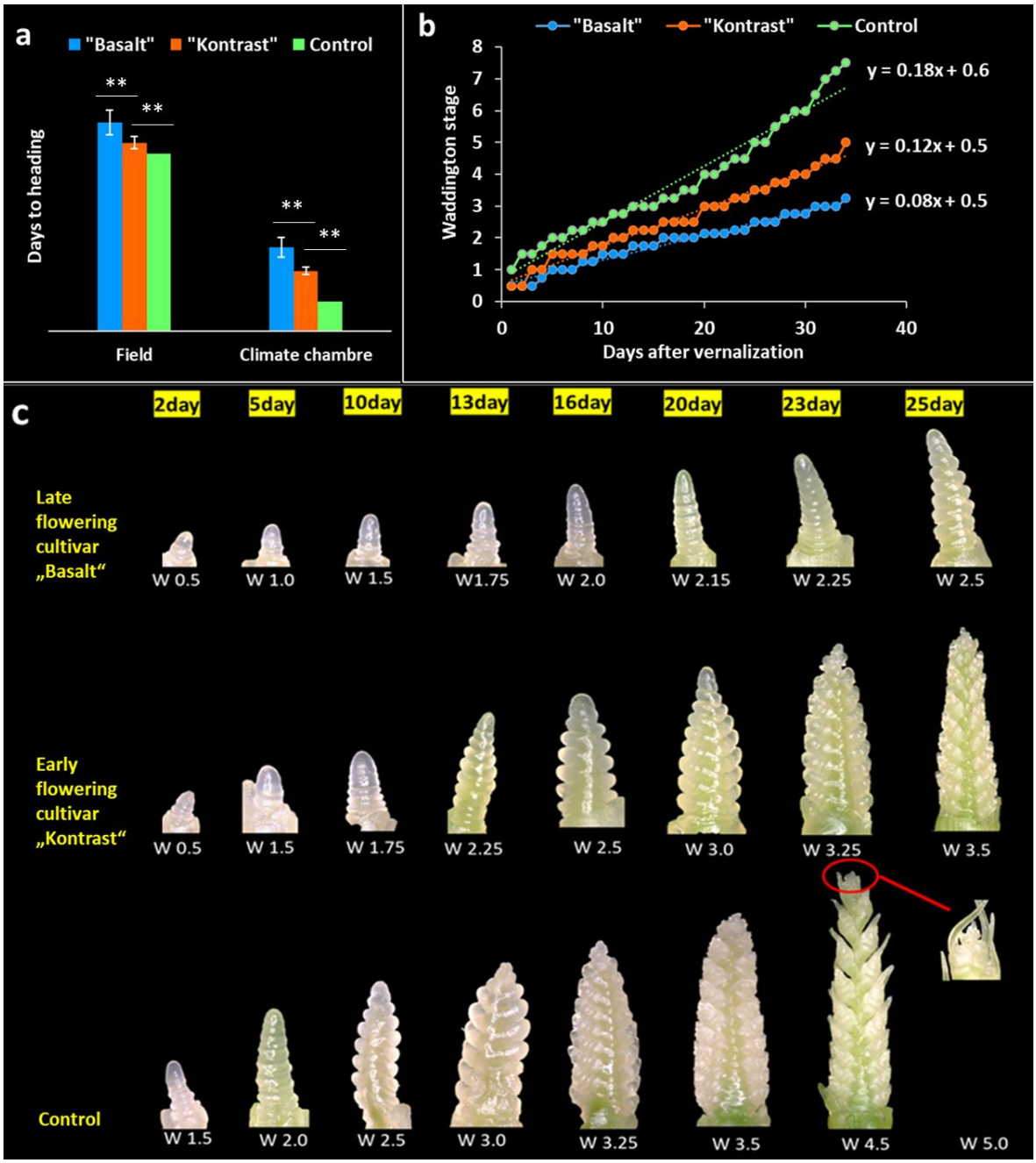

Figure 4. 1: Comparative microscopical development of shoot apical meristem of two adapted cultivars “Basalt” and “Kontrast” showing late and early heading time.

Comparative microscopical development of shoot apical meristem of two adapted cultivars “Basalt” and “Kontrast” showing late and early heading time, respectively. a: Days to heading scored in the field and the climate chamber for the control, “Kontrast” and “Basalt”. ** Significance at <0.01 of the probability level. b: Regression analysis of shoot apex development after vernalization of control, “Kontrast” and “Basalt” according to Waddington scale. c: Microscopical description of SAM development of control, “Kontrast” and “Basalt” from day 2 to day 25 after vernalization.

4.3.2 Description of transcription variants in leaves and shoot apex of early and late flowering cultivars

To identify candidate genes responsible for the floral switch, we conducted whole-transcriptome expression profiling of SAM and leaves of the two adapted early and late flowering cultivars in three selected time points. Counting only mapped and annotated genes, RNA-sequence analysis of 36 libraries yielded 10,533 DEGs in SAM, 31%, 18.4%, and 50.6% were found in time points 5, 13, and 25 DAV, respectively. In leaves, 16,007 DEGs remained, 33.3%, 21.1% and 45.6% were distributed in time points 5, 13 and 25 DAV, respectively. The hierarchical clustering revealed more closeness between the three biological replicates per cultivar and time point in SAM than in leaves. Transcriptional changes between time points occurred more frequently in leaves and the DEGs that showed higher expression levels than the average were more observed both more frequently in leaves as well. The number of positive high expression levels relative to average is greater in "Kontrast" than "Basalt" when considering the apex tissue (Figure 4. 2).

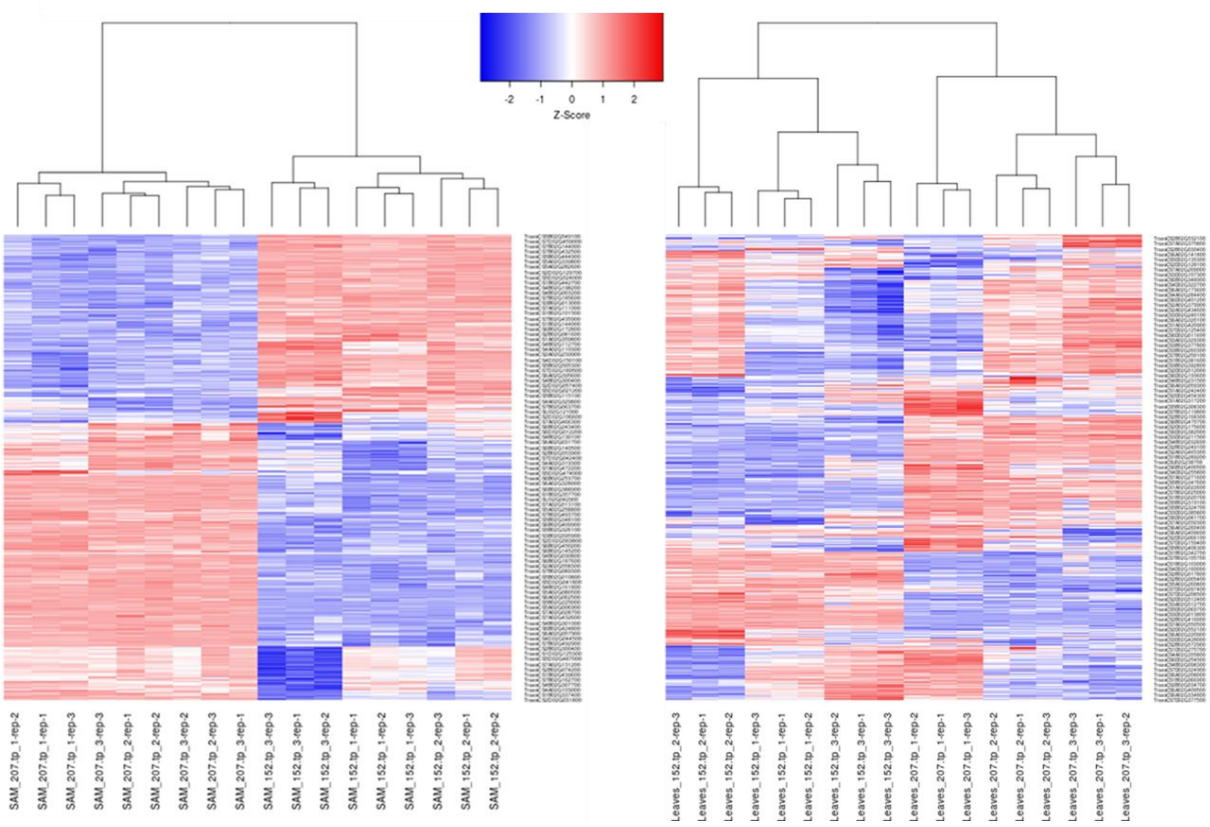

Figure 4. 2: Hierarchical clustering of mapped and annotated DEGs in "Kontrast" and "Basalt" in SAM (right) and leaves (left).

Hierarchical clustering of mapped and annotated DEGs in "Kontrast" and "Basalt" in SAM (right) and leaves (left). Z-score represents the standard deviation from the mean value of all samples. Samples are clustered, based on the Euclidean distance between the expression values of the samples.

4.3.3 Mapping the expressed flowering time regulators in the QTL intervals

The goal was to determine the genes involved in the transition from the vegetative to reproductive phase. For that, we applied a strategy to combine genetic analysis with comparative transcriptomics. The previously four uncovered loci involved in the regulation of flowering time detected in adapted German wheat cultivars (Benaouda et al., under review) plus 17 other significant QTL were used for downstream selection of DEGs comparing "Kontrast" to "Basalt". In total, 664 and 1075 genes were differentially expressed between the cultivars in SAM and leaves, respectively, and could be mapped to the 23 significant QTL intervals (Appendix 4.8 and Appendix 4.9, **https://doi.org/10.5281/zenodo.6624075**). The TAP involved 91 DEGs in SAM and 181 in leaves. In all, 26 DEGs were specific to 13 to DRS in the early flowering "Kontrast" at SAM (31) during the change to the LRP (Figure 4. 3a, b). By contrast, 26% of total DEGs in SAM were co-regulated during all time points, while only 6.2% of genes were continuously regulated in leaves samples. For both organs, the DRS yielded less number of DEGs in comparison to vegetative and reproductive time points. The visualization of DEGs regulation revealed the same three patterns of expression in SAM and leaves: stable up/downregulation in all-time points, up/downregulation in one and two-time points (Figure 4. 3c, d). The $|\log_2$ fold change| which indicates the log-ratio of a gene's expression values ranged from -11.3 for downregulated DEGs to +8.9 for upregulated ones.

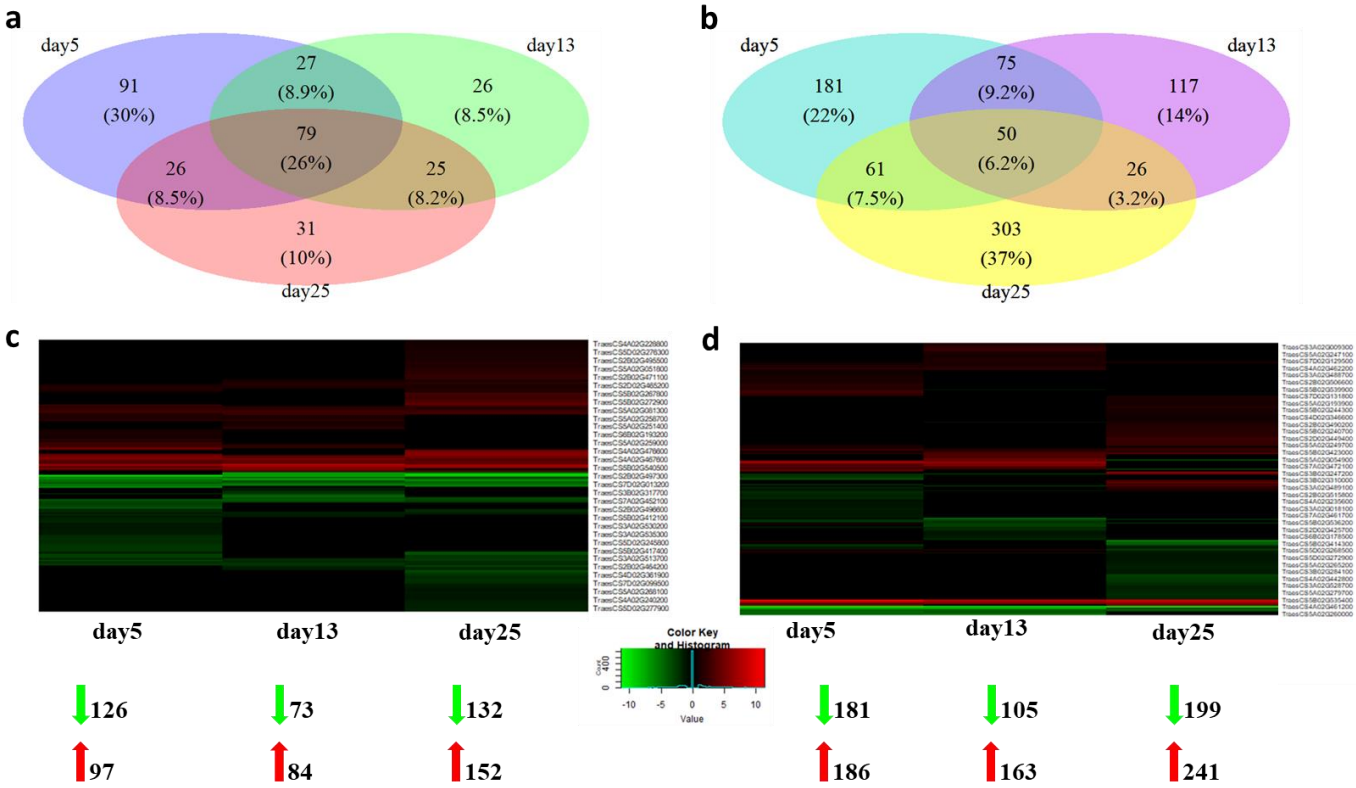

Figure 4. 3: Differential gene expression analysis in SAM and leaves mapped in 23 QTL intervals associated with flowering time trait.

Differential gene expression analysis in SAM and leaves mapped in 27 QTL intervals associated with flowering time trait. a and b: Venn diagrams showing the number and percentages of mapped DEGs in the early flowering "Kontrast" relatively to the late one "Basalt" in 5, 13, and 25 DAV in SAM and leaves, respectively. c and d: Heatmap for visualization of the regulation pattern of mapped DEGs based on fold change estimation between "Kontrast" relatively to "Basalt" in 5, 13, and 25 DAV in SAM and leaves, respectively. The mean value of Log_2 FC includes three biological replicates. Genes not passing FDR <0.05 Fold and change > (±) 2 were set to value =0 (black). The number of upregulated DEGs (red) and downregulated ones (green) are shown at the bottom.

4.3.4 GO enrichment analysis of DEGs in the apex and leaves at the transition phase

Overrepresented functional categories in each time point in the QTL intervals were identified by gene ontology (GO) enrichment analysis in the early flowering "Kontrast" relatively to "Basalt" ($p < 0.05$) (Appendix 4.10, **https://doi.org/10.5281/zenodo.6624075**). DEGs in SAM at TAP were assigned to 20 biological processes, 9 cellular components, and 12 molecular functions. The detected biological processes include cellular process (42.4%), metabolic process (32%), biological regulation (12%), and response to stimuli (8.8%). Most DEGs are localized in the cellular anatomical entity (51.3%), intracellular (36.5%), and membrane protein complex (12.2%). Almost 51% of DEGs have catalytic activity and 30% binding activity. Enriched GO terms for 80 upregulated DEGs were aggregated in histone *H3-K36* demethylation (GO:0070544), regulation of circadian rhythm (GO:0007623), Salicylic acid biosynthetic process (GO:0071446), Jasmonic acid stimulus (GO:0071395), and floral organ morphogenesis (GO:0048444). While the downregulated DEGs were enriched in terms of Cytokinin

transport (GO:0010184), response to temperature stimulus (GO:0009266), vernalization response (GO:0010048), response to light intensity (GO:0009642), and response to red or far-red light (GO:0009639). At DRS, the number of identified biological processes, cellular components, and molecular functions was 16, 8, and 8, respectively. In comparison to TAP, the biological regulation in this phase increased by 16%, while cellular process, metabolic process, and response to stimuli decreased slightly by 38%, 20%, and 7.8%, respectively. More DEGs were centered in intracellular component 40.5% and membrane protein complex 14.4%, and less in cellular anatomical entity 45%. Catalytic activity decreased as well, however, binding activity, enzyme, and transcription regulation activity augmented. Almost the same identified GO terms for upregulated DEGs as in TAP were found enriched in DRS, in addition to the cellular response to Abscisic acid stimulus (GO:0071215) and positive regulation of flower development (GO:0009911). The enriched downregulated DEGs include cellular response to Gibberellin stimulus (GO:0071370), methylation-dependent chromatin silencing (GO:0006346), and fatty acid elongation (GO:0030497). The LRP is characterized by increased biological processes, cellular components, and molecular functions to 25, 12, and 14, respectively. GO terms of upregulated DEGs were involved in the negative regulation of many processes such as MAP kinase activity (GO:0043407) and Cytokinin-activated signaling pathway (GO:0080037). By contrast, regulation of photoperiodism and flowering (GO:0009648) and Abscisic acid-activated signaling are positively controlled. Some downregulated DEGs were involved in the regulation of timing of meristematic phase transition (GO:0048506), floral organ morphogenesis (GO:0048444), and shoot system development (GO:0048367).

In leaves tissue, 367 detected DEGs at TAP are grouped in reproductive process (75), developmental process (107), cellular process (127), and response to stimulus (188). For molecular function, binding, transcription factor and transferase activities assemble 251, 34, and 98 genes, respectively. Involved cellular components are the endomembrane system, plasma membrane, and chloroplast thylakoid. Enriched GO terms for upregulated DEGs include primary shoot apical meristem specification GO: 0010072, histone lysine methylation (GO:0034968), photomorphogenesis (GO:0009640), and photoperiodism (GO:0009648). While the downregulated DEGs were enriched in terms of inflorescence morphogenesis (GO:0048281), regulation of reproductive process (GO:2000241) and flowering, photoperiodism (GO:0048573). In DRS, response to phytohormones such as Abscisic acid, Jasmonic acid, Auxin, and Brassinosteroid has upregulated as well the response to temperature stimulus. Among the negatively controlled GO terms, regulation of timing of the transition from vegetative to reproductive phase (GO:0048510) and vegetative phase change (GO:0010050) could be detected.

In the LRP, 92 DEGs were operating in signal transduction, 76 in reproductive structure development, and 102 in the cellular protein modification process. As molecular functions, nucleotide-binding (109), kinase activity (51) and nucleoside-triphosphatase activity (26) as well transporter activity (51) were detected. Those genes fall into the membrane (200), endomembrane system (76), and plasma membrane

(112). Most activated pathways are related to embryo development (GO:0009908), seed maturation, and the seed dormancy process. By contrast, circadian rhythm, response to Gibberellin, Abscisic acid, Jasmonic acid, and photoperiodism continue to be negatively controlled.

4.3.5 Organ-specific genes at transition phase detected in QTL intervals

This analysis is based on the DEGs detected (Figure 4. 3) and genetic analysis. Among the 91 DEGs specific to the TAP in the apex, three GO terms are related to flowering time: histone *H3-K36* demethylation, Cytokinin transport, and regulation of circadian rhythm (Appendix 4.10, **https://doi.org/10.5281/zenodo.6624075**). Histone *H3-K36* methylation is represented by three homoeologous genes on chromosome 5: *TraesCS5A02G265500*, *TraesCS5B02G265200* and *TraesCS5D02G273400* mapped in QTL TaHd112, TaHd124 and TaHd137, respectively. These genes, coding for the *CUPIN-LIKE* domain are also associated with the regulation of circadian rhythm. Far-red light phototransduction involves two genes *TraesCS3B02G318600* and *TraesCS5B02G422000* mapped in QTLTaHd054 and TaHd129, annotated as *SPA1-RELATED 3* and transcription factor *PIF5*, respectively. The first response to temperature could be detected in leaves tissue as well via the gene *TraesCS5A02G260600* from QTL TaHd112, which encodes a *HEAT SHOCK* protein.

The 26 DEGs, identified specifically in the DRS in the apex, are clustered in four significant ($p<0.05$) GO terms: G-protein coupled receptor signaling pathway, monovalent inorganic cation homeostasis, regulation of the cellular biosynthetic process, and plant-type cell wall modification. Blasting all genes of those pathways led to uncovering the gene *TraesCS3B02G318300* found in QTL TaHd054, which controls the regulation of floral organ identity via MADS-box transcription factor 32. Simultaneously, ethylene regulation is triggered in the leaves because of the expression of *ETHYLENE INSENSITIVE 3* related to gene *TraesCS5B02G265400* (QTLTaHd124) and its homoeologous *TraesCS5A02G265700* (QTLTaHd112). Under the regulation of stomatal movement GO:0010119, the gene *TraesCS7D02G111600* annotated as *FLOWERING LOCUS T* is mapped in the last QTL TaHd177 on chromosome 7D.

GLYCOSYLTRANSFERASE protein encoded by two genes *TraesCS2D02G462500* and *TraesCS3B02G313500*, mapped in loci TaHd038 and TaHd054, respectively, expressed exclusively in the apex at LRP. At this stage, three homoeologous genes *TraesCS5A02G264800*, *TraesCS5B02G264300* and *TraesCS5D02G272800*, localized in loci TaHd112, TaHd124 and TaHd137, respectively, encode the transcription factor *bHLH130* classified under photoperiodism and flowering (GO:0048573). The response to red and far light (GO: 0010114) was detected in the form of transcription factor *PIF3* encoded by *TraesCS2D02G461700* from QTL TaHd038. In leaves tissue, many genes expressed at LRP and related to the circadian clock (GO: 0042752) could be mapped in the identified QTL. For instance, *TraesCS7A02G431600* (TaHd166) and *TraesCS3A02G526600* (TaHd049) encodes *ADAGIO-LIKE* protein and *LUX/PCL1*, respectively. While,

TraesCS4A02G474100 (TaHd073) and *TraesCS7A02G470700* (TaHd166) encode the same Protein *REVEILLE 6 (RVE6).* The expression of the transcription factor *ASYMMETRIC LEAVES (AS1) was* reported to respond to Gibberellin acid encoded by the gene *TraesCS5A02G079100* mapped in the QTL TaHd102.

Among the genes mapped to QTLs that are consistently regulated in the three phases of the floral switch, 547 expressed and 150 GO annotated genes were found shared between SAM and leaves in at least one stage. In this category, *FRIGIDA-like* protein could be identified as a transcription product of the gene *TraesCS5B02G543400* localized in locus TaHd132. *FRIGIDA-like* protein is detected as well at TAP and DRS in the leaves. Many transcription factors were permanently controlled as a response to light such as light-inducible protein *CPRF2* encoded by the genes *TraesCS5A02G057500* (TaHd098) and *TraesCS6B02G182500* (TaHd152) found both in SAM and leaves. In leaves, mRNA cleavage and polyadenylation specificity factor are related to the gene *TraesCS5B02G536400* (TaHd132) and expressed in the three phases. The response to Cytokinin (*TraesCS4A02G228800*, TaHd071), Abscisic acid (*TraesCS5A02G069500*, TaHd099), Auxin (*TraesCS5A02G058700*, TaHd098) and other numerous continuously expressed regulatory transcripts related to glucose, metal (nitrate, iron, zink, and cadmium), phosphorylation, and fatty acid could be mapped in QTL intervals in SAM and leaves (Appendix 4.10, **https://doi.org/10.5281/zenodo.6624075**).

4.3.6 RT-qPCR expression analysis of selected flowering time candidate gene *AS1*

To check the reliability of the RNA-Seq data**, s**ix DEGs (three from each cultivar/time point) were randomly chosen for verification via qRT-PCR. The results showed that the relative gene expression levels of the selected DEGs were consistent with expression profiling resulting from the RNA-seq analysis. One locus TaHd102 (98.3-125.1 Mbp) mapped on chromosome 5A, showing a high association to flowering time trait ($P < 0.0001$) (Benaouda et al., under review), was used for further analysis of DEGs as inferred from the RNA-sequencing data. TaHd102 bears the gene *TraesCS5A02G079100* (98.4 Mbp), encoding the transcription factor *AS1*, which was selected for gene expression analysis using RT-quantitative PCR in SAM and leaves for the three-time points in the early "Kontrast", late "Basalt" and the control (Figure 4. 4a and b). In SAM, The analysis revealed that *AS1* reached its maximal expression in the control in TP1 and TP2, in "Kontrast" in TP2 and TP3, and in "Basalt" in TP3. The same expression pattern was observed in leaves, where the expression level of *AS1* in the late "Basalt" at TP3 is closer to the expression level in "Kontrast" and the control when they reached the DRS than in SAM. The RT-qPCR results are almost in line with RNA-seq expression profiles with more similarity in leaves than in SAM. *AS1* expression in SAM could not be detected via RNA-seq in "Basalt" at TP1 and showed very low levels at the other time points for the same cultivar. Comparing only "Kontrast" and "Basalt", the fold change of differential expression of *AS1* in "Kontrast" relatively to "Basalt" is much higher in RNA-seq output than in RT-qPCR.

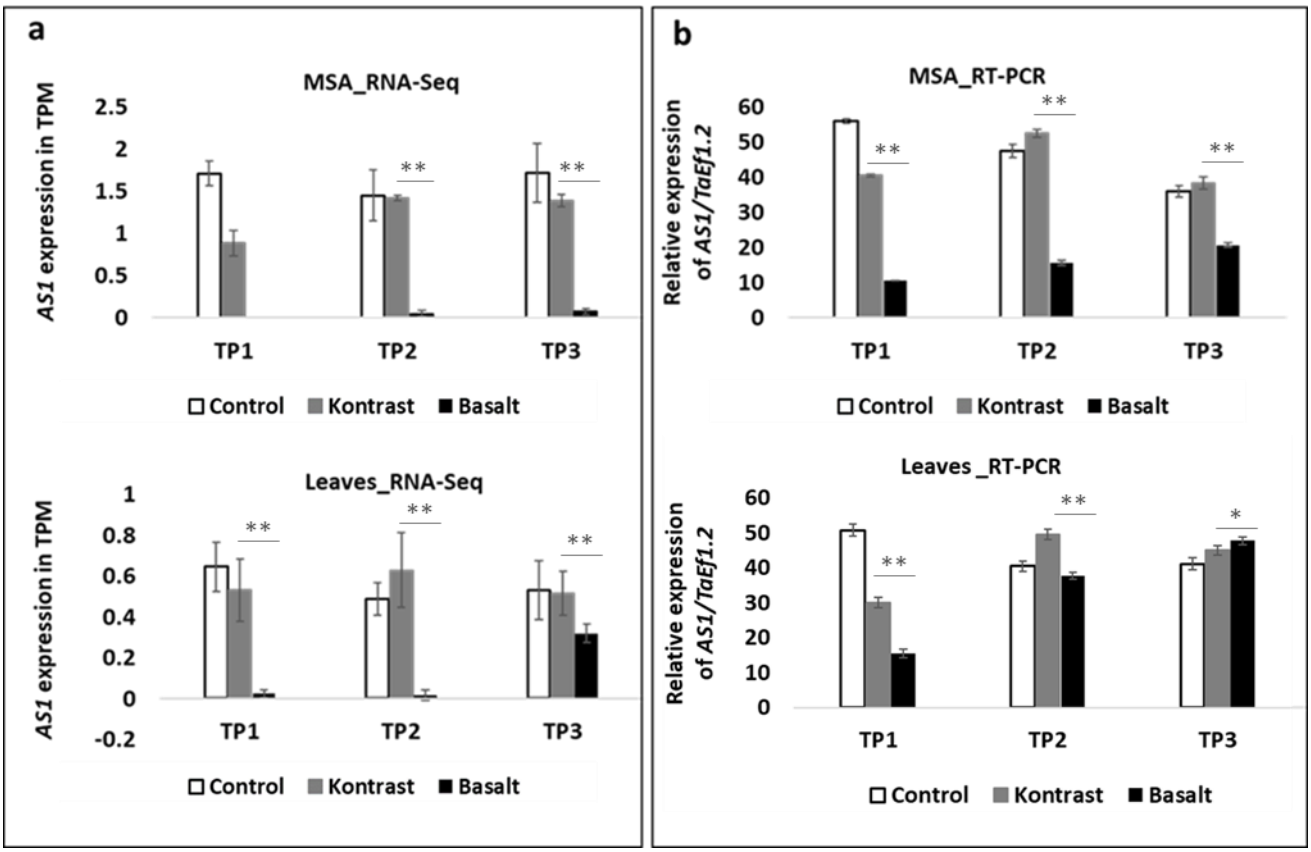

Figure 4. 4: Expression of *AS1* using RT-quantitative PCR in SAM and leaves.

Gene expression *AS1* for the three-time points: TP1 (TAP), TP2 (DRS), and TP3 (LRP) in "Kontrast", "Basalt" and the control. a. Gene expression of *AS1* in TPM (Transcripts Per Kilobase Million) in SAM (up) and leaves (down) using RNA-seq output. b. Expression of *AS1* relatively to the internal control *Ta.Ef1.2* in %. *, ** Significance at the 0.1 and 0.01 probability levels, respectively.

4.3.7 Promoter region analysis of transcription factor *AS1*

The promoter region of the *AS1* gene is highly conserved and 96% of the sequenced 2kb upstream of the start codon is similar in all cultivars (Appendix 4. 2) that share 94.8% of the conserved TF binding site of their 2kb promoter regions. The alignment output uncovered a deletion of eight single nucleotides in "Basalt" between positions 225 and 231 upstream of the translation initiation site compared to control. In the same region, "Kontrast" revealed a deletion of only three single nucleotides in its promoter region from the same region detected in the control (Figure 4. 5). This polymorphism is followed by one SNP (C/T) at position 232 where nucleotide T in the two adapted cultivars "Kontrast" and "Basalt" is substituted by C in the exotic control. The sequence TCCCCCCCTCTCTCTCTCTCT (http://planttfdb.gao-lab.org/tf.php?sp=Tae&did) is the core motif of the TF *Traes_1AL_6B108514B* from *MADS BOX* TF family.

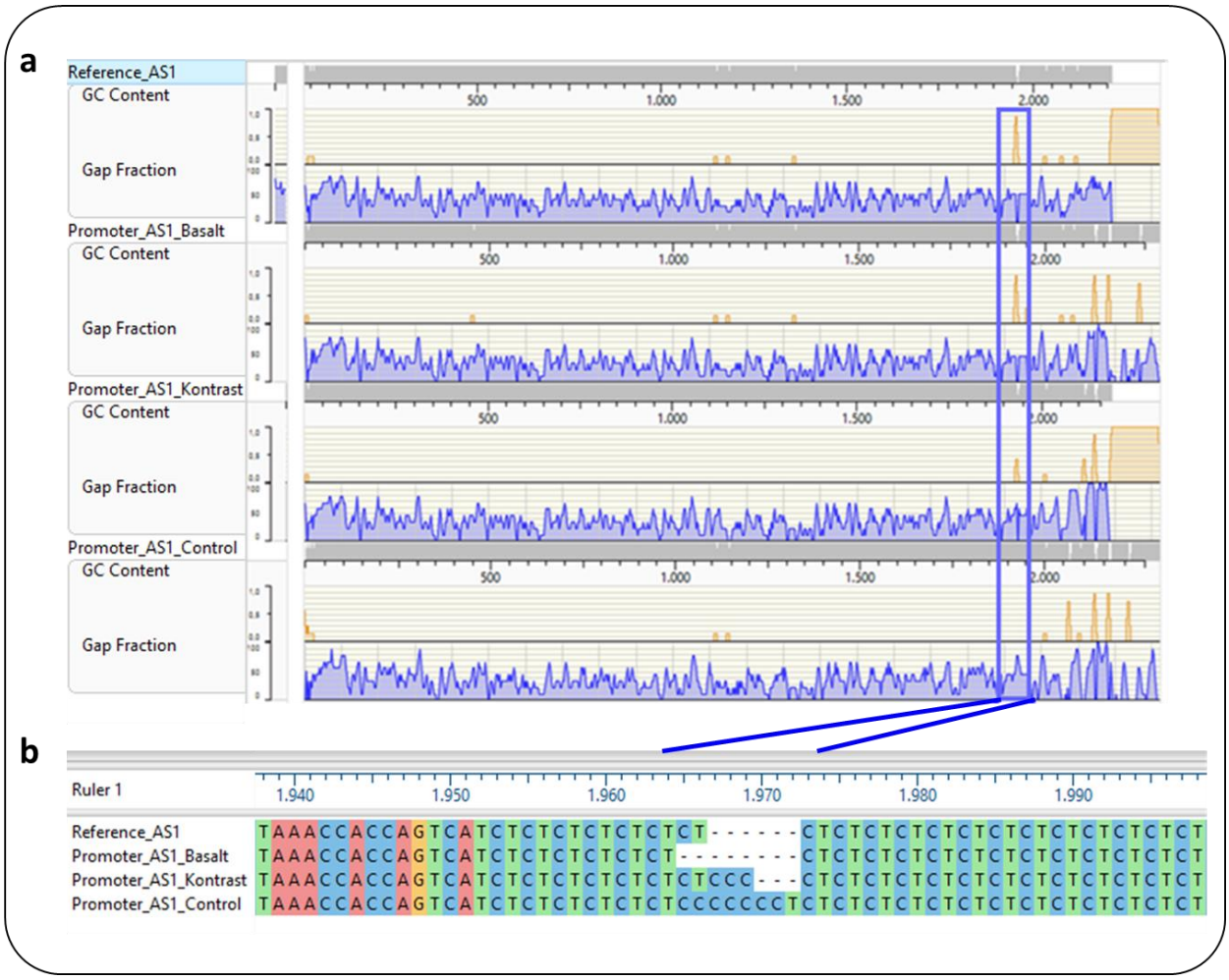

Figure 4. 5: Alignment of *AS1* promoter region (2kb) sequence in cultivars "Basalt", "Kontrast" and the control.

a. in cultivars "Basalt", "Kontrast" and control compared with the reference sequence from EnsemblPlant database. GC content and Gap fraction are indicated in blue and orange lines, respectively. b. Comparison of the motif sequence of the TFBS CTCTCTCCCCCCCTCTCTCTC in the three cultivars and the reference sequence at positions 1972-1966 bp.

4.4 Discussion

4.4.1 Assessment of flowering behavior by microscopical phenotyping of the SAM

In this study, the earliest and latest flowering cultivars “Kontrast” and “Basalt” were subject to microscopical visualization of SAM development. This comparative analysis revealed the acceleration of the apex development of “Kontrast” compared to “Basalt” in the three phases of the transition from vegetative to reproductive stage, and consequently, asserts the early flowering behavior of “Kontrast” in the field. Furthermore, from the vegetative apex stage, no overlapping in SAM growth was observed between both cultivars during the floral monitoring, which means that the difference in progress rate from one stage to the next was stable between both cultivars; this is shown by comparing the regression slopes of SAM development after vernalization in “Kontrast” and “Basalt”. Before the DRS, the spikelets are induced at day 5 in the control, whereas the LRP arises in more than 15 days. Thereby, spikelets are initiated at a much faster rate than after the DRS. Many studies have reported that the dynamic of the floral initiation marked by the first spikelet primordium until the initiation of the last one is much accelerated compared to that of the terminal spikelet to anthesis (floret primordia) (Ochagavía et al., 2018; Prieto et al., 2018). The duration of the early RP (double ridge) determines the number of spikelet primordia initiated on the shoot apex (Alqudah & Schnurbusch, 2014; Gustavo A Slafer et al., 2015). However, no significant difference in spikelet primordia counts (six to seven) was observed in the late flowering “basalt” compared to the early one “Kontrast”, even when the reproductive stage lasted 25 days in “Basalt”. The number of fertile florets developed within the spikelets is defined in the LRP (Gustavo A Slafer et al., 2015). For this trait, the comparison between “Kontrast” and the control (flowers earlier than “Kontrast”) showed no relation in the duration of the LRP. This can be explained by the fact that the final number of fertile florets is depending more on the number of florets that survived the degeneration and death mechanisms after floret initiation than on the duration of floret formation (Guo & Schnurbusch, 2015; Kirby, 1988). On the other hand, the switch to constant long days and ambient temperature conditions after vernalization reduced significantly the number of days to heading in all cultivars, including the control, compared to field conditions. This result leads to conclude that the response to environmental stimuli such as light, photoperiod, and ambient temperature has a quantitative nature, while the stable heading time range is due to established genotypic differences among cultivars.

4.4.2 Identifying candidate genes by integrating QTL mapping and RNA-seq

Few genes could be discovered in association with spike development in wheat (Boden et al., 2015; Dobrovolskaya et al., 2015; Feng et al., 2017). Flowering time is a measurable feature and quantitative trait whose genetic regulation is strongly relying on Genotype ^{X} Environment interaction. In a previous study on the genetic control of HD in multi-environment trials over Germany, 27 QTL stably expressed in different environments have been detected (Benaouda et al., under review). Merging QTL mapping and transcriptome sequencing analysis is a complementary strategy used successfully for studying

abiotic stress and flowering time mechanisms in important crops like rapeseed, maize, and wheat (Duarte-Delgado et al., 2020; J. Song et al., 2021; Wei et al., 2021).

4.4.3 Histone methylation and light response regulate the transition apex phase

Several pathways were upregulated in SAM and leaves tissues to promote the switch from vegetative to TAP (5 DAV). For example, genes Histone *H3K36* methylation are detected in three homoeologous loci (three QTL) on chromosomes 5A, 5B, and 5D. *H3K36* was found to induce flowering by activating alternative splicing and plant plasticity to fluctuating ambient temperature in *Arabidopsis* (Pajoro et al., 2017) and rice (Lu et al., 2013). Interestingly, the same homoeologous genes are involved in the regulation of circadian rhythm as well. Circadian clock and histone methylation are connected pathways. *H3-K36* was found to antagonize the binding of *Arabidopsis* clock repressor *TIMING OF CAB EXPRESSION(TOC1)* ensuring that repression occurred at the proper time during the day and night cycle (oscillation) via chromatin changes (Malapeira et al., 2012; Perales & Más, 2007; Song & Noh, 2012). Light is a signaling cue that controls many aspects of plant growth including the induction of flowering (Kami et al., 2010). Some expressed light signaling components were downregulated and mapped in two loci such as *SPA1 (SUPPRESSOR OF PHYA-105) -RELATED 3*/TaHd054 which reduces the persistence of *PHYA* signaling and function in concert with *PHOTOMORPHOGENIC1(COP1)* to suppress photomorphogenesis in the dark (Baumgardt et al., 2002; Ordoñez-Herrera et al., 2015). The second gene, *PHYTOCHROME INTERACTING FACTORS 5* (*PIF5*/TaHd129) functions negatively in *PHY*-mediated pathways and reduces red light sensitivity (Fujimori et al., 2004). S*PA* and *PIF-like* genes have not been functionally validated in temperate grasses thus far. The response to low light intensity stimulus was found to be downregulated at this stage as well. One gene annotated in wheat as "light-harvesting chlorophyll a/b-binding protein (*LHCB*)" is classified in very-low-fluence responses and involved in inhibition of hypocotyl elongation and promotion of cotyledon expansion (Chiara Mustilli & Bowler, 1997) in *Arabidopsis*. Moreover, the response to low-fluence blue light represses a *Pirin-like* gene. *M*utant plants for this gene in *Arabidopsis* flower earlier than wild-type plants (Orozco-Nunnelly et al., 2014).

4.4.4 *TaAGL14* activates the floral switch and SNP at *VRN3* represses it in the double ridge stage

The highlight result in the double ridge stage is the detection of the MADS-box transcription factor 32 in QTL TaHd054. MADSS32 wheat gene (*TraesCS3B02G318300*, SAM) is the ortholog of *OsMADS32* that regulates floral patterning in rice and takes charge of floral meristem identity and initiation through interactions with multiple floral homeotic genes to sustain floral organ development (Hu et al., 2021). BLAST results showed that the predicted protein of *TraesCS3B02G318300* is identical by 99% with *TaAGL14*, 98% with *TaAGL15* in wheat, and 87% with *OsMADS32* in rice. Furthermore, *TaAGL14*, *TaAGL15*, and *OsMADS32* together, form a distinctive clade of *MIKC*-type gene family found only in grasses with no representatives from *Arabidopsis* (Zhao et al., 2006, Liu et al.,2020) reported the

involvement of *TaAGL14* in stamen and pistils development in wheat. Here, we provide the first evidence about the function of the *TaAGL14* gene in an earlier reproductive stage in floral meristem activation in wheat, which may very likely be similar to *OsMADS32* function in rice. *TraesCS3B02G318300* was 4.5 fold more upregulated in "Kontrast" than in "Basalt", which is in line with the activator role of *OsMADS32* in initiating the floral meristem and its role in the termination of floral meristem activity and repressing its reversion to vegetative meristem (Hu et al., 2021). *FLOWERING LOCUS T* (*FT*) (QTL TaHd177), from *Phosphatidylethanolamine*-binding protein (*PEBP*), was exclusively detected in the DRS in leaves tissue. Surprisingly, *TaFT1* transcription was strongly downregulated by $\log_2$FC = - 8.6 in the early "Kontrast" relatively to late heading "Basalt" cultivar. This fact contrasts with the well-documented function of *FT* as a floral promoter in *Arabidopsis*, rice, barley, and wheat. Actually, *FT* can be a floral repressor, too. It was reported that, because of gene duplication event(s), paralogs of *FT* with an antagonistic function were generated in sugar beet (*Beta vulgari*s L.) and tobacco (*Nicotiana tabacum* L.). In sugar beet, the first protein *BvFT1* acts as an inhibitor of the floral switch, whereas a second *FT-like* paralog protein *BvFT2* works as a promoter (Pin et al., 2010). This is due to synonymous mutations in specific amino acids allowing the conversion of *BvFT1* to *BvFT2* and *vice versa* (Pin et al., 2010). The tobacco genome harbors three *FT* floral inhibitors *NtFT1*, *NtFT2*, and *NtFT3*, and the fourth paralog *NtFT4* is a floral inducer (Harig et al., 2012). The same phenomenon was discovered in *Arabidopsis* and tomato (Cao et al., 2016; Hanzawa et al., 2005). This means, we may detect a copy of *FT* in wheat with the QTL effect showing an opposite function and acting as a floral repressor, which can explain the negative regulation of *FT* transcription in the early flowering "Kontrast" genotype. To examine this hypothesis we sequenced the coding sequence of the gene *TraesCS7D02G111600* (1026 bp) and performed an alignment of translated amino acids against the *TaFT1(VRN3)* protein on chromosome 7B (Figure 4. 6a and b). Among seven SNPs, three found in the first exon are synonymous, where a substitution of single nucleotide T/G leads to the change of the third amino acid valine to glycine. The second SNP G/A in the 23rd amino acid substitutes valine with isoleucine and the third SNP G/C in the position 56th coverts glycine into alanine (Figure 4. 7a and b). In wheat, the role of *TaFT1(VRN3)* on chromosome 7B is determined, while no validation of the homologs function on chromosomes 7A and 7D as floral inducers were reported so far. On chromosome 7D, two copies of *PEBP* are localized at 68.4 and 191Mbp (Ensembl plants database). As locus TaHd177 (63.5-73.8Mbp) includes the first copy (68.4Mbp), we tend more towards the supposition that the antagonistic player of *TaFT1* on chromosome 7B is very likely its homoeolog *TraesCS7D02G111600* on chromosome 7D mapped at 68.4Mbp. Further analysis is required to prove the responsibility of substituted amino acids in altering the role of the wheat *FT* from an inducer (*TaFT1* in 7B) into an inhibitor (*TaFT1* in 7D) in the flowering time pathway, as it is the case in many other plant species.

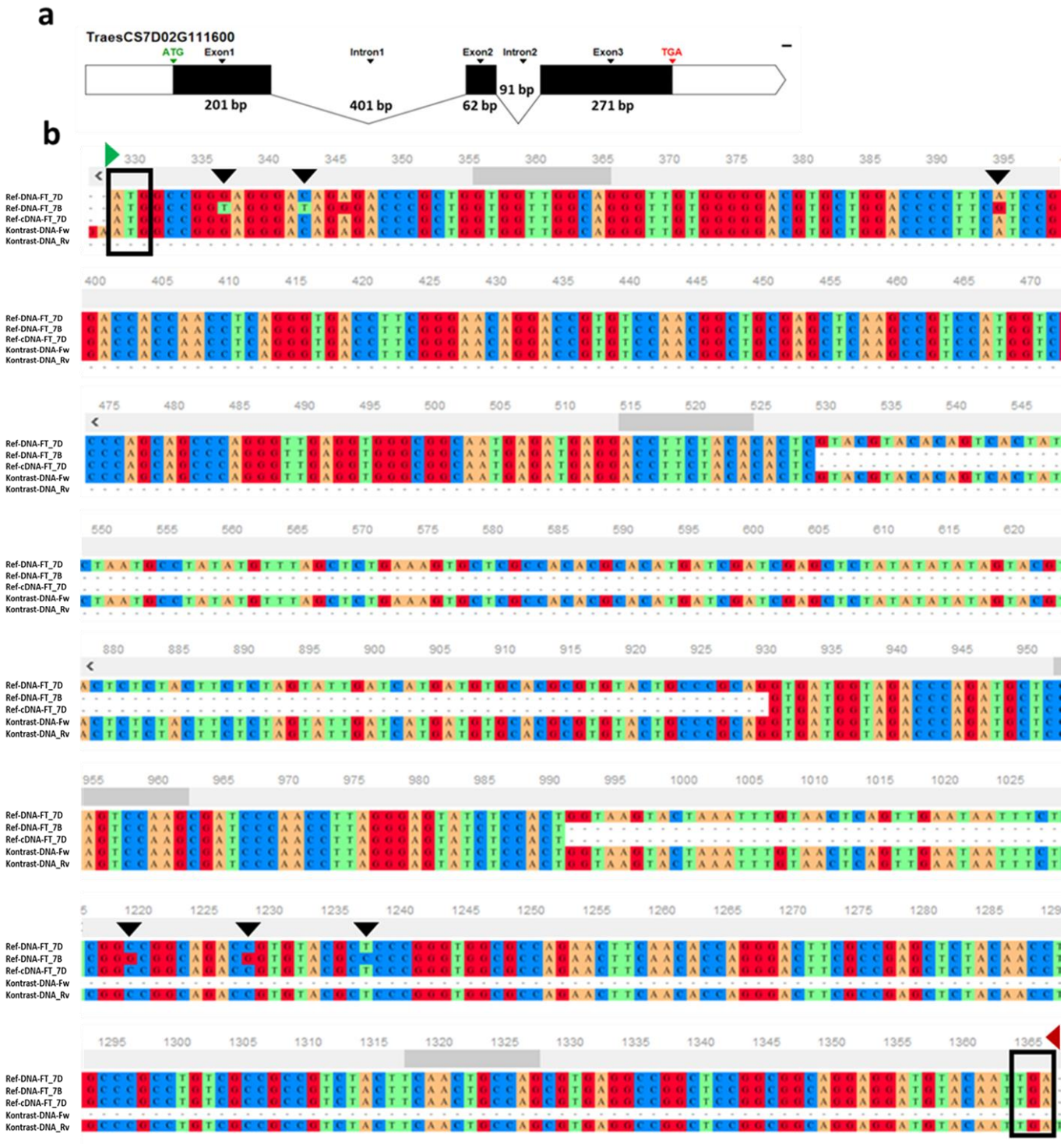

Figure 4. 6: Coding sequence alignment of the gene *TraesCS7D02G111600* encoding *Flowering locus T*.

a. Structure of the gene *TraesCS7D02G111600* mapped on chromosome 7D in early flowering cultivar "Kontrast" that contains three exons and two introns. b. Alignment output of the gene *TraesCS7D02G111600* (forward and reverse sequences) with its homoeologous *(TaFT1)* mapped on chromosome 7B and the in *Silico* reference cDNA. Start and stop codon's positions are indicated in green and red arrows, respectively. SNPs are highlighted with black arrows.

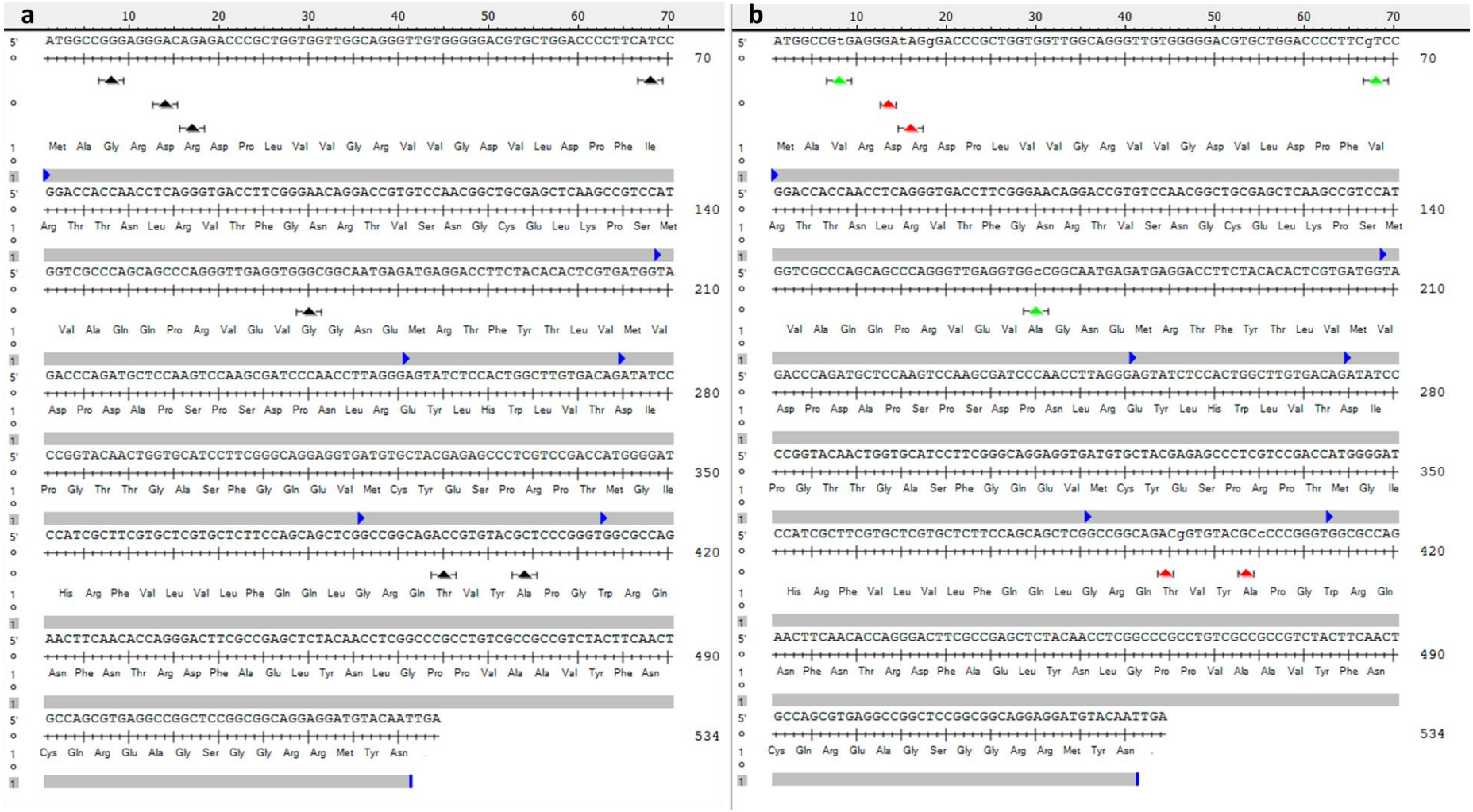

Figure 4. 7: Full translation of the *Flowering locus T* protein encoded by the gene *TraesCS7D02G111600*

a. Using the ORFs finder of DNAstar, Seqbuilder tool, the first ORF on top gave the longest and continued translation (176 amino acids). The alignment with the *VRN3* coding sequence lead to detect seven SNPs indicated with black arrows. b. Effect of nucleotide substitution on amino acid change. Synonymous and non-synonymous SNPs are indicated by green and red arrows, respectively.

4.4.5 Circadian clock is involved in hypocotyl and stem elongation in the reproductive phase

During the LRP, stem internodes elongate, and the floret primordia develop into flowers (Waddington et al., 1983). In this phase of spikelet development, some expressed flowering time key regulatory elements were mapped in QTL intervals. The transcription factor basic *HELIX–LOOP–HELIX* (*bHLH130*) was identified in three homoeologous loci on chromosomes 5A, 5B, and 5D. *bHLH130* annotated as *FBH4* (*AT2G42280*) binds to the E-box cis-elements in the *CONSTANS (CO)* promoter. The overexpression of *FBH4* strongly increases *CO* transcription and causes early flowering in *Arabidopsis* and rice (Ito et al., 2012). This is in full agreement with our results showing differential upregulation of *bHLH130* in "Kontrast" by 5.4, 8.5, and 4 fold at loci TaHd112, TaHd124, and TaHd137, respectively. We conclude that the copy mapped in QTL TaHd124 on chromosome 5B has more effect than other homoeologous regions. *LUX/PCL1* belongs to clock players of the evening complex expressed in the night to regulate the nocturnal rhythmicity of the circadian clock (Hazen et al., 2005). Moreover, the *ELF4-ELF3-LUX* complex is regulated by the clock and light. It represses the expression of *PIF4* and *PIF5* required for hypocotyl growth in the early evening. *PIF4/5* regulation is turned over at dawn to permit maximal hypocotyl growth in *Arabidopsis* (Nusinow et al., 2011). The expressed orthologue of *LUX/PCL1* in wheat was mapped in QTLTaHd049 and was by $\log_2$FC = 5.9 upregulated in "Kontrast". We deduce that the regulation of circadian rhythm is more pronounced in the early flowering cultivar and this occurs in the late reproductive phase where the stem elongation initiates. We suggest that *LUX/PCL1* may be involved in the oscillator growth of the stem under circadian clock control as in *Arabidopsis*. QTL TaHd166 harbors the gene encoding *ZTL* orthologue in wheat and was found downregulated in "Kontrast". This finding agrees with the reported results in *Arabidopsis* that over-expression of *ZTL* results in downregulation of *CO* and *FT* expression, leading to delayed flowering under long-day conditions (Kiyosue & Wada, 2000; Somers et al., 2004).

4.4.6 Allelic variation in the promoter of *AS1* is associated with HD variability

QTL TaHd102 on chromosome 5A is strongly associated with heading date and explains 13.8% of the genetic variance observed in the German wheat germplasm (Benaouda et al., under review). *AS1* is the only annotated transcript in this locus known to be involved in the flowering time pathway in the *Arabidopsis* background. We conclude that the effect of QTL TaHd102 on heading variation is most likely due to the gene *TraesCS5A02G079100* encoding AS1 protein. *AS1* is required for normal cell differentiation and leaves patterning by direct suppression of *KNOTTED-like HOMEOBOX (KNOX)* gene expression at leaves primordia in *Arabidopsis* (Byrne et al., 2000; M. Guo et al., 2008). *KNOX* proteins repress the GA biosynthesis gene *AtGA20ox1*, thus *AS1* is possibly mediating the Gibberellin pathway (Hay et al., 2002). In this study, RNA-seq and RT-qPCR confirmed the association of the expression of an *AS1* transcription factor with the early flowering time. This leads to conclude that the floral transition in wheat involves GA biosynthesis besides vernalization, photoperiod, and earliness *per se*. On the other hand, *AS1* forms a functional complex with *CONSTANS (CO)* to activate *FLOWERING*

LOCUS T in photoperiodic *Arabidopsis* as reported by Song et al. (2012). We found that transcription factor *bHLH130 (FBH4)* is strongly upregulated in the early flowering "Kontrast" and this *TF* binds directly to the E-box cis-elements in the *CONSTANS (CO)* promoter. We have no evidence that *AS1* is interacting with *CO*, as is the case in *Arabidopsis*; however, we provide first insight that *AS1* and *FBH4*, which activates *CO*, are inducing the floral switch and expressed both in leaves during the RP in wheat. In addition, the polymorphism in the promoter region of *AS1* in the studied cultivars concerns the core motif of the well-described *AGAMOUS-LIKE MADS-BOX* protein *AGL20* (*AT2G45660*) known as *SUPPRESSOR OF CONSTANS OVEREXPRESSION 1 (SOC1)*, which acts as an activator of flowering time in *Arabidopsis* (Lee et al., 2000) and rice as well (Lee et al., 2004). *SOC1* expression is induced as a response to GA (Moon et al., 2003) by integrating the signals from vernalization (Searle et al., 2006) and photoperiod (Hepworth et al., 2002) in *Arabidopsis*. In light of that, we deduce that the deletion of TFBS of *SOC1* in the promoter of *AS1* is likely associated with late flowering time in wheat and *AS1* requires *SOC1* to induce flowering time in GA response. The direct interaction between *SOC1* and *AS1* has been not reported so far, even in the *Arabidopsis* background. Further explorations are necessary to confirm this interaction *in vivo* and in *vitro.*

4.5 Conclusion

In the present study, we investigated the transcriptome profiling at the transition to the reproductive stage, which uncovered stage and spatial tissue-specific QTL in winter wheat. In total, 664 and 1075 DEGs in early "Kontrast" compared to late "Basalt" in SAM and leaves, respectively, could be mapped in 27 QTL intervals associated with heading time. We showed that the transition apex, double ridge stage, and reproductive phase are decisive steps in the floral switch process in which some key flowering time-related genes are activated for responding to external and internal stimuli such as light, ambient temperature, and day length change. The spatial expression of those genes in specific tissues grants first insights into possible cross-talk and signals migrations from leaves to SAM and *vice versa*. We have uncovered a potential antagonist of *VRN3* on chromosome 7D acting as a repressor of flowering time due to polymorphisms in critical amino acids of the coding sequence. The allele harboring SNPs are mapped in QTL177 showing significant association to heading trait. We detected the involvement of GA mechanisms in the flowering time pathway in wheat via the expression of *TraesCS5A02G079100* encoding *AS1* protein. *SOC1* binds *in silico* to a specific TFBS in the promoter of *AS1*, and both genes respond to GA biosynthesis for inducing flowering time. Our results enrich the knowledge and understanding gained so far in the transition to the reproductive phase in wheat on genetic and molecular levels.

Chapter 5: General discussion, conclusion, and perspectives

Why it is important to study flowering time?

Flowering is a developmental stage that permits the plant to develop its reproductive organs after reaching an advanced standard of growth. This critical physiological event is the response to environmental interaction, which causes biochemical cascades of reactions and interactions at different internal tissues, organs, and releases signals that make the plant moves from vegetative status to a reproductive phase. The start and duration of the floral transition depend on two physical dimensions: time and space. The plant senses what time of the year in what region on the earth flowering can take place. The plant senses the environment and adapts its flowering at the optimal time depending on space. Moreover, the plant can wait for favorable conditions to protect the sensitive and precious reproductive organs that guarantee the survival of its species. After starting, the flowering process can be accelerated or slowed down up to a couple of weeks, which reflects the huge elasticity and complexity of flowering time. Due to its property to be adaptable to a wide range of environments, which is becoming evident in many crops, flowering time is the "joker" trait that breeders can manipulate for producing high yield performant cultivars capable to acclimate to different climates and geographical regions (Guedira et al., 2016). In this chapter, we discuss how the findings of this thesis contribute to improving our understanding of the genetic regulation of one of the most perplexing phenological traits, having inscrutable interaction with the environment and great agronomical importance.

Genetic potential of the European wheat for studying flowering time

Over decades, an unlimited number of studies tried to investigate the genetic architecture of flowering time in *Arabidopsis* before extending the focus on more genetically complex but economically important monocots crops such as wheat. Wheat is cultivated worldwide by dint of its large natural variation, which has been favored by allelic diversity in genes regulating growth and developmental stages, especially flowering time. European wheat germplasm served as potential material for this purpose. This study is the first one to investigate the environmental effect on flowering time in 17 environments using a diverse panel of European winter wheat cultivars. Multi environmental trials repeated for more than one year lead to more credible estimations of genotypic variance. Our analysis showed that all cultivars respond very differently to the 17 environments and that the genetic response of HD is more dependent on location than on year. On one hand, this result is contrasting with the finding of Reif et al., (2011) and Langer et al., (2014), which reported that the variance components due to genotype by environment interaction are very low compared to the variance components of genotype. Experimental factors in both researches such as few and close locations, replication of only one year, and less number of tested genotypes per trial are very likely elements that can bias or underestimate the real magnitude of essential environmental factors namely location and year in explaining the genetic variance observed in flowering time. On the other hand, we confirm the high heritability mentioned previously, which ranges between 0.89 and 0.96. This indicates that genetic variation explains a large part of the phenotypic differences in the time of flowering. The European germplasm stores an immense genetic potency to dissect the

architecture of polygenic traits like flowering time, but not independently of the environment. Thus, this material can tell more about the climate effect and adaptation if it is efficiently exploited in multi-environment trials for a couple of years.

The competition between temperature and day length to induce heading

In this study, we propose for the first time the “growing degree day" (GDD) as a thermal growth indicator to estimate, not the duration of a phenological stage, but rather the beginning of the developmental stage “heading” for fixing a new reference date, which is environment depending date, recording thus the climatic effect. This approach enables the comparison of the measurements with those taken from one general fixed date. This allowed us to achieve one of the main goals of the study namely “to assess, with high accuracy, the interaction of heading time with the environmental stimuli in a geographical context. Very few publications analyzed the effect of environmental components on flowering time in *Arabidopsis* regarding a geographical dimension such as altitude (Lewandowska-Sabat et al., 2017), longitude (Samis et al., 2012), or latitude (Stinchcombe et al., 2004). In the current research, we present, the latitude-associated genotypic response linked to two major climatic factors (temperature and daylength) affecting HD. We showed that plants are adapted to use temperature as a sensor of favorable conditions for starting HD in lower latitudes but use photoperiod as a more reliable indicator of the changing seasons in higher ones. This cause-effect relationship (latitude, temperature, photoperiod, genotypic response, and heading time) has not been reported before. Villigas et al., (2016), by comparing the phenological development of spring wheat between Spain and Mexico, reported that the long day length is more responsible for short “sowing to anthesis” duration than the temperature in a latitude range of 22°. In this context, the clear relationship between latitude and heading could be easily uncovered. We conclude that the smallest the special scale is, the more complex the response of flowering time to the interplay of environmental factors. This assessment gained more evidence at least for the latitude gradient through this study based on well-structured and accurate statistical analysis.

GWAS and epistasis uncovered novel flowering time loci in wheat

Before looking for novel QTL involved in flowering time control, it was necessary to check first, the genetic background responsible for the growth habit of the studied association panel. All German adapted cultivars harbor the same winter alleles of vernalization genes *vrn-1/Vrn-2* that are behind the strict winter habit requiring a long exposure to cold. Up 95% of the adapted material carry the photoperiod sensitive allele *Ppd-D1b*, which indicates the successful establishment of specific *VRN* and *PPD* alleles as a result of long-term adaptation to winter conditions in the genetic background of the German elite cultivars. These results are in line with Langer et al., (2014) findings, except for the detection of the spring allele *Vrn-3Bc* in all adapted cultivars that our PCR screening showed. We cannot explain where this allele is coming from, but we are convinced of the PCR output, especially as the winter form *vrn3* could not be detected. The existence of this allele does not influence the vernalization

requirement of the cultivars that harbor it, due to the effect of *vrn-A1*, which has a greater impact on growth habit than *Vrn-3Bc* (Chen et al., 2013). Subsequently, 10.4 days difference in heading date observed in this germplasm is not due to allelic variation at vernalization or photoperiod genes, but rather to the genetic variation at other regulatory elements of flowering time. Indeed, incorporating QTL × environment interaction in GWAS uncovered the stable QTL TaHd102 on chromosome 5A. The allelic variation at this locus alters HD by 1.2 days independently of the environment and related climatic conditions. An SNP effect of 1.2 days is not to underestimate for adapted germplasm. Increasing the genetic variation using the non-adapted cultivars led to identifying the exotic allele at QTL TaHd044 on chromosome 3A, which decreases the heading time by 5.6 days and explains up to 33% of the genetic variance. The interplay of climate drivers and the effect of their competition, governed by latitude gradient, is translated into a selection of fine-tuning loci that respond to the dominant environmental factor in a specific latitude for the adjustment of flowering time. Thermosensitive genes seem to be selected in the response to temperature in lower latitudes, while a gene related to the circadian clock and photoperiod could be detected in higher ones. Comparing these results with other QTL previously reported (Griffiths et al., 2009; Hanocq et al., 2007; Kuchel et al., 2007; Langer et al., 2014; Zanke et al., 2014), we confirm that both QTL TaHd102 and TaHd044 have not been published before. As mentioned in chapter 2, the studies of the epistatic interactions involved in flowering time control in European wheat reported opposite results. Our analysis revealed significant interactions among the genetic loci that explain up to 7.8% of the genetic variance, which is not matching the output of Langer et al., (2014). This later reported that epistatic interactions have a very small contribution to the genetic regulation of flowering time. Furthermore, we discovered a pivotal epistatic role of *VRN2* in controlling heading time in wheat. Based on uncovered genetic interactions with other loci, we concluded the involvement of this known crucial flowering repressor in interplaying regulatory effects. Similarly, Reif et al., (2011) evoked the putative role of *VRN1* in epistatic interactions in heading time regulation. Remarkably, a locus TaHd098 that has a small QTL effect in the adapted wheat, showed a strong epistatic effect by the use of the non-adapted germplasm in the analysis. Some of the 15 interacting loci were mapped very close to key regulatory elements of flowering time in *Arabidopsis*.

Stage and spatial tissue-specific QTL regulating flowering time in winter wheat

Chapter 3 was dedicated to studying the environmental effect on heading date and the genetic response to the interaction with specific climate attributes. Many loci with stable, fine-tune and epistatic effects could be detected. In chapter 3, we described the molecular analysis, in which we joined loci showing stable effect to transcriptome profiling at the heading phase for identifying organ and stage-specific candidate genes in winter wheat. On one hand, stable QTL regulate flowering time independently of environment change due to location factor. On the other hand, adapted material showing as well a stable flowering behavior in different environments was logically selected for this analysis, as the loci were detected in the adapted germplasm. Even though four QTL were strongly associated with flowering

time, we extended the list to 23 loci that are statistically significant to explore as much the pathways and responses revealed by RNA-seq. Combining genetic and molecular analyses is a recent strategy that proved its efficacy in a couple of studies dealing with flowering time in Brassica species (Jian et al., 2019; Song et al., 2021; Wei et al., 2021) and maize (Song et al., 2017). In our study, this approach led to mapping 664 and 1076 DEGs in the early flowering cultivar compared to the late one in the SAM and leaf tissue, respectively. Candidate gene approach and association mapping through GWAS excluded the involvement of the known vernalization and photoperiod genes in controlling the genetic shape of flowering time in the adapted germplasm due to adaptation. However, RNA-seq gave insights that other genetic regulators related indirectly to these pathways, acts upstream or downstream of *VRN* and *PPD* genes, could be detected, like DEGs linked to circadian rhythm and the response to light, which are expressed mostly in TAP and DRS. This result is consistent with the finding of Jian et al., (2019). GWAS detected an important vernalization player mapped on chromosome 7D that we believed first is a promoter of flowering time like its homeolog *VRN3* located on chromosome 7B. Surprisingly, RNA-seq and sequencing of the coding region revealed that we have detected an antagonist of *VRN3*, acting as a repressor of flowering time in DRS. Several regulatory genes, classified under autonomous pathway, expressed in the biosynthesis of phytohormones, phosphorylation, fatty acid, sugar, amino acid, and metal ion transporters might prime the plant and increase its ability for starting the floral switch under long days (Digel et al., 2015). Gibberellin biosynthesis is one of the four mechanisms controlling flowering time in wheat. In response to Gibberellin signaling, wheat orthologous transcription factor *AS1 is* expressed in the LRP. The locus harboring this gene is the strongest QTL associated with the heading trait in the German cultivars which explains 13.8% of the genetic variance. Consequently, after analyzing all significant QTL and the expressed genes mapped in their intervals, we conclude that the Gibberellin biosynthesis is the mechanism that is mostly behind the HD variation in the adapted germplasm.

Conclusion

The present thesis provides a comprehensive investigation based on environmental, genome-wide scan, and RNA-sequencing studies to dissect the effect of the environment on the genetic and molecular architecture underlying flowering time regulation in winter wheat. The most important outcomes are:

1. GDD reflects reliably the impact of microclimate heterogeneity on flowering time, thus it leads to a better evaluation of HD and comparison of flowering behavior in interaction with the environment. Thence, using GDD to fix a specific date for each environment for scoring heading and measurement of climatic ques without including the vernalization period is an accurate approach that proved its efficacy through this research.
2. Plants are adapted to use temperature as a sensor of favorable conditions for starting HD in low latitudes as a response to high seasonal change of Tmax, while they use photoperiod as a more reliable proxy than the temperature in high latitudes for starting the transition to the reproductive

phase. The genetic response to this competition led to thermos-sensitive loci (fine-tuning QTL) in low latitudes and photoperiod susceptible loci in high ones for inducing flowering time.

3. Detection of novel stable allele mapped in QTL TaHd102 in adapted cultivars and another exotic allele located in QTL TaHd044 with great HD alteration effect by including the non-adapted material to the genome-wide scan. Besides the identification of QTL TaHd098 with multiple epistatic interactions by increasing the allelic variation.
4. The global transcriptomic at heading time uncovered stage and spatial tissue-specific QTL in winter wheat. By comparing the early and late flowering cultivars, 664 and 1076 differentially expressed genes in MSA and leaf tissue, respectively, could be mapped in 27 QTL intervals associated with the heading date. The QTL TaHd102 bears the transcription factor *AS1*. A mutation at the promoter region affects very likely the binding of the gene *SOC1*, which delays flowering time. *AS1 and SOC1* are involved in the biosynthesis of Gibberellin, which seems to be the mechanism that causes 13.8 % of the HD variation observed in the German winter wheat.

The findings of this dissertation improved our understanding of the genetic response of flowering time to the interplay of the environmental drivers. We showed how the spring temperature and the photoperiod compete with each other to control HD in a latitude range of 6°. This complex interaction can serve as a basis to elucidate the influence of interaction with the environment on HD at larger scales. The identified QTL can be exploited in the wheat breeding process for developing cultivars adapted to different environments. The novel adapted alleles that attribute stable effect independently of the environment can be used for the adjustment of HD in wide geographical regions. The exotic alleles allow the possibility through introgression in the adapted material to improve the adaptability of wheat cultivars to face challenging climate change. The fine-tune alleles responding to the temperature, day length, and solar radiation or other external stimuli enhance our comprehension of the delicate adaptation mechanism due to the allelic variation at loci with minor effects. The results of the transcriptomic profiling at the heading stage offer many new insights reported for the first time in a monocotyledon crop and enrich the knowledge gained so far in flowering time pathway in wheat on genetic and molecular levels. Taken together, the plant material, methods, and workflow presented in this thesis could successfully achieve the main objective and the partial goals planned previously.

Perspectives

Looking at the importance of the results obtained in this thesis, we highly recommend:

1. Analyze the expression of the differentially expressed genes in the intervals of QTL showing epistatic effect, especially TaHd098.
2. Validate the function of the gene *AS1* in a NIL for avoiding the interference of the genetic background with the gene effect.

We thank the German Research Foundation (DFG) for funding this research under the priority program 1530, “Flowering time control: From natural variation to crop improvement”. We address our acknowledgment also to the project partners of the BRIWECS project funded by the German Federal Ministry of Education and Research (BMBF) grant 031A354 and SECOBRA Saatzucht GmbH for the phenotypic data.

Chapter 6: References

Abe, M., Kobayashi, Y., Yamamoto, S., Daimon, Y., Yamaguchi, A., Ikeda, Y., Ichinoki, H., Notaguchi, M., Goto, K., & Araki, T. (2005). FD, a bZIP protein mediating signals from the floral pathway integrator FT at the shoot apex. *Science*, *309*(5737), 1052–1056.

Acevedo, E. (1987). *Assessing crop and plant attributes for cereal improvement in water-limited Mediterranean environments. Chapter 24.* Improving Winter Cereals for Moisture-limiting Areas. Capri (Italy). 27-31 ….

Achard, P., Baghour, M., Chapple, A., Hedden, P., Van Der Straeten, D., Genschik, P., Moritz, T., & Harberd, N. P. (2007). The plant stress hormone ethylene controls floral transition via DELLA-dependent regulation of floral meristem-identity genes. *Proceedings of the National Academy of Sciences*, *104*(15), 6484 LP – 6489. https://doi.org/10.1073/pnas.0610717104

Afsharyan, N. P., Sannemann, W., Léon, J., & Ballvora, A. (2020). Effect of epistasis and environment on flowering time in barley reveals a novel flowering-delaying QTL allele. *Journal of Experimental Botany*, *71*(3), 893–906.

Ahsan, A., Monir, M., Meng, X., Rahaman, M., Chen, H., & Chen, M. (2019). Identification of epistasis loci underlying rice flowering time by controlling population stratification and polygenic effect. *DNA Research*, *26*(2), 119–130.

Alexandratos, N., & Bruinsma, J. (2012). *World agriculture towards 2030/2050: the 2012 revision*.

Allard, V., Veisz, O., Kõszegi, B., Rousset, M., Le Gouis, J., & Martre, P. (2012). The quantitative response of wheat vernalization to environmental variables indicates that vernalization is not a response to cold temperature. *Journal of Experimental Botany*, *63*(2), 847–857.

Allen, A. M., Winfield, M. O., Burridge, A. J., Downie, R. C., Benbow, H. R., Barker, G. L. A., Wilkinson, P. A., Coghill, J., Waterfall, C., & Davassi, A. (2017). Characterization of a Wheat Breeders' Array suitable for high-throughput SNP genotyping of global accessions of hexaploid bread wheat (Triticum aestivum). *Plant Biotechnology Journal*, *15*(3), 390–401.

Alqudah, A. M., Sallam, A., Stephen Baenziger, P., & Börner, A. (2020). GWAS: Fast-forwarding gene identification and characterization in temperate Cereals: lessons from Barley – A review. *Journal of Advanced Research*, *22*, 119–135. https://doi.org/10.1016/j.jare.2019.10.013

Alqudah, A. M., & Schnurbusch, T. (2014). Awn primordium to tipping is the most decisive developmental phase for spikelet survival in barley. *Functional Plant Biology*, *41*(4), 424–436.

Alvarez, M. A., Tranquilli, G., Lewis, S., Kippes, N., & Dubcovsky, J. (2016). Genetic and physical mapping of the earliness per se locus Eps-A m 1 in Triticum monococcum identifies EARLY FLOWERING 3 (ELF3) as a candidate gene. *Functional & Integrative Genomics*, *16*(4), 365–382.

Anders, S., McCarthy, D. J., Chen, Y., Okoniewski, M., Smyth, G. K., Huber, W., & Robinson, M. D. (2013). Count-based differential expression analysis of RNA sequencing data using R and Bioconductor. *Nature Protocols*, *8*(9), 1765–1786.

Andrés, F., & Coupland, G. (2012). The genetic basis of flowering responses to seasonal cues. *Nature Reviews Genetics*, *13*(9), 627–639.

Appels, R., Eversole, K., Feuillet, C., Keller, B., Rogers, J., Stein, N., Pozniak, C. J., Choulet, F., Distelfeld, A., & Poland, J. (2018). Shifting the limits in wheat research and breeding using a fully annotated reference genome. *Science*, *361*(6403), eaar7191.

Appendino, M. L., Bartoloni, N., & Slafer, G. A. (2003). Vernalization response and earliness per se in cultivars representing different eras of wheat breeding in Argentina. *Euphytica*, *130*(1), 61–69.

Baker, C. K., & Gallagher, J. N. (1983). The development of winter wheat in the field. 2. The control of primordium initiation rate by temperature and photoperiod. *The Journal of Agricultural Science*, *101*(2), 337–344.

Barth, C., De Tullio, M., & Conklin, P. L. (2006). The role of ascorbic acid in the control of flowering time and the onset of senescence. *Journal of Experimental Botany*, *57*(8), 1657–1665. https://doi.org/10.1093/jxb/erj198

Bateson, W. (1909). Mendel's Principles of Heredity: Cambridge University Press. *März 1909; 2nd Impr*, *3*, 1913.

Bauer, A. M., Hoti, F., Von Korff, M., Pillen, K., Léon, J., & Sillanpää, M. J. (2009). Advanced backcross-QTL analysis in spring barley (H. vulgare ssp. spontaneum) comparing a REML versus a Bayesian model in multi-environmental field trials. *Theoretical and Applied Genetics*, *119*(1), 105–123.

Baumgardt, R.-L., Oliverio, K. A., Casal, J. J., & Hoecker, U. (2002). SPA1, a component of phytochrome A signal transduction, regulates the light signaling current. *Planta*, *215*(5), 745–753.

Beales, J., Turner, A., Griffiths, S., Snape, J. W., & Laurie, D. A. (2007). A pseudo-response regulator is misexpressed in the photoperiod insensitive Ppd-D1a mutant of wheat (Triticum aestivum L.). *Theoretical and Applied Genetics*, *115*(5), 721–733.

Benaouda, S., Dadshani, S., Koua, P., Léon, J., & Ballvora, A. (2021). *Latitude and epistatic effects uncover novel stable regulators of flowering time on chromosomes 5A and 3A in winter wheat*.

Beniston, M., Stephenson, D. B., Christensen, O. B., Ferro, C. A. T., Frei, C., Goyette, S., Halsnaes, K., Holt, T., Jylhä, K., & Koffi, B. (2007). Future extreme events in European climate: an exploration of regional climate model projections. *Climatic Change*, *81*(1), 71–95.

Benjamini, Y., & Hochberg, Y. (1995). Controlling the false discovery rate: a practical and powerful approach to multiple testing. *Journal of the Royal Statistical Society: Series B (Methodological)*, *57*(1), 289–300.

Bentley, A. R., Horsnell, R., Werner, C. P., Turner, A. S., Rose, G. A., Bedard, C., Howell, P., Wilhelm, E. P., Mackay, I. J., & Howells, R. M. (2013). Short, natural, and extended photoperiod response in BC2F4 lines of bread wheat with different Photoperiod-1 (Ppd-1) alleles. *Journal of Experimental Botany*, *64*(7), 1783–1793.

Bernier, G. (2013). My favourite flowering image: the role of cytokinin as a flowering signal. *Journal of Experimental Botany*, *64*(18), 5795–5799. https://doi.org/10.1093/jxb/err114

Bertone, P., Stolc, V., Royce, T. E., Rozowsky, J. S., Urban, A. E., Zhu, X., Rinn, J. L., Tongprasit, W., Samanta, M., & Weissman, S. (2004). Global identification of human transcribed sequences with genome tiling arrays. *Science*, *306*(5705), 2242–2246.

Bevan, M. W., & Uauy, C. (2013). Genomics reveals new landscapes for crop improvement. *Genome Biology*, *14*(6), 1–11.

Blair, E. J., Bonnot, T., Hummel, M., Hay, E., Marzolino, J. M., Quijada, I. A., & Nagel, D. H. (2019). Contribution of time of day and the circadian clock to the heat stress responsive transcriptome in Arabidopsis. *Scientific Reports*, *9*(1), 1–12.

Blümel, M., Dally, N., & Jung, C. (2015). Flowering time regulation in crops—what did we learn from Arabidopsis? *Current Opinion in Biotechnology*, *32*, 121–129.

Boden, S. A., Cavanagh, C., Cullis, B. R., Ramm, K., Greenwood, J., Finnegan, E. J., Trevaskis, B., & Swain, S. M. (2015). Ppd-1 is a key regulator of inflorescence architecture and paired spikelet development in wheat. *Nature Plants*, *1*(2), 1–6.

Boeven, P. H. G., Longin, C. F. H., Leiser, W. L., Kollers, S., Ebmeyer, E., & Würschum, T. (2016). Genetic architecture of male floral traits required for hybrid wheat breeding. *Theoretical and Applied Genetics*, *129*(12), 2343–2357.

Bolser, D. M., Staines, D. M., Perry, E., & Kersey, P. J. (2017). Ensembl plants: integrating tools for visualizing, mining, and analyzing plant genomic data. In *Plant genomics databases* (pp. 1–31). Springer.

Bonnett, O. T. (1936). The development of the wheat spike. *J. Agric. Res*, *53*(6), 445–451.

Borlaug, N. E. (1983). Contributions of conventional plant breeding to food production. *Science*, *219*(4585), 689–693.

Börner, A., Worland, A. J., Plaschke, J., Schumann, E., & Law, C. N. (1993). Pleiotropic effects of genes for reduced height (Rht) and day-length insensitivity (Ppd) on yield and its components for wheat grown in middle Europe. *Plant Breeding*, *111*(3), 204–216.

Bornman, J. F., Barnes, P. W., Robinson, S. A., Ballare, C. L., Flint, S. D., & Caldwell, M. M. (2015). Solar ultraviolet radiation and ozone depletion-driven climate change: effects on terrestrial ecosystems. *Photochemical & Photobiological Sciences*, *14*(1), 88–107.

Brachi, B., Faure, N., Horton, M., Flahauw, E., Vazquez, A., Nordborg, M., Bergelson, J., Cuguen, J., & Roux, F. (2010). Linkage and association mapping of Arabidopsis thaliana flowering time in nature. *PLoS Genetics*, *6*(5), e1000940.

Bradbury, P. J., Zhang, Z., Kroon, D. E., Casstevens, T. M., Ramdoss, Y., & Buckler, E. S. (2007). TASSEL: software for association mapping of complex traits in diverse samples. *Bioinformatics*, *23*(19), 2633–2635.

Broman, K. W., Wu, H., Sen, Ś., & Churchill, G. A. (2003). R/qtl: QTL mapping in experimental crosses. *Bioinformatics*, *19*(7), 889–890.

Buckler, E. S., Holland, J. B., Bradbury, P. J., Acharya, C. B., Brown, P. J., Browne, C., Ersoz, E., Flint-Garcia, S., Garcia, A., & Glaubitz, J. C. (2009). The genetic architecture of maize flowering time. *Science*, *325*(5941), 714–718.

Byrne, M. E., Barley, R., Curtis, M., Arroyo, J. M., Dunham, M., Hudson, A., & Martienssen, R. A. (2000). Asymmetric leaves1 mediates leaf patterning and stem cell function in Arabidopsis. *Nature*, *408*(6815), 967–971.

Camargo, A. V, Mott, R., Gardner, K. A., Mackay, I. J., Corke, F., Doonan, J. H., Kim, J. T., & Bentley, A. R. (2016). Determining phenological patterns associated with the onset of senescence in a wheat MAGIC mapping population. *Frontiers in Plant Science*, *7*, 1540.

Cantor, R. M., Lange, K., & Sinsheimer, J. S. (2010). Prioritizing GWAS results: a review of statistical methods and recommendations for their application. *The American Journal of Human Genetics*, *86*(1), 6–22.

Cao, K., Cui, L., Zhou, X., Ye, L., Zou, Z., & Deng, S. (2016). Four tomato FLOWERING LOCUS T-like proteins act antagonistically to regulate floral initiation. *Frontiers in Plant Science*, *6*, 1213.

Cao, W., & Moss, D. N. (1989). Temperature Effect on Leaf Emergence and Phyllochron in Wheat and Barley. *Crop Science*, *29*(4), cropsci1989.0011183X002900040038x. https://doi.org/https://doi.org/10.2135/cropsci1989.0011183X002900040038x

Cardon, L. R., & Palmer, L. J. (2003). Population stratification and spurious allelic association. *The Lancet*, *361*(9357), 598–604.

Carlborg, Ö., Andersson, L., & Kinghorn, B. (2000). The use of a genetic algorithm for simultaneous mapping of multiple interacting quantitative trait loci. *Genetics*, *155*(4), 2003–2010.

Carlborg, Ö., & Haley, C. S. (2004). Epistasis: too often neglected in complex trait studies? *Nature Reviews Genetics*, *5*(8), 618–625. https://doi.org/10.1038/nrg1407

Carlborg, Ö., Kerje, S., Schütz, K., Jacobsson, L., Jensen, P., & Andersson, L. (2003). A global search reveals epistatic interaction between QTL for early growth in the chicken. *Genome Research*, *13*(3), 413–421.

Carlson, C. S., Eberle, M. A., Kruglyak, L., & Nickerson, D. A. (2004). Mapping complex disease loci in whole-genome association studies. *Nature*, *429*(6990), 446–452.

Casal, J. J., Candia, A. N., & Sellaro, R. (2014). Light perception and signalling by phytochrome A. *Journal of Experimental Botany*, *65*(11), 2835–2845.

Cavanagh, C. R., Chao, S., Wang, S., Huang, B. E., Stephen, S., Kiani, S., Forrest, K., Saintenac, C., Brown-Guedira, G. L., & Akhunova, A. (2013). Genome-wide comparative diversity uncovers multiple targets of selection for improvement in hexaploid wheat landraces and cultivars. *Proceedings of the National Academy of Sciences*, *110*(20), 8057–8062.

Chang, C., Bowman, J. L., DeJohn, A. W., Lander, E. S., & Meyerowitz, E. M. (1988). Restriction fragment length polymorphism linkage map for Arabidopsis thaliana. *Proceedings of the National Academy of Sciences*, *85*(18), 6856–6860.

Chang, C. C., Chow, C. C., Tellier, L. C. A. M., Vattikuti, S., Purcell, S. M., & Lee, J. J. (2015). Second-generation PLINK: rising to the challenge of larger and richer datasets. *Gigascience*, *4*(1), s13742-015.

Chen, A., & Dubcovsky, J. (2012). Wheat TILLING mutants show that the vernalization gene VRN1 down-regulates the flowering repressor VRN2 in leaves but is not essential for flowering. *PLoS Genetics*, *8*(12), e1003134.

Chen, A., Li, C., Hu, W., Lau, M. Y., Lin, H., Rockwell, N. C., Martin, S. S., Jernstedt, J. A., Lagarias, J. C., & Dubcovsky, J. (2014). PHYTOCHROME C plays a major role in the acceleration of wheat flowering under long-day photoperiod. *Proceedings of the National Academy of Sciences*, *111*(28), 10037–10044.

Chen, F., Gao, M., Zhang, J., Zuo, A., Shang, X., & Cui, D. (2013). Molecular characterization of vernalization and response genes in bread wheat from the Yellow and Huai Valley of

China. *BMC Plant Biology*, *13*(1), 199.

Chen, Liang, Du, Y., Lu, Q., Chen, H., Meng, R., Cui, C., Lu, S., Yang, Y., Chai, Y., & Li, J. (2018). The photoperiod-insensitive allele Ppd-D1a promotes earlier flowering in Rht12 dwarf plants of bread wheat. *Frontiers in Plant Science*, *9*, 1312.

Chen, Liyuan, Bernhardt, A., Lee, J., & Hellmann, H. (2015). Identification of Arabidopsis MYB56 as a novel substrate for CRL3BPM E3 ligases. *Molecular Plant*, *8*(2), 242–250.

Chen, P., Jäger, G., & Zheng, B. (2010). Transfer RNA modifications and genes for modifying enzymes in Arabidopsis thaliana. *BMC Plant Biology*, *10*(1), 201.

Chiang, C., Aas, O. T., Jetmundsen, M. R., Lee, Y., Torre, S., Fløistad, I. S., & Olsen, J. E. (2018). Day extension with far-red light enhances growth of subalpine fir (Abies lasiocarpa (hooker) Nuttall) seedlings. *Forests*, *9*(4), 175.

Chiara Mustilli, A., & Bowler, C. (1997). Tuning in to the signals controlling photoregulated gene expression in plants. *The EMBO Journal*, *16*(19), 5801–5806.

Chouard, P. (1960). Vernalization and its relations to dormancy. *Annual Review of Plant Physiology*, *11*(1), 191–238.

Chu, C. G., Tan, C. T., Yu, G. T., Zhong, S., Xu, S. S., & Yan, L. (2011). A novel retrotransposon inserted in the dominant Vrn-B1 allele confers spring growth habit in tetraploid wheat (Triticum turgidum L.). *G3: Genes| Genomes| Genetics*, *1*(7), 637–645.

Chuck, G., Meeley, R. B., & Hake, S. (1998). The control of maize spikelet meristem fate by theAPETALA2-like gene indeterminate spikelet1. *Genes & Development*, *12*(8), 1145–1154.

Clapham, D. H., Ekberg, I., Eriksson, G., Norell, L., & Vince-Prue, D. (2002). Requirement for far-red light to maintain secondary needle extension growth in northern but not southern populations of Pinus sylvestris (Scots pine). *Physiologia Plantarum*, *114*(2), 207–212.

Cockram, J., Jones, H., Leigh, F. J., O'Sullivan, D., Powell, W., Laurie, D. A., & Greenland, A. J. (2007). Control of flowering time in temperate cereals: genes, domestication, and sustainable productivity. *Journal of Experimental Botany*, *58*(6), 1231–1244.

Consortium, S. (2014). A comprehensive assessment of RNA-seq accuracy, reproducibility and information content by the Sequencing Quality Control Consortium. *Nature Biotechnology*, *32*(9), 903.

Cooper, M., & DeLacy, I. H. (1994). Relationships among analytical methods used to study genotypic variation and genotype-by-environment interaction in plant breeding multi-environment experiments. *Theoretical and Applied Genetics*, *88*(5), 561–572.

Corbesier, L., Prinsen, E., Jacqmard, A., Lejeune, P., Van Onckelen, H., Périlleux, C., & Bernier, G. (2003). Cytokinin levels in leaves, leaf exudate and shoot apical meristem of Arabidopsis thaliana during floral transition. *Journal of Experimental Botany*, *54*(392), 2511–2517.

Corbesier, L., Vincent, C., Jang, S., Fornara, F., Fan, Q., Searle, I., Giakountis, A., Farrona, S., Gissot, L., & Turnbull, C. (2007). FT protein movement contributes to long-distance signaling in floral induction of Arabidopsis. *Science*, *316*(5827), 1030–1033.

Corchete, L. A., Rojas, E. A., Alonso-López, D., De Las Rivas, J., Gutiérrez, N. C., & Burguillo, F. J. (2020). Systematic comparison and assessment of RNA-seq procedures for gene

expression quantitative analysis. *Scientific Reports*, *10*(1), 1–15.

Covington, M. F., & Harmer, S. L. (2007). The circadian clock regulates auxin signaling and responses in Arabidopsis. *PLoS Biol*, *5*(8), e222.

Craufurd, P. Q., & Wheeler, T. R. (2009). Climate change and the flowering time of annual crops. *Journal of Experimental Botany*, *60*(9), 2529–2539.

Crossa, J., Campos, G. de los, Pérez, P., Gianola, D., Burgueño, J., Araus, J. L., Makumbi, D., Singh, R. P., Dreisigacker, S., & Yan, J. (2010). Prediction of genetic values of quantitative traits in plant breeding using pedigree and molecular markers. *Genetics*, *186*(2), 713–724.

Cuesta-Marcos, A., Casas, A. M., Hayes, P. M., Gracia, M. P., Lasa, J. M., Ciudad, F., Codesal, P., Molina-Cano, J. L., & Igartua, E. (2009). Yield QTL affected by heading date in Mediterranean grown barley. *Plant Breeding*, *128*(1), 46–53.

Cui, F., Zhang, N., Fan, X., Zhang, W., Zhao, C., Yang, L., Pan, R., Chen, M., Han, J., & Zhao, X. (2017). Utilization of a Wheat660K SNP array-derived high-density genetic map for high-resolution mapping of a major QTL for kernel number. *Scientific Reports*, *7*(1), 1–12.

Curtis, B. C., Rajaram, S., & Gómez Macpherson, H. (2002). *Wheat in the world*.

Dadshani, S., Mathew, B., Ballvora, A., Mason, A. S., & Léon, J. (2021). Detection of breeding signatures in wheat using a linkage disequilibrium-corrected mapping approach. *Scientific Reports*, *11*(1), 1–12.

Dahlgren, J. P., von Zeipel, H., & Ehrlén, J. (2007). Variation in vegetative and flowering phenology in a forest herb caused by environmental heterogeneity. *American Journal of Botany*, *94*(9), 1570–1576. https://doi.org/https://doi.org/10.3732/ajb.94.9.1570

Danyluk, J., Kane, N. A., Breton, G., Limin, A. E., Fowler, D. B., & Sarhan, F. (2003). TaVRT-1, a putative transcription factor associated with vegetative to reproductive transition in cereals. *Plant Physiology*, *132*(4), 1849–1860.

Davis, S. J. (2009). Integrating hormones into the floral-transition pathway of Arabidopsis thaliana. *Plant, Cell & Environment*, *32*(9), 1201–1210.

Deng, W., Casao, M. C., Wang, P., Sato, K., Hayes, P. M., Finnegan, E. J., & Trevaskis, B. (2015). Direct links between the vernalization response and other key traits of cereal crops. *Nature Communications*, *6*(1), 1–8.

Dennis, E. S., & Peacock, W. J. (2009). Vernalization in cereals. *Journal of Biology*, *8*(6), 1–4.

Díaz, A., Zikhali, M., Turner, A. S., Isaac, P., & Laurie, D. A. (2012). Copy number variation affecting the Photoperiod-B1 and Vernalization-A1 genes is associated with altered flowering time in wheat (Triticum aestivum). *PloS One*, *7*(3), e33234.

Digel, B., Pankin, A., & von Korff, M. (2015). Global transcriptome profiling of developing leaf and shoot apices reveals distinct genetic and environmental control of floral transition and inflorescence development in barley. *The Plant Cell*, *27*(9), 2318–2334.

Distelfeld, A, Li, C., & Dubcovsky, J. (2009). Regulation of flowering in temperate cereals. *Current Opinion in Plant Biology*, *12*(2), 178–184.

Distelfeld, Assaf, Tranquilli, G., Li, C., Yan, L., & Dubcovsky, J. (2009). Genetic and molecular characterization of the VRN2 loci in tetraploid wheat. *Plant Physiology*, *149*(1), 245–257.

Dodd, A. N., Salathia, N., Hall, A., Kévei, E., Tóth, R., Nagy, F., Hibberd, J. M., Millar, A. J., & Webb, A. A. R. (2005). Plant circadian clocks increase photosynthesis, growth, survival, and competitive advantage. *Science*, *309*(5734), 630–633.

Duan, J., Yu, H., Yuan, K., Liao, Z., Meng, X., Jing, Y., Liu, G., Chu, J., & Li, J. (2019). Strigolactone promotes cytokinin degradation through transcriptional activation of CYTOKININ OXIDASE/DEHYDROGENASE 9 in rice. *Proceedings of the National Academy of Sciences*, *116*(28), 14319–14324.

Duarte-Delgado, D., Dadshani, S., Schoof, H., Oyiga, B. C., Schneider, M., Mathew, B., Léon, J., & Ballvora, A. (2020). Transcriptome profiling at osmotic and ionic phases of salt stress response in bread wheat uncovers trait-specific candidate genes. *BMC Plant Biology*, *20*(1), 1–18.

Dubcovsky, J, Lijavetzky, D., Appendino, L., & Tranquilli, G. (1998). Comparative RFLP mapping of Triticum monococcum genes controlling vernalization requirement. *Theoretical and Applied Genetics*, *97*(5–6), 968–975.

Dubcovsky, Jorge, Loukoianov, A., Fu, D., Valarik, M., Sanchez, A., & Yan, L. (2006). Effect of photoperiod on the regulation of wheat vernalization genes VRN1 and VRN2. *Plant Molecular Biology*, *60*(4), 469–480.

Durand, E., Bouchet, S., Bertin, P., Ressayre, A., Jamin, P., Charcosset, A., Dillmann, C., & Tenaillon, M. I. (2012). Flowering time in maize: linkage and epistasis at a major effect locus. *Genetics*, *190*(4), 1547–1562.

Eagles, H. A., Cane, K., Kuchel, H., Hollamby, G. J., Vallance, N., Eastwood, R. F., Gororo, N. N., & Martin, P. J. (2010). Photoperiod and vernalization gene effects in southern Australian wheat. *Crop and Pasture Science*, *61*(9), 721–730.

Eagles, H. A., Cane, K., & Vallance, N. (2009). The flow of alleles of important photoperiod and vernalisation genes through Australian wheat. *Crop and Pasture Science*, *60*(7), 646–657.

Ehrenreich, I. M., Hanzawa, Y., Chou, L., Roe, J. L., Kover, P. X., & Purugganan, M. D. (2009). Candidate gene association mapping of Arabidopsis flowering time. *Genetics*, *183*(1), 325–335.

Ehrenreich, I. M., Stafford, P. A., & Purugganan, M. D. (2007). The genetic architecture of shoot branching in Arabidopsis thaliana: a comparative assessment of candidate gene associations vs. quantitative trait locus mapping. *Genetics*, *176*(2), 1223–1236.

Elshire, R. J., Glaubitz, J. C., Sun, Q., Poland, J. A., Kawamoto, K., Buckler, E. S., & Mitchell, S. E. (2011). A robust, simple genotyping-by-sequencing (GBS) approach for high diversity species. *PloS One*, *6*(5), e19379.

Endelman, J. B. (2011). Ridge regression and other kernels for genomic selection with R package rrBLUP. *The Plant Genome*, *4*(3), 250–255.

Ersoz, E. S., Yu, J., Buckler, E. S., Varshney, R. K., & Tuberosa, R. (2007). *Genomics-assisted Crop Improvement, Vol. 1: Genomics Approaches and Platforms*.

Evans, L. T., Blundell, C., & King, R. W. (1995). Developmental responses by tall and dwarf isogenic lines of spring wheat to applied gibberellins. *Functional Plant Biology*, *22*(3), 365–371.

Eveland, A. L., Goldshmidt, A., Pautler, M., Morohashi, K., Liseron-Monfils, C., Lewis, M.

W., Kumari, S., Hiraga, S., Yang, F., & Unger-Wallace, E. (2014). Regulatory modules controlling maize inflorescence architecture. *Genome Research*, *24*(3), 431–443.

Fabian, M., Gao, M., Zhang, X.-N., Shi, J., Kim, S.-H., Patel, P., Hu, A. R., & Lu, H. (2021). The Flowering Time Regulator FLK Controls Pathogen Defense in Arabidopsis thaliana. *BioRxiv*.

Falconer, D. S. (1996). *Introduction to quantitative genetics*. Pearson Education India.

FAO. (2019). *No Title*. FAOSTAT Statistics Database: Crops, Available at Www.Fao.Org/Faostat/En/#data/QC.

Faricelli, M. E., Valárik, M., & Dubcovsky, J. (2010). Control of flowering time and spike development in cereals: the earliness per se Eps-1 region in wheat, rice, and Brachypodium. *Functional & Integrative Genomics*, *10*(2), 293–306.

Feng, N., Song, G., Guan, J., Chen, K., Jia, M., Huang, D., Wu, J., Zhang, L., Kong, X., Geng, S., Liu, J., Li, A., & Mao, L. (2017). Transcriptome Profiling of Wheat Inflorescence Development from Spikelet Initiation to Floral Patterning Identified Stage-Specific Regulatory Genes. *Plant Physiology*, *174*(3), 1779 LP – 1794. https://doi.org/10.1104/pp.17.00310

Ferrara, G. O., Mosaad, M. G., Mahalakshmi, V., & Rajaram, S. (1997). Photoperiod and vernalisation response of Mediterranean wheats, and implications for adaptation. In *Wheat: Prospects for Global Improvement* (pp. 509–516). Springer.

Feuillet, C., Travella, S., Stein, N., Albar, L., Nublat, A., & Keller, B. (2003). Map-based isolation of the leaf rust disease resistance gene Lr10 from the hexaploid wheat (Triticum aestivum L.) genome. *Proceedings of the National Academy of Sciences*, *100*(25), 15253–15258.

Fischer, R. A., & Kohn, G. (1966). The relationship of grain yield to vegetative growth and post-flowering leaf area in the wheat crop under conditions of limited soil moisture. *Australian Journal of Agricultural Research*, *17*(3), 281–295.

Fisher, R. A. (1919). XV.—The correlation between relatives on the supposition of Mendelian inheritance. *Earth and Environmental Science Transactions of the Royal Society of Edinburgh*, *52*(2), 399–433.

Fjellheim, S., Boden, S., & Trevaskis, B. (2014). The role of seasonal flowering responses in adaptation of grasses to temperate climates. *Frontiers in Plant Science*, *5*, 431.

Flint-Garcia, S. A., Thuillet, A., Yu, J., Pressoir, G., Romero, S. M., Mitchell, S. E., Doebley, J., Kresovich, S., Goodman, M. M., & Buckler, E. S. (2005). Maize association population: a high-resolution platform for quantitative trait locus dissection. *The Plant Journal*, *44*(6), 1054–1064.

FLOOD, R. G., & Halloran, G. M. (1984). The nature and duration of gene action for vernalization response in wheat. *Annals of Botany*, *53*(3), 363–368.

Ford, B., Deng, W., Clausen, J., Oliver, S., Boden, S., Hemming, M., & Trevaskis, B. (2016). Barley (Hordeum vulgare) circadian clock genes can respond rapidly to temperature in an EARLY FLOWERING 3-dependent manner. *Journal of Experimental Botany*, *67*(18), 5517–5528.

Fornara, F., de Montaigu, A., & Coupland, G. (2010). SnapShot: control of flowering in Arabidopsis. *Cell*, *141*(3), 550.

Franklin, K. A., & Quail, P. H. (2010). Phytochrome functions in Arabidopsis development. *Journal of Experimental Botany*, *61*(1), 11–24.

Frazer, K. A., Eskin, E., Kang, H. M., Bogue, M. A., Hinds, D. A., Beilharz, E. J., Gupta, R. V, Montgomery, J., Morenzoni, M. M., & Nilsen, G. B. (2007). A sequence-based variation map of 8.27 million SNPs in inbred mouse strains. *Nature*, *448*(7157), 1050–1053.

Fu, D., Szűcs, P., Yan, L., Helguera, M., Skinner, J. S., Von Zitzewitz, J., Hayes, P. M., & Dubcovsky, J. (2005). Large deletions within the first intron in VRN-1 are associated with spring growth habit in barley and wheat. *Molecular Genetics and Genomics*, *273*(1), 54–65.

Fujimori, T., Yamashino, T., Kato, T., & Mizuno, T. (2004). Circadian-controlled basic/helix-loop-helix factor, PIL6, implicated in light-signal transduction in Arabidopsis thaliana. *Plant and Cell Physiology*, *45*(8), 1078–1086.

Gassner, G. (1918). *Beiträge zur physiologischen Charakteristik sommer-und winterannueller Gewächse, insbesondere der Getreidepflanzen*.

Gawroński, P., & Schnurbusch, T. (2012). High-density mapping of the earliness per se-3Am (Eps-3A m) locus in diploid einkorn wheat and its relation to the syntenic regions in rice and Brachypodium distachyon L. *Molecular Breeding : New Strategies in Plant Improvement*, *30*(2), 1097—1108. https://doi.org/10.1007/s11032-011-9697-0

Geldermann, H. (1975). Investigations on inheritance of quantitative characters in animals by gene markers I. Methods. *Theoretical and Applied Genetics*, *46*(7), 319–330.

Georges, F., Das, S., Ray, H., Bock, C., Nokhrina, K., Kolla, V. A., & Keller, W. (2009). Over-expression of Brassica napus phosphatidylinositol-phospholipase C2 in canola induces significant changes in gene expression and phytohormone distribution patterns, enhances drought tolerance and promotes early flowering and maturation. *Plant, Cell & Environment*, *32*(12), 1664–1681.

Gerhard, D. S., Wagner, L., Feingold, E. A., Shenmen, C. M., Grouse, L. H., Schuler, G., Klein, S. L., Old, S., Rasooly, R., & Good, P. (2004). The status, quality, and expansion of the NIH full-length cDNA project: the Mammalian Gene Collection (MGC). *Genome Research*, *14*(10 B), 2121–2127.

Gilmour, A. R., Thompson, R., & Cullis, B. R. (1995). Average information REML: an efficient algorithm for variance parameter estimation in linear mixed models. *Biometrics*, 1440–1450.

Gizaw, S. A., Godoy, J. G. V, Pumphrey, M. O., & Carter, A. H. (2018). Spectral Reflectance for Indirect Selection and Genome-Wide Association Analyses of Grain Yield and Drought Tolerance in North American Spring Wheat. *Crop Science*, *58*(6), 2289–2301.

Godfray, H. C. J., Beddington, J. R., Crute, I. R., Haddad, L., Lawrence, D., Muir, J. F., Pretty, J., Robinson, S., Thomas, S. M., & Toulmin, C. (2010). Food security: the challenge of feeding 9 billion people. *Science*, *327*(5967), 812–818.

Gol, L., Haraldsson, E. B., & von Korff, M. (2021). Ppd-H1 integrates drought stress signals to control spike development and flowering time in barley. *Journal of Experimental Botany*, *72*(1), 122–136.

Golembeski, G. S., & Imaizumi, T. (2015). Photoperiodic regulation of florigen function in Arabidopsis thaliana. *The Arabidopsis Book/American Society of Plant Biologists*, *13*.

González-Martínez, S. C., Wheeler, N. C., Ersoz, E., Nelson, C. D., & Neale, D. B. (2007). Association genetics in Pinus taeda LI Wood property traits. *Genetics*, *175*(1), 399–409.

González, F. G., Slafer, G. A., & Miralles, D. J. (2005). Pre-anthesis development and number of fertile florets in wheat as affected by photoperiod sensitivity genes Ppd-D1 and Ppd-B1. *Euphytica*, *146*(3), 253–269.

GOTT, M. B., Gregory, F. G., & Purvis, O. N. (1955). Studies in Vernalisation of Cereals: XIII. Photoperiodic Control of Stages in Flowering between Initiation and Ear Formation in Vernalised and Unvernalised Petkus Winter Rye. *Annals of Botany*, *19*(1), 87–126.

Goulart, M. F., Lemos Filho, J. P., & Lovato, M. B. (2005). Phenological variation within and among populations of Plathymenia reticulata in Brazilian Cerrado, the Atlantic Forest and transitional sites. *Annals of Botany*, *96*(3), 445–455.

Griffiths, S., Simmonds, J., Leverington, M., Wang, Y., Fish, L., Sayers, L., Alibert, L., Orford, S., Wingen, L., Herry, L., Faure, S., Laurie, D., Bilham, L., & Snape, J. (2009). Meta-QTL analysis of the genetic control of ear emergence in elite European winter wheat germplasm. *Theoretical and Applied Genetics*, *119*(3), 383–395. https://doi.org/10.1007/s00122-009-1046-x

Grogan, S., Anderson, J., Baenziger, P., Frels, K., Guttieri, M., Haley, S., Kim, K.-S., Liu, S., McMaster, G., Newell, M., Prasad, P. V. V., Reid, S., Shroyer, K., Zhang, G., Akhunov, E., & Byrne, P. (2016). Phenotypic Plasticity of Winter Wheat Heading Date and Grain Yield across the US Great Plains. *Crop Science*, *56*. https://doi.org/10.2135/cropsci2015.06.0357

Grogan, S. M., Brown-Guedira, G., Haley, S. D., McMaster, G. S., Reid, S. D., Smith, J., & Byrne, P. F. (2016). Allelic variation in developmental genes and effects on winter wheat heading date in the US Great Plains. *PloS One*, *11*(4), e0152852.

Guedira, M., Xiong, M., Hao, Y. F., Johnson, J., Harrison, S., Marshall, D., & Brown-Guedira, G. (2016). Heading date QTL in winter wheat (Triticum aestivum L.) coincide with major developmental genes VERNALIZATION1 and PHOTOPERIOD1. *PloS One*, *11*(5).

Guo, M., Thomas, J., Collins, G., & Timmermans, M. C. P. (2008). Direct repression of KNOX loci by the ASYMMETRIC LEAVES1 complex of Arabidopsis. *The Plant Cell*, *20*(1), 48–58.

Guo, Q., Ng, P. Q., Shi, S., Fan, D., Li, J., Zhao, J., Wang, H., David, R., Mittal, P., & Do, T. (2019). Arabidopsis TRM5 encodes a nuclear-localised bifunctional tRNA guanine and inosine-N1-methyltransferase that is important for growth. *PloS One*, *14*(11), e0225064.

Guo, Z., & Schnurbusch, T. (2015). Variation of floret fertility in hexaploid wheat revealed by tiller removal. *Journal of Experimental Botany*, *66*(19), 5945–5958.

Gupta, P. K., Rustgi, S., & Kulwal, P. L. (2005). Linkage disequilibrium and association studies in higher plants: present status and future prospects. *Plant Molecular Biology*, *57*(4), 461–485.

Gustafson, P., Raskina, O., Ma, X., & Nevo, E. (2009). Wheat evolution, domestication, and improvement. *Wheat: Science and Trade. Wiley, Danvers*, 5–30.

Habib, A., Powell, J. J., Stiller, J., Liu, M., Shabala, S., Zhou, M., Gardiner, D. M., & Liu, C. (2018). A multiple near isogenic line (multi-NIL) RNA-seq approach to identify candidate genes underpinning QTL. *Theoretical and Applied Genetics*, *131*(3), 613–624.

Haley, C. S., & Knott, S. A. (1992). A simple regression method for mapping quantitative trait loci in line crosses using flanking markers. *Heredity*, *69*(4), 315–324.

Han, Y., Zhang, X., Wang, Y., & Ming, F. (2013). The suppression of WRKY44 by GIGANTEA-miR172 pathway is involved in drought response of Arabidopsis thaliana. *PLoS One*, *8*(11), e73541.

Hanocq, E., Laperche, A., Jaminon, O., Lainé, A.-L., & Le Gouis, J. (2007). Most significant genome regions involved in the control of earliness traits in bread wheat, as revealed by QTL meta-analysis. *Theoretical and Applied Genetics*, *114*(3), 569–584.

Hanzawa, Y., Money, T., & Bradley, D. (2005). A single amino acid converts a repressor to an activator of flowering. *Proceedings of the National Academy of Sciences*, *102*(21), 7748–7753.

Harig, L., Beinecke, F. A., Oltmanns, J., Muth, J., Müller, O., Rüping, B., Twyman, R. M., Fischer, R., Prüfer, D., & Noll, G. A. (2012). Proteins from the FLOWERING LOCUS T-like subclade of the PEBP family act antagonistically to regulate floral initiation in tobacco. *The Plant Journal*, *72*(6), 908–921.

Harmer, S. L. (2009). The circadian system in higher plants. *Annual Review of Plant Biology*, *60*, 357–377.

Harrop, T. W. R., Ud Din, I., Gregis, V., Osnato, M., Jouannic, S., Adam, H., & Kater, M. M. (2016). Gene expression profiling of reproductive meristem types in early rice inflorescences by laser microdissection. *The Plant Journal*, *86*(1), 75–88.

Hay, A., Kaur, H., Phillips, A., Hedden, P., Hake, S., & Tsiantis, M. (2002). The gibberellin pathway mediates KNOTTED1-type homeobox function in plants with different body plans. *Current Biology*, *12*(18), 1557–1565.

Hazebroek, J. P., & Metzger, J. D. (1990). Thermoinductive regulation of gibberellin metabolism in Thlaspi arvense L.: I. Metabolism of [2H]-ent-Kaurenoic Acid and [14C] Gibberellin A12-Aldehyde. *Plant Physiology*, *94*(1), 157–165.

Hazen, S. P., Schultz, T. F., Pruneda-Paz, J. L., Borevitz, J. O., Ecker, J. R., & Kay, S. A. (2005). LUX ARRHYTHMO encodes a Myb domain protein essential for circadian rhythms. *Proceedings of the National Academy of Sciences*, *102*(29), 10387–10392.

He, J., Zhao, X., Laroche, A., Lu, Z.-X., Liu, H., & Li, Z. (2014). Genotyping-by-sequencing (GBS), an ultimate marker-assisted selection (MAS) tool to accelerate plant breeding. *Frontiers in Plant Science*, *5*, 484.

Hemming, M. N., Peacock, W. J., Dennis, E. S., & Trevaskis, B. (2008). Low-temperature and daylength cues are integrated to regulate FLOWERING LOCUS T in barley. *Plant Physiology*, *147*(1), 355–366.

Henderson, I. R., & Dean, C. (2004). Control of Arabidopsis flowering: the chill before the bloom. *Development*, *131*(16), 3829–3838.

Hepworth, S. R., Valverde, F., Ravenscroft, D., Mouradov, A., & Coupland, G. (2002). Antagonistic regulation of flowering-time gene SOC1 by CONSTANS and FLC via separate promoter motifs. *The EMBO Journal*, *21*(16), 4327–4337.

Herndl, M., White, J. W., Graeff, S., & Claupein, W. (2008). The impact of vernalization requirement, photoperiod sensitivity and earliness per se on grain protein content of bread wheat (Triticum aestivum L.). *Euphytica*, *163*(2), 309–320.

Holland, J. B., Nyquist, W. E., & Cervantes-Martínez, C. T. (2003). Estimating and interpreting heritability for plant breeding: an update. *Plant Breeding Reviews*, *22*.

Holm, S. (1979). A simple sequentially rejective multiple test procedure. *Scandinavian Journal of Statistics*, 65–70.

Hsu, P. Y., & Harmer, S. L. (2014). Wheels within wheels: the plant circadian system. *Trends in Plant Science*, *19*(4), 240–249.

Hu, Y., Wang, L., Jia, R., Liang, W., Zhang, X., Xu, J., Chen, X., Lu, D., Chen, M., & Luo, Z. (2021). Rice transcription factor MADS32 regulates floral patterning through interactions with multiple floral homeotic genes. *Journal of Experimental Botany*, *72*(7), 2434–2449.

Huang, B. E., George, A. W., Forrest, K. L., Kilian, A., Hayden, M. J., Morell, M. K., & Cavanagh, C. R. (2012). A multiparent advanced generation inter-cross population for genetic analysis in wheat. *Plant Biotechnology Journal*, *10*(7), 826–839.

Huang, W., Richards, S., Carbone, M. A., Zhu, D., Anholt, R. R. H., Ayroles, J. F., Duncan, L., Jordan, K. W., Lawrence, F., & Magwire, M. M. (2012). Epistasis dominates the genetic architecture of Drosophila quantitative traits. *Proceedings of the National Academy of Sciences*, *109*(39), 15553–15559.

Inouye, D. W., Saavedra, F., & Lee-Yang, W. (2003). Environmental influences on the phenology and abundance of flowering by Androsace septentrionalis (Primulaceae). *American Journal of Botany*, *90*(6), 905–910.

Iqbal, M., Navabi, A., Yang, R.-C., Salmon, D. F., & Spaner, D. (2007). Molecular characterization of vernalization response genes in Canadian spring wheat. *Genome*, *50*(5), 511–516.

Ito, S., Song, Y. H., Josephson-Day, A. R., Miller, R. J., Breton, G., Olmstead, R. G., & Imaizumi, T. (2012). FLOWERING BHLH transcriptional activators control expression of the photoperiodic flowering regulator CONSTANS in Arabidopsis. *Proceedings of the National Academy of Sciences*, *109*(9), 3582–3587.

Jackson, M. T. (1966). Effects of microclimate on spring flowering phenology. *Ecology*, *47*(3), 407–415.

Jacob, Y., Mongkolsiriwatana, C., Veley, K. M., Kim, S. Y., & Michaels, S. D. (2007). The nuclear pore protein AtTPR is required for RNA homeostasis, flowering time, and auxin signaling. *Plant Physiology*, *144*(3), 1383–1390.

Jaeger, K. E., & Wigge, P. A. (2007). FT protein acts as a long-range signal in Arabidopsis. *Current Biology*, *17*(12), 1050–1054.

Jander, G., Norris, S. R., Rounsley, S. D., Bush, D. F., Levin, I. M., & Last, R. L. (2002). Arabidopsis map-based cloning in the post-genome era. *Plant Physiology*, *129*(2), 440–450.

Jannink, J.-L., & Jansen, R. (2001). Mapping epistatic quantitative trait loci with one-dimensional genome searches. *Genetics*, *157*(1), 445–454.

Jian, H., Zhang, A., Ma, J., Wang, T., Yang, B., Shuang, L. S., Liu, M., Li, J., Xu, X., Paterson, A. H., & Liu, L. (2019). Joint QTL mapping and transcriptome sequencing analysis reveal candidate flowering time genes in Brassica napus L. *BMC Genomics*, *20*(1), 21. https://doi.org/10.1186/s12864-018-5356-8

Jiang, Li, Yan, S., Yang, W., Li, Y., Xia, M., Chen, Z., Wang, Q., Yan, L., Song, X., & Liu, R. (2015). Transcriptomic analysis reveals the roles of microtubule-related genes and transcription factors in fruit length regulation in cucumber (Cucumis sativus L.). *Scientific Reports*, *5*(1), 1–11.

Jiang, Lingyan, Chen, Y., Luo, L., & Peck, S. C. (2018). Central roles and regulatory mechanisms of dual-specificity MAPK phosphatases in developmental and stress signaling. *Frontiers in Plant Science*, *9*, 1697.

Jiang, Y., Schmidt, R. H., Zhao, Y., & Reif, J. C. (2017). A quantitative genetic framework highlights the role of epistatic effects for grain-yield heterosis in bread wheat. *Nature Genetics*, *49*(12), 1741–1746.

Johal, G. S., & Briggs, S. P. (1992). Reductase activity encoded by the HM1 disease resistance gene in maize. *Science*, *258*(5084), 985–987.

Jones, P. G., & Thornton, P. K. (2003). The potential impacts of climate change on maize production in Africa and Latin America in 2055. *Global Environmental Change*, *13*(1), 51–59.

Kaler, A. S., Gillman, J. D., Beissinger, T., & Purcell, L. C. (2020). Comparing different statistical models and multiple testing corrections for association mapping in soybean and maize. *Frontiers in Plant Science*, *10*, 1794.

Kami, C., Lorrain, S., Hornitschek, P., & Fankhauser, C. (2010). Light-regulated plant growth and development. *Current Topics in Developmental Biology*, *91*, 29–66.

Kamran, A., Iqbal, M., & Spaner, D. (2014). Flowering time in wheat (Triticum aestivum L.): a key factor for global adaptability. *Euphytica*, *197*(1), 1–26.

Kamran, A., Randhawa, H. S., Yang, R., & Spaner, D. (2014). The effect of VRN1 genes on important agronomic traits in high-yielding C anadian soft white spring wheat. *Plant Breeding*, *133*(3), 321–326.

Kang, H. M., Zaitlen, N. A., Wade, C. M., Kirby, A., Heckerman, D., Daly, M. J., & Eskin, E. (2008). Efficient Control of Population Structure in Model Organism Association Mapping. *Genetics*, *178*(3), 1709 LP – 1723. https://doi.org/10.1534/genetics.107.080101

Kärkkäinen, H. P., Li, Z., & Sillanpää, M. J. (2015). An efficient genome-wide multilocus epistasis search. *Genetics*, *201*(3), 865–870.

Kato, K., Miura, H., & Sawada, S. (2000). Mapping QTLs controlling grain yield and its components on chromosome 5A of wheat. *Theoretical and Applied Genetics*, *101*(7), 1114–1121.

Kearsey, M. J. (1998). The principles of QTL analysis (a minimal mathematics approach). *Journal of Experimental Botany*, *49*(327), 1619–1623.

Keller, B., Feuillet, C., & Yahiaoui, N. (2005). Map-based isolation of disease resistance genes from bread wheat: cloning in a supersize genome. *Genetics Research*, *85*(2), 93–100.

Kelly, J. K., & Mojica, J. P. (2011). Interactions among flower-size QTL of Mimulus guttatus are abundant but highly variable in nature. *Genetics*, *189*(4), 1461–1471.

Kilpikari, R., & Sillanpää, M. J. (2003). Bayesian analysis of multilocus association in quantitative and qualitative traits. *Genetic Epidemiology: The Official Publication of the International Genetic Epidemiology Society*, *25*(2), 122–135.

Kim, D.-H., Kang, J.-G., Yang, S.-S., Chung, K.-S., Song, P.-S., & Park, C.-M. (2002). A phytochrome-associated protein phosphatase 2A modulates light signals in flowering time control in Arabidopsis. *The Plant Cell*, *14*(12), 3043–3056.

Kim, K.-H., Song, K., Park, J.-M., Kim, J.-Y., & Lee, B.-M. (2021). RNA-Seq Analysis of Gene Expression Changes Related to Delay of Flowering Time under Drought Stress in Tropical Maize. *Applied Sciences*, *11*(9), 4273.

Kim, S. (2015). ppcor: an R package for a fast calculation to semi-partial correlation coefficients. *Communications for Statistical Applications and Methods*, *22*(6), 665.

King, R. W., & Heide, O. M. (2009). Seasonal flowering and evolution: the heritage from Charles Darwin. *Functional Plant Biology : FPB*, *36*(12), 1027—1036. https://doi.org/10.1071/fp09170

King, R. W., Pate, J. S., & Johnston, J. (1996). Ecotyptic Differences in the Flowering of Pimelea ferruginea (Thymelaeaceae) in Response to Cool Temperatures. *Australian Journal of Botany*, *44*(1), 47–55.

Kippes, N., Chen, A., Zhang, X., Lukaszewski, A. J., & Dubcovsky, J. (2016). Development and characterization of a spring hexaploid wheat line with no functional VRN2 genes. *Theoretical and Applied Genetics*, *129*(7), 1417–1428.

Kippes, N., Debernardi, J. M., Vasquez-Gross, H. A., Akpinar, B. A., Budak, H., Kato, K., Chao, S., Akhunov, E., & Dubcovsky, J. (2015). Identification of the VERNALIZATION 4 gene reveals the origin of spring growth habit in ancient wheats from South Asia. *Proceedings of the National Academy of Sciences*, *112*(39), E5401–E5410.

Kippes, N., Guedira, M., Lin, L., Alvarez, M. A., Brown-Guedira, G. L., & Dubcovsky, J. (2018). Single nucleotide polymorphisms in a regulatory site of VRN-A1 first intron are associated with differences in vernalization requirement in winter wheat. *Molecular Genetics and Genomics*, *293*(5), 1231–1243.

Kippes, N., Zhu, J., Chen, A., Vanzetti, L., Lukaszewski, A., Nishida, H., Kato, K., Dvorak, J., & Dubcovsky, J. (2014). Fine mapping and epistatic interactions of the vernalization gene VRN-D4 in hexaploid wheat. *Molecular Genetics and Genomics*, *289*(1), 47–62.

Kirby, E. J. M. (1988). Analysis of leaf, stem and ear growth in wheat from terminal spikelet stage to anthesis. *Field Crops Research*, *18*(2–3), 127–140.

Kiseleva, A. A., & Salina, E. A. (2018). Genetic regulation of common wheat heading time. *Russian Journal of Genetics*, *54*(4), 375–388.

Kiyosue, T., & Wada, M. (2000). LKP1 (LOV kelch protein 1): a factor involved in the regulation of flowering time in Arabidopsis. *The Plant Journal*, *23*(6), 807–815.

Kobayashi, F., Tanaka, T., Kanamori, H., Wu, J., Katayose, Y., & Handa, H. (2016). Characterization of a mini core collection of Japanese wheat varieties using single-nucleotide polymorphisms generated by genotyping-by-sequencing. *Breeding Science*, *66*(2), 213–225.

Kobayashi, Y., Kaya, H., Goto, K., Iwabuchi, M., & Araki, T. (1999). A pair of related genes with antagonistic roles in mediating flowering signals. *Science*, *286*(5446), 1960–1962.

Koornneef, M., Blankestijn-de Vries, H., Hanhart, C., Soppe, W., & Peeters, T. (1994). The phenotype of some late-flowering mutants is enhanced by a locus on chromosome 5 that is not effective in the Landsberg erecta wild-type. *The Plant Journal*, *6*(6), 911–919.

Korte, A., & Farlow, A. (2013). The advantages and limitations of trait analysis with GWAS: a review. *Plant Methods*, *9*(1), 1–9.

KOUCHAKI, A. L. I. R., & NASIRI, M. M. (2008). *Impacts of climate change and CO2 concentration on wheat yield in Iran and adaptation strategies*.

Krizek, B. A. (2011). Aintegumenta and Aintegumenta-Like6 regulate auxin-mediated flower development in Arabidopsis. *BMC Research Notes*, *4*(1), 1–8.

Kuchel, H., Williams, K. J., Langridge, P., Eagles, H. A., & Jefferies, S. P. (2007). Genetic dissection of grain yield in bread wheat. I. QTL analysis. *Theoretical and Applied Genetics*, *115*(8), 1029–1041.

Kusterer, B., Muminovic, J., Utz, H. F., Piepho, H.-P., Barth, S., Heckenberger, M., Meyer, R. C., Altmann, T., & Melchinger, A. E. (2007). Analysis of a triple testcross design with recombinant inbred lines reveals a significant role of epistasis in heterosis for biomass-related traits in Arabidopsis. *Genetics*, *175*(4), 2009–2017.

Kwon, J. M., & Goate, A. M. (2000). The candidate gene approach. *Alcohol Research & Health*, *24*(3), 164.

Lamkey, K. R., Schnicker, B. J., & Melchinger, A. E. (1995). Epistasis in an elite maize hybrid and choice of generation for inbred line development. *Crop Science*, *35*(5), 1272.

Lander, E. S., & Botstein, D. (1989). Mapping mendelian factors underlying quantitative traits using RFLP linkage maps. *Genetics*, *121*(1), 185–199.

Lang, A. (1957). The effect of gibberellin upon flower formation. *Proceedings of the National Academy of Sciences of the United States of America*, *43*(8), 709.

Langer, S. M., Longin, C. F. H., & Würschum, T. (2014). Flowering time control in European winter wheat. *Frontiers in Plant Science*, *5*(OCT), 1–11. https://doi.org/10.3389/fpls.2014.00537

Larsson, S. J., Lipka, A. E., & Buckler, E. S. (2013). Lessons from Dwarf8 on the strengths and weaknesses of structured association mapping. *PLoS Genetics*, *9*(2), e1003246.

Laurie, C. C., Chasalow, S. D., LeDeaux, J. R., McCarroll, R., Bush, D., Hauge, B., Lai, C., Clark, D., Rocheford, T. R., & Dudley, J. W. (2004). The genetic architecture of response to long-term artificial selection for oil concentration in the maize kernel. *Genetics*, *168*(4), 2141–2155.

Laurie, D. A. (1997). Comparative genetics of flowering time. *Oryza: From Molecule to Plant*, 167–177.

Law, C. N., Sutka, J., & Worland, A. J. (1978). A genetic study of day-length response in wheat. *Heredity*, *41*(2), 185–191.

Law, C. N., & Worland, A. J. (1997). Genetic analysis of some flowering time and adaptive traits in wheat. *New Phytologist*, *137*(1), 19–28.

Law, C. W., Chen, Y., Shi, W., & Smyth, G. K. (2014). voom: Precision weights unlock linear model analysis tools for RNA-seq read counts. *Genome Biology*, *15*(2), 1–17.

Lawlor, D. W., & Mitchell, R. A. C. (2000). Crop ecosystem responses to climatic change: wheat. *Climate Change and Global Crop Productivity*, 57–80.

Lee, H., Suh, S.-S., Park, E., Cho, E., Ahn, J. H., Kim, S.-G., Lee, J. S., Kwon, Y. M., & Lee,

I. (2000). The AGAMOUS-LIKE 20 MADS domain protein integrates floral inductive pathways in Arabidopsis. *Genes & Development*, *14*(18), 2366–2376.

Lee, I., & Amasino, R. M. (1995). Effect of vernalization, photoperiod, and light quality on the flowering phenotype of Arabidopsis plants containing the FRIGIDA gene. *Plant Physiology*, *108*(1), 157–162.

Lee, J. A., Cockerham, C. C., & Smith, F. H. (1968). The inheritance of gossypol level in gossypium i. additive, dominance, epistatic, and maternal effects associated with seed gossypol in two varieties of gossypium hirsutum l. *Genetics*, *59*(2), 285.

Lee, S., Kim, J., Han, J., Han, M., & An, G. (2004). Functional analyses of the flowering time gene OsMADS50, the putative SUPPRESSOR OF OVEREXPRESSION OF CO 1/AGAMOUS-LIKE 20 (SOC1/AGL20) ortholog in rice. *The Plant Journal*, *38*(5), 754–764.

Lewandowska-Sabat, A. M., Fjellheim, S., Olsen, J. E., & Rognli, O. A. (2017). Local populations of Arabidopsis thaliana show clear relationship between photoperiodic sensitivity of flowering time and altitude. *Frontiers in Plant Science*, *8*, 1046.

Lewis, S., Faricelli, M. E., Appendino, M. L., Valárik, M., & Dubcovsky, J. (2008). The chromosome region including the earliness per se locus Eps-Am1 affects the duration of early developmental phases and spikelet number in diploid wheat. *Journal of Experimental Botany*, *59*(13), 3595–3607.

Li, B., Suzuki, J.-I., & Hara, T. (1998). Latitudinal variation in plant size and relative growth rate in Arabidopsis thaliana. *Oecologia*, *115*(3), 293–301.

Li, Chengqi, Fu, Y., Sun, R., Wang, Y., & Wang, Q. (2018). Single-locus and multi-locus genome-wide association studies in the genetic dissection of fiber quality traits in upland cotton (Gossypium hirsutum L.). *Frontiers in Plant Science*, *9*, 1083.

Li, Chengxia, & Dubcovsky, J. (2008). Wheat FT protein regulates VRN1 transcription through interactions with FDL2. *The Plant Journal*, *55*(4), 543–554.

Li, F.-W., Melkonian, M., Rothfels, C. J., Villarreal, J. C., Stevenson, D. W., Graham, S. W., Wong, G. K.-S., Pryer, K. M., & Mathews, S. (2015). Phytochrome diversity in green plants and the origin of canonical plant phytochromes. *Nature Communications*, *6*(1), 1–12.

Li, J., Yang, J., Li, Y., & Ma, L. (2020). Current strategies and advances in wheat biology. *The Crop Journal*, *8*(6), 879–891.

Li, L., Lu, K., Chen, Z., Mu, T., Hu, Z., & Li, X. (2008). Dominance, overdominance and epistasis condition the heterosis in two heterotic rice hybrids. *Genetics*, *180*(3), 1725–1742.

Li, R., Zhu, H., Ruan, J., Qian, W., Fang, X., Shi, Z., Li, Y., Li, S., Shan, G., & Kristiansen, K. (2010). De novo assembly of human genomes with massively parallel short read sequencing. *Genome Research*, *20*(2), 265–272.

Li, W., Wang, T., Zhang, Y., & Li, Y. (2016). Overexpression of soybean miR172c confers tolerance to water deficit and salt stress, but increases ABA sensitivity in transgenic Arabidopsis thaliana. *Journal of Experimental Botany*, *67*(1), 175–194.

Li, Y., Fu, X., Zhao, M., Zhang, W., Li, B., An, D., Li, J., Zhang, A., Liu, R., & Liu, X. (2018). A genome-wide view of transcriptome dynamics during early spike development in bread

wheat. *Scientific Reports*, *8*(1), 1–16.

Li, Z., & Sillanpää, M. J. (2012). Estimation of quantitative trait locus effects with epistasis by variational Bayes algorithms. *Genetics*, *190*(1), 231–249.

Lin, C. (2000). Photoreceptors and regulation of flowering time. *Plant Physiology*, *123*(1), 39–50.

Lin, Y.-R., Schertz, K. F., & Paterson, A. H. (1995). Comparative analysis of QTLs affecting plant height and maturity across the Poaceae, in reference to an interspecific sorghum population. *Genetics*, *141*(1), 391–411.

Liu, B., Jiang, G., Zhang, Y., Li, J., Li, X., Yue, J., Chen, F., Liu, H., Li, H., & Zhu, S. (2011). Analysis of transcriptome differences between resistant and susceptible strains of the citrus red mite Panonychus citri (Acari: Tetranychidae). *PloS One*, *6*(12), e28516.

Liu, C., Tu, Y., Liao, S., Fu, X., Lian, X., He, Y., Xie, W., & Wang, G. (2021). Genome-wide association study of flowering time reveals complex genetic heterogeneity and epistatic interactions in rice. *Gene*, *770*, 145353.

Liu, L., Liu, C., Hou, X., Xi, W., Shen, L., Tao, Z., Wang, Y., & Yu, H. (2012). FTIP1 is an essential regulator required for florigen transport. *PLoS Biol*, *10*(4), e1001313.

Liu, Q., Liu, Z., Li, W., & Song, X. (2020). Comparative transcriptome analysis indicates conversion of stamens into pistil-like structures in male sterile wheat (Triticum aestivum L.) with Aegilops crassa cytoplasm. *BMC Genomics*, *21*(1), 1–17.

Liu, X., Huang, M., Fan, B., Buckler, E. S., & Zhang, Z. (2016). Iterative usage of fixed and random effect models for powerful and efficient genome-wide association studies. *PLoS Genetics*, *12*(2), e1005767.

Liu, Y., He, Z., Appels, R., & Xia, X. (2012). Functional markers in wheat: current status and future prospects. *Theoretical and Applied Genetics*, *125*(1), 1–10.

Livak, K. J., & Schmittgen, T. D. (2001). Analysis of relative gene expression data using real-time quantitative PCR and the 2− ΔΔCT method. *Methods*, *25*(4), 402–408.

Lu, Z., Huang, X., Ouyang, Y., & Yao, J. (2013). Genome-wide identification, phylogenetic and co-expression analysis of OsSET gene family in rice. *PLoS One*, *8*(6), e65426.

Lukens, L. N., & Doebley, J. (1999). Epistatic and environmental interactions for quantitative trait loci involved in maize evolution. *Genetics Research*, *74*(3), 291–302.

Lukowitz, W., Gillmor, C. S., & Scheible, W.-R. (2000). Positional cloning in Arabidopsis. Why it feels good to have a genome initiative working for you. *Plant Physiology*, *123*(3), 795–806.

Lv, B., Nitcher, R., Han, X., Wang, S., Ni, F., Li, K., Pearce, S., Wu, J., Dubcovsky, J., & Fu, D. (2014). Characterization of FLOWERING LOCUS T1 (FT1) gene in Brachypodium and wheat. *PLoS One*, *9*(4), e94171.

Lynch, M., & Walsh, B. (1998). *Genetics and analysis of quantitative traits*.

Lyons, R., Rusu, A., Stiller, J., Powell, J., Manners, J. M., & Kazan, K. (2015). Investigating the association between flowering time and defense in the Arabidopsis thaliana-Fusarium oxysporum interaction. *PloS One*, *10*(6), e0127699.

Mackay, I. J., Bansept-Basler, P., Barber, T., Bentley, A. R., Cockram, J., Gosman, N.,

Greenland, A. J., Horsnell, R., Howells, R., & O'Sullivan, D. M. (2014). An eight-parent multiparent advanced generation inter-cross population for winter-sown wheat: creation, properties, and validation. *G3: Genes, Genomes, Genetics*, *4*(9), 1603–1610.

Mackay, T. F. C. (2001). Quantitative trait loci in Drosophila. *Nature Reviews Genetics*, *2*(1), 11–20.

MacMillan, C. P., Blundell, C. A., & King, R. W. (2005). Flowering of the grass Lolium perenne. Effects of vernalization and long days on gibberellin biosynthesis and signaling. *Plant Physiology*, *138*(3), 1794–1806.

Malapeira, J., Khaitova, L. C., & Mas, P. (2012). Ordered changes in histone modifications at the core of the Arabidopsis circadian clock. *Proceedings of the National Academy of Sciences*, *109*(52), 21540–21545.

Mall, R. K., & Aggarwal, P. K. (2002). Climate change and rice yields in diverse agro-environments of India. I. Evaluation of impact assessment models. *Climatic Change*, *52*(3), 315–330.

Malmberg, R. L., Held, S., Waits, A., & Mauricio, R. (2005). Epistasis for fitness-related quantitative traits in Arabidopsis thaliana grown in the field and in the greenhouse. *Genetics*, *171*(4), 2013–2027.

Manderscheid, R., Burkart, S., Bramm, A., & Weigel, H.-J. (2003). Effect of CO2 enrichment on growth and daily radiation use efficiency of wheat in relation to temperature and growth stage. *European Journal of Agronomy*, *19*(3), 411–425.

Marquis, R. J. (1988). Phenological variation in the neotropical understory shrub Piper arielanum: causes and consequences. *Ecology*, *69*(5), 1552–1565.

Martin, G. B., Brommonschenkel, S. H., Chunwongse, J., Frary, A., Ganal, M. W., Spivey, R., Wu, T., Earle, E. D., & Tanksley, S. D. (1993). Map-based cloning of a protein kinase gene conferring disease resistance in tomato. *Science*, *262*(5138), 1432–1436.

Martínez, C., Pons, E., Prats, G., & León, J. (2004). Salicylic acid regulates flowering time and links defence responses and reproductive development. *The Plant Journal*, *37*(2), 209–217.

Mathew, B., Léon, J., Sannemann, W., & Sillanpää, M. J. (2018). Detection of epistasis for flowering time using Bayesian multilocus estimation in a barley MAGIC population. *Genetics*, *208*(2), 525–536.

Mathews, S. (2010). Evolutionary studies illuminate the structural-functional model of plant phytochromes. *The Plant Cell*, *22*(1), 4–16.

McKinney, H. H. (1940). Vernalization and the growth-phase concept. *The Botanical Review*, *6*(1), 25.

Meier, U. (1997). *Growth stages of mono-and dicotyledonous plants*. Blackwell Wissenschafts-Verlag.

Menzel, A., Sparks, T. H., Estrella, N., Koch, E., Aaasa, A., Ahas, R., Alm-Kübler, K., Bissolli, P., Braslavská, O., Briede, A., Chmielewski, F. M., Crepinsek, Z., Curnel, Y., Dahl, Å., Defila, C., Donnelly, A., Filella, Y., Jatczak, K., Måge, F., … Zust, A. (2006). European phenological response to climate change matches the warming pattern. *Global Change Biology*, *12*(10), 1969–1976. https://doi.org/10.1111/j.1365-2486.2006.01193.x

Michaels, S. D., & Amasino, R. M. (1999). FLOWERING LOCUS C encodes a novel MADS domain protein that acts as a repressor of flowering. *The Plant Cell*, *11*(5), 949–956.

Miller-Rushing, A. J., Katsuki, T., Primack, R. B., Ishii, Y., Sang, D. L., & Higuchi, H. (2007). Impact of global warming on a group of related species and their hybrids: Cherry tree (Rosaceae) flowering at Mt. Takao, Japan. *American Journal of Botany*, *94*(9), 1470–1478. https://doi.org/10.3732/ajb.94.9.1470

Mizuno, T., & Nakamichi, N. (2005). Pseudo-response regulators (PRRs) or true oscillator components (TOCs). *Plant and Cell Physiology*, *46*(5), 677–685.

Möglich, A., Yang, X., Ayers, R. A., & Moffat, K. (2010). Structure and function of plant photoreceptors. *Annual Review of Plant Biology*, *61*, 21–47.

Monte, E., Alonso, J. M., Ecker, J. R., Zhang, Y., Li, X., Young, J., Austin-Phillips, S., & Quail, P. H. (2003). Isolation and characterization of phyC mutants in Arabidopsis reveals complex crosstalk between phytochrome signaling pathways. *The Plant Cell*, *15*(9), 1962–1980.

Moon, J., Suh, S., Lee, H., Choi, K., Hong, C. B., Paek, N., Kim, S., & Lee, I. (2003). The SOC1 MADS-box gene integrates vernalization and gibberellin signals for flowering in Arabidopsis. *The Plant Journal*, *35*(5), 613–623.

Moore, J. H. (2003). The ubiquitous nature of epistasis in determining susceptibility to common human diseases. *Human Heredity*, *56*(1–3), 73–82.

Moore, L. M., & Lauenroth, W. K. (2017). Differential effects of temperature and precipitation on early- vs. Late-flowering species. *Ecosphere*, *8*(5). https://doi.org/10.1002/ecs2.1819

Morrell, P. L., Buckler, E. S., & Ross-Ibarra, J. (2012). Crop genomics: advances and applications. *Nature Reviews Genetics*, *13*(2), 85–96.

Mortazavi, A., Williams, B. A., McCue, K., Schaeffer, L., & Wold, B. (2008). Mapping and quantifying mammalian transcriptomes by RNA-Seq. *Nature Methods*, *5*(7), 621–628.

Murai, K., Miyamae, M., Kato, H., Takumi, S., & Ogihara, Y. (2003). WAP1, a wheat APETALA1 homolog, plays a central role in the phase transition from vegetative to reproductive growth. *Plant and Cell Physiology*, *44*(12), 1255–1265.

Myles, S., Peiffer, J., Brown, P. J., Ersoz, E. S., Zhang, Z., Costich, D. E., & Buckler, E. (2009). Association mapping: Critical considerations shift from genotyping to experimental design. *Plant Cell*, *21*(8), 2194–2202. https://doi.org/10.1105/tpc.109.068437

Nagalakshmi, U., Wang, Z., Waern, K., Shou, C., Raha, D., Gerstein, M., & Snyder, M. (2008). The transcriptional landscape of the yeast genome defined by RNA sequencing. *Science*, *320*(5881), 1344–1349.

Nam, H.-G., Giraudat, J., Den Boer, B., Moonan, F., Loos, W. D. B., Hauge, B. M., & Goodman, H. M. (1989). Restriction fragment length polymorphism linkage map of Arabidopsis thaliana. *The Plant Cell*, *1*(7), 699–705.

Nemoto, Y., Kisaka, M., Fuse, T., Yano, M., & Ogihara, Y. (2003). Characterization and functional analysis of three wheat genes with homology to the CONSTANS flowering time gene in transgenic rice. *The Plant Journal*, *36*(1), 82–93.

Nishida, H., Yoshida, T., Kawakami, K., Fujita, M., Long, B., Akashi, Y., Laurie, D. A., & Kato, K. (2013). Structural variation in the 5′ upstream region of photoperiod-insensitive

alleles Ppd-A1a and Ppd-B1a identified in hexaploid wheat (Triticum aestivum L.), and their effect on heading time. *Molecular Breeding*, *31*(1), 27–37.

Nusinow, D. A., Helfer, A., Hamilton, E. E., King, J. J., Imaizumi, T., Schultz, T. F., Farré, E. M., & Kay, S. A. (2011). The ELF4–ELF3–LUX complex links the circadian clock to diurnal control of hypocotyl growth. *Nature*, *475*(7356), 398–402.

Ó'Maoiléidigh, D. S., Graciet, E., & Wellmer, F. (2014). Gene networks controlling A rabidopsis thaliana flower development. *New Phytologist*, *201*(1), 16–30.

Ochagavía, H., Prieto, P., Savin, R., Griffiths, S., & Slafer, G. (2018). Dynamics of leaf and spikelet primordia initiation in wheat as affected by Ppd-1a alleles under field conditions. *Journal of Experimental Botany*, *69*(10), 2621–2631.

Ochagavía, H., Prieto, P., Zikhali, M., Griffiths, S., & Slafer, G. A. (2019). Earliness Per Se by Temperature Interaction on Wheat Development. *Scientific Reports*, *9*(1), 2584. https://doi.org/10.1038/s41598-019-39201-6

Ogonowska, H., Barchacka, K., Gasparis, S., Jablonski, B., Orczyk, W., Dmochowska-Boguta, M., & Nadolska-Orczyk, A. (2019). Specificity of expression of TaCKX family genes in developing plants of wheat and their co-operation within and among organs. *PloS One*, *14*(4), e0214239.

Oliver, S. N., Finnegan, E. J., Dennis, E. S., Peacock, W. J., & Trevaskis, B. (2009). Vernalization-induced flowering in cereals is associated with changes in histone methylation at the VERNALIZATION1 gene. *Proceedings of the National Academy of Sciences*, *106*(20), 8386–8391.

Opseth, L., Holefors, A., Rosnes, A. K. R., Lee, Y., & Olsen, J. E. (2016). FTL2 expression preceding bud set corresponds with timing of bud set in Norway spruce under different light quality treatments. *Environmental and Experimental Botany*, *121*, 121–131.

Ordoñez-Herrera, N., Fackendahl, P., Yu, X., Schaefer, S., Koncz, C., & Hoecker, U. (2015). A cop1 spa mutant deficient in COP1 and SPA proteins reveals partial co-action of COP1 and SPA during Arabidopsis post-embryonic development and photomorphogenesis. *Molecular Plant*, *8*(3), 479–481.

Orozco-Nunnelly, D. A., Muhammad, D., Mezzich, R., Lee, B.-S., Jayathilaka, L., Kaufman, L. S., & Warpeha, K. M. (2014). Pirin1 (PRN1) is a multifunctional protein that regulates quercetin, and impacts specific light and UV responses in the seed-to-seedling transition of Arabidopsis thaliana. *PLoS One*, *9*(4), e93371.

Ovcharenko, I., Loots, G. G., Giardine, B. M., Hou, M., Ma, J., Hardison, R. C., Stubbs, L., & Miller, W. (2005). Mulan: multiple-sequence local alignment and visualization for studying function and evolution. *Genome Research*, *15*(1), 184–194.

Oyiga, B. C., Sharma, R. C., Baum, M., Ogbonnaya, F. C., Léon, J., & Ballvora, A. (2018). Allelic variations and differential expressions detected at quantitative trait loci for salt stress tolerance in wheat. *Plant, Cell & Environment*, *41*(5), 919–935.

Pajoro, A., Severing, E., Angenent, G. C., & Immink, R. G. H. (2017). Histone H3 lysine 36 methylation affects temperature-induced alternative splicing and flowering in plants. *Genome Biology*, *18*(1), 1–12.

Palmer, N. A., Saathoff, A. J., Kim, J., Benson, A., Tobias, C. M., Twigg, P., Vogel, K. P., Madhavan, S., & Sarath, G. (2012). Next-generation sequencing of crown and rhizome

transcriptome from an upland, tetraploid switchgrass. *Bioenergy Research*, *5*(3), 649–661.

Pánková, K., Milec, Z., Simmonds, J., Leverington-Waite, M., Fish, L., & Snape, J. W. (2008). Genetic mapping of a new flowering time gene on chromosome 3B of wheat. *Euphytica*, *164*(3), 779–787. https://doi.org/10.1007/s10681-008-9727-0

Park, D. H., Somers, D. E., Kim, Y. S., Choy, Y. H., Lim, H. K., Soh, M. S., Kim, H. J., Kay, S. A., & Nam, H. G. (1999). Control of circadian rhythms and photoperiodic flowering by the Arabidopsis GIGANTEA gene. *Science*, *285*(5433), 1579–1582.

Pasam, R. K., Sharma, R., Malosetti, M., van Eeuwijk, F. A., Haseneyer, G., Kilian, B., & Graner, A. (2012). Genome-wide association studies for agronomical traits in a world wide spring barley collection. *BMC Plant Biology*, *12*(1), 1–22.

Pearce, S., Kippes, N., Chen, A., Debernardi, J. M., & Dubcovsky, J. (2016). RNA-seq studies using wheat PHYTOCHROME B and PHYTOCHROME C mutants reveal shared and specific functions in the regulation of flowering and shade-avoidance pathways. *BMC Plant Biology*, *16*(1), 1–19.

Pearce, S., Saville, R., Vaughan, S. P., Chandler, P. M., Wilhelm, E. P., Sparks, C. A., Al-Kaff, N., Korolev, A., Boulton, M. I., & Phillips, A. L. (2011). Molecular characterization of Rht-1 dwarfing genes in hexaploid wheat. *Plant Physiology*, *157*(4), 1820–1831.

Pearce, S., Vanzetti, L. S., & Dubcovsky, J. (2013). Exogenous gibberellins induce wheat spike development under short days only in the presence of VERNALIZATION1. *Plant Physiology*, *163*(3), 1433–1445.

Peng, J., Richards, D. E., Hartley, N. M., Murphy, G. P., Devos, K. M., Flintham, J. E., Beales, J., Fish, L. J., Worland, A. J., & Pelica, F. (1999). 'Green revolution'genes encode mutant gibberellin response modulators. *Nature*, *400*(6741), 256–261.

Perales, M., & Más, P. (2007). A functional link between rhythmic changes in chromatin structure and the Arabidopsis biological clock. *The Plant Cell*, *19*(7), 2111–2123.

Peterson, R. F. (1965). Wheat crop series, Ed. Polunin, N. *Inter Science Publication Inc. New York*, *422*.

Phillips, Patrick C. (2008a). Epistasis--the essential role of gene interactions in the structure and evolution of genetic systems. *Nature Reviews. Genetics*, *9*(11), 855–867. https://doi.org/10.1038/nrg2452

Phillips, Patrick C. (2008b). Epistasis--the essential role of gene interactions in the structure and evolution of genetic systems. *Nature Reviews. Genetics*, *9*(11), 855–867. https://doi.org/10.1038/nrg2452

Phillips, PATRICK C, Otto, S. P., Whitlock, M. C., Wolf, J. D., Brodie, E. D. I., & Wade, M. J. (2000). Beyond the average: the evolutionary importance of gene interactions and variability of epistatic effects. *Epistasis and the Evolutionary Process*, 20–38.

Piepho, H. P., Möhring, J., Melchinger, A. E., & Büchse, A. (2008). BLUP for phenotypic selection in plant breeding and variety testing. *Euphytica*, *161*(1), 209–228.

Piétu, G., Mariage-Samson, R., Fayein, N.-A., Matingou, C., Eveno, E., Houlgatte, R., Decraene, C., Vandenbrouck, Y., Tahi, F., & Devignes, M.-D. (1999). The Genexpress IMAGE knowledge base of the human brain transcriptome: a prototype integrated resource for functional and computational genomics. *Genome Research*, *9*(2), 195–209.

Pin, P. A., Benlloch, R., Bonnet, D., Wremerth-Weich, E., Kraft, T., Gielen, J. J. L., & Nilsson, O. (2010). An antagonistic pair of FT homologs mediates the control of flowering time in sugar beet. *Science*, *330*(6009), 1397–1400.

Platt, A., Vilhjálmsson, B. J., & Nordborg, M. (2010). Conditions under which genome-wide association studies will be positively misleading. *Genetics*, *186*(3), 1045–1052.

Pletcher, M. T., McClurg, P., Batalov, S., Su, A. I., Barnes, S. W., Lagler, E., Korstanje, R., Wang, X., Nusskern, D., & Bogue, M. A. (2004). Use of a dense single nucleotide polymorphism map for in silico mapping in the mouse. *PLoS Biology*, *2*(12).

Pokhilko, A., Fernández, A. P., Edwards, K. D., Southern, M. M., Halliday, K. J., & Millar, A. J. (2012). The clock gene circuit in Arabidopsis includes a repressilator with additional feedback loops. *Molecular Systems Biology*, *8*(1), 574.

Poland, J. A., Brown, P. J., Sorrells, M. E., & Jannink, J.-L. (2012). Development of high-density genetic maps for barley and wheat using a novel two-enzyme genotyping-by-sequencing approach. *PloS One*, *7*(2), e32253.

Prasad, P. V. V, Boote, K. J., Allen Jr, L. H., Sheehy, J. E., & Thomas, J. M. G. (2006). Species, ecotype and cultivar differences in spikelet fertility and harvest index of rice in response to high temperature stress. *Field Crops Research*, *95*(2–3), 398–411.

Price, A. L., Patterson, N. J., Plenge, R. M., Weinblatt, M. E., Shadick, N. A., & Reich, D. (2006). Principal components analysis corrects for stratification in genome-wide association studies. *Nature Genetics*, *38*(8), 904–909.

Prieto, P., Ochagavía, H., Savin, R., Griffiths, S., & Slafer, G. A. (2018). Dynamics of floret initiation/death determining spike fertility in wheat as affected by Ppd genes under field conditions. *Journal of Experimental Botany*, *69*(10), 2633–2645.

Pritchard, J. K., Stephens, M., Rosenberg, N. A., & Donnelly, P. (2000). Association mapping in structured populations. *The American Journal of Human Genetics*, *67*(1), 170–181.

Pugsley, A. T. (1971). A genetic analysis of the spring-winter habit of growth in wheat. *Australian Journal of Agricultural Research*, *22*(1), 21–31.

Purvis, O. N. (1934). An analysis of the influence of temperature during germination on the subsequent development of certain winter cereals and its relation to the effect of length of day. *Annals of Botany*, *48*(192), 919–955.

Putterill, J., Robson, F., Lee, K., Simon, R., & Coupland, G. (1995). The CONSTANS gene of Arabidopsis promotes flowering and encodes a protein showing similarities to zinc finger transcription factors. *Cell*, *80*(6), 847–857.

Rafalski, J. A. (2010). Association genetics in crop improvement. *Current Opinion in Plant Biology*, *13*(2), 174–180. https://doi.org/10.1016/j.pbi.2009.12.004

Rahimi, Y., Bihamta, M. R., Taleei, A., Alipour, H., & Ingvarsson, P. K. (2019). Genome-wide association study of agronomic traits in bread wheat reveals novel putative alleles for future breeding programs. *BMC Plant Biology*, *19*(1), 1–19.

Rajaram, S., & Ginkel, M. Van. (2001). *México: 50 years of international wheat breeding. The world wheat book: a history of wheat breeding.*

Ramirez-Gonzalez, R. H., Segovia, V., Bird, N., Fenwick, P., Holdgate, S., Berry, S., Jack, P., Caccamo, M., & Uauy, C. (2015). RNA-S eq bulked segregant analysis enables the

identification of high-resolution genetic markers for breeding in hexaploid wheat. *Plant Biotechnology Journal*, *13*(5), 613–624.

Razumov, V. I. (1960). The effect of gibberellic acid on development of winter cereals. *Botanicheskii Zhurnal*, *45*(12), 1732–1738.

Record, P. (2009). The Responses of Species to Climate Over Two Centuries : An Analysis of the Marsham Author (s): T . H . Sparks and P . D . Carey Published by : British Ecological Society Stable URL : http://www.jstor.org/stable/2261570. *Society*, *83*(2), 321–329.

Reif, J. C., Maurer, H. P., Korzun, V., Ebmeyer, E., Miedaner, T., & Würschum, T. (2011). Mapping QTLs with main and epistatic effects underlying grain yield and heading time in soft winter wheat. *Theoretical and Applied Genetics*, *123*(2), 283–292. https://doi.org/10.1007/s00122-011-1583-y

Reynolds, M., Foulkes, J., Furbank, R., Griffiths, S., King, J., Murchie, E., Parry, M., & Slafer, G. (2012). Achieving yield gains in wheat. *Plant, Cell & Environment*, *35*(10), 1799–1823.

Risch, N., & Merikangas, K. (1996). The future of genetic studies of complex human diseases. *Science*, *273*(5281), 1516–1517.

Robinson, M. D., McCarthy, D. J., & Smyth, G. K. (2010). edgeR: a Bioconductor package for differential expression analysis of digital gene expression data. *Bioinformatics*, *26*(1), 139–140.

Robson, F., Costa, M. M. R., Hepworth, S. R., Vizir, I., Pin˜ eiro, M., Reeves, P. H., Putterill, J., & Coupland, G. (2001). Functional importance of conserved domains in the flowering-time gene CONSTANS demonstrated by analysis of mutant alleles and transgenic plants. *The Plant Journal*, *28*(6), 619–631.

Romera-Branchat, M., Andrés, F., & Coupland, G. (2014). Flowering responses to seasonal cues: what's new? *Current Opinion in Plant Biology*, *21*, 120–127.

Roro, A. G., Terfa, M. T., Solhaug, K. A., Tsegaye, A., Olsen, J. E., & Torre, S. (2016). The impact of UV radiation at high altitudes close to the equator on morphology and productivity of pea (Pisum sativum) in different seasons. *South African Journal of Botany*, *106*, 119–128. https://doi.org/https://doi.org/10.1016/j.sajb.2016.05.011

Rousset, M., Bonnin, I., Remoué, C., Falque, M., Rhoné, B., Veyrieras, J.-B., Madur, D., Murigneux, A., Balfourier, F., & Le Gouis, J. (2011). Deciphering the genetics of flowering time by an association study on candidate genes in bread wheat (Triticum aestivum L.). *Theoretical and Applied Genetics*, *123*(6), 907.

Saile-Mark, M., Tevini, M., & Mark, U. (1996). Effects of solar UVB radiation on growth, flowering and yield of central and southern European maize cultivars (Zea mays L.). *Photochemistry and Photobiology*, *64*(3), 457–463.

Salomé, P. A., & McClung, C. R. (2005). PSEUDO-RESPONSE REGULATOR 7 and 9 are partially redundant genes essential for the temperature responsiveness of the Arabidopsis circadian clock. *The Plant Cell*, *17*(3), 791–803.

Samis, K. E., Murren, C. J., Bossdorf, O., Donohue, K., Fenster, C. B., Malmberg, R. L., Purugganan, M. D., & Stinchcombe, J. R. (2012). Longitudinal trends in climate drive flowering time clines in North American Arabidopsis thaliana. *Ecology and Evolution*, *2*(6), 1162–1180.

Sannemann, W., Huang, B. E., Mathew, B., & Léon, J. (2015). Multi-parent advanced

generation inter-cross in barley: high-resolution quantitative trait locus mapping for flowering time as a proof of concept. *Molecular Breeding*, *35*(3), 1–16.

Santra, D. K., Santra, M., Allan, R. E., Campbell, K. G., & Kidwell, K. K. (2009). Genetic and molecular characterization of vernalization genes Vrn-A1, Vrn-B1, and Vrn-D1 in spring wheat germplasm from the Pacific Northwest region of the USA. *Plant Breeding*, *128*(6), 576–584.

Schaffer, R., Ramsay, N., Samach, A., Corden, S., Putterill, J., Carré, I. A., & Coupland, G. (1998). The late elongated hypocotyl mutation of Arabidopsis disrupts circadian rhythms and the photoperiodic control of flowering. *Cell*, *93*(7), 1219–1229.

Schläppi, M. (2001). RNA levels and activity of FLOWERING LOCUS C are modified in mixed genetic backgrounds of Arabidopsis thaliana. *International Journal of Plant Sciences*, *162*(3), 527–537.

Scott, M. F., Ladejobi, O., Amer, S., Bentley, A. R., Biernaskie, J., Boden, S. A., Clark, M., Dell'Acqua, M., Dixon, L. E., & Filippi, C. V. (2020). Multi-parent populations in crops: a toolbox integrating genomics and genetic mapping with breeding. *Heredity*, *125*(6), 396–416.

Searle, I., & Coupland, G. (2004). Induction of flowering by seasonal changes in photoperiod. *The EMBO Journal*, *23*(6), 1217–1222.

Searle, I., He, Y., Turck, F., Vincent, C., Fornara, F., Kröber, S., Amasino, R. A., & Coupland, G. (2006). The transcription factor FLC confers a flowering response to vernalization by repressing meristem competence and systemic signaling in Arabidopsis. *Genes & Development*, *20*(7), 898–912.

Segura, V., Vilhjálmsson, B. J., Platt, A., Korte, A., Seren, Ü., Long, Q., & Nordborg, M. (2012). An efficient multi-locus mixed-model approach for genome-wide association studies in structured populations. *Nature Genetics*, *44*(7), 825–830.

Semagn, K., Bjørnstad, Å., & Xu, Y. (2010). The genetic dissection of quantitative traits in crops. *Electronic Journal of Biotechnology*, *13*(5), 16–17.

Shahid, S. A., & Al-Shankiti, A. (2013). Sustainable food production in marginal lands—Case of GDLA member countries. *International Soil and Water Conservation Research*, *1*(1), 24–38.

Shaw, L. M., Turner, A. S., Herry, L., Griffiths, S., & Laurie, D. A. (2013). Mutant alleles of Photoperiod-1 in wheat (Triticum aestivum L.) that confer a late flowering phenotype in long days. *PLoS One*, *8*(11), e79459.

Shaw, L. M., Turner, A. S., & Laurie, D. A. (2012). The impact of photoperiod insensitive Ppd-1a mutations on the photoperiod pathway across the three genomes of hexaploid wheat (Triticum aestivum). *The Plant Journal*, *71*(1), 71–84.

Sheldon, C. C., Burn, J. E., Perez, P. P., Metzger, J., Edwards, J. A., Peacock, W. J., & Dennis, E. S. (1999). The FLF MADS box gene: a repressor of flowering in Arabidopsis regulated by vernalization and methylation. *The Plant Cell*, *11*(3), 445–458.

Shen, G., Zhan, W., Chen, H., & Xing, Y. (2014). Dominance and epistasis are the main contributors to heterosis for plant height in rice. *Plant Science*, *215*, 11–18.

Shi, C., Zhao, L., Zhang, X., Lv, G., Pan, Y., & Chen, F. (2019). Gene regulatory network and abundant genetic variation play critical roles in heading stage of polyploidy wheat. *BMC*

Plant Biology, *19*(1), 1–16.

Shimada, S., Ogawa, T., Kitagawa, S., Suzuki, T., Ikari, C., Shitsukawa, N., Abe, T., Kawahigashi, H., Kikuchi, R., & Handa, H. (2009). A genetic network of flowering-time genes in wheat leaves, in which an APETALA1/FRUITFULL-like gene, VRN1, is upstream of FLOWERING LOCUS T. *The Plant Journal*, *58*(4), 668–681.

Shoaib, M., Yang, W., Shan, Q., Sajjad, M., & Zhang, A. (2019). Genome-wide identification and expression analysis of new cytokinin metabolic genes in bread wheat (Triticum aestivum L.). Peer J., 7: e6300. *Doi. Org/10.7717/Peerj*, *6300*.

Shourbalal, S. K. S., Soleymani, A., & Javanmard, H. R. (2019). Shortening vernalization in winter wheat (Triticum aestivum L.) using plant growth regulators and cold stratification. *Journal of Cleaner Production*, *219*, 443–450.

Shu, K., Chen, Q., Wu, Y., Liu, R., Zhang, H., Wang, S., Tang, S., Yang, W., & Xie, Q. (2016). ABSCISIC ACID-INSENSITIVE 4 negatively regulates flowering through directly promoting Arabidopsis FLOWERING LOCUS C transcription. *Journal of Experimental Botany*, *67*(1), 195–205.

Singh, V. K., & Jain, M. (2014). Transcriptome profiling for discovery of genes involved in shoot apical meristem and flower development. *Genomics Data*, *2*, 135–138.

Slafer, G A. (2003). Genetic basis of yield as viewed from a crop physiologist's perspective. *Annals of Applied Biology*, *142*(2), 117–128.

Slafer, G A, Abeledo, L. G., Miralles, D. J., Gonzalez, F. G., & Whitechurch, E. M. (2001). Photoperiod sensitivity during stem elongation as an avenue to raise potential yield in wheat. In *Wheat in a global environment* (pp. 487–496). Springer.

Slafer, Gustavo A. (1996). Differences in phasic development rate amongst wheat cultivars independent of responses to photoperiod and vernalization. A viewpoint of the intrinsic earliness hypothesis. *The Journal of Agricultural Science*, *126*(4), 403–419.

Slafer, Gustavo A, Kantolic, A. G., Appendino, M. L., Tranquilli, G., Miralles, D. J., & Savin, R. (2015). Genetic and environmental effects on crop development determining adaptation and yield. In *Crop Physiology* (pp. 285–319). Elsevier.

Slafer, Gustavo A, & Rawson, H. M. (1994). Sensitivity of wheat phasic development to major environmental factors: a re-examination of some assumptions made by physiologists and modellers. *Functional Plant Biology*, *21*(4), 393–426.

Slatkin, M. (2008). Linkage disequilibrium—understanding the evolutionary past and mapping the medical future. *Nature Reviews Genetics*, *9*(6), 477–485.

Snape, J. W., Butterworth, K., Whitechurch, E., & Worland, A. J. (2001). Waiting for fine times: genetics of flowering time in wheat. In *Wheat in a global environment* (pp. 67–74). Springer.

Snape, J. W., Law, C. N., & Worland, A. J. (1976). Chromosome variation for loci controlling ear emergence time on chromosome 5A of wheat. *Heredity*, *37*(3), 335–340. https://doi.org/10.1038/hdy.1976.97

Somers, D. E., Kim, W.-Y., & Geng, R. (2004). The F-box protein ZEITLUPE confers dosage-dependent control on the circadian clock, photomorphogenesis, and flowering time. *The Plant Cell*, *16*(3), 769–782.

Soneson, C., & Delorenzi, M. (2013). A comparison of methods for differential expression analysis of RNA-seq data. *BMC Bioinformatics*, *14*(1), 1–18.

Song, G., Zhang, R., Zhang, S., Li, Y., Gao, J., Han, X., Chen, M., Wang, J., Li, W., & Li, G. (2017). Response of microRNAs to cold treatment in the young spikes of common wheat. *BMC Genomics*, *18*(1), 1–15.

Song, H.-R., & Noh, Y.-S. (2012). Rhythmic oscillation of histone acetylation and methylation at the Arabidopsis central clock loci. *Molecules and Cells*, *34*(3), 279–287.

Song, J., Li, B., Cui, Y., Zhuo, C., Gu, Y., Hu, K., Wen, J., Yi, B., Shen, J., & Ma, C. (2021). QTL Mapping and Diurnal Transcriptome Analysis Identify Candidate Genes Regulating Brassica napus Flowering Time. *International Journal of Molecular Sciences*, *22*(14), 7559.

Song, K., Kim, H. C., Shin, S., Kim, K.-H., Moon, J.-C., Kim, J. Y., & Lee, B.-M. (2017). Transcriptome analysis of flowering time genes under drought stress in maize leaves. *Frontiers in Plant Science*, *8*, 267.

Song, W.-Y., Wang, G.-L., Chen, L.-L., Kim, H.-S., Pi, L.-Y., Holsten, T., Gardner, J., Wang, B., Zhai, W.-X., & Zhu, L.-H. (1995). A receptor kinase-like protein encoded by the rice disease resistance gene, Xa21. *Science*, *270*(5243), 1804–1806.

Song, Y. H., Lee, I., Lee, S. Y., Imaizumi, T., & Hong, J. C. (2012). CONSTANS and ASYMMETRIC LEAVES 1 complex is involved in the induction of FLOWERING LOCUS T in photoperiodic flowering in Arabidopsis. *The Plant Journal*, *69*(2), 332–342.

Sønsteby, A., & Heide, O. M. (2008). Environmental control of growth and flowering of Rubus idaeus L. cv. Glen Ample. *Scientia Horticulturae*, *117*(3), 249–256.

Soto-Cerda, B. J., & Cloutier, S. (2012). Association mapping in plant genomes. *Genetic Diversity in Plants*, 29–54.

Spilde, L. A. (1989). Influence of seed size and test weight on several agronomic traits of barley and hard red spring wheat. *Journal of Production Agriculture*, *2*(2), 169–172.

Staskawicz, B. J., Ausubel, F. M., Baker, B. J., Ellis, J. G., & Jones, J. D. (1995). Molecular genetics of plant disease resistance. *Science*, *268*(5211), 661–667.

Steinhoff, J., Liu, W., Reif, J. C., Della Porta, G., Ranc, N., & Würschum, T. (2012). Detection of QTL for flowering time in multiple families of elite maize. *Theoretical and Applied Genetics*, *125*(7), 1539–1551.

Stinchcombe, J. R., Weinig, C., Ungerer, M., Olsen, K. M., Mays, C., Halldorsdottir, S. S., Purugganan, M. D., & Schmitt, J. (2004). A latitudinal cline in flowering time in Arabidopsis thaliana modulated by the flowering time gene FRIGIDA. *Proceedings of the National Academy of Sciences*, *101*(13), 4712–4717.

Strayer, C., Oyama, T., Schultz, T. F., Raman, R., Somers, D. E., Más, P., Panda, S., Kreps, J. A., & Kay, S. A. (2000). Cloning of the Arabidopsis clock gene TOC1, an autoregulatory response regulator homolog. *Science*, *289*(5480), 768–771.

Sun, X.-D., & Ni, M. (2011). HYPOSENSITIVE TO LIGHT, an alpha/beta fold protein, acts downstream of ELONGATED HYPOCOTYL 5 to regulate seedling de-etiolation. *Molecular Plant*, *4*(1), 116–126.

Supply, F. A. O. C., & Brief, D. (2020). *Food and Agriculturre Organization of the United*

Nations. Rome.

Tabor, H. K., Risch, N. J., & Myers, R. M. (2002). Candidate-gene approaches for studying complex genetic traits: practical considerations. *Nature Reviews Genetics*, *3*(5), 391–397.

Takano, M., Inagaki, N., Xie, X., Yuzurihara, N., Hihara, F., Ishizuka, T., Yano, M., Nishimura, M., Miyao, A., & Hirochika, H. (2005). Distinct and cooperative functions of phytochromes A, B, and C in the control of deetiolation and flowering in rice. *The Plant Cell*, *17*(12), 3311–3325.

Tan, C., & Yan, L. (2016). Duplicated, deleted and translocated VRN2 genes in hexaploid wheat. *Euphytica*, *208*(2), 277–284.

Tanksley, S. D., & Nelson, J. C. (1996). Advanced backcross QTL analysis: a method for the simultaneous discovery and transfer of valuable QTLs from unadapted germplasm into elite breeding lines. *Theoretical and Applied Genetics*, *92*(2), 191–203.

Team, R. C. (2013). *R: A language and environment for statistical computing*.

Terfa, M. T., Roro, A. G., Olsen, J. E., & Torre, S. (2014). Effects of UV radiation on growth and postharvest characteristics of three pot rose cultivars grown at different altitudes. *Scientia Horticulturae*, *178*, 184–191.

Thomas, B., & Vince-Prue, D. (1996). *Photoperiodism in plants*. Elsevier.

Thomas, D. (2010). Gene–environment-wide association studies: emerging approaches. *Nature Reviews Genetics*, *11*(4), 259–272.

Tian, T., Liu, Y., Yan, H., You, Q., Yi, X., Du, Z., Xu, W., & Su, Z. (2017). agriGO v2. 0: a GO analysis toolkit for the agricultural community, 2017 update. *Nucleic Acids Research*, *45*(W1), W122–W129.

Trevaskis, B., Bagnall, D. J., Ellis, M. H., Peacock, W. J., & Dennis, E. S. (2003). MADS box genes control vernalization-induced flowering in cereals. *Proceedings of the National Academy of Sciences*, *100*(22), 13099–13104.

Trevaskis, B., Hemming, M. N., Dennis, E. S., & Peacock, W. J. (2007). The molecular basis of vernalization-induced flowering in cereals. *Trends in Plant Science*, *12*(8), 352–357.

Tsegay, B. A., Lund, L., Nilsen, J., Olsen, J. E., Molmann, J. M., Ernsten, A., & Juntttila, O. (2005). Growth responses of Betula pendula ecotypes to red and far-red light. *Electronic Journal of Biotechnology*, *8*(1), 17–23.

Turck, F., Fornara, F., & Coupland, G. (2008). Regulation and identity of florigen: FLOWERING LOCUS T moves center stage. *Annu. Rev. Plant Biol.*, *59*, 573–594.

Turner, A., Beales, J., Faure, S., Dunford, R. P., & Laurie, D. A. (2005). The pseudo-response regulator Ppd-H1 provides adaptation to photoperiod in barley. *Science*, *310*(5750), 1031–1034.

Turner, A. S., Faure, S., Zhang, Y., & Laurie, D. A. (2013). The effect of day-neutral mutations in barley and wheat on the interaction between photoperiod and vernalization. *Theoretical and Applied Genetics*, *126*(9), 2267–2277.

Uchiyama, K., Iwata, H., Moriguchi, Y., Ujino-Ihara, T., Ueno, S., Taguchi, Y., Tsubomura, M., Mishima, K., Iki, T., & Watanabe, A. (2013). Demonstration of genome-wide association studies for identifying markers for wood property and male strobili traits in Cryptomeria japonica. *PloS One*, *8*(11), e79866.

Ueda, A., Li, P., Feng, Y., Vikram, M., Kim, S., Kang, C. H., Kang, J. S., Bahk, J. D., Lee, S. Y., & Fukuhara, T. (2008). The Arabidopsis thaliana carboxyl-terminal domain phosphatase-like 2 regulates plant growth, stress and auxin responses. *Plant Molecular Biology*, *67*(6), 683.

Ueda, H., Howson, J. M. M., Esposito, L., Heward, J., Chamberlain, G., Rainbow, D. B., Hunter, K. M. D., Smith, A. N., Di Genova, G., & Herr, M. H. (2003). Association of the T-cell regulatory gene CTLA4 with susceptibility to autoimmune disease. *Nature*, *423*(6939), 506–511.

Vaisse, C., Clement, K., Durand, E., Hercberg, S., Guy-Grand, B., & Froguel, P. (2000). Melanocortin-4 receptor mutations are a frequent and heterogeneous cause of morbid obesity. *The Journal of Clinical Investigation*, *106*(2), 253–262.

Valverde, F., Mouradov, A., Soppe, W., Ravenscroft, D., Samach, A., & Coupland, G. (2004). Photoreceptor regulation of CONSTANS protein in photoperiodic flowering. *Science*, *303*(5660), 1003–1006.

Velculescu, V. E., Zhang, L., Zhou, W., Vogelstein, J., Basrai, M. A., Bassett Jr, D. E., Hieter, P., Vogelstein, B., & Kinzler, K. W. (1997). Characterization of the yeast transcriptome. *Cell*, *88*(2), 243–251.

Villegas, D., Alfaro, C., Ammar, K., Cátedra, M. M., Crossa, J., del Moral, L. F., & Royo, C. (2016). Daylength, Temperature and Solar Radiation Effects on the Phenology and Yield Formation of Spring Durum Wheat. *Journal of Agronomy and Crop Science*, *202*(3), 203–216. https://doi.org/https://doi.org/10.1111/jac.12146

Visscher, P. M., Brown, M. A., McCarthy, M. I., & Yang, J. (2012). Five years of GWAS discovery. *The American Journal of Human Genetics*, *90*(1), 7–24.

Voss-Fels, K. P., Stahl, A., Wittkop, B., Lichthardt, C., Nagler, S., Rose, T., Chen, T.-W., Zetzsche, H., Seddig, S., & Baig, M. M. (2019). Breeding improves wheat productivity under contrasting agrochemical input levels. *Nature Plants*, *5*(7), 706–714.

Waddington, S. R., Cartwright, P. M., & Wall, P. C. (1983). A quantitative scale of spike initial and pistil development in barley and wheat. *Annals of Botany*, *51*(1), 119–130.

Wallace, M. R., Marchuk, D. A., Andersen, L. B., Letcher, R., Odeh, H. M., Saulino, A. M., Fountain, J. W., Brereton, A., Nicholson, J., & Mitchell, A. L. (1990). Type 1 neurofibromatosis gene: identification of a large transcript disrupted in three NF1 patients. *Science*, *249*(4965), 181–186.

Wang, B., Smith, S. M., & Li, J. (2018). Genetic regulation of shoot architecture. *Annual Review of Plant Biology*, *69*, 437–468.

Wang, G., Cai, G., Xu, N., Zhang, L., Sun, X., Guan, J., & Meng, Q. (2019). Novel DnaJ protein facilitates thermotolerance of transgenic tomatoes. *International Journal of Molecular Sciences*, *20*(2), 367.

Wang, L., Feng, Z., Wang, X., Wang, X., & Zhang, X. (2010). DEGseq: an R package for identifying differentially expressed genes from RNA-seq data. *Bioinformatics*, *26*(1), 136–138.

Wang, S.-B., Feng, J.-Y., Ren, W.-L., Huang, B., Zhou, L., Wen, Y.-J., Zhang, J., Dunwell, J. M., Xu, S., & Zhang, Y.-M. (2016). Improving power and accuracy of genome-wide association studies via a multi-locus mixed linear model methodology. *Scientific Reports*,

6(1), 1–10.

Wang, S., Wong, D., Forrest, K., Allen, A., Chao, S., Huang, B. E., Maccaferri, M., Salvi, S., Milner, S. G., & Cattivelli, L. (2014). Characterization of polyploid wheat genomic diversity using a high-density 90 000 single nucleotide polymorphism array. *Plant Biotechnology Journal*, *12*(6), 787–796.

Wang, Y., Li, L., Ye, T., Lu, Y., Chen, X., & Wu, Y. (2013). The inhibitory effect of ABA on floral transition is mediated by ABI5 in Arabidopsis. *Journal of Experimental Botany*, *64*(2), 675–684.

Wang, Z., Gerstein, M., & Snyder, M. (2009). RNA-Seq: a revolutionary tool for transcriptomics. *Nature Reviews Genetics*, *10*(1), 57–63.

Wei, X., Rahim, M. A., Zhao, Y., Yang, S., Wang, Z., Su, H., Li, L., Niu, L., Rashid, M. H.-U., & Yuan, Y. (2021). Comparative Transcriptome Analysis of Early-and Late-Bolting Traits in Chinese Cabbage (Brassica rapa). *Frontiers in Genetics*, *12*, 119.

Welsh, J. R. (1973). Genetic control of photoperiod response in wheat. *Proc. 4th Int. Wheat Genet. Symp., Columbia, USA, 1973*, 879–884.

Wenkel, S., Turck, F., Singer, K., Gissot, L., Le Gourrierec, J., Samach, A., & Coupland, G. (2006). CONSTANS and the CCAAT box binding complex share a functionally important domain and interact to regulate flowering of Arabidopsis. *The Plant Cell*, *18*(11), 2971–2984.

Werner, T., Köllmer, I., Bartrina, I., Holst, K., & Schmülling, T. (2006). New insights into the biology of cytokinin degradation. *Plant Biology*, *8*(03), 371–381.

Wilczek, A. M., Burghardt, L. T., Cobb, A. R., Cooper, M. D., Welch, S. M., & Schmitt, J. (2010). Genetic and physiological bases for phenological responses to current and predicted climates. *Philosophical Transactions of the Royal Society B: Biological Sciences*, *365*(1555), 3129–3147.

Wilhelm, B. T., Marguerat, S., Watt, S., Schubert, F., Wood, V., Goodhead, I., Penkett, C. J., Rogers, J., & Bähler, J. (2008). Dynamic repertoire of a eukaryotic transcriptome surveyed at single-nucleotide resolution. *Nature*, *453*(7199), 1239–1243.

Williams, I. H. (1960). Effects of environment on Rubus idaeus LV Dormancy and flowering of the mature shoot. *Journal of Horticultural Science*, *35*(3), 214–220.

Wilson, L. M., Whitt, S. R., Ibaéñez, A. M., Rocheford, T. R., Goodman, M. M., & Buckler IV, E. S. (2004). Dissection of maize kernel composition and starch production by candidate gene association. *The Plant Cell*, *16*(10), 2719–2733.

Wilson, P. B., Streich, J. C., Murray, K. D., Eichten, S. R., Cheng, R., Aitken, N. C., Spokas, K., Warthmann, N., Gordon, S. P., & Accession, C. (2019). Global diversity of the Brachypodium species complex as a resource for genome-wide association studies demonstrated for agronomic traits in response to climate. *Genetics*, *211*(1), 317–331.

Winfield, M. O., Allen, A. M., Burridge, A. J., Barker, G. L. A., Benbow, H. R., Wilkinson, P. A., Coghill, J., Waterfall, C., Davassi, A., & Scopes, G. (2016). High-density SNP genotyping array for hexaploid wheat and its secondary and tertiary gene pool. *Plant Biotechnology Journal*, *14*(5), 1195–1206.

Worland, A J, Börner, A., Korzun, V., Li, W. M., Petrovic, S., & Sayers, E. J. (1998). The influence of photoperiod genes on the adaptability of European winter wheats. *Euphytica*,

100(1), 385–394.

Worland, A J, Petrovic, S., & Law, C. N. (1988). Genetic Analysis of Chromosome 2D of Wheat: II. The Importance of this Chromosome to Yugoslavian Varieties. *Plant Breeding*, *100*(4), 247–259.

Worland, Anthony John. (1996). The influence of flowering time genes on environmental adaptability in European wheats. *Euphytica*, *89*(1), 49–57.

Worland, T. (2001). Genetic basis of worldwide wheat varietal improvement. *The World Wheat Book: A History of Wheat BreedingWorland, T. (2001). Genetic Basis of Worldwide Wheat Varietal Improvement. The World Wheat Book: A History of Wheat Breeding, 59–100.*, 59–100.

Wray, N., & Visscher, P. (2008). Estimating trait heritability. *Nature Education*, *1*(1), 29.

Wu, Chao, Cui, K., Wang, W., Li, Q., Fahad, S., Hu, Q., Huang, J., Nie, L., Mohapatra, P. K., & Peng, S. (2017). Heat-induced cytokinin transportation and degradation are associated with reduced panicle cytokinin expression and fewer spikelets per panicle in rice. *Frontiers in Plant Science*, *8*, 371.

Wu, Chengqing, DeWan, A., Hoh, J., & Wang, Z. (2011). A comparison of association methods correcting for population stratification in case–control studies. *Annals of Human Genetics*, *75*(3), 418–427.

Würschum, T., Maurer, H. P., Dreyer, F., & Reif, J. C. (2013). Effect of inter-and intragenic epistasis on the heritability of oil content in rapeseed (Brassica napus L.). *Theoretical and Applied Genetics*, *126*(2), 435–441.

Xu, C., Xia, Z., Huang, Z., Xia, C., Huang, J., Zha, M., Wang, S., Imran, M., Casteel, S., & Jiang, Y. (2019). Understanding the physiological and transcriptional mechanism of reproductive stage soybean in response to heat stress. *Crop Breeding, Genetics and Genomics*, *2*(1).

Xu, Shizhong. (2007). An empirical Bayes method for estimating epistatic effects of quantitative trait loci. *Biometrics*, *63*(2), 513–521.

Xu, Shujuan, Xiao, J., Yin, F., Guo, X., Xing, L., Xu, Y., & Chong, K. (2019). The protein modifications of O-GlcNAcylation and phosphorylation mediate vernalization response for flowering in winter wheat. *Plant Physiology*, *180*(3), 1436–1449.

Xu, Y., Li, P., Yang, Z., & Xu, C. (2017). Genetic mapping of quantitative trait loci in crops. *The Crop Journal*, *5*(2), 175–184.

Yan, L, Helguera, M., Kato, K., Fukuyama, S., Sherman, J., & Dubcovsky, J. (2004). Allelic variation at the VRN-1 promoter region in polyploid wheat. *Theoretical and Applied Genetics*, *109*(8), 1677–1686.

Yan, Limei, Fu, D., Li, C., Blechl, A., Tranquilli, G., Bonafede, M., Sanchez, A., Valarik, M., Yasuda, S., & Dubcovsky, J. (2006). The wheat and barley vernalization gene VRN3 is an orthologue of FT. *Proceedings of the National Academy of Sciences*, *103*(51), 19581–19586.

Yan, Liuling, Loukoianov, A., Blechl, A., Tranquilli, G., Ramakrishna, W., SanMiguel, P., Bennetzen, J. L., Echenique, V., & Dubcovsky, J. (2004). The wheat VRN2 gene is a flowering repressor down-regulated by vernalization. *Science*, *303*(5664), 1640–1644.

Yan, Liuling, Loukoianov, A., Tranquilli, G., Helguera, M., Fahima, T., & Dubcovsky, J. (2003). Positional cloning of the wheat vernalization gene VRN1. *Proceedings of the National Academy of Sciences*, *100*(10), 6263–6268.

Yang, Y., Zhang, X., Wu, L., Zhang, L., Liu, G., Xia, C., Liu, X., & Kong, X. (2021). Transcriptome profiling of developing leaf and shoot apices to reveal the molecular mechanism and co-expression genes responsible for the wheat heading date. *BMC Genomics*, *22*(1), 1–13.

Yanofsky, M. F., Ma, H., Bowman, J. L., Drews, G. N., Feldmann, K. A., & Meyerowitz, E. M. (1990). The protein encoded by the Arabidopsis homeotic gene agamous resembles transcription factors. *Nature*, *346*(6279), 35–39.

Yasuda, S., & Shimoyama, H. (1965). Analysis of internal factors influencing the heading time of wheat varieties. *Berichte Des Ohara Instituts Für Landwirtschaftliche Biologie, Okayama Universität*, *13*(1), 23–38.

Yu, J., Pressoir, G., Briggs, W. H., Bi, I. V., Yamasaki, M., Doebley, J. F., McMullen, M. D., Gaut, B. S., Nielsen, D. M., & Holland, J. B. (2006). A unified mixed-model method for association mapping that accounts for multiple levels of relatedness. *Nature Genetics*, *38*(2), 203–208.

Zadoks, J. C., Chang, T. T., & Konzak, C. F. (1974). A decimal code for the growth stages of cereals. *Weed Research*, *14*(6), 415–421.

Zanke, C., Ling, J., Plieske, J., Kollers, S., Ebmeyer, E., Korzun, V., Argillier, O., Stiewe, G., Hinze, M., Beier, S., Ganal, M. W., & Röder, M. S. (2014). Genetic architecture of main effect QTL for heading date in European winter wheat. *Frontiers in Plant Science*, *5*(MAY), 1–12. https://doi.org/10.3389/fpls.2014.00217

Zeng, Z.-B. (1993). Theoretical basis for separation of multiple linked gene effects in mapping quantitative trait loci. *Proceedings of the National Academy of Sciences*, *90*(23), 10972–10976.

Zhai, Q., Zhang, X., Wu, F., Feng, H., Deng, L., Xu, L., Zhang, M., Wang, Q., & Li, C. (2015). Transcriptional mechanism of jasmonate receptor COI1-mediated delay of flowering time in Arabidopsis. *The Plant Cell*, *27*(10), 2814–2828.

Zhang, J., Wang, Y., Wu, S., Yang, J., Liu, H., & Zhou, Y. (2012). A single nucleotide polymorphism at the Vrn-D1 promoter region in common wheat is associated with vernalization response. *Theoretical and Applied Genetics*, *125*(8), 1697–1704.

Zhang, X., Chen, J., Yan, Y., Yan, X., Shi, C., Zhao, L., & Chen, F. (2018). Genome-wide association study of heading and flowering dates and construction of its prediction equation in Chinese common wheat. *Theoretical and Applied Genetics*, *131*(11), 2271–2285.

Zhang, Z., Ersoz, E., Lai, C.-Q., Todhunter, R. J., Tiwari, H. K., Gore, M. A., Bradbury, P. J., Yu, J., Arnett, D. K., & Ordovas, J. M. (2010). Mixed linear model approach adapted for genome-wide association studies. *Nature Genetics*, *42*(4), 355–360.

Zhao, T., Ni, Z., Dai, Y., Yao, Y., Nie, X., & Sun, Q. (2006). Characterization and expression of 42 MADS-box genes in wheat (Triticum aestivum L.). *Molecular Genetics and Genomics*, *276*(4), 334–350.

Zheng, J., Ge, Q., Hao, Z., & Wang, W. C. (2006). Spring phenophases in recent decades over

eastern china and its possible link to climate changes. *Climatic Change*, *77*(3–4), 449–462. https://doi.org/10.1007/s10584-005-9038-6

Zhu, M., & Zhao, S. (2007). Candidate gene identification approach: progress and challenges. *International Journal of Biological Sciences*, *3*(7), 420.

Zhu, T., Wang, L., Rimbert, H., Rodriguez, J. C., Deal, K. R., De Oliveira, R., Choulet, F., Keeble-Gagnère, G., Tibbits, J., & Rogers, J. (2021). Optical maps refine the bread wheat Triticum aestivum cv. Chinese Spring genome assembly. *The Plant Journal*.

Zhu, X., Tan, C., Cao, S., & Yan, L. (2011). Molecular differentiation of null alleles at ZCCT-1 genes on the A, B, and D genomes of hexaploid wheat. *Molecular Breeding*, *27*(4), 501–510.

Zikhali, M., Griffiths, S., & Ogihara, Y. (2015). The effect of Earliness per se (Eps) genes on flowering time in bread wheat. *Advances in Wheat Genetics: From Genome to Field*, 339–345.

Zikhali, M., Leverington-Waite, M., Fish, L., Simmonds, J., Orford, S., Wingen, L. U., Goram, R., Gosman, N., Bentley, A., & Griffiths, S. (2014). Validation of a 1DL earliness per se (eps) flowering QTL in bread wheat (Triticum aestivum). *Molecular Breeding*, *34*(3), 1023–1033.

Zikhali, M., Wingen, L. U., Leverington-Waite, M., Specel, S., & Griffiths, S. (2017). The identification of new candidate genes Triticum aestivum FLOWERING LOCUS T3-B1 (TaFT3-B1) and TARGET OF EAT1 (TaTOE1-B1) controlling the short-day photoperiod response in bread wheat. *Plant, Cell & Environment*, *40*(11), 2678–2690.

Chapter 7: Appendixes

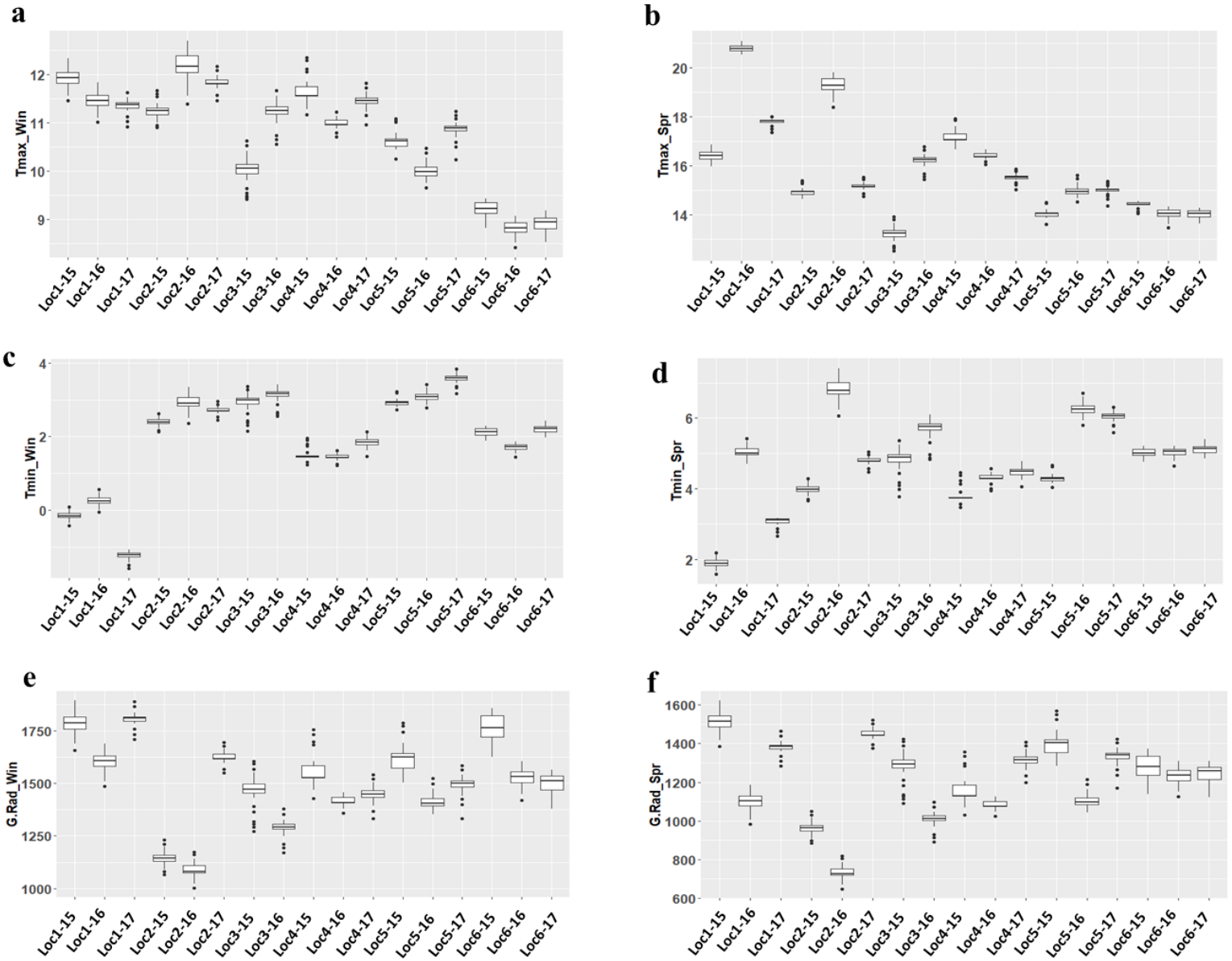
a
Tmax_Win
b
Tmax_Spr
c
Tmin_Win
d
Tmin_Spr
e
G.Rad_Win
f
G.Rad_Spr
Loc1-15 Loc1-16 Loc1-17 Loc2-15 Loc2-16 Loc2-17 Loc3-15 Loc3-16 Loc4-15 Loc4-16 Loc4-17 Loc5-15 Loc5-16 Loc5-17 Loc6-15 Loc6-16 Loc6-17

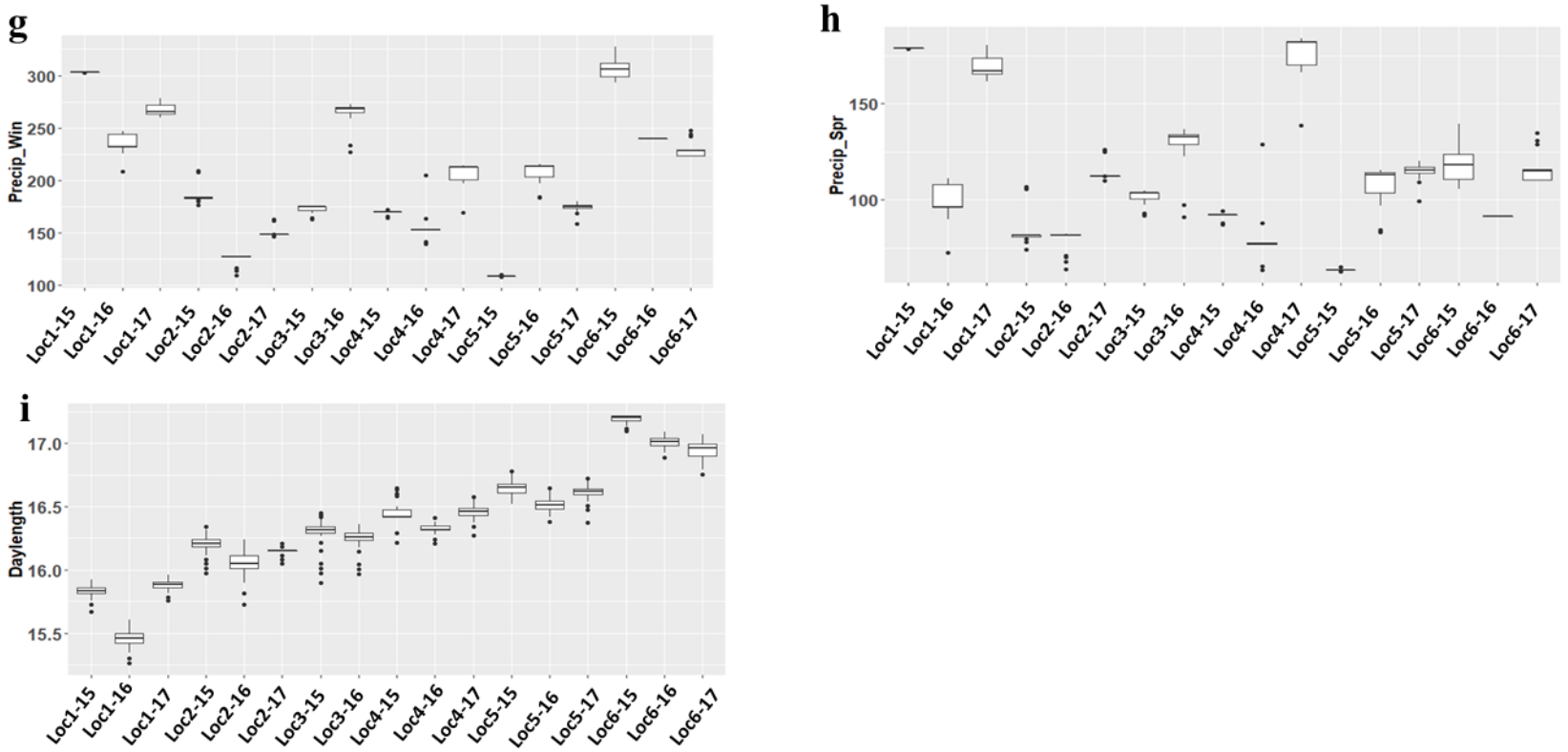

Appendix 3. 1: Boxplots showing the measurements of climatic factors per environment according to winter and spring reference dates. Each boxplot in each measurement is based on the scorings per genotype. The mean was considered for the comparison between environments. a, b) The maximal temperature in °C. c, d) The minimal temperature in °C. e, f)The accumulative global radiation in $Mj/m^2/day$. g, h) The accumulative precipitations in mm. i) The day length in hours

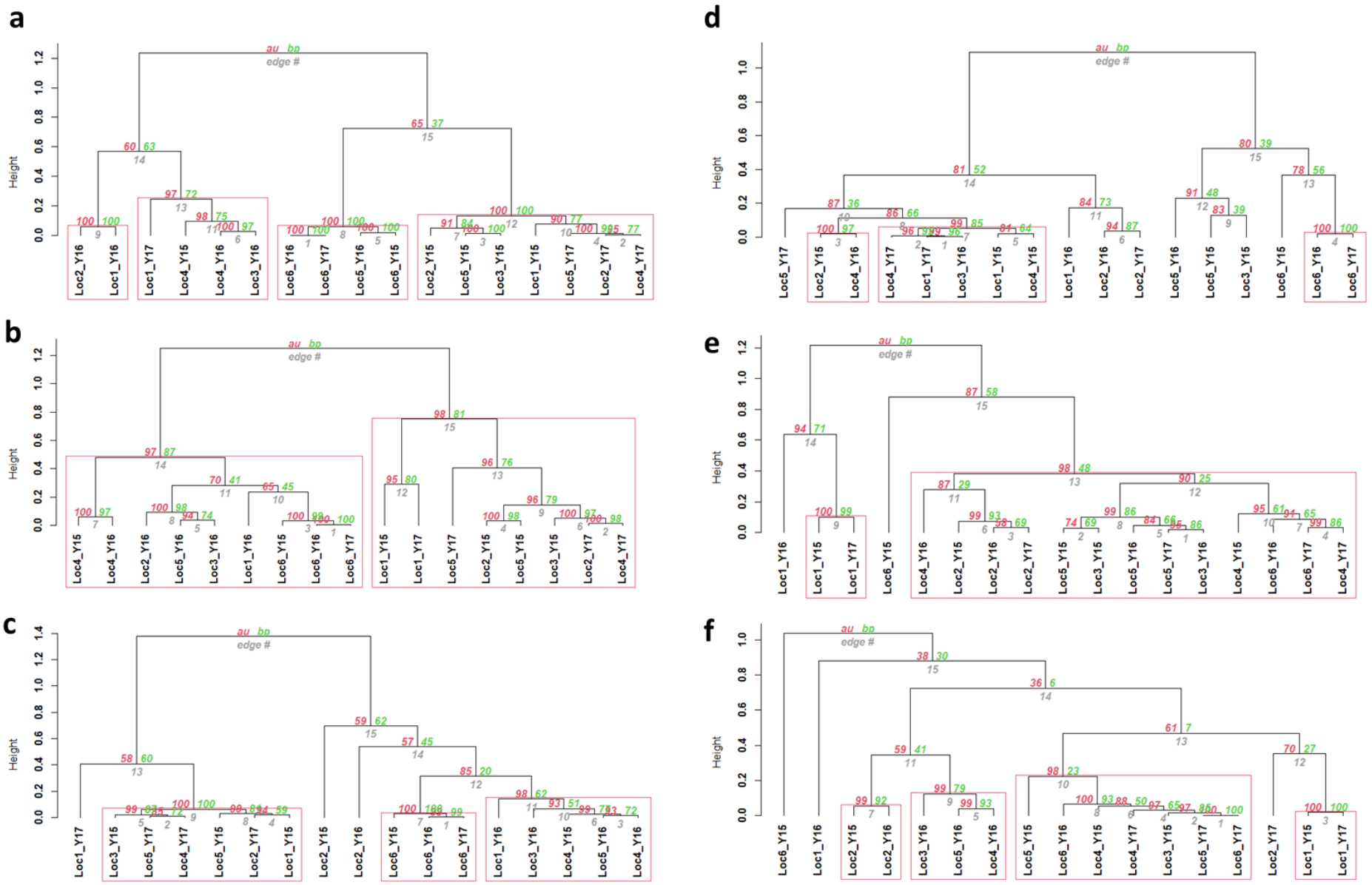
a
b
c
d
e
f
au bp
edge #
Height

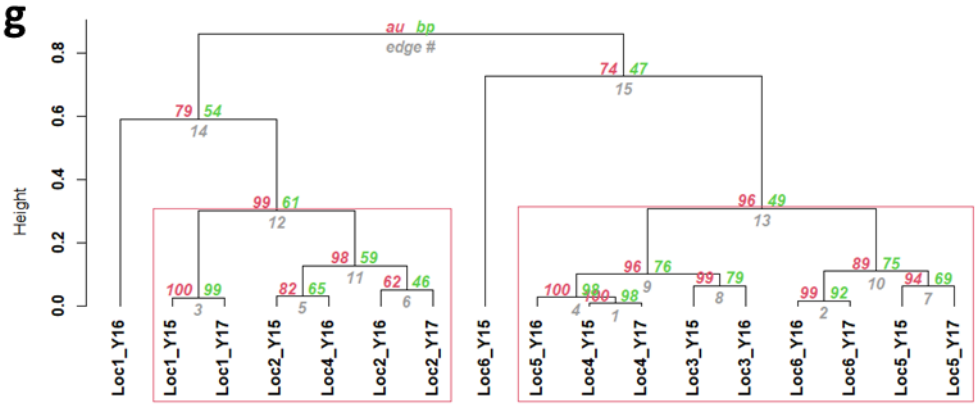

Appendix 3. 2: Dendrogram with p-values (%) showing the hierarchical clustering of the interaction HD*environmental factors including six locations and three years. Green numbers are the bootstrap probability*100 (bp). Red numbers indicate the approximately unbiased p-value*100 (au). Grey numbers specify the rank of the cluster (from 1 to 15). Clusters with "au" larger than 95% are highlighted by the red rectangle. The y-axis represents the correlation distance or dissimilarity between clusters using the 1-cor (Loc_iY_j, Loc_kY_m) function. e. HD*Tmax-spring, b. HD*Tmin_spring, c. HD*global radiation_spring, d. HD*Tmax_winter, e. HD*Tmin_winter, f. HD*global radiation_winter, g. HD*daylength.

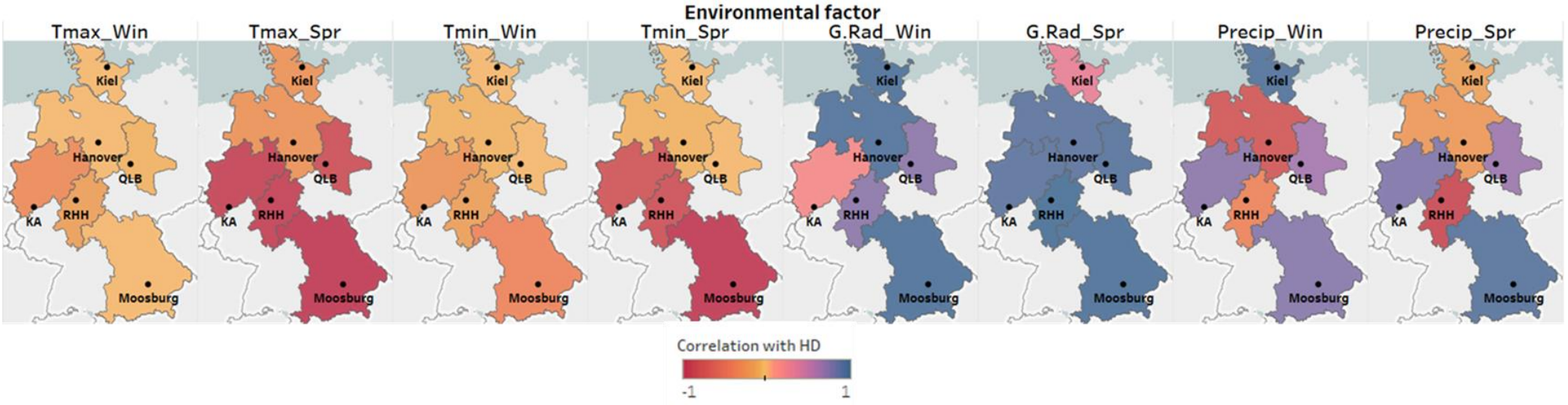

Appendix 3. 3: Geographical heatmap summarizing the correlation between the climatic factors (The minimal and maximal temperature, the global radiation, and the amount of precipitations) with HD based on winter and spring records per location. Each correlation was run separately including HD scores of three years per location. (*), (**) indicate level of significance p< 0.1 and p< 0.01 as shown in the table below. Loc1: Moosburg, Loc2: Klein-Altendorf (KA), Loc3: RHH, Loc4; Quedlinburg, Loc5: Hannover, Loc6: Kiel.

Location	Tmax_Win	Tmax_Spr	Tmin_win	Tmin_Spr	G.Rad_Win	G.Rad_Spr	Precip_Win	Precip_Spr
Loc1	-0.10*	-0.98**	-0.35**	-0.98**	0.99**	0.99**	0.77**	0.95**
Loc2	-0.31**	-0.91**	-0.18**	-0.79**	0.2*	0.92**	0.74**	0.78**
Loc3	-0.16**	-0.93**	-0.23**	-0.81**	0.74**	1**	-0.35**	-0.88**
Loc4	-0.04**	-0.83**	0	0	0.75**	0.94**	0.64**	0.68**
Loc5	0.02**	-0.25**	-0.04	-0.04*	0.97**	0.92**	-0.75**	-0.21**
Loc6	0.06*	-0.26**	0	0	0.99**	0.33**	0.97**	-0.13**

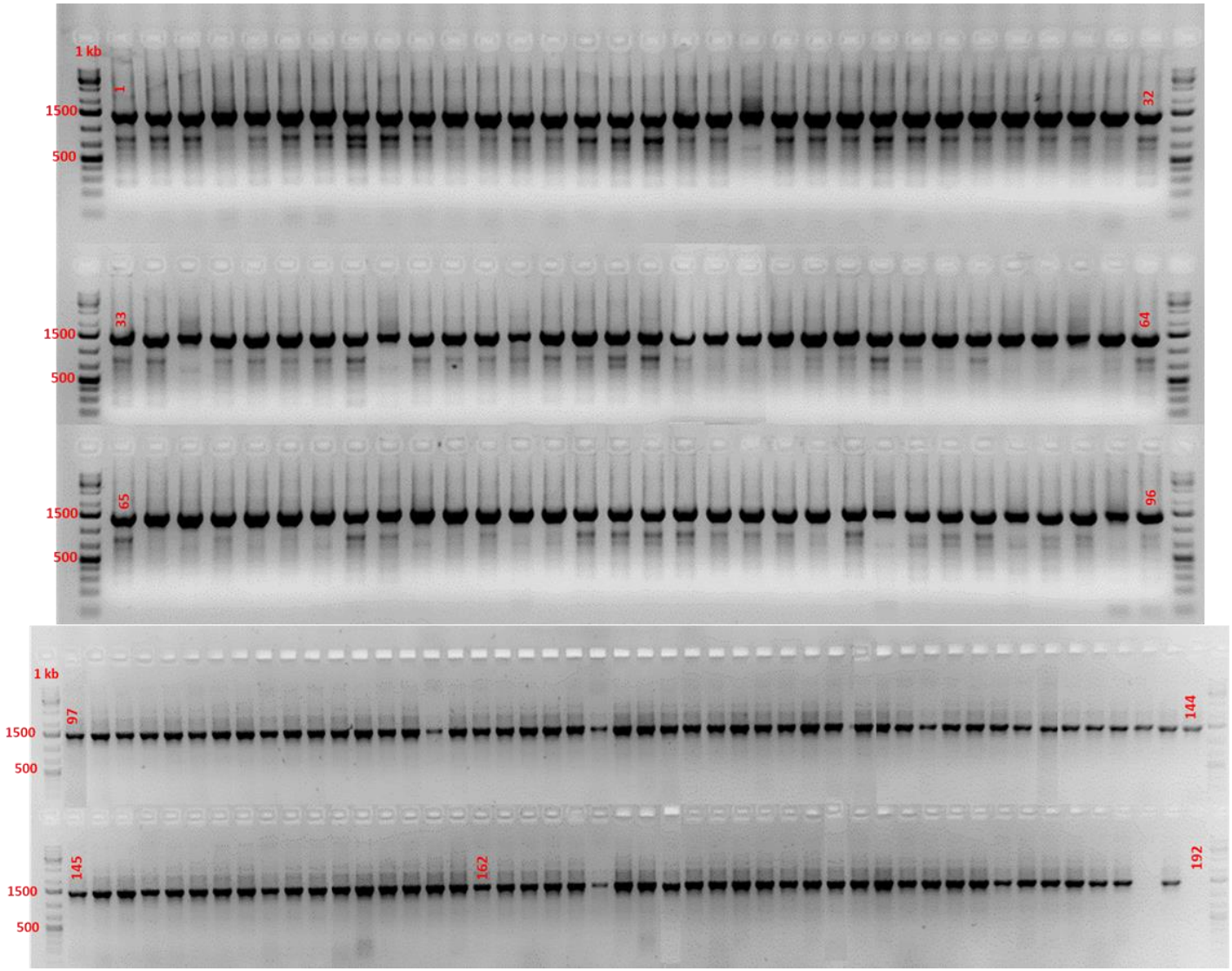

Appendix 3. 4: PCR pattern screening of adapted cultivars (162) at *Vrn-3Bc*, visualized in 2% electrophoresis gel. The size of the amplified gene is 1401bp

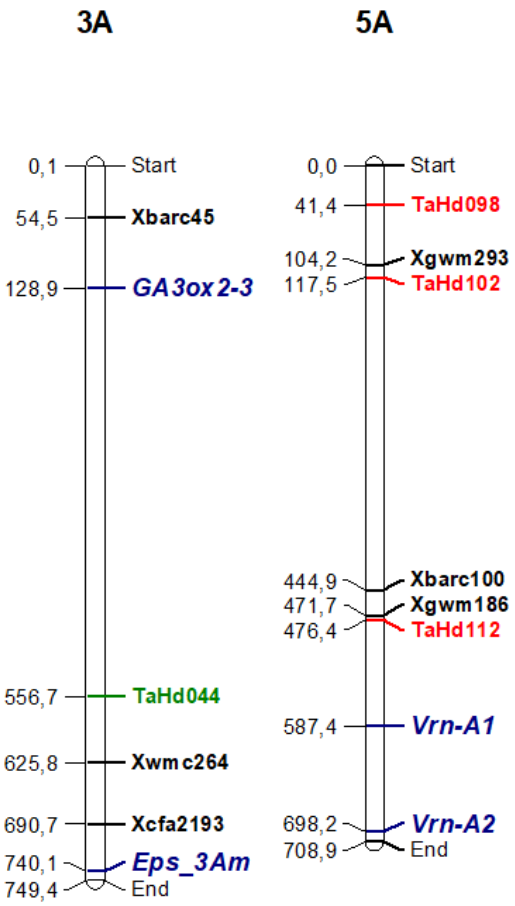

Appendix 3. 5: Physical mapping of strongest detected QTL for heading date trait using panel1 (marker in red color) and panel2 (marked in green color) on chromosomes 5A and 3A, respectively. Known genes involved in flowering time control are highlighted in blue. The previously reported SSR marker are indicated in black and mapped in bp as following: Xbarc45 104,225,386-104,225,406. The numbers on the right of the depicted chromosomes indicate physical positions in bp*10^3.

Appendix 3. 6: Summary of Heading date scoring and daily measurements of environmental factors per location and year

Location	Year	Heading (days)		Global radiation (Mj/m2/day)		Precipitations mm		Tmin (°C)		Tmax (°C)		Daylength (h)
		Winter	Spring	Winter	Spring	Winter	Spring	Winter	Spring	Winter	Spring	
Loc1 48°08'N	2015	153.03	97.03	1788.18	1517.13	303.4	178.8	-0.13	1.9	11.94	16.43	15.84
	2016	140.85	56.85	1602.06	1098.65	235.11	99.11	0.25	5.02	11.45	20.79	15.45
	2017	154.73	80.73	1802.77	1379.71	266.07	167.97	-1.23	3.07	11.34	17.8	15.88
Loc2 50°44'N	2015	151.04	91.04	1144.43	963.77	185.34	83.29	2.39	3.99	11.25	14.93	16.20
	2016	146.91	64.91	1094.04	739.25	126.01	80.3	2.95	6.88	12.22	19.33	16.07
	2017	149.31	104.31	1623.28	1449.76	149.26	112.52	2.71	4.79	11.83	15.15	16.15
Loc3 50°46'N	2015	156.1	96.1	1476.31	1295.99	173.72	102.57	2.98	4.87	10.05	13.23	16.32
	2016	154.02	77.02	1296.5	1016.5	267.43	131.43	3.16	5.75	11.27	16.26	16.26
Loc4 51°47'N	2015	153.62	70.62	1546.63	1147.53	169.46	91.86	1.46	3.76	11.61	17.13	16.43
	2016	150.32	71.32	1414.83	1082.2	155.62	79.82	1.44	4.3	10.99	16.4	16.32
	2017	154.28	103.28	1453.86	1320.47	209.07	178.47	1.87	4.5	11.47	15.53	16.46
Loc5 52°22'N	2015	158.17	94.17	1624.62	1404.52	109.01	63.79	2.93	4.3	10.63	14.04	16.65
	2016	152.27	73.27	1416.93	1107.62	209.4	109.4	3.09	6.27	10.02	14.99	16.52
	2017	154.99	98.99	1495.8	1335.48	175.14	115.62	3.59	6.06	10.88	15.01	16.62
Loc6 54°19'N	2015	167.94	73.94	1769.23	1284.66	307.71	119.71	2.13	5.03	9.22	14.43	16.20
	2016	156.82	78.82	1524.93	1229.84	239.9	91.4	1.71	5.03	8.81	14.02	17.01
	2017	154.64	77.64	1501.91	1246.89	229.42	116.12	2.2	5.12	8.92	14.03	16.95

Appendix 3. 7: Primer used for the analysis of allelic variation at *VRN* and *PPD* genes

Gene	Allele/ target		Name of primer	Genotype at the locus	Primer sequence (5´- 3´)	Amplicon size [bp]	Annealing temperature [°C]	Reference	Growth habit
VRN1	*vrn-A1*		Intr1/C/F	Recessive	GCACTCCTAACCCACTAACC	1068	56	Yan et al.(2004)	Winter
			Intr1/AB/R		TCATCCATCATCAAGGCAAA				
	Vrn-A1a		VRN1AF	Dominant	GAAAGGAAAAATTCTGCTCG	650+750	55	Yan et al.(2004)	Spring
			VRN1R		TGCACCTTCCCCCGCCCCAT				
	Vrn-A1b		VRN1AF	Dominant	GAAAGGAAAAATTCTGCTCG	≈480		Yan et al.(2004)	Spring
			VRN1R		TGCACCTTCCCGCGCCCCAT				
	Vrn-A1c		Intr1/A/F2	Dominant	AGCCTCCACGGTTTGAAAGTAA	1170	58.9	Yan et al.(2004)	Spring
			Intr1/A/R3		AAGTAAGACAACACGAATGTGAGA				
	vrn-B1		Intr1/B/F	Recessive	CAAGTGGAACGGTTAGGACA	1149	56.4	Chu et al.(2011)	Winter
			Intr1/B/R4		CAAATGAAAAGGAATGAGAGCA				
	Vrn-B1a		Intr/B/F	Dominant	CAAGTGGAACGGTTAGGACA	709	58	Chu et al.(2011)	Spring
			Intr/B/R3		CTCATGCCAAAAATTGAAGATGA				
	Vrn-B1b		Vrn-P7_F	Dominant	CCAATCTCACATGCCTCCAA	215 or 252	59	Santra et al.(2009)	Spring
			Vrn-P7_R		ATGCGCCATGAACAACAAAG				
	vrn-D1		Intr1/D/F	Recessive	GTTGTCTGCCTCATCAAATCC	997	61	Fu et al. (2005)	Winter
			Intr1/D/R4		AAATGAAAAGGAACGAGAGCG				
	Vrn-D1a		Intr1/D/F	Dominant	GTTGTCTGCCTCATCAAATCC	1671	61	Fu et al. (2005)	Spring
			Intr/D/R3		GGTCACTGGTGGTCTGTGC				
	Vrn-D1b		VRN1DF	Dominant	CGACCCGGGCGGCACGAGTG	612	65	Zhang et al. (2012)	Spring
			VRN1-SANP161CR		AGGATGGCCAGGCCAAAACG				
VRN2	Null allele	*ZCCT-A1*	V2A-F1	Abscent	CATTAGTTGAGCAATATTTTGA	320	50*	Zhu et al. (2010)	Winter
			V2ABD-R4	Present	TGAATGGGCGAGACCATGAG				Spring
		ZCCT-B1	V2B-F2	Abscent	ATGTGAGAGAGAGACGCAGTA	1126	57	Zhu et al. (2010)	Winter
			V2B-R1	Present	AAGAGATATGTTATATTATCGAAATT				Spring
		ZCCT-D1	V2B-F2	Abscent	TTTGCTAATTCCCATATTGAT	260	50*	Zhu et al. (2010)	Winter
			V2ABD-R3	Present	CAAACCGCATGACATGGACAT				Spring

	Functional allele	*ZCCT-A2*	VRN2/A2/F4	Abscent	AAAAAGTTAGCGCCATGTAACC	994	58	Distelfeld et al.(2009)	Spring
			VRN2/A2/R4	Present	CTAATAGTGCTGGTGAATGCAG				Winter
		ZCCT-B2	VRN2/B2/F2	Abscent	ATACATATGTCCGCGCCTTC	1106/1107	60	Distelfeld et al.(2009)	Spring
			VRN2/B2/R5	Present	TAACTCCTCCAACCGGTCAA				Winter
		ZCCT-D2	ZCCT-D2-F	Abscent	ATGCCCATGTCATGCAGT	800	62	Kippes et al.(2016)	Spring
			ZCCT-D2-R	Present	TACCGGAACCATCCGAGG				Winter
VRN3***	*vrn-B3*		Vrn-P12_F	Recessive	ATGCTTTCGCTTGCCATCC	1140 or 2030	56	Chen et al. (2013)	Winter
			Vrn-P12_R		CTATCCCTACCGGCCATTAG				
	Vrn-B3a		Vrn-P13_F	Dominant	CATAATGCCAAGCCGGTGAGTAC	1200	59	Chen et al. (2013)	Spring
			Vrn-P13_R		ATGTCTGCCAATTAGCTAGC				
	Vrn-B3b		Vrn-P17_F	Dominant	GCTTTCGCTTGCCATCCCAT	898	62	Chen et al. (2013)	Spring
			Vrn-P17_R		GCGGGAACGCTAATCTCCTG				
	Vrn-B3c		Vrn-P14-F	Dominant	GCTTTGAACTCCAAGGAGAA	1401	52	Chen et al. (2013)	Spring
			Vrn_P14-R		ATAATCAGCAGGTGAACCAG				
PPD	*Ppd-A1a*		TaPpd-A1prodelF	Insensitive	CGTACTCCCTCCGTTTCTTT	338	57	Nishida et al. (2013)	Spring
			TaPpd-A1prodelR3		AATTTACGGGGACCAAATACC				
	Ppd-A1b		TaPpd-A1prodelF	Sensitive	CGTACTCCCTCCGTTTCTTT	299	57	Nishida et al. (2013)	Winter
			TaPpd-A1prodelR2		GTTGGGGTCGTTTGGTGGTG				
	Ppd-B1a/b		TaPpd-B1proinF1	a= Insensitive	CAGCTCCTCCGTTTGCTTCC	620 or 312	60**	Nishida et al. (2013)	Spring
			TaPpd-B1proinR1	b= Sensitive	CAGAGGAGTAGTCCGCGTGT				Winter
	Ppd-D1a		Ppd-D1_F1	Insensitive	ACGCCTCCCACTACACTG	288	54	Beales et al. (2007)	Spring
			Ppd-D1_R2		CACTGGTGGTAGCTGAGATT				
	Ppd-D1b		Ppd-D1_F1	Sensitive	ACGCCTCCCACTACACTG	414	54	Beales et al. (2007)	Winter
			Ppd-D1_R1		GTTGGTTCAAACAGAGAGC				

* A touch-down program (57°C down to 51°C for annealing temperature) was performed before the regular program was performed

** A touch-down program (70°C down to 61°C for annealing temperature) was performed before the regular program was performed

*** Natural variation for Vrn-3 has been found only in the B genome

Appendix 3. 8: Physical mapping of *VRN* and *PPD* genes based on reported flanking Marker in Centimorgan (cM)

Gene	Reported flanking markers	Chromosome	Arm	Reference	Position bp	Gene ID	database
Vrn-A1	Xwg644, Xcdo504, Xpsr426	5A	long arm	Galiba et al.(1995)	587,411,454	TraesCS5A02G391700	IWGSC RefSeq v1.1
Vrn-B1	Xgwm408, Xgwm604	5B	longarm	Leonova et al. (2003)	573,802,883	TraesCS5B02G396600	IWGSC RefSeq v1.1
Vrn-D1	Xrz395, Xbcd450	5D	long arm	Nelson et al. (1995)	467,176,609	TraesCS5D02G401500	IWGSC RefSeq v1.1
Vrn-A2	Xbcd402, Xb-Amy-1	5A	long arm	Dubcovsky et al. (1998)	698,162,058	TraesCS5A02G541200	IWGSC RefSeq v1.1
Vrn-B2	SNP62771400, SNP19707472	4B	long arm	Tan et al.(2016)	657,515,589	TraesCS4B02G372700	IWGSC RefSeq v1.1
Vrn-D2	SNP62771400, SNP19707472	4D	long arm	Tan et al.(2016)	509,282,253	TraesCS4D02G364400	IWGSC RefSeq v1.1
Vrn-A3 (TaFTA)	wmc283, barc154	7A	short arm	Bonnin et al. (2008)	71,669,854	TraesCS7A02G115400	IWGSC RefSeq v1.1
Vrn-B3 (TaFTB)	GWM569, ABC158	7B	short arm	McIntosh et al.(2003), Yan et al. (2006)	9,703,454	TraesCS7B02G013100	IWGSC RefSeq v1.1
Vrn-D3 (TaFTD)	barc295, gwm44	7D	short arm	Bonnin et al. (2008)	68,415,945	TraesCS7D02G111600	IWGSC RefSeq v1.1
Vrn-D4 *	Xcfd78,Xbarc205	5D	centromeric region	Yoshida et al.(2010)	156,572,984	TraesCS5D02G118200	IWGSC RefSeq v1.1
Ppd-A1	Xwmc453, Xwmc 181	2A	short arm	Allen et al (2011)	36,933,684	TraesCS2A02G081900	IWGSC RefSeq v1.1
Ppd-B1	XE36M54-312, XE36M52-97	2B	short arm	Mohler et al.(2004)	67,078,632	LOC119362183	NCBI
Ppd-D1	Xfba400-2D, Xcdo1379-2D	2D	short arm	Börner et al.(2002)	33,953,403	TraesCS2D01G079600	IWGSC RefSeq v1.1

* Found only in the D genome

Appendix 3. 9: Student's t-test results of significant Heading date difference between subset1 and subset2

Difference Scores Calculations
subset1
N_1: 162
$df_1 = N - 1 = 162 - 1 = 161$
M_1: 153.24
SS_1: 426.01
$s^2_1 = SS_1/(N - 1) = 426.01/(162-1) = 2.65$
subset2
N_2: 213
$df_2 = N - 1 = 213 - 1 = 212$
M_2: 152.32
SS_2: 1547.46
$s^2_2 = SS_2/(N - 1) = 1547.46/(213-1) = 7.3$
T-value Calculation
$s^2_p = ((df_1/(df_1 + df_2)) * s^2_1) + ((df_2/(df_2 + df_2)) * s^2_2) = ((161/373) * 2.65) + ((212/373) * 7.3) = 5.29$
$s^2_{M1} = s^2_p/N_1 = 5.29/162 = 0.03$
$s^2_{M2} = s^2_p/N_2 = 5.29/213 = 0.02$
$t = (M_1 - M_2)/\sqrt{(s^2_{M1} + s^2_{M2})} = 0.93/\sqrt{0.06} = 3.87$
the *t*-value is 3.86811. The *p*-value is .000065. The result is significant at $p < .01$.

Appendix 3. 10: ANOVA

ANOVA of climatic variable and heading date depending on location and year

Source of variance	Mean square	%	F-value	Pr > F
Tmax*Genotype*Location	283.1232	0.53	14.87	<.0001
Daylength*Genotype*Location	179.9556	0.34	6.25	<.0001
Radiation*Genotype*Location	69.502	0.13	5.29	<.0001
Error	0.1233			

ANOVA of climatic variable and heading date depending on the year

Source of variance	Mean square	%	F-value	Pr > F
Tmax*Genotype*Year	394.4418	0.70	11.64	<.0001
Daylength*Genotype*Year	66.0961	0.12	2.59	<.0001
Radiation*Genotype*Year	103.364	0.18	6.25	<.0001
Error	0.1343			

Appendix 3. 11: Pearson coefficients of correlation and partial correlation between HD and the environmental parameters

Pearson coefficients of correlation (r)

Location	Tmax_Win	Tmax_Spr	Tmin_win	Tmin_Spr	G.Rad_Win	G.Rad_Spr	Precip_Win	Precip_Spr
Loc1	-0.10*	-0.98**	-0.35**	-0.98**	0.99**	0.99**	0.77**	0.95**
Loc2	-0.31**	-0.91**	-0.18**	-0.79**	0.2*	0.92**	0.74**	0.78**
Loc3	-0.16**	-0.93**	-0.23**	-0.81**	0.74**	1**	-0.35**	-0.88**
Loc4	-0.04**	-0.83**	0	0	0.75**	0.94**	0.64**	0.68**
Loc5	0.02**	-0.25**	-0.04	-0.04*	0.97**	0.92**	-0.75**	-0.21**
Loc6	0.06*	-0.26**	0	0	0.99**	0.33**	0.97**	-0.13**

** Significance at the 0.01 probability level

Pearson coefficients of partial correlation (r´)

HD_winter			Variable Z			
Location	Variable X	Variable Y	Tmax	Tmin	G.rad	Precip
Loc1	HD	Tmax		-0.10**	-0.59**	-0.62**
	HD	Tmin	-0.12**		-0.06**	-0.92**
	HD	G.rad	0.99**	0.99**		0.97**
	HD	Precip	0.85**	0.93**	0.00**	
Loc2	HD	Tmax		-0.20**	-0.33**	0.86**
	HD	Tmin	-0.41**		-0.25**	0.89**
	HD	G.rad	0.24**	0.22**		0.32**
	HD	Precip	0.93**	0.95**	0.76**	
Loc3	HD	Tmax		-0.18**	-0.23**	0.91**
	HD	Tmin	-0.18**		-0.20**	1.00**
	HD	G.rad	0.99**	1.00**		0.99**
	HD	Precip	-0.92**	-0.98**	0.99**	
Loc4	HD	Tmax		-0.07**	-0.14**	0.87**
	HD	Tmin	-0.33**		-0.28**	0.43**
	HD	G.rad	-0.30**	0.98**		0.90**
	HD	Precip	0.46**	-0.08**	0.86**	
Loc5	HD	Tmax		-0.08**	-0.39**	0.56**
	HD	Tmin	-0.10**		-0.16**	0.45**
	HD	G.rad	0.94**	0.98**		0.99**
	HD	Precip	-0.66**	-0.81**	0.94**	
Loc6	HD	Tmax		0.09**	-0.28**	0.71**
	HD	Tmin	-0.16**		-0.05**	0.21**
	HD	G.rad	0.97**	1.00**		0.89**
	HD	Precip	0.93**	0.97**	0.07**	

HD_spring			Variable Z			
Location	Variable X	Variable Y	Tmax	Tmin	G.rad	Precip
Loc1	HD	Tmax		-0.89**	-0.83**	-0.78**
	HD	Tmin	-0.83**		-0.84**	-0.83**
	HD	G.rad	0.86**	0.91**		0.89**
	HD	Precip	0.15**	0.42**	-0.15**	
Loc2	HD	Tmax		-0.97**	-0.95**	-0.97**
	HD	Tmin	-0.74**		-0.96**	-0.96**
	HD	G.rad	0.96**	0.98**		0.86**
	HD	Precip	0.94**	0.96**	-0.56**	
Loc3	HD	Tmax		-0.98**	-0.75**	-0.72**
	HD	Tmin	-0.71**		-0.62**	-0.45**
	HD	G.rad	0.99**	1.00**		0.99**
	HD	Precip	0.37**	-0.70**	-0.41**	
Loc4	HD	Tmax		-0.74**	-0.80**	-0.62**
	HD	Tmin	-0.18**		-0.25**	-0.69**
	HD	G.rad	1.00**	0.92**		0.17**
	HD	Precip	0.96**	0.98**	0.84**	
Loc5	HD	Tmax		-0.13**	-0.33**	-0.18**
	HD	Tmin	-0.12**		0.76**	-0.87**
	HD	G.rad	0.95**	0.96**		0.98**
	HD	Precip	0.12**	0.85**	0.84**	
Loc6	HD	Tmax		-0.20**	-0.35**	-0.23**
	HD	Tmin	-0.05**		-0.72**	-0.87**
	HD	G.rad	0.85**	0.38**		0.58**
	HD	Precip	0.02**	-0.71**	-0.52**	

Variable "Z" is considered as constant in the correlation (X, Y, Z)

Appendix 3. 12: PCR screening of 213 cultivars at known *VRN* and *PPD* genes

					VRN1									
Genotype	**Cultivar name**	**Year of Release**	**Origin**	**Type**	***vrn-A1***	***Vrn-A1a***	***Vrn-A1b***	***Vrn-A1c***	***vrn-B1***	***Vrn-B1a***	***Vrn-B1b***	***vrn-D1***	***Vrn-D1a***	***Vrn-D1b***
Bri_003	Jafet	2008	Germany	Winter	+	-	-	-	+	-	-	+	-	-
Bri_005	Rebell	2013	Germany	Winter	+	-	-	-	+	-	-	+	-	-
Bri_006	Memory	2013	Germany	Winter	+	-	-	-	+	-	-	+	-	-
Bri_007	Kurt	2013	Germany	Winter	+	-	-	-	+	-	-	+	-	-
Bri_008	Zappa	2009	Germany	Winter	+	-	-	-	+	-	-	+	-	-
Bri_010	Gordian	2013	Germany	Winter	+	-	-	-	+	-	-	+	-	-
Bri_011	Mentor	2012	Germany	Winter	+	-	-	-	+	-	-	+	-	-
Bri_012	Meister	2010	Germany	Winter	+	-	-	-	+	-	-	+	-	-
Bri_015	Profilus	2008	Germany	Winter	+	-	-	-	+	-	-	+	-	-
Bri_017	KWS Pius	2010	Germany	Winter	+	-	-	-	+	-	-	+	-	-
Bri_018	Paroli	2004	Germany	Winter	+	-	-	-	+	-	-	+	-	-
Bri_019	Estivus	2012	Germany	Winter	+	-	-	-	+	-	-	+	-	-
Bri_020	Kronjuwel	1980	Germany	Winter	+	-	-	-	+	-	-	+	-	-
Bri_021	Desamo	2013	Germany	Winter	+	-	-	-	+	-	-	+	-	-
Bri_022	Carenius	2006	Germany	Winter	+	-	-	-	+	-	-	+	-	-
Bri_023	Mulan	2006	Germany	Winter	+	-	-	-	+	-	-	+	-	-
Bri_024	Kredo	2009	Germany	Winter	+	-	-	-	+	-	-	+	-	-
Bri_025	Nelson	2011	Germany	Winter	+	-	-	-	+	-	-	+	-	-
Bri_026	Patras	2012	Germany	Winter	+	-	-	-	+	-	-	+	-	-
Bri_027	Götz	1978	Germany	Winter	+	-	-	-	+	-	-	+	-	-
Bri_029	Anapolis	2013	Germany	Winter	+	-	-	-	+	-	-	+	-	-
Bri_031	Biscay	2000	Germany	Winter	+	-	-	-	+	-	-	+	-	-
Bri_032	Capone	2012	Germany	Winter	+	-	-	-	+	-	-	+	-	-

Bri_033	Tabasco	2008	Germany	Winter	+	-	-	-	+	-	-	+	-	-
Bri_034	Kometus	2011	Germany	Winter	+	-	-	-	+	-	-	+	-	-
Bri_035	Cubus	2002	Germany	Winter	+	-	-	-	+	-	-	+	-	-
Bri_036	Edward	2013	Germany	Winter	+	-	-	-	+	-	-	+	-	-
Bri_037	Famulus	2010	Germany	Winter	+	-	-	-	+	-	-	+	-	-
Bri_038	Dekan	1999	Germany	Winter	+	-	-	-	+	-	-	+	-	-
Bri_039	SW Topper	2002	Germany	Winter	+	-	-	-	+	-	-	+	-	-
Bri_040	Matrix	2010	Germany	Winter	+	-	-	-	+	-	-	+	-	-
Bri_041	Jenga	2007	Germany	Winter	+	-	-	-	+	-	-	+	-	-
Bri_042	Linus	2010	Germany	Winter	+	-	-	-	+	-	-	+	-	-
Bri_044	Forum	2012	Germany	Winter	+	-	-	-	+	-	-	+	-	-
Bri_045	Colonia	2011	Germany	Winter	+	-	-	-	+	-	-	+	-	-
Bri_046	Transit	1994	Germany	Winter	+	-	-	-	+	-	-	+	-	-
Bri_047	Potenzial	2006	Germany	Winter	+	-	-	-	+	-	-	+	-	-
Bri_049	Tarso	1994	Germany	Winter	+	-	-	-	+	-	-	+	-	-
Bri_050	Hermann	2004	Germany	Winter	+	-	-	-	+	-	-	+	-	-
Bri_051	Glaucus	2011	Germany	Winter	+	-	-	-	+	-	-	+	-	-
Bri_052	Tuareg	2005	Germany	Winter	+	-	-	-	+	-	-	+	-	-
Bri_053	Atomic	2012	Germany	Winter	+	-	-	-	+	-	-	+	-	-
Bri_054	Tobak	2011	Germany	Winter	+	-	-	-	+	-	-	+	-	-
Bri_055	Pionier	2013	Germany	Winter	+	-	-	-	+	-	-	+	-	-
Bri_056	Manager	2006	Germany	Winter	+	-	-	-	+	-	-	+	-	-
Bri_057	Gourmet	2013	Germany	Winter	+	-	-	-	+	-	-	+	-	-
Bri_058	Limes	2003	Germany	Winter	+	-	-	-	+	-	-	+	-	-
Bri_059	Ritmo	1993	Germany	Winter	+	-	-	-	+	-	-	+	-	-
Bri_060	Kalahari	2010	Germany	Winter	+	-	-	-	+	-	-	+	-	-
Bri_061	Intro	2011	Germany	Winter	+	-	-	-	+	-	-	+	-	-
Bri_062	Oxal	2010	Germany	Winter	+	-	-	-	+	-	-	+	-	-
Bri_063	Zobel	2006	Germany	Winter	+	-	-	-	+	-	-	+	-	-

Bri_064	Event	2009	Germany	Winter	+	-	-	-	+	-	-	+	-	-
Bri_065	Joker	2012	Germany	Winter	+	-	-	-	+	-	-	+	-	-
Bri_066	Global	2009	Germany	Winter	+	-	-	-	+	-	-	+	-	-
Bri_067	Elixer	2012	Germany	Winter	+	-	-	-	+	-	-	+	-	-
Bri_068	Fedor	2007	Germany	Winter	+	-	-	-	+	-	-	+	-	-
Bri_069	Türkis	2004	Germany	Winter	+	-	-	-	+	-	-	+	-	-
Bri_070	Skagen	2006	Germany	Winter	+	-	-	-	+	-	-	+	-	-
Bri_071	Greif	1989	Germany	Winter	+	-	-	-	+	-	-	+	-	-
Bri_072	Esket	2007	Germany	Winter	+	-	-	-	+	-	-	+	-	-
Bri_073	Primus	2009	Germany	Winter	+	-	-	-	+	-	-	+	-	-
Bri_074	Skalmeje	2006	Germany	Winter	+	-	-	-	+	-	-	+	-	-
Bri_075	Genius	2009	Germany	Winter	+	-	-	-	+	-	-	+	-	-
Bri_076	Enorm	2002	Germany	Winter	+	-	-	-	+	-	-	+	-	-
Bri_077	Florian	2010	Germany	Winter	+	-	-	-	+	-	-	+	-	-
Bri_078	Skater	2000	Germany	Winter	+	-	-	-	+	-	-	+	-	-
Bri_079	Brillant	2005	Germany	Winter	+	-	-	-	+	-	-	+	-	-
Bri_080	Inspiration	2007	Germany	Winter	+	-	-	-	+	-	-	+	-	-
Bri_081	Apertus	2013	Germany	Winter	+	-	-	-	+	-	-	+	-	-
Bri_082	Ellvis	2002	Germany	Winter	+	-	-	-	+	-	-	+	-	-
Bri_083	Edgar	2010	Germany	Winter	+	-	-	-	+	-	-	+	-	-
Bri_085	SY Ferry	2012	Germany	Winter	+	-	-	-	+	-	-	+	-	-
Bri_086	Landsknecht	2013	Germany	Winter	+	-	-	-	+	-	-	+	-	-
Bri_088	Impression	2005	Germany	Winter	+	-	-	-	+	-	-	+	-	-
Bri_089	Winnetou	2002	Germany	Winter	+	-	-	-	+	-	-	+	-	-
Bri_090	Toronto	1990	Germany	Winter	+	-	-	-	+	-	-	+	-	-
Bri_091	Torrild	2005	Germany	Winter	+	-	-	-	+	-	-	+	-	-
Bri_092	Contra	1990	Germany	Winter	+	-	-	-	+	-	-	+	-	-
Bri_093	Schamane	2005	Germany	Winter	+	-	-	-	+	-	-	+	-	-
Bri_094	Granada	1980	Germany	Winter	+	-	-	-	+	-	-	+	-	-

Bri_095	KWS Cobalt	2013	Germany	Winter	+	-	-	-	+	-	-	+	-	-
Bri_096	Tommi	2002	Germany	Winter	+	-	-	-	+	-	-	+	-	-
Bri_097	Saturn	1973	Germany	Winter	+	-	-	-	+	-	-	+	-	-
Bri_098	Severin	1980	Germany	Winter	+	-	-	-	+	-	-	+	-	-
Bri_099	JB Asano	2008	Germany	Winter	+	-	-	-	+	-	-	+	-	-
Bri_100	Kerubino	2004	Germany	Winter	+	-	-	-	+	-	-	+	-	-
Bri_101	Arktis	2010	Germany	Winter	+	-	-	-	+	-	-	+	-	-
Bri_102	Urban	1980	Germany	Winter	+	-	-	-	+	-	-	+	-	-
Bri_103	Orestis	1988	Germany	Winter	+	-	-	-	+	-	-	+	-	-
Bri_104	Flair	1996	Germany	Winter	+	-	-	-	+	-	-	+	-	-
Bri_105	Anthus	2005	Germany	Winter	+	-	-	-	+	-	-	+	-	-
Bri_106	Bombus	2012	Germany	Winter	+	-	-	-	+	-	-	+	-	-
Bri_107	Lucius	2006	Germany	Winter	+	-	-	-	+	-	-	+	-	-
Bri_108	Herzog	1986	Germany	Winter	+	-	-	-	+	-	-	+	-	-
Bri_109	Sorbas	1985	Germany	Winter	+	-	-	-	+	-	-	+	-	-
Bri_110	Tabor	1979	Germany	Winter	+	-	-	-	+	-	-	+	-	-
Bri_111	Terrier	2001	Germany	Winter	+	-	-	-	+	-	-	+	-	-
Bri_112	Magister	2005	Germany	Winter	+	-	-	-	+	-	-	+	-	-
Bri_113	Altos	2000	Germany	Winter	+	-	-	-	+	-	-	+	-	-
Bri_114	Progress	2007	Germany	Winter	+	-	-	-	+	-	-	+	-	-
Bri_115	Xantippe	2011	Germany	Winter	+	-	-	-	+	-	-	+	-	-
Bri_116	Avenir	2013	Germany	Winter	+	-	-	-	+	-	-	+	-	-
Bri_117	Pantus	1966	Germany	Winter	+	-	-	-	+	-	-	+	-	-
Bri_118	Drifter	1999	Germany	Winter	+	-	-	-	+	-	-	+	-	-
Bri_119	Joss	1972	Germany	Winter	+	-	-	-	+	-	-	+	-	-
Bri_120	Kranich	2007	Germany	Winter	+	-	-	-	+	-	-	+	-	-
Bri_121	Sperber	1982	Germany	Winter	+	-	-	-	+	-	-	+	-	-
Bri_122	Discus	2007	Germany	Winter	+	-	-	-	+	-	-	+	-	-
Bri_125	Magnus	2000	Germany	Winter	+	-	-	-	+	-	-	+	-	-

Bri_126	Disponent	1975	Germany	Winter	+	-	-	-	+	-	-	+	-	-
Bri_127	Tambor	1993	Germany	Winter	+	-	-	-	+	-	-	+	-	-
Bri_128	Boxer	2013	Germany	Winter	+	-	-	-	+	-	-	+	-	-
Bri_129	Sokrates	2001	Germany	Winter	+	-	-	-	+	-	-	+	-	-
Bri_130	Carisuper	1975	Germany	Winter	+	-	-	-	+	-	-	+	-	-
Bri_131	Rektor	1980	Germany	Winter	+	-	-	-	+	-	-	+	-	-
Bri_132	Alves	2010	Germany	Winter	+	-	-	-	+	-	-	+	-	-
Bri_133	NaturaStar	2002	Germany	Winter	+	-	-	-	+	-	-	+	-	-
Bri_134	Alidos	1987	Germany	Winter	+	-	-	-	+	-	-	+	-	-
Bri_135	Monopol	1975	Germany	Winter	+	-	-	-	+	-	-	+	-	-
Bri_136	Akratos	2004	Germany	Winter	+	-	-	-	+	-	-	+	-	-
Bri_137	Knirps	1985	Germany	Winter	+	-	-	-	+	-	-	+	-	-
Bri_138	Bussard	1990	Germany	Winter	+	-	-	-	+	-	-	+	-	-
Bri_139	Oberst	1980	Germany	Winter	+	-	-	-	+	-	-	+	-	-
Bri_141	Tiger	2001	Germany	Winter	+	-	-	-	+	-	-	+	-	-
Bri_142	Ibis	1991	Germany	Winter	+	-	-	-	+	-	-	+	-	-
Bri_143	Batis	1994	Germany	Winter	+	-	-	-	+	-	-	+	-	-
Bri_144	Topfit	1972	Germany	Winter	+	-	-	-	+	-	-	+	-	-
Bri_145	Akteur	2003	Germany	Winter	+	-	-	-	+	-	-	+	-	-
Bri_146	Ludwig	1998	Germany	Winter	+	-	-	-	+	-	-	+	-	-
Bri_147	Asketis	1998	Germany	Winter	+	-	-	-	+	-	-	+	-	-
Bri_148	Aristos	1997	Germany	Winter	+	-	-	-	+	-	-	+	-	-
Bri_149	Zentos	1989	Germany	Winter	+	-	-	-	+	-	-	+	-	-
Bri_150	Diplomat	1966	Germany	Winter	+	-	-	-	+	-	-	+	-	-
Bri_151	Astron	1989	Germany	Winter	+	-	-	-	+	-	-	+	-	-
Bri_152	Basalt	1980	Germany	Winter	+	-	-	-	+	-	-	+	-	-
Bri_153	Kormoran	1973	Germany	Winter	+	-	-	-	+	-	-	+	-	-
Bri_154	Aron	1992	Germany	Winter	+	-	-	-	+	-	-	+	-	-

Bri_155	KWS Milaneco	2013	Germany	Winter	+	-	-	-	+	-	-	+	-	-
Bri_156	Aszita	2005	Germany	Winter	+	-	-	-	+	-	-	+	-	-
Bri_157	Kobold	2014	Germany	Winter	+	-	-	-	+	-	-	+	-	-
Bri_158	Carimulti	1975	Germany	Winter	+	-	-	-	+	-	-	+	-	-
Bri_159	Admiral	1968	Germany	Winter	+	-	-	-	+	-	-	+	-	-
Bri_160	Vuka	1975	Germany	Winter	+	-	-	-	+	-	-	+	-	-
Bri_161	Benno	1973	Germany	Winter	+	-	-	-	+	-	-	+	-	-
Bri_162	Apollo	1984	Germany	Winter	+	-	-	-	+	-	-	+	-	-
Bri_164	Kanzler	1980	Germany	Winter	+	-	-	-	+	-	-	+	-	-
Bri_165	Kraka	1997	Germany	Winter	+	-	-	-	+	-	-	+	-	-
Bri_166	Caribo	1968	Germany	Winter	+	-	-	-	+	-	-	+	-	-
Bri_167	Butaro	2009	Germany	Winter	+	-	-	-	+	-	-	+	-	-
Bri_168	Konsul	1990	Germany	Winter	+	-	-	-	+	-	-	+	-	-
Bri_169	Ares	1983	Germany	Winter	+	-	-	-	+	-	-	+	-	-
Bri_186	KWS Ferrum	2012	Germany	Winter	+	-	-	-	+	-	-	+	-	-
Bri_188	Cardos	1998	Germany	Winter	+	-	-	-	+	-	-	+	-	-
Bri_193	Camp Remy	1980	Germany	Winter	+	-	-	-	+	-	-	+	-	-
Bri_200	Orcas	2010	Germany	Winter	+	-	-	-	+	-	-	+	-	-
Bri_201	Nimbus	1975	Germany	Winter	+	-	-	-	+	-	-	+	-	-
Bri_202	Muskat	2010	Germany	Winter	+	-	-	-	+	-	-	+	-	-
Bri_204	Rumor	2013	Germany	Winter	+	-	-	-	+	-	-	+	-	-
Bri_207	Kontrast	1990	Germany	Winter	+	-	-	-	+	-	-	+	-	-
Bri_208	WW 4180 (Kongo)	2012	Germany	Winter	+	-	-	-	+	-	-	+	-	-
Bri_213	Pegassos	1994	Germany	Winter	+	-	-	-	+	-	-	+	-	-
Bri_001	Einstein	2002	UK	Winter	+	-	-	-	+	-	-	+	-	-
Bri_002	Oakley	2005	UK	Winter	+	-	-	-	+	-	-	+	-	-
Bri_004	Claire	1997	UK	Winter	+	-	-	-	+	-	-	+	-	-

Bri_009	Chevalier	2005	Austria	Winter	+	-	-	-	+	-	-	+	-	-
Bri_013	KWS Santiago	2009	UK	Winter	+	-	-	-	+	-	-	+	-	-
Bri_014	Brigand	1979	UK	Winter	+	-	-	-	+	-	-	+	-	-
Bri_016	Durin	1975	France	Winter	+	-	-	-	+	-	-	-	+	-
Bri_028	Robigous	1999	UK	Winter	+	-	-	-	+	-	-	+	-	-
Bri_030	Solstice	2001	UK	Winter	+	-	-	-	+	-	-	+	-	-
Bri_043	TJB 990.15	1980	UK	Winter	+	-	-	-	+	-	-	+	-	-
Bri_084	Maris Huntsman	1971	UK	Winter	+	-	-	-	+	-	-	+	-	-
Bri_087	Sponsor	1994	France	Winter	+	-	-	-	+	-	-	-	+	-
Bri_124	Obelisk	1987	NL	Winter	+	-	-	-	+	-	-	+	-	-
Bri_140	Capelle Desprez	1946	France	Winter	+	-	-	-	+	-	-	+	-	-
Bri_163	Aquila	1977	GBR	Winter	+	-	-	-	+	-	-	+	-	-
Bri_171	NS 22/92	1971	Serbia	Winter	+	-	-	-	+	-	-	-	+	-
Bri_176	Mironovska 808	1963	Ukraine	Winter	+	-	-	-	+	-	-	+	-	-
Bri_177	Caphorn	2001	France	Winter	+	-	-	-	+	-	-	+	-	-
Bri_178	Cordiale	2004	GBR	Winter	+	-	-	-	+	-	-	+	-	-
Bri_179	Apache	1999	CZ	Winter	+	-	-	-	+	-	-	+	-	-
Bri_180	Premio	2007	France	Winter	+	-	-	-	+	-	-	+	-	-
Bri_181	Isengrain	1996	France	Winter	+	-	-	-	+	-	-	+	-	-
Bri_182	Alixan	2005	France	Winter	+	-	-	-	+	-	-	-	+	-
Bri_183	Boregan	2007	France	Winter	+	-	-	-	+	-	-	+	-	-
Bri_184	Renesansa	1995	Serbia	Winter	+	-	-	-	-	+	-	+	-	-
Bri_185	Tremie	1992	France	Winter	+	-	-	-	+	-	-	+	-	-
Bri_189	Soissons	1987	France	Winter	+	-	-	-	+	-	-	+	-	-
Bri_191	Arlequin	2007	France	Winter	+	-	-	-	+	-	-	+	-	-
Bri_195	Avalon	1980	GBR	Winter	+	-	-	-	+	-	-	+	-	-

Bri_196	Ivanka	1998	Serbia	Winter	+	-	-	-	-	+	-	-	+	-
Bri_197	Pobeda	1990	Serbia	Winter	+	-	-	-	+	-	-	+	-	-
Bri_198	NS 66/92	1992	Serbia	Winter	+	-	-	-	+	-	-	+	-	-
Bri_205	Highbury	1968	GBR	Spring	+	-	-	-	+	-	-	+	-	-
Bri_210	NS 46/90	1990	Serbia	Winter	+	-	-	-	+	-	-	-	+	-
Bri_048	Gaucho	1993	USA	Winter	+	-	-	-	+	-	-	+	+	-
Bri_123	Helios	1980	USA	Winter	+	-	-	-	+	-	-	-	+	-
Bri_170	Centurk	1971	USA	Winter	+	-	-	-	+	-	-	-	+	-
Bri_172	Benni multifloret	1980	USA	Winter	+	-	-	-	+	-	-	+	-	-
Bri_173	Hope	1948	USA	Winter	+	-	-	-	+	-	-	-	+	-
Bri_174	Vel	1976	USA	Winter	+	-	-	-	+	-	-	-	+	-
Bri_175	Phoenix	1981	USA	Winter	+	-	-	-	-	+	-	-	+	-
Bri_187	Triple dirk "S"	1968	Australia	Spring	-	+	-	-	+	-	-	-	+	-
Bri_190	BCD 1302/83	1983	Moldava	Winter	-	+	-	-	+	-	-	-	+	-
Bri_192	Sonalika	1967	India	Spring	+	-	-	-	+	-	-	-	+	-
Bri_194	Cajeme 71	1971	Mexico	Spring	+	-	-	-	-	+	-	-	+	-
Bri_199	Mex. 3	1971	Mexico	Spring	+	-	-	-	-	+	-	-	+	-
Bri_203	Florida	1985	USA	Winter	+	-	-	-	+	-	-	+	-	-
Bri_206	Siete Cerros	1966	Mexico	Spring	+	-	-	-	-	+	-	-	+	-
Bri_209	INTRO 615	1980	USA	Winter	+	-	-	-	+	-	-	-	+	-
Bri_211	Mex. 17 bb	1971	Mexico	Winter	+	-	-	-	-	+	-	+	-	-
Bri_212	Lambriego Inia	1980	Chile	Winter	-	+	-	-	+	-	-	-	+	-

					VRN2						***VRN3***			
					Null allele			**Functional allele**						
Genotype	**Cultivar name**	**Year of Release**	**Origin**	**Type**	***ZCCT-A1***	***ZCCT-B1***	***ZCCT-D1***	***ZCCT-A2***	***ZCCT-B2***	***ZCCT-D2***	***vrn-B3***	***Vrn-B3a***	***Vrn-B3b***	***Vrn-B3c***
Bri_003	Jafet	2008	Germany	Winter	+	-	+	-	+	+	-	-	-	+
Bri_005	Rebell	2013	Germany	Winter	+	-	+	-	+	+	-	-	-	+
Bri_006	Memory	2013	Germany	Winter	+	-	+	-	+	+	-	-	-	+
Bri_007	Kurt	2013	Germany	Winter	+	-	+	-	+	+	-	-	-	+
Bri_008	Zappa	2009	Germany	Winter	+	-	+	-	+	+	-	-	-	+
Bri_010	Gordian	2013	Germany	Winter	+	-	+	-	+	+	-	-	-	+
Bri_011	Mentor	2012	Germany	Winter	+	-	+	-	+	+	-	-	-	+
Bri_012	Meister	2010	Germany	Winter	+	-	+	-	+	+	-	-	-	+
Bri_015	Profilus	2008	Germany	Winter	+	-	+	-	+	+	-	-	-	+
Bri_017	KWS Pius	2010	Germany	Winter	+	-	+	-	+	+	-	-	-	+
Bri_018	Paroli	2004	Germany	Winter	+	-	+	-	+	+	-	-	-	+
Bri_019	Estivus	2012	Germany	Winter	+	-	+	-	+	+	-	-	-	+
Bri_020	Kronjuwel	1980	Germany	Winter	+	-	+	-	+	+	-	-	-	+
Bri_021	Desamo	2013	Germany	Winter	+	-	+	-	+	+	-	-	-	+
Bri_022	Carenius	2006	Germany	Winter	+	-	+	-	+	+	-	-	-	+
Bri_023	Mulan	2006	Germany	Winter	+	-	+	-	+	+	-	-	-	+
Bri_024	Kredo	2009	Germany	Winter	+	-	+	-	+	+	-	-	-	+
Bri_025	Nelson	2011	Germany	Winter	+	-	+	-	+	+	-	-	-	+
Bri_026	Patras	2012	Germany	Winter	+	-	+	-	+	+	-	-	-	+
Bri_027	Götz	1978	Germany	Winter	+	-	+	-	+	+	-	-	-	+
Bri_029	Anapolis	2013	Germany	Winter	+	-	+	-	+	+	-	-	-	+
Bri_031	Biscay	2000	Germany	Winter	+	-	+	-	+	+	-	-	-	+
Bri_032	Capone	2012	Germany	Winter	+	-	+	-	+	+	-	-	-	+

Bri_033	Tabasco	2008	Germany	Winter	+	-	+	-	+	+	-	-	-	+
Bri_034	Kometus	2011	Germany	Winter	+	-	+	-	+	+	-	-	-	+
Bri_035	Cubus	2002	Germany	Winter	+	-	+	-	+	+	-	-	-	+
Bri_036	Edward	2013	Germany	Winter	+	-	+	-	+	+	-	-	-	+
Bri_037	Famulus	2010	Germany	Winter	+	-	+	-	+	+	-	-	-	+
Bri_038	Dekan	1999	Germany	Winter	+	-	+	-	+	+	-	-	-	+
Bri_039	SW Topper	2002	Germany	Winter	+	-	+	-	+	+	-	-	-	+
Bri_040	Matrix	2010	Germany	Winter	+	-	+	-	+	+	-	-	-	+
Bri_041	Jenga	2007	Germany	Winter	+	-	+	-	+	+	-	-	-	+
Bri_042	Linus	2010	Germany	Winter	+	-	+	-	+	+	-	-	-	+
Bri_044	Forum	2012	Germany	Winter	+	-	+	-	+	+	-	-	-	+
Bri_045	Colonia	2011	Germany	Winter	+	-	+	-	+	+	-	-	-	+
Bri_046	Transit	1994	Germany	Winter	+	-	+	-	+	+	-	-	-	+
Bri_047	Potenzial	2006	Germany	Winter	+	-	+	-	+	+	-	-	-	+
Bri_049	Tarso	1994	Germany	Winter	+	-	+	-	+	+	-	-	-	+
Bri_050	Hermann	2004	Germany	Winter	+	-	+	-	+	+	-	-	-	+
Bri_051	Glaucus	2011	Germany	Winter	+	-	+	-	+	+	-	-	-	+
Bri_052	Tuareg	2005	Germany	Winter	+	-	+	-	+	+	-	-	-	+
Bri_053	Atomic	2012	Germany	Winter	+	-	+	-	+	+	-	-	-	+
Bri_054	Tobak	2011	Germany	Winter	+	-	+	-	+	+	-	-	-	+
Bri_055	Pionier	2013	Germany	Winter	+	-	+	-	+	+	-	-	-	+
Bri_056	Manager	2006	Germany	Winter	+	-	+	-	+	+	-	-	-	+
Bri_057	Gourmet	2013	Germany	Winter	+	-	+	-	+	+	-	-	-	+
Bri_058	Limes	2003	Germany	Winter	+	-	+	-	+	+	-	-	-	+
Bri_059	Ritmo	1993	Germany	Winter	+	-	+	-	+	+	-	-	-	+
Bri_060	Kalahari	2010	Germany	Winter	+	-	+	-	+	+	-	-	-	+
Bri_061	Intro	2011	Germany	Winter	+	-	+	-	+	+	-	-	-	+
Bri_062	Oxal	2010	Germany	Winter	+	-	+	-	+	+	-	-	-	+
Bri_063	Zobel	2006	Germany	Winter	+	-	+	-	+	+	-	-	-	+

Bri_064	Event	2009	Germany	Winter	+	-	+	-	+	+	-	-	-	+
Bri_065	Joker	2012	Germany	Winter	+	-	+	-	+	+	-	-	-	+
Bri_066	Global	2009	Germany	Winter	+	-	+	-	+	+	-	-	-	+
Bri_067	Elixer	2012	Germany	Winter	+	-	+	-	+	+	-	-	-	+
Bri_068	Fedor	2007	Germany	Winter	+	-	+	-	+	+	-	-	-	+
Bri_069	Türkis	2004	Germany	Winter	+	-	+	-	+	+	-	-	-	+
Bri_070	Skagen	2006	Germany	Winter	+	-	+	-	+	+	-	-	-	+
Bri_071	Greif	1989	Germany	Winter	+	-	+	-	+	+	-	-	-	+
Bri_072	Esket	2007	Germany	Winter	+	-	+	-	+	+	-	-	-	+
Bri_073	Primus	2009	Germany	Winter	+	-	+	-	+	+	-	-	-	+
Bri_074	Skalmeje	2006	Germany	Winter	+	-	+	-	+	+	-	-	-	+
Bri_075	Genius	2009	Germany	Winter	+	-	+	-	+	+	-	-	-	+
Bri_076	Enorm	2002	Germany	Winter	+	-	+	-	+	+	-	-	-	+
Bri_077	Florian	2010	Germany	Winter	+	-	+	-	+	+	-	-	-	+
Bri_078	Skater	2000	Germany	Winter	+	-	+	-	+	+	-	-	-	+
Bri_079	Brillant	2005	Germany	Winter	+	-	+	-	+	+	-	-	-	+
Bri_080	Inspiration	2007	Germany	Winter	+	-	+	-	+	+	-	-	-	+
Bri_081	Apertus	2013	Germany	Winter	+	-	+	-	+	+	-	-	-	+
Bri_082	Ellvis	2002	Germany	Winter	+	-	+	-	+	+	-	-	-	+
Bri_083	Edgar	2010	Germany	Winter	+	-	+	-	+	+	-	-	-	+
Bri_085	SY Ferry	2012	Germany	Winter	+	-	+	-	+	+	-	-	-	+
Bri_086	Landsknecht	2013	Germany	Winter	+	-	+	-	+	+	-	-	-	+
Bri_088	Impression	2005	Germany	Winter	+	-	+	-	+	+	-	-	-	+
Bri_089	Winnetou	2002	Germany	Winter	+	-	+	-	+	+	-	-	-	+
Bri_090	Toronto	1990	Germany	Winter	+	-	+	-	+	+	-	-	-	+
Bri_091	Torrild	2005	Germany	Winter	+	-	+	-	+	+	-	-	-	+
Bri_092	Contra	1990	Germany	Winter	+	-	+	-	+	+	-	-	-	+
Bri_093	Schamane	2005	Germany	Winter	+	-	+	-	+	+	-	-	-	+
Bri_094	Granada	1980	Germany	Winter	+	-	+	-	+	+	-	-	-	+

Bri_095	KWS Cobalt	2013	Germany	Winter	+	-	+	-	+	+	-	-	-	+
Bri_096	Tommi	2002	Germany	Winter	+	-	+	-	+	+	-	-	-	+
Bri_097	Saturn	1973	Germany	Winter	+	-	+	-	+	+	-	-	-	+
Bri_098	Severin	1980	Germany	Winter	+	-	+	-	+	+	-	-	-	+
Bri_099	JB Asano	2008	Germany	Winter	+	-	+	-	+	+	-	-	-	+
Bri_100	Kerubino	2004	Germany	Winter	+	-	+	-	+	+	-	-	-	+
Bri_101	Arktis	2010	Germany	Winter	+	-	+	-	+	+	-	-	-	+
Bri_102	Urban	1980	Germany	Winter	+	-	+	-	+	+	-	-	-	+
Bri_103	Orestis	1988	Germany	Winter	+	-	+	-	+	+	-	-	-	+
Bri_104	Flair	1996	Germany	Winter	+	-	+	-	+	+	-	-	-	+
Bri_105	Anthus	2005	Germany	Winter	+	-	+	-	+	+	-	-	-	+
Bri_106	Bombus	2012	Germany	Winter	+	-	+	-	+	+	-	-	-	+
Bri_107	Lucius	2006	Germany	Winter	+	-	+	-	+	+	-	-	-	+
Bri_108	Herzog	1986	Germany	Winter	+	-	+	-	+	+	-	-	-	+
Bri_109	Sorbas	1985	Germany	Winter	+	-	+	-	+	+	-	-	-	+
Bri_110	Tabor	1979	Germany	Winter	+	-	+	-	+	+	-	-	-	+
Bri_111	Terrier	2001	Germany	Winter	+	-	+	-	+	+	-	-	-	+
Bri_112	Magister	2005	Germany	Winter	+	-	+	-	+	+	-	-	-	+
Bri_113	Altos	2000	Germany	Winter	+	-	+	-	+	+	-	-	-	+
Bri_114	Progress	2007	Germany	Winter	+	-	+	-	+	+	-	-	-	+
Bri_115	Xantippe	2011	Germany	Winter	+	-	+	-	+	+	-	-	-	+
Bri_116	Avenir	2013	Germany	Winter	+	-	+	-	+	+	-	-	-	+
Bri_117	Pantus	1966	Germany	Winter	+	-	+	-	+	+	-	-	-	+
Bri_118	Drifter	1999	Germany	Winter	+	-	+	-	+	+	-	-	-	+
Bri_119	Joss	1972	Germany	Winter	+	-	+	-	+	+	-	-	-	+
Bri_120	Kranich	2007	Germany	Winter	+	-	+	-	+	+	-	-	-	+
Bri_121	Sperber	1982	Germany	Winter	+	-	+	-	+	+	-	-	-	+
Bri_122	Discus	2007	Germany	Winter	+	-	+	-	+	+	-	-	-	+
Bri_125	Magnus	2000	Germany	Winter	+	-	+	-	+	+	-	-	-	+

Bri_126	Disponent	1975	Germany	Winter	+	-	+	-	+	+	-	-	-	+
Bri_127	Tambor	1993	Germany	Winter	+	-	+	-	+	+	-	-	-	+
Bri_128	Boxer	2013	Germany	Winter	+	-	+	-	+	+	-	-	-	+
Bri_129	Sokrates	2001	Germany	Winter	+	-	+	-	+	+	-	-	-	+
Bri_130	Carisuper	1975	Germany	Winter	+	-	+	-	+	+	-	-	-	+
Bri_131	Rektor	1980	Germany	Winter	+	-	+	-	+	+	-	-	-	+
Bri_132	Alves	2010	Germany	Winter	+	-	+	-	+	+	-	-	-	+
Bri_133	NaturaStar	2002	Germany	Winter	+	-	+	-	+	+	-	-	-	+
Bri_134	Alidos	1987	Germany	Winter	+	-	+	-	+	+	-	-	-	+
Bri_135	Monopol	1975	Germany	Winter	+	-	+	-	+	+	-	-	-	+
Bri_136	Akratos	2004	Germany	Winter	+	-	+	-	+	+	-	-	-	+
Bri_137	Knirps	1985	Germany	Winter	+	-	+	-	+	+	-	-	-	+
Bri_138	Bussard	1990	Germany	Winter	+	-	+	-	+	+	-	-	-	+
Bri_139	Oberst	1980	Germany	Winter	+	-	+	-	+	+	-	-	-	+
Bri_141	Tiger	2001	Germany	Winter	+	-	+	-	+	+	-	-	-	+
Bri_142	Ibis	1991	Germany	Winter	+	-	+	-	+	+	-	-	-	+
Bri_143	Batis	1994	Germany	Winter	+	-	+	-	+	+	-	-	-	+
Bri_144	Topfit	1972	Germany	Winter	+	-	+	-	+	+	-	-	-	+
Bri_145	Akteur	2003	Germany	Winter	+	-	+	-	+	+	-	-	-	+
Bri_146	Ludwig	1998	Germany	Winter	+	-	+	-	+	+	-	-	-	+
Bri_147	Asketis	1998	Germany	Winter	+	-	+	-	+	+	-	-	-	+
Bri_148	Aristos	1997	Germany	Winter	+	-	+	-	+	+	-	-	-	+
Bri_149	Zentos	1989	Germany	Winter	+	-	+	-	+	+	-	-	-	+
Bri_150	Diplomat	1966	Germany	Winter	+	-	+	-	+	+	-	-	-	+
Bri_151	Astron	1989	Germany	Winter	+	-	+	-	+	+	-	-	-	+
Bri_152	Basalt	1980	Germany	Winter	+	-	+	-	+	+	-	-	-	+
Bri_153	Kormoran	1973	Germany	Winter	+	-	+	-	+	+	-	-	-	+
Bri_154	Aron	1992	Germany	Winter	+	-	+	-	+	+	-	-	-	+

Bri_155	KWS Milaneco	2013	Germany	Winter	+	-	+	-	+	+	-	-	-	+
Bri_156	Aszita	2005	Germany	Winter	+	-	+	-	+	+	-	-	-	+
Bri_157	Kobold	2014	Germany	Winter	+	-	+	-	+	+	-	-	-	+
Bri_158	Carimulti	1975	Germany	Winter	+	-	+	-	+	+	-	-	-	+
Bri_159	Admiral	1968	Germany	Winter	+	-	+	-	+	+	-	-	-	+
Bri_160	Vuka	1975	Germany	Winter	+	-	+	-	+	+	-	-	-	+
Bri_161	Benno	1973	Germany	Winter	+	-	+	-	+	+	-	-	-	+
Bri_162	Apollo	1984	Germany	Winter	+	-	+	-	+	+	-	-	-	+
Bri_164	Kanzler	1980	Germany	Winter	+	-	+	-	+	+	-	-	-	+
Bri_165	Kraka	1997	Germany	Winter	+	-	+	-	+	+	-	-	-	+
Bri_166	Caribo	1968	Germany	Winter	+	-	+	-	+	+	-	-	-	+
Bri_167	Butaro	2009	Germany	Winter	+	-	+	-	+	+	-	-	-	+
Bri_168	Konsul	1990	Germany	Winter	+	-	+	-	+	+	-	-	-	+
Bri_169	Ares	1983	Germany	Winter	+	-	+	-	+	+	-	-	-	+
Bri_186	KWS Ferrum	2012	Germany	Winter	+	-	+	-	+	+	-	-	-	+
Bri_188	Cardos	1998	Germany	Winter	+	-	+	-	+	+	-	-	-	+
Bri_193	Camp Remy	1980	Germany	Winter	+	-	+	-	+	+	-	-	-	+
Bri_200	Orcas	2010	Germany	Winter	+	-	+	-	+	+	-	-	-	+
Bri_201	Nimbus	1975	Germany	Winter	+	-	+	-	+	+	-	-	-	+
Bri_202	Muskat	2010	Germany	Winter	+	-	+	-	+	+	-	-	-	+
Bri_204	Rumor	2013	Germany	Winter	+	-	+	-	+	+	-	-	-	+
Bri_207	Kontrast	1990	Germany	Winter	+	-	+	-	+	+	-	-	-	+
Bri_208	WW 4180 (Kongo)	2012	Germany	Winter	+	-	+	-	+	+	-	-	-	+
Bri_213	Pegassos	1994	Germany	Winter	+	-	+	-	+	+	-	-	-	+
Bri_001	Einstein	2002	UK	Winter	+	-	+	-	+	+	-	-	-	+
Bri_002	Oakley	2005	UK	Winter	+	-	+	-	+	+	-	-	-	+
Bri_004	Claire	1997	UK	Winter	+	-	+	-	+	+	-	-	-	+

Bri_009	Chevalier	2005	Austria	Winter	+	-	+	-	+	+	-	-	-	+
Bri_013	KWS Santiago	2009	UK	Winter	+	-	+	-	+	+	-	-	-	+
Bri_014	Brigand	1979	UK	Winter	+	-	+	-	+	+	-	-	-	+
Bri_016	Durin	1975	France	Winter	+	-	+	-	+	+	-	-	-	+
Bri_028	Robigous	1999	UK	Winter	+	-	+	-	+	+	-	-	-	+
Bri_030	Solstice	2001	UK	Winter	+	-	+	-	+	+	-	-	-	+
Bri_043	TJB 990.15	1980	UK	Winter	+	-	+	-	+	+	-	-	-	+
Bri_084	Maris Huntsman	1971	UK	Winter	+	-	+	-	+	+	-	-	-	+
Bri_087	Sponsor	1994	France	Winter	+	-	+	-	+	+	-	-	-	+
Bri_124	Obelisk	1987	NL	Winter	+	-	+	-	+	+	-	-	-	+
Bri_140	Capelle Desprez	1946	France	Winter	+	-	+	-	+	+	-	-	-	+
Bri_163	Aquila	1977	GBR	Winter	+	-	+	-	+	+	-	-	-	+
Bri_171	NS 22/92	1971	Serbia	Winter	+	-	+	-	+	+	-	-	-	+
Bri_176	Mironovska 808	1963	Ukraine	Winter	+	-	+	-	+	+	-	-	-	+
Bri_177	Caphorn	2001	France	Winter	+	-	+	-	+	+	-	-	-	+
Bri_178	Cordiale	2004	GBR	Winter	+	-	+	-	+	+	-	-	-	+
Bri_179	Apache	1999	CZ	Winter	+	-	+	-	+	+	-	-	-	+
Bri_180	Premio	2007	France	Winter	+	-	+	-	+	+	-	-	-	+
Bri_181	Isengrain	1996	France	Winter	+	-	+	-	+	+	-	-	-	+
Bri_182	Alixan	2005	France	Winter	+	-	+	-	+	+	-	-	-	+
Bri_183	Boregan	2007	France	Winter	+	-	+	-	+	+	-	-	-	+
Bri_184	Renesansa	1995	Serbia	Winter	+	-	+	-	+	+	-	-	-	+
Bri_185	Tremie	1992	France	Winter	+	-	+	-	+	+	-	-	-	+
Bri_189	Soissons	1987	France	Winter	+	-	+	-	+	+	-	-	-	+
Bri_191	Arlequin	2007	France	Winter	+	-	+	-	+	+	-	-	-	+
Bri_195	Avalon	1980	GBR	Winter	+	-	+	-	+	+	-	-	-	+

Bri_196	Ivanka	1998	Serbia	Winter	+	-	+	-	+	+	-	-	-	+
Bri_197	Pobeda	1990	Serbia	Winter	+	-	+	-	+	+	-	-	-	+
Bri_198	NS 66/92	1992	Serbia	Winter	+	-	+	-	+	+	-	-	-	+
Bri_205	Highbury	1968	GBR	Spring	+	-	+	-	+	+	-	-	-	+
Bri_210	NS 46/90	1990	Serbia	Winter	+	-	+	-	+	+	-	-	-	+
Bri_048	Gaucho	1993	USA	Winter	+	-	+	-	+	+	-	-	-	+
Bri_123	Helios	1980	USA	Winter	+	-	+	-	+	+	-	-	-	+
Bri_170	Centurk	1971	USA	Winter	+	-	+	-	+	+	-	-	-	+
Bri_172	Benni multifloret	1980	USA	Winter	+	-	+	-	+	+	-	-	-	+
Bri_173	Hope	1948	USA	Winter	+	-	+	-	+	+	-	-	-	+
Bri_174	Vel	1976	USA	Winter	+	-	+	-	+	+	-	-	-	+
Bri_175	Phoenix	1981	USA	Winter	+	-	+	-	+	+	-	-	-	+
Bri_187	Triple dirk "S"	1968	Australia	Spring	+	-	+	-	+	+	-	-	-	+
Bri_190	BCD 1302/83	1983	Moldava	Winter	+	-	+	-	+	+	-	-	-	+
Bri_192	Sonalika	1967	India	Spring	+	-	+	-	+	+	-	-	-	+
Bri_194	Cajeme 71	1971	Mexico	Spring	+	-	+	-	+	+	-	-	-	+
Bri_199	Mex. 3	1971	Mexico	Spring	+	-	+	-	+	+	-	-	-	+
Bri_203	Florida	1985	USA	Winter	+	-	+	-	+	+	-	-	-	+
Bri_206	Siete Cerros	1966	Mexico	Spring	+	-	+	-	+	+	-	-	-	+
Bri_209	INTRO 615	1980	USA	Winter	+	-	+	-	+	+	-	-	-	+
Bri_211	Mex. 17 bb	1971	Mexico	Winter	+	-	+	-	+	+	-	-	-	+
Bri_212	Lambriego Inia	1980	Chile	Winter	+	-	+	-	+	+	-	-	-	+

					PPD-1				
Genotype	**Cultivar name**	**Year of Release**	**Origin**	**Type**	***Ppd-A1a***	***Ppd-A1b***	***Ppd-B1a/b***	***Ppd-D1a***	***Ppd-D1b***
Bri_003	Jafet	2008	Germany	Winter	-	-	-	-	+
Bri_005	Rebell	2013	Germany	Winter	-	-	-	-	+
Bri_006	Memory	2013	Germany	Winter	-	-	-	-	+
Bri_007	Kurt	2013	Germany	Winter	-	-	-	-	+
Bri_008	Zappa	2009	Germany	Winter	-	-	-	-	+
Bri_010	Gordian	2013	Germany	Winter	-	-	-	-	+
Bri_011	Mentor	2012	Germany	Winter	-	-	-	-	+
Bri_012	Meister	2010	Germany	Winter	-	-	-	-	+
Bri_015	Profilus	2008	Germany	Winter	-	-	-	-	+
Bri_017	KWS Pius	2010	Germany	Winter	-	-	-	-	+
Bri_018	Paroli	2004	Germany	Winter	-	-	-	-	+
Bri_019	Estivus	2012	Germany	Winter	-	-	-	-	+
Bri_020	Kronjuwel	1980	Germany	Winter	-	-	-	-	+
Bri_021	Desamo	2013	Germany	Winter	-	-	-	-	+
Bri_022	Carenius	2006	Germany	Winter	-	-	-	-	+
Bri_023	Mulan	2006	Germany	Winter	-	-	-	-	+
Bri_024	Kredo	2009	Germany	Winter	-	-	-	-	+
Bri_025	Nelson	2011	Germany	Winter	-	-	-	-	+
Bri_026	Patras	2012	Germany	Winter	-	-	-	+	-
Bri_027	Götz	1978	Germany	Winter	-	-	-	-	+
Bri_029	Anapolis	2013	Germany	Winter	-	-	-	-	+
Bri_031	Biscay	2000	Germany	Winter	-	-	-	-	+
Bri_032	Capone	2012	Germany	Winter	-	-	-	-	+
Bri_033	Tabasco	2008	Germany	Winter	-	-	-	-	+
Bri_034	Kometus	2011	Germany	Winter	-	-	-	+	-

Bri_035	Cubus	2002	Germany	Winter	-	-	-	-	+
Bri_036	Edward	2013	Germany	Winter	-	-	-	-	+
Bri_037	Famulus	2010	Germany	Winter	-	-	-	-	+
Bri_038	Dekan	1999	Germany	Winter	-	-	-	-	+
Bri_039	SW Topper	2002	Germany	Winter	-	-	-	-	+
Bri_040	Matrix	2010	Germany	Winter	-	-	-	-	+
Bri_041	Jenga	2007	Germany	Winter	-	-	-	-	+
Bri_042	Linus	2010	Germany	Winter	-	-	-	-	+
Bri_044	Forum	2012	Germany	Winter	-	-	-	-	+
Bri_045	Colonia	2011	Germany	Winter	-	-	-	-	+
Bri_046	Transit	1994	Germany	Winter	-	-	-	-	+
Bri_047	Potenzial	2006	Germany	Winter	-	-	-	-	+
Bri_049	Tarso	1994	Germany	Winter	-	-	-	-	+
Bri_050	Hermann	2004	Germany	Winter	-	-	-	-	+
Bri_051	Glaucus	2011	Germany	Winter	-	-	-	-	+
Bri_052	Tuareg	2005	Germany	Winter	-	-	-	-	+
Bri_053	Atomic	2012	Germany	Winter	-	-	-	-	+
Bri_054	Tobak	2011	Germany	Winter	-	-	-	-	+
Bri_055	Pionier	2013	Germany	Winter	-	-	-	-	+
Bri_056	Manager	2006	Germany	Winter	-	-	-	-	+
Bri_057	Gourmet	2013	Germany	Winter	-	-	-	-	+
Bri_058	Limes	2003	Germany	Winter	-	-	-	-	+
Bri_059	Ritmo	1993	Germany	Winter	-	-	-	-	+
Bri_060	Kalahari	2010	Germany	Winter	-	-	-	-	+
Bri_061	Intro	2011	Germany	Winter	-	-	-	-	+
Bri_062	Oxal	2010	Germany	Winter	-	-	-	-	+
Bri_063	Zobel	2006	Germany	Winter	-	-	-	-	+
Bri_064	Event	2009	Germany	Winter	-	-	-	-	+
Bri_065	Joker	2012	Germany	Winter	-	-	-	-	+

Bri_066	Global	2009	Germany	Winter	-	-	-	-	+
Bri_067	Elixer	2012	Germany	Winter	-	-	-	-	+
Bri_068	Fedor	2007	Germany	Winter	-	-	-	-	+
Bri_069	Türkis	2004	Germany	Winter	-	-	-	-	+
Bri_070	Skagen	2006	Germany	Winter	-	-	-	-	+
Bri_071	Greif	1989	Germany	Winter	-	-	-	-	+
Bri_072	Esket	2007	Germany	Winter	-	-	-	-	+
Bri_073	Primus	2009	Germany	Winter	-	-	-	-	+
Bri_074	Skalmeje	2006	Germany	Winter	-	-	-	-	+
Bri_075	Genius	2009	Germany	Winter	-	-	-	-	+
Bri_076	Enorm	2002	Germany	Winter	-	-	-	-	+
Bri_077	Florian	2010	Germany	Winter	-	-	-	-	+
Bri_078	Skater	2000	Germany	Winter	-	-	-	-	+
Bri_079	Brillant	2005	Germany	Winter	-	-	-	-	+
Bri_080	Inspiration	2007	Germany	Winter	-	-	-	-	+
Bri_081	Apertus	2013	Germany	Winter	-	-	-	-	+
Bri_082	Ellvis	2002	Germany	Winter	-	-	-	-	+
Bri_083	Edgar	2010	Germany	Winter	-	-	-	-	+
Bri_085	SY Ferry	2012	Germany	Winter	-	-	-	-	+
Bri_086	Landsknecht	2013	Germany	Winter	-	-	-	-	+
Bri_088	Impression	2005	Germany	Winter	-	-	-	-	+
Bri_089	Winnetou	2002	Germany	Winter	-	-	-	-	+
Bri_090	Toronto	1990	Germany	Winter	-	-	-	-	+
Bri_091	Torrild	2005	Germany	Winter	-	-	-	-	+
Bri_092	Contra	1990	Germany	Winter	-	-	-	-	+
Bri_093	Schamane	2005	Germany	Winter	-	-	-	-	+
Bri_094	Granada	1980	Germany	Winter	-	-	-	-	+
Bri_095	KWS Cobalt	2013	Germany	Winter	-	-	-	-	+
Bri_096	Tommi	2002	Germany	Winter	-	-	-	-	+

Bri_097	Saturn	1973	Germany	Winter	-	-	-	-	+
Bri_098	Severin	1980	Germany	Winter	-	-	-	-	+
Bri_099	JB Asano	2008	Germany	Winter	-	-	-	-	+
Bri_100	Kerubino	2004	Germany	Winter	-	-	-	-	+
Bri_101	Arktis	2010	Germany	Winter	-	-	-	-	+
Bri_102	Urban	1980	Germany	Winter	-	-	-	-	+
Bri_103	Orestis	1988	Germany	Winter	-	-	-	-	+
Bri_104	Flair	1996	Germany	Winter	-	-	-	-	+
Bri_105	Anthus	2005	Germany	Winter	-	-	-	-	+
Bri_106	Bombus	2012	Germany	Winter	-	-	-	-	+
Bri_107	Lucius	2006	Germany	Winter	-	-	-	-	+
Bri_108	Herzog	1986	Germany	Winter	-	-	-	-	+
Bri_109	Sorbas	1985	Germany	Winter	-	-	-	-	+
Bri_110	Tabor	1979	Germany	Winter	-	-	-	-	+
Bri_111	Terrier	2001	Germany	Winter	-	-	-	-	+
Bri_112	Magister	2005	Germany	Winter	-	-	-	-	+
Bri_113	Altos	2000	Germany	Winter	-	-	-	-	+
Bri_114	Progress	2007	Germany	Winter	-	-	-	-	+
Bri_115	Xantippe	2011	Germany	Winter	-	-	-	-	+
Bri_116	Avenir	2013	Germany	Winter	-	-	-	-	+
Bri_117	Pantus	1966	Germany	Winter	-	-	-	-	+
Bri_118	Drifter	1999	Germany	Winter	-	-	-	-	+
Bri_119	Joss	1972	Germany	Winter	-	-	-	-	+
Bri_120	Kranich	2007	Germany	Winter	-	-	-	-	+
Bri_121	Sperber	1982	Germany	Winter	-	-	-	-	+
Bri_122	Discus	2007	Germany	Winter	-	-	-	+	-
Bri_125	Magnus	2000	Germany	Winter	-	-	-	-	+
Bri_126	Disponent	1975	Germany	Winter	-	-	-	-	+
Bri_127	Tambor	1993	Germany	Winter	-	-	-	-	+

Bri_128	Boxer	2013	Germany	Winter	-	-	-	-	+
Bri_129	Sokrates	2001	Germany	Winter	-	-	-	-	+
Bri_130	Carisuper	1975	Germany	Winter	-	-	-	-	+
Bri_131	Rektor	1980	Germany	Winter	-	-	-	-	+
Bri_132	Alves	2010	Germany	Winter	-	-	-	-	+
Bri_133	NaturaStar	2002	Germany	Winter	-	-	-	-	+
Bri_134	Alidos	1987	Germany	Winter	-	-	-	-	+
Bri_135	Monopol	1975	Germany	Winter	-	-	-	-	+
Bri_136	Akratos	2004	Germany	Winter	-	-	-	-	+
Bri_137	Knirps	1985	Germany	Winter	-	-	-	-	+
Bri_138	Bussard	1990	Germany	Winter	-	-	-	-	+
Bri_139	Oberst	1980	Germany	Winter	-	-	-	-	+
Bri_141	Tiger	2001	Germany	Winter	-	-	-	-	+
Bri_142	Ibis	1991	Germany	Winter	-	-	-	-	+
Bri_143	Batis	1994	Germany	Winter	-	-	-	-	+
Bri_144	Topfit	1972	Germany	Winter	-	-	-	-	+
Bri_145	Akteur	2003	Germany	Winter	-	-	-	-	+
Bri_146	Ludwig	1998	Germany	Winter	-	-	-	-	+
Bri_147	Asketis	1998	Germany	Winter	-	-	-	-	+
Bri_148	Aristos	1997	Germany	Winter	-	-	-	-	+
Bri_149	Zentos	1989	Germany	Winter	-	-	-	-	+
Bri_150	Diplomat	1966	Germany	Winter	-	-	-	-	+
Bri_151	Astron	1989	Germany	Winter	-	-	-	-	+
Bri_152	Basalt	1980	Germany	Winter	-	-	-	-	+
Bri_153	Kormoran	1973	Germany	Winter	-	-	-	-	+
Bri_154	Aron	1992	Germany	Winter	-	-	-	-	+
Bri_155	KWS Milaneco	2013	Germany	Winter	-	-	-	-	+
Bri_156	Aszita	2005	Germany	Winter	-	-	-	-	+
Bri_157	Kobold	2014	Germany	Winter	-	-	-	-	+

Bri_158	Carimulti	1975	Germany	Winter	-	-	-	-	+
Bri_159	Admiral	1968	Germany	Winter	-	-	-	-	+
Bri_160	Vuka	1975	Germany	Winter	-	-	-	-	+
Bri_161	Benno	1973	Germany	Winter	-	-	-	-	+
Bri_162	Apollo	1984	Germany	Winter	-	-	-	-	+
Bri_164	Kanzler	1980	Germany	Winter	-	-	-	-	+
Bri_165	Kraka	1997	Germany	Winter	-	-	-	-	+
Bri_166	Caribo	1968	Germany	Winter	-	-	-	-	+
Bri_167	Butaro	2009	Germany	Winter	-	-	-	-	+
Bri_168	Konsul	1990	Germany	Winter	-	-	-	-	+
Bri_169	Ares	1983	Germany	Winter	-	-	-	-	+
Bri_186	KWS Ferrum	2012	Germany	Winter	-	-	-	-	+
Bri_188	Cardos	1998	Germany	Winter	-	-	-	+	-
Bri_193	Camp Remy	1980	Germany	Winter	-	-	-	+	-
Bri_200	Orcas	2010	Germany	Winter	-	-	-	+	-
Bri_201	Nimbus	1975	Germany	Winter	-	-	-	+	-
Bri_202	Muskat	2010	Germany	Winter	-	-	-	+	-
Bri_204	Rumor	2013	Germany	Winter	-	-	-	+	-
Bri_207	Kontrast	1990	Germany	Winter	-	-	-	-	+
Bri_208	WW 4180 (Kongo)	2012	Germany	Winter	-	-	-	-	+
Bri_213	Pegassos	1994	Germany	Winter	-	-	-	-	+
Bri_001	Einstein	2002	UK	Winter	-	-	-	-	+
Bri_002	Oakley	2005	UK	Winter	-	-	-	-	+
Bri_004	Claire	1997	UK	Winter	-	-	-	-	+
Bri_009	Chevalier	2005	Austria	Winter	-	-	-	+	-
Bri_013	KWS Santiago	2009	UK	Winter	-	-	-	-	+
Bri_014	Brigand	1979	UK	Winter	-	-	-	-	+
Bri_016	Durin	1975	France	Winter	-	-	-	+	+
Bri_028	Robigous	1999	UK	Winter	-	-	-	-	+

Bri_030	Solstice	2001	UK	Winter	-	-	-	-	+
Bri_043	TJB 990.15	1980	UK	Winter	-	-	-	+	-
Bri_084	Maris Huntsman	1971	UK	Winter	-	-	-	+	-
Bri_087	Sponsor	1994	France	Winter	-	-	-	-	+
Bri_124	Obelisk	1987	NL	Winter	-	-	-	-	+
Bri_140	Capelle Desprez	1946	France	Winter	-	-	-	-	+
Bri_163	Aquila	1977	GBR	Winter	-	-	-	-	+
Bri_171	NS 22/92	1971	Serbia	Winter	-	-	-	+	-
Bri_176	Mironovska 808	1963	Ukraine	Winter	-	-	-	-	+
Bri_177	Caphorn	2001	France	Winter	-	-	-	-	+
Bri_178	Cordiale	2004	GBR	Winter	-	-	-	-	+
Bri_179	Apache	1999	CZ	Winter	-	-	-	-	+
Bri_180	Premio	2007	France	Winter	-	-	-	+	-
Bri_181	Isengrain	1996	France	Winter	-	-	-	+	-
Bri_182	Alixan	2005	France	Winter	-	-	-	+	-
Bri_183	Boregan	2007	France	Winter	-	-	-	-	+
Bri_184	Renesansa	1995	Serbia	Winter	-	-	-	-	+
Bri_185	Tremie	1992	France	Winter	-	-	-	-	+
Bri_189	Soissons	1987	France	Winter	-	-	-	-	+
Bri_191	Arlequin	2007	France	Winter	-	-	-	-	+
Bri_195	Avalon	1980	GBR	Winter	-	-	-	+	-
Bri_196	Ivanka	1998	Serbia	Winter	-	-	-	-	+
Bri_197	Pobeda	1990	Serbia	Winter	-	-	-	-	+
Bri_198	NS 66/92	1992	Serbia	Winter	-	-	-	-	+
Bri_205	Highbury	1968	GBR	Spring	-	-	-	+	-
Bri_210	NS 46/90	1990	Serbia	Winter	-	-	-	-	+
Bri_048	Gaucho	1993	USA	Winter	-	-	-	-	+
Bri_123	Helios	1980	USA	Winter	-	-	-	-	+
Bri_170	Centurk	1971	USA	Winter	-	-	-	-	+

Bri_172	Benni multifloret	1980	USA	Winter	-	-	-	-	+
Bri_173	Hope	1948	USA	Winter	-	-	-	-	+
Bri_174	Vel	1976	USA	Winter	-	-	-	-	+
Bri_175	Phoenix	1981	USA	Winter	-	-	+	-	-
Bri_187	Triple dirk "S"	1968	Australia	Spring	+	-	-	-	-
Bri_190	BCD 1302/83	1983	Moldava	Winter	+	-	-	-	-
Bri_192	Sonalika	1967	India	Spring	+	-	-	-	-
Bri_194	Cajeme 71	1971	Mexico	Spring	-	-	+	-	-
Bri_199	Mex. 3	1971	Mexico	Spring	-	-	+	-	-
Bri_203	Florida	1985	USA	Winter	-	-	-	-	+
Bri_206	Siete Cerros	1966	Mexico	Spring	-	-	+	-	-
Bri_209	INTRO 615	1980	USA	Winter	-	-	-	-	+
Bri_211	Mex. 17 bb	1971	Mexico	Winter	-	-	+	-	-
Bri_212	Lambriego Inia	1980	Chile	Winter	-	-	-	-	+

Appendix 3. 13: Genotypic variance of QTL TaHd044 compared with *VRN* and *PPD* genes

Source of variance	**DF**	**Type I SS**	**Mean Square**	**F Value**	**Pr > F**					
Year	2	37125.8144	9281.45361	1260.81	<.0001					
Location	5	20291.3201	3381.88668	459.4	<.0001					
Year*Location	9	11895.9205	1699.41721	230.85	<.0001					
Genotype	212	**19866.5276**	146.07741	47.08	<.0001	**Genotypic variance**	**%**	**Gene**	**Position bp**	**Chromosome**
TaHd044	1	**6576.4804**	6576.4804	893.36	<.0001	0.33	33.1	Novel QTL	556,662,059	3A
TaHd006	1	**232.4569**	232.4569	31.58	<.0001	0.01	1.17	*VRN-A2*	698,507,476	5A
TaHd093	1	**0**	.	.	.	0	0	*VRN-D2*	509,666,717	4D
TaHd115	1	**401.40983**	401.40983	54.53	<.0001	0.02	2.02	*VRN-B1*	581,141,294	5B
TaHd128	1	**7.75418**	7.75418	1.05	0.3048	0	0.04	*VRN-A1*	586,152,803	5A
TaHd020	1	**303.5732**	**303.5732**	28.7	<.0001	0.02	2.02	close to *Ppd-A1*	70,940,322	2A
TaHd030	1	**290.3465**	**290.3465**	35.53	<.0001	0.01	1.17	close to *Ppd-B1*	91,836,538	2B

Abbreviation:

Degree of freedom (DF), Type I SS (Type I sum of squares), F-Test (F), Level of significance (Pr).

Appendix 3. 14: Fine-tuning QTL per location and year in subset1

Location	Year	QTL	Marker	Chr	pos	MAF	Flanking	F_Value	Prob	FDR	Explained_ gen_Variance	SNP effect
Loc1 48°08'N	2015	TaHd008	AX-158545204	1B	41,095,790	0.13	36,273,096 - 51,590,002	26.47	8.74E-07	1.31E-03	16.60	2.13
		TaHd017	AX-86184877	1B	687,718,518	0.41	687,718,493 - 687,718,518	12.33	5.97E-04	3.44E-02	7.71	0.62
		TaHd024	BS00064813_51	2A	779,295,382	0.24	772,460,881 - 781,710,314	30.28	1.09E-07	5.50E-04	10.97	-1.36
		TaHd076	AX-158538813	4B	17,091,460	0.43	17,090,624 - 17,091,460	15.88	1.07E-04	1.51E-02	11.31	0.68
		TaHd102	GENE_3500_336	5A	117,495,484	0.47	98,329,421 - 125,143,323	16.70	7.28E-05	1.24E-02	11.24	-0.7
		TaHd114	AX-158538901	5A	546,531,300	0.45	540,239,141 - 547,383,900	17.86	4.26E-05	1.02E-02	10.87	-0.72
		TaHd120	AX-158565287	5A	698,124,968	0.47	689,708,574 - 700, 455,357	25.98	1.09E-06	1.31E-03	15.34	-0.86
		TaHd178	AX-111597215	7D	90,634,513	0.04	80,696,313 - 94,712,158	35.81	1.70E-08	2.23E-04	21.40	2.41
	2016	TaHd059	AX-158548744	3B	548,044,112	0.44	531,400,517 - 556,486,889	17.77	4.37E-05	3.48E-02	9.99	-1.05
		TaHd088	Tdurum_contig10978_1074	4B	667,614,273	0.23	590,156,901 - 612,544,008	26.75	8.73E-05	1.46E-02	14.74	-2.47
		TaHd092	AX-158619147	4D	503,744,119	0.14	498,241,876 - 512,102,050	31.17	1.11E-07	3.70E-04	17.27	2.97
		TaHd119	AX-158584540	5A	689,708,574	0.27	679,138,395 - 689,896,831	18.94	2.51E-05	2.22E-02	10.15	-1.15

	2017	TaHd038	AX-158610976	2D	556,054,721	0.14	533,165,115 - 577,108,685	46.31	2.38E-10	9.55E-07	22.98	2.72
		TaHd060	AX-158579208	3B	552,441,534	0.44	531,400,517 - 556,486,889	26.63	7.97E-07	8.24E-04	16.92	-0.97
		TaHd113	wsnp_Ex_c7383_12655992	5A	481,900,684	0.25	478,007,505 - 487,540,032	22.04	6.06E-06	3.07E-03	18.60	0.95
		TaHd164	BS00006674_51	7A	511,497,094	0.43	485,611,893 - 511,497,094	17.03	6.23E-05	9.36E-03	7.40	-0.78
Loc2 50°44'N	2015	TaHd040	RAC875_c27530_860	2D	630,395,021	0.47	628,546,933 - 634,879,867	11.76	7.72E-04	8.52E-03	12.70	0.5
		TaHd102	GENE_3500_336	5A	117,495,484	0.47	98,329,421 - 125,143,323	23.03	3.68E-06	3.64E-03	11.95	-1.34
		TaHd177	AX-111073271	7D	73,548,381	0.14	53,260,043 - 83,063,146	57.95	2.25E-12	0.00E+00	26.38	4.45
	2016	TaHd032	AX-158547474	2B	154,252,646	0.37	143,488,881 - 159,888,549	11.53	8.68E-04	3.80E-02	3.64	-0.7
		TaHd059	AX-111155128	3B	548,044,112	0.44	531,400,517 - 556,486,889	16.36	8.15E-05	3.42E-02	9.07	-1.16
		TaHd071	AX-158549898	4A	541,682,624	0.14	531,236,819 - 555,440,210	17.34	5.10E-05	1.07E-02	9.86	1.75
		TaHd088	Tdurum_contig10978_1074	4B	667,614,273	0.11	662,388,150 - 670,730,258	22.37	4.42E-04	2.79E-02	5.70	2.452
		TaHd112	BS00022191_51	5A	476,402,782	0.35	459,777,087 - 477,393,365	28.54	3.14E-07	4.72E-04	7.95	1.05
		TaHd131	AX-158621334	5B	655,450,076	0.44	650,133,415 - 658,962,357	14.83	1.70E-04	1.82E-02	6.58	0.75
		TaHd133	wsnp_Ra_c17541_26430903	5D	94,339,848	0.46	90,352,453 - 96,766,280	50.21	4.31E-11	0.00E+00	24.04	-1.21

	2017	TaHd061	BS00066466_51	3B	553,733,007	0.27	531,400,517 - 561,094,273	21.17	8.60E-06	1.90E-03	10.21	-0.61
		TaHd085	AX-158598874	4B	575,905,334	0.05	570,223,560 - 582,150,443	14.72	1.80E-04	9.13E-03	9.57	-0.83
		TaHd102	GENE_3500_336	5A	117,495,484	0.47	98,329,421 - 125,143,323	31.11	1.04E-07	1.10E-04	15.46	-0.55
		TaHd120	AX-158565287	5A	698,124,968	0.47	689,708,574 - 700, 455,357	11.83	7.47E-04	2.04E-02	5.41	-0.36
		TaHd136	AX-111012253	5D	354,268,986	0.14	354,268,986 - 364,591,550	24.23	2.12E-06	8.39E-04	8.75	0.68
		TaHd173	GENE_2677_330	7B	443,852,093	0.41	440,555,110 - 445,028,364	14.94	1.62E-04	8.55E-03	6.15	-0.42
		TaHd177	AX-111073271	7D	73,548,381	0.14	53,260,043 - 83,063,146	52.26	1.92E-11	0.00E+00	18.59	1.54
Loc3 50°46'N	2015	TaHd036	RAC875_c22328_1356	2B	775,368,670	0.08	770,024,758 - 778,336, 544	15.59	1.18E-04	2.12E-02	12.13	1.76
		TaHd111	Kukri_c17430_972	5A	468,467,263	0.49	459,777,087 - 477,393,365	20.37	3.70E-05	2.28E-02	14.43	0.92
		TaHd155	wsnp_BQ171182B_Ta_1_1	6B	652,640,002	0.08	651,010,174 - 657,061,081	22.45	1.53E-04	3.81E-02	15.20	1.64
		TaHd163	AX-158591518	7A	116,124,115	0.49	115,814,853 - 116,124,115	16.72	2.67E-04	4.17E-02	10.73	0.96
		TaHd177	AX-111073271	7D	73,548,381	0.14	53,260,043 - 83,063,146	28.28	2.46E-05	2.28E-02	19.03	2.74
	2016	TaHd059	AX-111155128	3B	548,044,112	0.44	531,400,517 - 556,486,889	34.55	2.40E-08	9.97E-05	13.08	-0.64
		TaHd065	AX-158580668	3D	43,729,571	0.16	42,789,665 - 45,069,812	28.38	3.41E-07	2.78E-04	25.04	0.7

		TaHd080	BS00018707_51	4B	95,108,661	0.35	86,064,624 - 95,186,494	23.41	3.15E-06	7.76E-04	15.22	-0.56
		TaHd088	Tdurum_contig10978_1074	4B	667,614,273	0.24	615,727,691 - 623,477,041	30.42	5.96E-06	1.27E-03	5.40	0.48
		TaHd102	GENE_3500_336	5A	117,495,484	0.47	98,329,421 - 125,143,323	18.94	2.43E-05	2.57E-03	9.97	-0.47
		TaHd109	BS00066916_51	5A	466,013,993	0.23	459,777,087 - 470,971,334	34.74	2.20E-08	9.97E-05	15.82	0.73
		TaHd118	TA001299_0711	5A	666,706,446	0.48	665,301,472 - 686,547,174	16.42	7.93E-05	4.17E-03	9.16	0.44
		TaHd126	IAAV5683	5B	513,608,096	0.07	513,608,096 - 515,577,945	30.80	1.17E-07	1.80E-04	24.59	1.43
		TaHd143	AX-158566109	6A	506,638,784	0.42	503,903,286 - 510,246,544	14.21	2.31E-04	7.27E-03	13.84	0.42
		TaHd168	AX-158590557	7A	688,947,056	0.17	688,947,056 - 688,967,503	22.47	4.73E-06	9.49E-04	15.26	0.69
		TaHd177	AX-111073271	7D	73,548,381	0.14	53,260,043 - 83,063,146	24.59	1.81E-06	6.42E-04	15.71	1.2
Loc4 51°47'N	2015	TaHd026	IACX1098	2B	58,324,615	0.13	50,123,410 - 62,202,352	17.74	4.22E-05	1.04E-02	12.73	-1.27
		TaHd069	D_contig04964_668	3D	613,709,181	0.16	611,558,324 - 614,269,346	26.03	9.61E-07	3.33E-03	17.07	-1.41
		TaHd090	AX-158550554	4D	40,561,790	0.39	39,122,660 - 43,084,614	15.38	1.30E-04	1.15E-02	10.62	0.86
		TaHd096	AX-158620979	5A	18,837,764	0.18	14,844,440 - 26,130,955	17.57	4.59E-05	1.04E-02	14.43	-1.45
		TaHd134	AX-158543080	5D	206,103,101	0.42	201,333,651 - 210,800,713	21.23	8.36E-06	5.79E-03	13.24	-1

		TaHd149	BobWhite_c23416_168	6B	42,318,724	0.09	36,422,613 - 45,021,305	25.12	1.41E-06	3.33E-03	12.08	-2.41
	2016	TaHd008	AX-158545204	1B	41,095,790	0.13	36,273,096 - 51,590,002	17.28	5.25E-05	2.02E-02	10.72	1.51
		TaHd018	AX-158561465	1D	11,683,390	0.46	11,524,360 - 11,754,646	14.85	1.69E-04	2.83E-02	8.87	0.58
		TaHd025	RAC875_c87052_193	2B	18,176,413	0.15	18,176,413 - 18,386,107	12.54	5.22E-04	4.22E-02	9.19	-0.79
		TaHd080	BS00018707_51	4B	95,108,661	0.35	86,064,624 - 95,186,494	12.72	4.81E-04	4.15E-02	5.90	-0.58
		TaHd102	GENE_3500_336	5A	117,495,484	0.47	98,329,421 - 125,143,323	28.71	2.92E-07	4.05E-03	11.00	-0.76
	2017	TaHd002	AX-111125508	1A	8,634,114	0.23	8,329,289 - 10,048,650	13.72	2.94E-04	4.47E-03	9.06	0.63
		TaHd032	AX-158547474	2B	154,252,646	0.37	143,488,881 - 159,888,549	19.70	1.70E-05	6.94E-04	2.71	-0.67
		TaHd037	GENE_1213_138	2D	425,743,395	0.47	417,130,569 - 428,825,608	11.76	7.72E-04	8.52E-03	12.70	0.5
		TaHd062	BS00097383_51	3B	633,375,071	0.05	623,656,449 - 636,269,864	32.67	5.30E-08	1.52E-05	7.28	-1.62
		TaHd102	GENE_3500_336	5A	117,495,484	0.47	98,329,421 - 125,143,323	53.62	1.17E-11	1.62E-07	23.58	-0.93
		TaHd140	AX-108809122	6A	818,389	0.16	287,347 - 2,972,633	34.44	2.50E-08	1.03E-05	14.35	1.11
		TaHd158	wsnp_Ex_c18632_27501724	6B	680,543,072	0.45	680,308,324 - 680,862,683	24.79	1.65E-06	1.68E-04	13.30	-0.72
		TaHd179	AX-158595243	7D	145,781,043	0.06	141,195,382 - 150,001,953	12.58	5.11E-04	6.61E-03	2.23	-1.65

Loc5 52°22'N	2015	TaHd026	IACX1098	2B	58,324,615	0.13	50,123,410 - 62,202,352	17.74	4.22E-05	1.04E-02	12.73	-1.27
		TaHd050	Excalibur_c14803_1088	3B	370,966,100	0.28	367,835,451 - 372,896,058	14.97	1.60E-04	3.44E-02	8.15	-0.81
		TaHd064	TA005738_0654	3B	782,845,348	0.21	779,662,814 - 785,674,115	21.88	6.14E-06	5.62E-03	11.81	1.04
		TaHd066	AX-158615052	3D	535,583,661	0.04	529,021,359 - 538,469,877	13.40	3.42E-04	4.60E-02	7.91	-2.33
		TaHd122	AX-109317915	5A	26,130,955	-0.06	21,822,390 - 35,631,193	15.18	3.52E-04	4.03E-02	9.05	-2.22
		TaHd097	wsnp_Ra_rep_c69221_66574148	5A	41,427,419	0.36	35,631,193 - 41,458,586	35.22	1.80E-08	1.53E-04	18.75	1.17
		TaHd132	BS00024829_51	5B	693,611,551	0.26	693,611,551 - 693,679,909	17.20	5.45E-05	1.80E-02	8.98	-0.97
		TaHd153	Excalibur_rep_c94584_98	6B	539,539,566	0.32	531,523,292 - 539,539,566	18.24	3.34E-05	1.40E-02	10.58	-0.88
	2016	TaHd003	AX-158569579	1A	25,922,488	0.09	22,933,255 - 28,751,901	11.98	6.91E-04	2.69E-02	8.10	-1.49
		TaHd042	AX-89691002	3A	23,829,167	0.11	21,043,648 - 24,581,600	14.11	2.42E-04	1.62E-02	6.94	1.06
		TaHd043	AX-158613127	3A	79,328,347	0.05	69,497,860 - 83,722,110	44.04	4.74E-10	5.00E-06	18.39	-2.62
		TaHd063	AX-158538304	3B	760,711,086	0.26	760,709,431 - 760,714,102	20.20	1.35E-05	3.36E-03	13.39	0.85
		TaHd151	AX-158529603	6B	88,826,937	0.10	84,846,642 - 94,000,039	21.49	7.35E-06	2.83E-03	13.86	-1.51
		TaHd181	AX-89664808	7D	581,297,867	0.13	575,365,411 - 582,509,671	16.32	8.32E-05	9.18E-03	7.90	1.02

	2017	TaHd035	RAC875_c16752_283	2B	745,716,997	0.08	745,716,997 - 746,131,888	15.59	1.18E-04	2.12E-02	12.13	-1.36
		TaHd060	AX-158579208	3B	552,441,534	0.44	531,400,517 - 561,094,273	20.27	1.30E-05	7.42E-03	14.90	-0.83
		TaHd085	AX-158598874	4B	575,905,334	0.05	570,223,560 - 582,150,443	14.68	1.83E-04	2.85E-02	8.50	-1.43
		TaHd089	AX-158583760	4D	14,847,876	0.04	10,138,474 - 16,680,532	18.27	3.33E-05	1.17E-02	14.20	-1.67
		TaHd111	Kukri_c17430_972	5A	468,467,263	0.49	459,777,087 - 477,393,365	23.28	3.27E-06	4.11E-03	10.82	0.85
		TaHd177	AX-111073271	7D	73,548,381	0.14	53,260,043 - 83,063,146	41.78	1.00E-09	1.60E-05	12.51	2.36
Loc6 54°19'N	2015	TaHd095	BS00079189_51	5A	15,851,069	0.43	14,844,440 - 26,130,955	22.60	4.45E-06	2.57E-02	12.51	-2.41
		TaHd122	AX-109317915	5A	26,130,955	0.11	21,822,390 - 35,631,193	20.30	7.95E-06	3.15E-03	14.62	1.142
	2017	TaHd008	AX-158545204	1B	41,095,790	0.13	36,273,096 - 51,590,002	21.91	6.12E-06	2.73E-03	12.50	2.09
		TaHd050	Excalibur_c14803_1088	3B	370,966,100	0.28	367,835,451 - 372,896,058	22.69	4.35E-06	2.36E-03	16.18	-0.91
		TaHd091	RAC875_c61493_327	4D	166,147,990	0.49	163,067,252 - 169,720,006	19.29	2.05E-05	5.77E-03	15.31	0.81
		TaHd102	GENE_3500_336	5A	117,495,484	0.47	98,329,421 - 125,143,323	39.09	4.00E-09	5.12E-05	15.71	-1.07
		TaHd163	AX-158591518	7A	116,124,115	0.49	115,670,157 - 116,124,115	21.32	8.15E-06	3.41E-03	12.42	0.86

Appendix 3. 15: GWAS of HD [x] correlation coefficients between HD and the mean records of climate variables in February, March and April

Trait	QTL	Marker	Chr	Position	MAF	F_value	ProbF	FDR	Explained_Var %	Annotation
Corr coef.HD*daylength	TaHd031	Tdurum_contig59780_988	2B	98,365,757	0.17	14.41	2.09E-04	0.0430	8.19	Potassium transporter
Corr coef.HD*daylength	TaHd045	AX-158532821	3A	653,349,400	0.20	18.39	3.11E-05	0.0289	9.70	WUSCHEL Homeobox
Corr coef.HD*daylength	TaHd068	BS00003119_51	3D	612,272,421	0.20	16.93	6.20E-05	0.0202	8.83	Agamous-like MADS-box protein AGL62
Corr coef.HD*daylength	TaHd117	AX-89478130	5A	657,206,392	0.29	20.55	1.13E-05	0.0152	11.11	S-adenosyl-L-methionine-dependent methyltransferase
Corr coef.HD*daylength	TaHd147	wsnp_Ex_c56091_58346859	6B	26,633,165	0.27	17.28	5.25E-05	0.0470	9.65	Affinity nitrate transporter
Corr coef.HD*daylength	TaHd148	AX-158589486	6B	32,834,416	0.25	14.97	1.59E-04	0.0430	8.41	Histone H2B
Corr coef.HD*daylength	TaHd175	Excalibur_c81824_411	7B	739,931,842	0.20	13.70	2.94E-04	0.0486	7.85	Argonaute
Corr coef.HD*Temperature	TaHd012	AX-158531922	1B	568,532,403	0.16	32.19	6.39E-08	0.0002	16.70	Tesmin/TSO1-like CXC domain-containing protein
Corr coef.HD*Temperature	TaHd156	AX-109435918	6B	656,544,675	0.14	18.12	3.53E-05	0.0315	10.17	Eukaryotic translation initiation factor 3
Corr coef.HD*Temperature	TaHd161	Kukri_c38025_633	6D	462,840,323	0.11	25.22	1.35E-06	0.0327	13.62	F-box/FBD/LRR-repeat protein

Corr coef.HD*Temperature	TaHd174	AX-158592494	7B	702,474,597	0.19	16.65	7.06E-05	0.0454	9.37	FBD domain
Corr coef.HD*Radiation	TaHd004	AX-110588375	1A	539,965,663	0.11	23.42	3.05E-06	0.0092	12.74	Endonuclease/exonuclease/phosphatase
Corr coef.HD*Radiation	TaHd046	AX-158577185	3A	714,722,922	0.13	26.01	9.50E-07	0.0058	13.69	Speckle-type POZ
Corr coef.HD*Radiation	TaHd070	AX-158549975	4A	88,016,603	0.07	25.07	1.44E-06	0.0058	13.51	Beta-galactosidase
Corr coef.HD*Radiation	TaHd142	BobWhite_c62620_150	6A	38,470,584	0.12	18.79	2.58E-05	0.0476	10.51	Glutamate--tRNA ligase
Corr coef.HD*Radiation	TaHd161	Kukri_c38025_633	6D	462,840,323	0.05	25.39	1.26E-06	0.0015	13.69	F-box domain

Appendix 3. 16: Epistatic interactions detected in subset1

QTL1	Marker1	Chr. Marker1	Pos. Marker1	QTL2	Marker2	Chr. Marker2	Pos. Marker2	Epi_F _Value	Epi_ Prob_F	Epi_ FDR	Genetic explaination %	SNP effect
TaHd008	AX-158545204	1B	41,095,790	TaHd120	AX-158565287	5A	698,124,968	16.57	2.22E-09	5.39E-06	3.76	1.97
TaHd011	AX-89615400	1B	566,980,275	TaHd145	GENE_4208_229	6A	613,483,581	10.34	3.06E-06	8.58E-05	0.99	-0.78
TaHd011	AX-89615400	1B	566,980,275	TaHd159	Kukri_c66579_206	6B	712,672,683	10.28	3.25E-06	8.93E-05	1.27	1.95
TaHd016	AX-89537486	1B	671,196,915	TaHd127	BS00076169_51	5B	555,179,293	9.85	5.55E-06	1.27E-04	0.82	0.79
TaHd032	AX-158547474	2B	154,252,646	TaHd150	TA003528_0548	6B	71,038,456	13.59	6.52E-08	1.17E-05	0.82	1.98
TaHd050	Excalibur_c14803_1088	3B	370,966,100	TaHd001	Kukri_c8390_1102	1A	6,323,655	9.53	8.37E-06	1.69E-04	0.14	-1.69
TaHd056	AX-158536736	3B	502,922,399	TaHd050	Excalibur_c14803_1088	3B	370,966,100	11.47	7.99E-07	3.95E-05	0.00	-1.69
TaHd073	AX-110415935	4A	725,662,722	TaHd120	AX-158565287	5A	698,124,968	10.04	4.73E-06	1.14E-04	0.70	-0.92
TaHd074	AX-110504460	4B	13,427,465	TaHd120	AX-158565287	5A	698,124,968	10.27	3.34E-06	9.07E-05	0.09	-0.89
TaHd076	AX-158538813	4B	17,091,460	TaHd120	AX-158565287	5A	698,124,968	9.56	8.01E-06	1.64E-04	0.42	1.74
TaHd077	AX-158583100	4B	49,936,874	TaHd085	AX-158598920	4B	575,908,171	12.07	3.90E-07	2.72E-05	0.00	-1.36
TaHd078	AX-158583105	4B	52,833,650	TaHd085	AX-158598920	4B	575,908,171	10.51	2.57E-06	7.69E-05	0.14	1.95
TaHd079	AX-158583099	4B	76,127,758	TaHd085	AX-158598920	4B	575,908,171	10.42	2.78E-06	8.11E-05	0.07	1.94
TaHd082	AX-158583101	4B	226,851,988	TaHd085	AX-158598920	4B	575,908,171	11.07	1.27E-06	5.09E-05	0.00	0.97
TaHd083	AX-158550351	4B	295,048,265	TaHd050	Excalibur_c14803_1088	3B	370,966,100	11.49	7.82E-07	3.90E-05	0.07	-1.10
TaHd083	AX-158550351	4B	295,048,265	TaHd131	AX-158621334	5B	655,450,076	9.53	8.16E-06	1.66E-04	0.00	-1.09
TaHd101	AX-110574552	5A	88,032,042	TaHd120	AX-158565287	5A	698,124,968	9.91	5.22E-06	1.22E-04	0.40	-1.11
TaHd120	AX-158565287	5A	698,124,968	TaHd026	IACX1098	2B	58,324,615	10.83	1.71E-06	6.07E-05	0.18	-1.20
TaHd120	AX-158565287	5A	698,124,968	TaHd050	Excalibur_c14803_1088	3B	370,966,100	9.65	7.19E-06	1.53E-04	0.00	0.84
TaHd120	AX-158565287	5A	698,124,968	TaHd094	BS00100185_51	5A	14,844,440	10.39	2.89E-06	8.28E-05	0.12	0.91
TaHd120	AX-158565287	5A	698,124,968	TaHd097	wsnp_Ra_rep_c69221_66574148	5A	41,427,419	10.61	2.24E-06	7.09E-05	0.01	-1.02
TaHd120	AX-158565287	5A	698,124,968	TaHd102	GENE_3500_336	5A	117,495,484	12.09	3.80E-07	2.70E-05	0.00	-0.91
TaHd120	AX-158565287	5A	698,124,968	TaHd106	BS00062996_51	5A	304,460,984	9.90	5.24E-06	1.23E-04	0.01	-0.87

TaHd120	AX-158565287	5A	698,124,968	TaHd107	RAC875_c12507_531	5A	393,918,811	10.14	3.99E-06	1.02E-04	0.07	1.03
TaHd120	AX-158565287	5A	698,124,968	TaHd130	AX-158621280	5B	646,230,623	9.59	7.59E-06	1.58E-04	0.05	1.05
TaHd120	AX-158565287	5A	698,124,968	TaHd133	wsnp_Ra_c17541_26430903	5D	94,339,848	12.16	3.53E-07	2.63E-05	0.00	1.02
TaHd129	AX-111486916	5B	587,071,168	TaHd077	AX-158583100	4B	49,936,874	10.42	2.77E-06	8.09E-05	0.04	-2.06
TaHd129	AX-111486916	5B	587,071,168	TaHd078	AX-158583105	4B	52,833,650	9.51	8.54E-06	1.71E-04	0.07	-1.19
TaHd129	AX-111486916	5B	587,071,168	TaHd079	AX-158583099	4B	76,127,758	9.42	9.26E-06	1.81E-04	0.23	0.97
TaHd139	BS00003995_51	5D	558,242,589	TaHd102	GENE_3500_336	5A	117,495,484	13.75	5.38E-08	1.05E-05	0.03	1.96
TaHd146	AX-158589441	6B	23,619,520	TaHd050	Excalibur_c14803_1088	3B	370,966,100	12.39	2.66E-07	2.24E-05	0.00	-0.83
TaHd177	AX-111073271	7D	73,548,381	TaHd165	wsnp_Ra_rep_c105182_89171305	7A	585,066,140	17.87	5.07E-10	5.39E-06	0.00	1.98

Appendix 3. 17: Epistatic interactions detected in subset2

QTL1	Marker1	Chr. Marker1	Pos. Marker1	QTL2	Marker2	Chr. Marker2	Pos. Marker2	Epi_F _Value	Epi_ Prob_F	Epi_ FDR	Genetic explaination %	SNP effect
TaHd015	AX-158544963	1B	654,714,930	TaHd104	wsnp_BE444644A_Ta_2_1	5A	158,247,085	21.17	5.52E-12	8.57E-07	7.77	2.02
TaHd029	AX-158597419	2B	89,552,907	TaHd098	Ra_c69221_1167	5A	41,427,501	21.18	5.92E-12	8.57E-07	2.61	4.64
TaHd005	AX-158569194	1A	549,425,883	TaHd098	Ra_c69221_1167	5A	41,427,501	20.84	8.09E-12	8.57E-07	0.83	3.57
TaHd015	AX-158544963	1B	654,714,930	TaHd098	Ra_c69221_1167	5A	41,427,501	20.63	1.04E-11	8.57E-07	0.10	2.85
TaHd005	AX-158569194	1A	549,425,883	TaHd104	wsnp_BE444644A_Ta_2_1	5A	158,247,085	19.70	2.86E-11	1.25E-06	0.00	2.57
TaHd013	AX-158544962	1B	639,071,657	TaHd104	wsnp_BE444644A_Ta_2_1	5A	158,247,085	19.57	3.33E-11	1.25E-06	1.14	1.82
TaHd033	BS00016650_51	2B	683,029,170	TaHd047	Ra_c4373_453	3A	720,436,430	19.61	3.43E-11	1.25E-06	0.34	-1.56
TaHd033	BS00016650_51	2B	683,029,170	TaHd007	BS00066271_51	1B	6,867,216	19.57	3.48E-11	1.25E-06	1.92	0.98
TaHd028	AX-158547347	2B	79,248,172	TaHd098	Ra_c69221_1167	5A	41,427,501	19.48	3.95E-11	1.25E-06	0.27	2.25
TaHd075	AX-158618765	4B	14,396,083	TaHd104	wsnp_BE444644A_Ta_2_1	5A	158,247,085	19.38	4.17E-11	1.25E-06	0.42	2.06
TaHd027	AX-89718064	2B	63,781,688	TaHd098	Ra_c69221_1167	5A	41,427,501	19.44	4.18E-11	1.25E-06	0.11	1.85
TaHd013	AX-158544962	1B	639,071,657	TaHd082	AX-158583101	4B	226,851,953	19.10	5.75E-11	1.58E-06	0.30	1.36
TaHd009	Excalibur_c95656_129	1B	44,933,639	TaHd098	Ra_c69221_1167	5A	41,427,501	19.07	7.24E-11	1.83E-06	0.13	2.22

TaHd075	AX-158618765	4B	14,396,083	TaHd098	Ra_c69221_1167	5A	41,427,501	18.86	7.80E-11	1.83E-06	0.02	2.67
TaHd013	AX-158544962	1B	639,071,657	TaHd098	Ra_c69221_1167	5A	41,427,501	18.75	8.85E-11	1.94E-06	0.00	2.20
TaHd027	AX-89718064	2B	63,781,688	TaHd104	wsnp_BE444644A_Ta_2_1	5A	158,247,085	18.62	1.04E-10	2.15E-06	0.05	1.70
TaHd098	Ra_c69221_1167	5A	41,427,501	TaHd010	wsnp_BG606586B_Ta_2_13	1B	530,481,020	18.59	1.16E-10	2.15E-06	0.04	0.17
TaHd013	AX-158544962	1B	639,071,657	TaHd033	BS00016650_51	2B	683,029,170	18.49	1.18E-10	2.15E-06	0.11	0.70
TaHd029	AX-158597419	2B	89,552,907	TaHd102	GENE_3500_336	5A	117,495,535	18.36	1.44E-10	2.33E-06	0.14	0.27
TaHd013	AX-158544962	1B	639,071,657	TaHd079	AX-158583099	4B	76,127,793	18.25	1.56E-10	2.33E-06	0.65	1.35
TaHd170	BS00061911_51	7A	722,573,912	TaHd098	Ra_c69221_1167	5A	41,427,501	18.30	1.60E-10	2.33E-06	0.03	1.92
TaHd127	BS00076169_51	5B	555,179,343	TaHd098	Ra_c69221_1167	5A	41,427,501	18.28	1.61E-10	2.33E-06	0.03	0.09
TaHd007	BS00066271_51	1B	6,867,216	TaHd098	Ra_c69221_1167	5A	41,427,501	18.22	1.67E-10	2.33E-06	0.00	2.14
TaHd028	AX-158547347	2B	79,248,172	TaHd104	wsnp_BE444644A_Ta_2_1	5A	158,247,085	18.19	1.72E-10	2.33E-06	1.41	1.81
TaHd160	AX-110612307	6D	402,872,625	TaHd023	AX-158596231	2A	764,103,038	18.12	1.82E-10	2.33E-06	0.23	0.73
TaHd104	wsnp_BE444644A_Ta_2_1	5A	158,247,085	TaHd010	wsnp_BG606586B_Ta_2_13	1B	530,481,020	18.17	1.84E-10	2.33E-06	0.06	0.23
TaHd135	AX-158587070	5D	307,085,234	TaHd098	Ra_c69221_1167	5A	41,427,501	18.10	1.93E-10	2.35E-06	0.15	2.08
TaHd048	AX-158523630	3A	724,058,885	TaHd098	Ra_c69221_1167	5A	41,427,501	18.02	2.07E-10	2.42E-06	0.09	1.81
TaHd116	AX-158542764	5A	619,687,804	TaHd098	Ra_c69221_1167	5A	41,427,501	17.99	2.13E-10	2.42E-06	0.08	2.21
TaHd015	AX-158544963	1B	654,714,930	TaHd033	BS00016650_51	2B	683,029,170	17.89	2.40E-10	2.54E-06	0.03	0.81

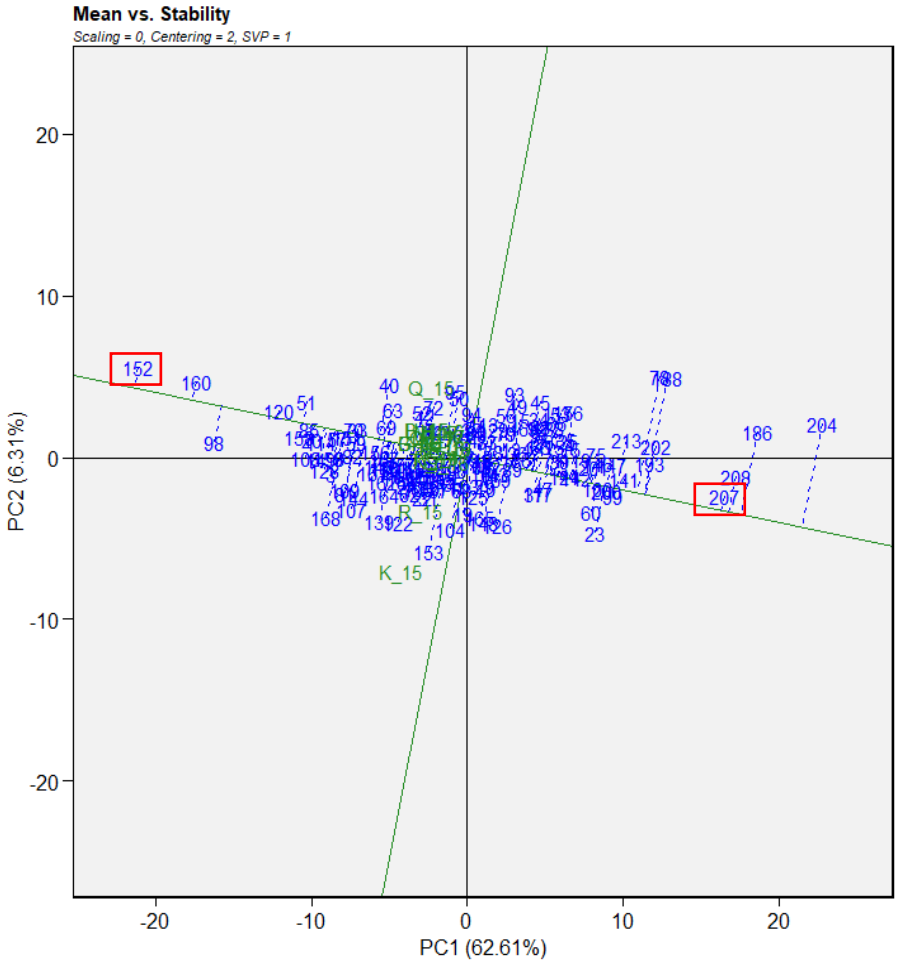

Appendix 4. 1: Mean vs. stability plot of heading date showing the principal components analysis of the stability/heterogeneity of 162 adapted cultivars bred in Germany. The early flowering cultivar 207 "Kontrast "and the late flowering one 152 "Basalt" are selected for their stable flowering behavior in different environments indicated in green (six locations and three years, Benaouda et al., under review), cultivars are shown in blue. The green line passing through the biplot is referring to the average-environmental axis. The early flowering cultivars are clustered on the right side of the plot, the late flowering ones on the left side. The closest the cultivar to the green line, the more stable in all environments.

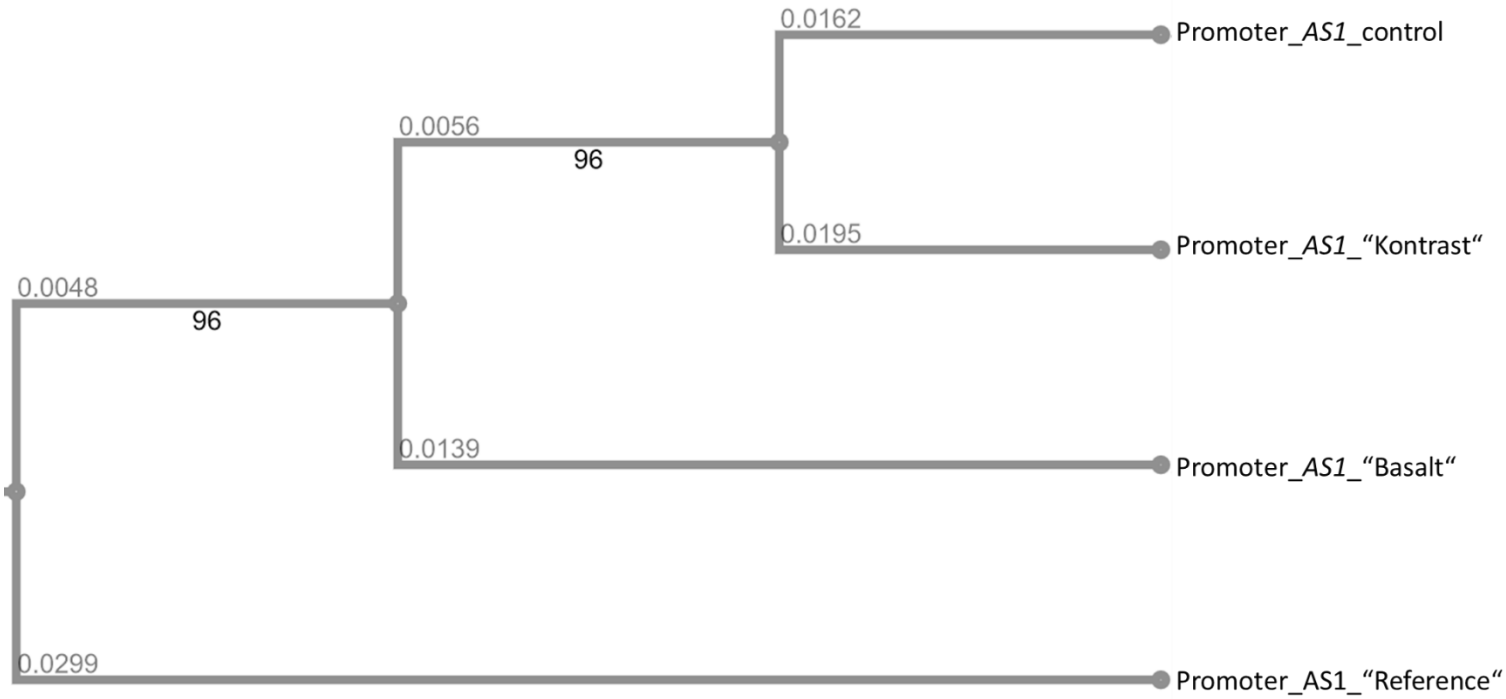

Appendix 4. 2: Alignment tree of the sequenced promoter region (2kb upstream of the start codon) of *AS1* gene of the control and the cultivars "Kontrast" and "Basalt". Level of significance is indicated in grey numbers. Percentage of the shared sequence is highlighted in black.

Appendix 4. 3: Extended list of significant QTL for heading trait in the Germany adapted wheat germplasm

QTL	Marker	Chr.	Position bp	MAF	Flanking	F_Value	Prob	LOD	FDR	Pg*	Pg**	Mark_1	Mark_3	SNP effect
TaHd008	AX-158545204	1B	41,095,790	0.13	36,273,096 - 51,590,002	17.58	4.55E-05	4.34	0.01004526	11.66	0	147.01	145.04	1.97
TaHd033	BS00016650_51	2B	683,029,120	0.50	676,128,349 - 683,029,120	16.32	8.31E-05	4.08	0.01355402	7.33	0.06	146.54	147.32	-0.78
TaHd038	AX-158610976	2D	556,054,721	0.14	533,165,115 - 577,108,685	19.70	1.67E-05	4.78	0.00553398	11.66	0	147.01	145.05	1.95
TaHd041	wsnp_Ku_c10362_17156084	3A	12,781,385	0.43	7,653,355 - 16,620,265	16.53	7.49E-05	4.13	0.01296732	11.39	0.49	147.26	146.47	0.79
TaHd049	AX-110532172	3A	737,651,746	0.13	708,931,624 - 746,917,073	17.63	4.43E-05	4.35	0.01004526	10.07	0.01	147.00	145.02	1.98
TaHd052	AX-111077221	3B	417,374,267	0.05	393,227,687 - 428,432,204	18.13	3.50E-05	4.45	0.00900022	6.23	1.47	146.81	148.50	-1.69
TaHd054	wsnp_Ex_c123_244117	3B	485,388,729	0.31	452,696,385 - 513,566,452	17.79	4.19E-05	4.38	0.00984437	9.68	1.32	146.64	147.56	-0.92
TaHd071	AX-158549898	4A	541,682,624	0.14	531,236,819 - 555,440,210	17.34	5.10E-05	4.29	0.01067905	9.86	0.03	147.01	145.26	1.74
TaHd073	AX-110415935	4A	725,662,722	0.10	709,612,413 - 735,484,113	17.44	5.03E-05	4.30	0.01067905	14.57	6.23	146.73	148.09	-1.36
TaHd081	AX-158582925	4B	221,188,841	0.14	191,079,567 - 262,707,612	19.60	1.76E-05	4.75	0.0055565	11.66	0	147.01	145.05	1.95
TaHd092	AX-158619147	4D	503,744,119	0.14	491,378,204 - 509,504,323	19.74	1.65E-05	4.78	0.00553398	11.66	0	146.99	145.05	1.94
TaHd098	Ra_c69221_1167	5A	41,427,451	0.37	35,626,865 - 59,618,615	26.06	9.40E-07	6.03	0.00090047	13.45	1.24	147.28	146.30	0.97
TaHd099	AX-158599370	5A	77,795,806	0.47	68,545,022 - 94,689,952	39.88	2.58E-09	8.59	8.954E-06	19.97	0	146.40	147.50	-1.10
TaHd102	GENE_3500_336	5A	117,495,484	0.47	98,329,421 - 125,143,323	49.30	6.14E-11	10.21	4.2523E-07	23.78	13.32	146.34	147.54	-1.20
TaHd107	RAC875_c12507_531	5A	393,918,811	0.43	375,286,301 - 413,409,682	24.57	1.85E-06	5.73	0.00150953	8.78	0.01	146.48	147.38	-0.91
TaHd112	BS00022191_51	5A	476,402,782	0.35	461,485,853 - 481,199,152	28.54	3.13E-07	6.50	0.00047181	7.95	0.52	147.26	146.21	1.05
TaHd124	Tdurum_contig10987_800	5B	436,210,304	0.26	418,811,456 - 458,896,741	22.79	4.08E-06	5.39	0.0028301	9.54	0.31	147.19	146.17	1.02
TaHd129	AX-111486916	5B	587,071,168	0.05	580,073,175 - 599,121,152	19.71	1.67E-05	4.78	0.00553398	1.75	0.00	146.81	148.87	-2.06
TaHd132	BS00024829_51	5B	693,611,551	0.26	691,411,951 - 697,289,998	28.11	3.74E-07	6.43	0.00047181	15.34	2.80	146.65	147.83	-1.19
TaHd137	wsnp_Ex_c24594_33843836	5D	367,813,913	0.22	341,039,070 - 381,816,517	17.58	4.57E-05	4.34	0.01004526	7.14	0.02	147.12	146.15	0.97
TaHd152	AX-158529291	6B	207,923,670	0.14	199,746,493 - 227,641,866	19.76	1.64E-05	4.78	0.00553398	11.66	0	147.01	145.05	1.96
TaHd166	AX-158553288	7A	644,705,755	0.43	628,482,675 - 668,251,770	18.46	3.02E-05	4.52	0.00820052	4.76	1.06	146.51	147.34	-0.83
TaHd177	AX-111073271	7D	73,548,381	0.14	53,260,043 - 83,063,146	22.26	5.17E-06	5.29	0.00311816	11.66	2.63	147.04	145.05	1.98

PG* : Total proportion of PG explained by the first selected marker including all markers with QTL effect in the Anova model

PG** : Individual proportion of PG of each marker is calculated without including other markers in the Anova model

Appendix 4. 4: List of primers used for RT-qPCR and sequencing of candidate gene

Gene ID	Chr	Gene target	Primer	Sequence (5' - 3')	Melting Temp (Â°C)	Size of amplified region (bp)	Application	Goal	Organ
TraesCS5B02G543400	5B	*Frigida_like*	Forward	CTCGCCTGCTTCAACGAC	60.71	294	RT-PCR	gene expression	Shoot apex +Leaf
			Reverse	GAGGGGATCTTCTCCGGT	58.98				
TraesCS2D02G434500	2D	*Ascorbate peroxidase 4*	Forward	GACGACGATGACCCCAAG	60.05	195	RT-PCR	gene expression	Shoot apex +Leaf
			Reverse	GAGGGGATCTTCTCCGGT	58.98				
TraesCS3A02G488400	3A	Calcium-binding protein	Forward	GCGTCTCTCGCGGACATT	62.54	154	RT-PCR	gene expression	Shoot apex +Leaf
			Reverse	GCTTGGGGTCATCGTCGT	62.54				
TraesCS6B02G182500	6B	Light-inducible protein	Forward	CTCAGACCCTCAATGGAACC	59.51	476	RT-PCR	gene expression	Shoot apex +Leaf
			Reverse	CTTCACCTTGACCCGCAGA	62.38				
TraesCS4B02G150800	4B	*HUA2-LIKE 3-like*	Forward	TTAGTGATACAAAACCAATCGGC	60.25	251	RT-PCR	gene expression	Shoot apex +Leaf
			Reverse	CATCATTACTTCAAATGTTCGG	57.2				
TraesCS5A02G250100	5A	*C2H2*-type domain-containing protein	Forward	AAGGCGAGGAATTCGAGG	60.29	273	RT-PCR	gene expression	Shoot apex +Leaf
			Reverse	GCACGTTTAATATGGATGACTG	57.22				
TraesCS3B02G318300	3B	*MADS-box transcription factor TaAGL14*	Forward	TTTGAGCTCGAGTGTTATGTCAA	59.93	211	RT-PCR	gene expression	Shoot apex +Leaf
			Reverse	GAACTAGAGCAAGAAGTGACCG	58.28				
TraesCS5A02G079100	5A	Transcription factor *AS1*	Forward	GGAAAGAGGCCTCGTGGA	61.31	200	RT-PCR	gene expression	Shoot apex +Leaf
			Reverse	CTCCTTGAGCTCGGCATC	59.61				
TraesCS7D02G111600	7D	*Flowering locus T*	Forward	CGGTACAACTGGTGCATCCT	60.98	127	RT-PCR	gene expression	Shoot apex +Leaf
			Reverse	GGGAGCGTACACGGTCTG	60.27				
TraesCS5D02G238700	2D	Elongation factor *Ef1a* (Housekeeping gene)	Forward	TCGTTTGTTCGTTTGTTCGTTTG	60	110	RT-PCR	gene expression	Shoot apex +Leaf
			Reverse	GTATAAAGAATAGGATTGGATACA	60				
TraesCS5A02G079100	5A	*AS1*_Gene	Forward	ACCACCAGTCATCTCTCTCTCTC	58.97	1778	PCR	Sequencing	Shoot apex +Leaf
			Reverse	AATGCACCCTGTTGCACTACT	59.68				
TraesCS5A02G079100	5A	*AS1*_Promoter	Forward	GCTGCCTCCTGTCTCCCA	62.6	2198	PCR	Sequencing	Shoot apex +Leaf

			Reverse	CTTCATCTCCATCCGCACCT	62.51				
TraesCS7D02G111600	7D	*Flowering locus T*_Gene	Forward	CATCGGTCTCTCGCTGCT	60.59	1914	PCR	Sequencing	Shoot apex +Leaf
			Reverse	GCCATAATCATGAGGGCG	59.99				
TraesCS7D02G111600	7D	*Flowering locus T_Promoter*	Forward	AAAAATTAGGCAGTGTCGTGTGG	62.43	2261	PCR	Sequencing	Shoot apex +Leaf
			Reverse	GCTTCCCAGCACCCAAAGT	62.53				

Appendix 4. 5: Student t-test results of significant Waddington scores difference between "Tripe Dirk S" and the German early and late flowering cultivar "Kontrast" and "Basalt".

Difference Scores Calculations
Treatment 1
N_1: 34
$df_1 = N - 1 = 34 - 1 = 33$
M_1: 1.88
SS_1: 20.96
$s^2_1 = SS_1/(N - 1) = 20.96/(34-1) = 0.64$
Treatment 2
N_2: 34
$df_2 = N - 1 = 34 - 1 = 33$
M_2: 2.62
SS_2: 46.91
$s^2_2 = SS_2/(N - 1) = 46.91/(34-1) = 1.42$
T-value Calculation
$s^2_p = ((df_1/(df_1 + df_2)) * s^2_1) + ((df_2/(df_2 + df_2)) * s^2_2) = ((33/66) * 0.64) + ((33/66) * 1.42) = 1.03$
$s^2_{M1} = s^2_p/N_1 = 1.03/34 = 0.03$
$s^2_{M2} = s^2_p/N_2 = 1.03/34 = 0.03$
$t = (M_1 - M_2)/\sqrt{(s^2_{M1} + s^2_{M2})} = -0.74/\sqrt{0.06} = -3.03$
The *t*-value is -3.0256. The *p*-value is .001767. The result is significant at $p < .01$.

Appendix 4. 6: Student t-test results of significant Waddington scores difference between "Tripe Dirk S" and the German late flowering cultivar "Basalt"

Difference Scores Calculations
Treatment 1
N_1: 34
$df_1 = N - 1 = 34 - 1 = 33$
M_1: 3.79
SS_1: 110.68
$s^2_1 = SS_1/(N - 1) = 110.68/(34-1) = 3.35$
Treatment 2
N_2: 34
$df_2 = N - 1 = 34 - 1 = 33$
M_2: 1.88
SS_2: 20.96
$s^2_2 = SS_2/(N - 1) = 20.96/(34-1) = 0.64$
T-value Calculation
$s^2_p = ((df_1/(df_1 + df_2)) * s^2_1) + ((df_2/(df_2 + df_2)) * s^2_2) = ((33/66) * 3.35) + ((33/66) * 0.64) = 1.99$
$s^2_{M1} = s^2_p/N_1 = 1.99/34 = 0.06$
$s^2_{M2} = s^2_p/N_2 = 1.99/34 = 0.06$
$t = (M_1 - M_2)/\sqrt{(s^2_{M1} + s^2_{M2})} = 1.91/\sqrt{0.12} = 5.59$
The *t*-value is 5.58553. The *p*-value is < .00001. The result is significant at *p* < .01.

Appendix 4. 7: Student t-test results of significant Waddington scores difference between the control "Tripe Dirk S" and the German early flowering cultivar "Kontrast"

Difference Scores Calculations
Treatment 1
N_1: 34
$df_1 = N - 1 = 34 - 1 = 33$
M_1: 3.79
SS_1: 110.68
$s^2_1 = SS_1/(N - 1) = 110.68/(34-1) = 3.35$
Treatment 2
N_2: 34
$df_2 = N - 1 = 34 - 1 = 33$
M_2: 2.62
SS_2: 46.91
$s^2_2 = SS_2/(N - 1) = 46.91/(34-1) = 1.42$
T-value Calculation
$s^2_p = ((df_1/(df_1 + df_2)) * s^2_1) + ((df_2/(df_2 + df_2)) * s^2_2) = ((33/66) * 3.35) + ((33/66) * 1.42) = 2.39$
$s^2_{M1} = s^2_p/N_1 = 2.39/34 = 0.07$
$s^2_{M2} = s^2_p/N_2 = 2.39/34 = 0.07$
$t = (M_1 - M_2)/\sqrt{(s^2_{M1} + s^2_{M2})} = 1.17/\sqrt{0.14} = 3.12$
The *t*-value is 3.11954. The *p*-value is .001343. The result is significant at $p < .01$.

Presentations und Posters

Salma Benaouda, Said Dadschani, Jens Léon, Agim Ballvora. Genetic and molecular analysis of heading day trait in wheat under different climatic conditions. International Symposium of the Society for Plant Breeding, February 11-13, 2020 |Tulln – Austria.

Salma Benaouda, Jens Léon , Agim Ballvora. Genetische und molekulare Analyse des Blühzeitpunktes in verschiedenen Weizen Populationen. Gemeinschaft zur Förderung von Pflanzeninnovation e. V.(GFPi) Tagung 23.05.2018 in Kleinaltendorf.

Salma Benaouda, Jens Léon , Agim Ballvora. Genetic and molecular analysis of flowering time pathways identified in Wheat populations. Deutsche Forschungsgemeinschaft (DFG) Projekt meetings am 07.09.2016 in Siebeldingen, 21.06.2017 in Gatersleben and 16.03.2018 in Kiel.

Publikationen

Salma Benaouda, Said Dadshani, Patrice Koua, Jens Léon, Agim Ballvora. Response to environment and epistasis uncover novel regulators of flowering time on chromosomes 5A and 3A in winter wheat. (In review in TAAG-D-22-00023R1).

Salma Benaouda, Tyll Stöcker, Heiko Schoof, Jens Léon, Agim Ballvora. Transcriptome profiling at transition to reproductive stage uncovers spatial and tissue specific genes for heading regulation in wheat. (Under internal review).

Koua P. A., Oyiga, B. C., Rasher U., **Benaouda S**., Léon J. & Ballvora, A. Chromosome 3A harbors several pleiotropic and stable droughts inducible QTLs (SNPs) selected through breeding and associated with photosynthesis activity (In review in Plant Direct: 2021-00775R1)